ZooKeys 744: 1–18 (2018)
doi: 10.3897/zookeys.744.23265
http://zookeys.pensoft.net

RESEARCH ARTICLE

A peer-reviewed open-access journal
ZooKeys
Launched to accelerate biodiversity research

Description of *Longidorus cheni* sp. n. (Nematoda, Longidoridae) from China

Eda Marie Barsalote[1], Hoa Thi Pham[1], Stela Lazarova[2], Vlada Peneva[2], Jingwu Zheng[1,3]

1 *Laboratory of Plant Nematology, Institute of Biotechnology, College of Agriculture & Biotechnology, Zhejiang University, Hangzhou 310058, China* **2** *Institute of Biodiversity and Ecosystem Research, Bulgarian Academy of Sciences, 2 Gagarin Street, 1113 Sofia, Bulgaria* **3** *Ministry of Agriculture Key Lab of Molecular Biology of Crop Pathogens and Insects, Hangzhou 310058, China*

Corresponding author: *Jingwu Zheng* (jwzheng@zju.edu.cn)

Academic editor: *S. Subbotin* | Received 24 December 2017 | Accepted 4 February 2018 | Published 19 March 2018

http://zoobank.org/E369B1BD-3C2C-409E-98B3-F4F9C64B9CF8

Citation: Barsalote EM, Pham HT, Lazarova S, Peneva V, Zheng J (2018) Description of *Longidorus cheni* sp. n. (Nematoda, Longidoridae) from China. ZooKeys 744: 1–18. https://doi.org/10.3897/zookeys.744.23265

Abstract

Longidorus cheni **sp. n.**, an amphimictic species recovered from the rhizosphere of *Larix principis-rupprechtii* and *Pyracantha fortuneana* in Shanxi and Beijing, China, is described and illustrated. The taxonomic position of *L. cheni* **sp. n.** among other species within the genus was elucidated using morphometric and molecular data, and phylogenetic relationships were inferred using D2–D3 expansion domains of 28S and 18S rRNA genes by Bayesian Inference (BI) method. The new species is characterised by females with a medium body size (L = 4.9–6.6 mm), a lip region slightly expanded, broadly rounded frontally and laterally, the amphidial fovea broad and symmetrically bilobed at base, odontostyle long and slender (143–168 µm), odonthophore slightly swollen at the base, tail short bluntly conoid to rounded. Guide ring located far posterior from the oral aperture (70–93 µm). Males with two ad-cloacal pairs of supplements preceded by a row of 10–14 ventromedian supplements, with robust spicules measuring 111–126 µm along the median line. Three juvenile stages were present, tail shape of J1 elongate conoid while in J2 and J3 the tail gradually becomes bluntly rounded. Codes for identifying the new species are: A6-B3-C5-D2-E2-F3-G1-H1-I2-J2-K2. *Longidorus cheni* **sp. n.** belongs to a group of species with a guide ring at the mid-odontostyle position that have a predominantly Asiatic origin. It differs from all of them by a combination of morphological characters and unique sequences of partial 18S and D2–D3 region of 28S rRNA genes. The percentage dissimilarities in partial 18S and D2–D3 28S rRNA genes of *L. cheni* to the closest species (*L. litchii*, *L. fangi*, *L. jonesi* and *L. juglans*) were 1.5 %–1.8 % and 16.8–18.3 %, respectively.

Keywords
D2–D3 region of large subunit (LSU) 28S rDNA, morphology, phylogeny, small subunit (SSU) 18S rDNA, taxonomy

Introduction

Longidorids, despite their long history of research (the first species of the family *Longidorus elongatus* (de Man, 1876) was described almost one hundred and fifty years ago) continue to attract the attention of scientists due to their high species diversity, wide distribution, and economic importance. The valid *Longidorus* Micoletzky, 1922 species described to date reached 167 (Peneva et al. 2013, Xu et al. 2017) with the proposed synonymy of two species (Sturhan 2014, Tanha Maafi et al. 2015). Present records of *Longidorus* distribution in mainland China reported by Guo et al. (2011) and Xu et al. (2017) include 16 species, half of which were originally described from the country: *L. jiangsuensis* Xu & Hooper, 1990, *L. fangi* Xu & Cheng 1991, *L. henanus* Xu & Cheng 1992, *L. litchii* Xu & Cheng 1992, *L. hangzhouensis* Zheng, Peng, Robbins & Brown, 2001, *L. camelliae* Zheng, Peneva & Brown, 2000, *L. asiaticus* Triscuizzi, Archidona-Yuste, Troccoli, Fanelli, Luca, Vovlas & Castillo, 2015 and *L. juglans* Xu, Ye, Wang, Zeng & Zhao, 2017.

In a survey during August 2014 and May 2015, a new species of *Longidorus* was recovered from native conifers growing in a mountainous region of Shanxi and evergreen shrubs growing in a botanic garden in Beijing, the localities situated in northern and northeastern China, respectively. Molecular approaches and phylogenetic studies in combination with morphometric characters are used as a taxonomic standard for species identification and delimitation (Gutiérrez-Gutiérrez et al. 2013, Peneva et al. 2013, Archidona-Yuste et al. 2016). The study aims to characterise this undescribed nematode species based on morphological characters coupled with molecular data and infer the phylogenetic relationships with the other species of genus *Longidorus*.

Materials and methods

Nematode sampling

Specimens examined in this study were extracted from soil samples collected from the rhizosphere of *Larix principis-rupprechtii* Mayr. from Shanxi and *Pyracantha fortuneana* (Maxim.) from Beijing, China. Five hundred grams (500 g) of soil were mixed and washed using a decanting and sieving technique (Brown and Boag 1988). The extract was left for two days on a Baermann funnel and the suspension was collected afterwards. Collected nematodes were examined under a stereomicroscope and *Longidorus* specimens were picked out and transferred to Syracuse dishes for storage. For morphometric studies the nematodes were killed, fixed with hot formalin, and processed to glycerine (Seinhorst 1959) as modified by De Grisse (1969). The micrographs, measurements, and drawings of nematodes were completed with the help of Nikon eclipse Ni-U 931845 compound microscope. All measurements were presented in micrometres (µm) and expressed as a mean ± standard deviation.

DNA Extraction, amplifications, and sequencing

DNA was extracted from a single adult nematode, carefully handpicked from nematode suspensions, transferred onto a glass slide containing a 13 µl H_2O, and cut into two pieces using a sterilised scalpel. The nematode fragments were pipetted up to 10 µl and transferred to Eppendorf tubes with 8 µl Mg+ free buffer and 2 µl proteinase K (Ye et al. 2004). PCR tubes were centrifuged at 12000 rpm for 2 minutes and immediately frozen at -70 °C for at least 30 minutes. Subsequently, each tube was incubated for 65 °C for 3 hours and nematode was digested at 75 °C for 60 minutes and 95 °C for 10 minutes. Finally, the DNA suspensions were cooled down at 8 °C and stored at -20 °C until use. A total of 25 µl PCR mixture was prepared containing 2.5 µl LA buffer, 2 µl dNTP, 1.5 µl each primer (synthesized by Takara Company, Shanghai, China) and 3 µl DNA template, 0.3 µl LATaq and 14.2 µl distilled water. All PCR reactions were conducted in the S1000 thermal cycler (BIO-RAD). Fragments of 18S and 28S region were amplified using two sets of primers: forward primer SSU_F_07 (5' AAA GAT TAA GCC ATG CAT G 3') and reverse primer SSU_R_81 (5' TGA TCC ACC TGC AGG TTC AC 3') (Gutiérrez-Gutiérrez et al. 2011) and forward primer D2A (5' ACA AGT ACC GTG AGG GAA AGT TG 3') and reverse primer D3B (5'-TCG GAA GGA ACC AGC TAC TA-3') (De Ley et al. 1999), respectively. The thermal cycling protocol consisted of denaturation at 95 °C for 5 minutes, followed by 35 cycles of denaturation at 94 °C for 30 seconds, annealing at 55 °C for 45 seconds, extension at 72 °C for 2 minutes and a final extension at 72 °C for 10 minutes. After DNA amplification, 2.5 µl aliquots of PCR products were analysed by gel electrophoresis in 1 % agarose gel (100V, 400 mA, 30 minutes) stained in ethidium bromide for 10 minutes and DNA were visualized under UV illumination. Amplified PCR products were purified following the instructions as described in the nucleic acid purification kit of AXYGEN (catalogue No. AP-GX-250) of the AXYGEN Biotechnology Co., Ltd. Hangzhou, China. Purified DNA were ligated to pUCM-T vector and transformed in to DH 5alpha competent cells. The transformants were screened on an ampicillin agar LB plates containing 400 ml IPTG, X-Gal and left at 37 °C overnight. White colonies were selected, transferred to 5 ml LB containing 100 mg/ml ampicillin, and incubated at 37 °C for 16–24 hours. PCR amplification was further confirmed with the primer insertion and expected band; four clones were sequenced per population. Sequencing was done at the SANGON Biotechnology Co., Ltd. Since the clones were identical, only one sequence for each gene has been deposited in GenBank sequence database with the following accession numbers: KY284157 and KF270638 for D2–D3 expansion domains of 28S rDNA, KF261570 and MG656980 for the 18S rDNA region.

Sequence and phylogenetic analyses

The D2–D3 28S and 18S rDNA sequences were compared with those of other nematode species deposited in GenBank database using BLASTn similarity search tool. The homologous sequences nearest to those of the new species were aligned using the GUIDANCE2 Server available at http://guidance.tau.ac.il/ with default parameters (Sela et al. 2015) and manually trimmed and edited in Mega 7 (Kumar et al. 2016). Bayesian Inference (BI) algorithm implemented in MrBayes 3.2.5 was used for phylogenetic relationships reconstructions (Huelsenbeck and Ronquist 2001, Ronquist et al. 2012). For further details, see Lazarova et al. (2016). The 50 % majority rule consensus BI trees of *Longidorus* and *Paralongidorus* spp. are based on a multiple sequence alignment data sets that included: a) 57 sequences and 700 total characters for D2–D3 28S rRNA gene and b) 48 sequences and 993 total characters for 18S rRNA gene.

Taxonomy

***Longidorus cheni* sp. n.**
http://zoobank.org/AD7993D5-AB3D-4436-863D-2D469EEE49CA
Figures 1–5

Material examined. Twelve females, twelve males, fifty-two juveniles (J1-J3) from Shanxi province and ten females, four males, thirty juveniles (J1-J3) from Beijing.

Description. *Measurements* (see Tables 1 and 2).

Female. Body habitus G-shaped when relaxed by gentle heat (Fig. 1M) gradually tapering in both ends. Cuticle under light microscope with three distinct layers, the middle one consisting of several sub-layers, slightly refractive, most pronounced at labial and tail regions, the inner one thicker at labial and tail region with radial striations, cuticle 6 μm thick at post-labial area, 5 μm along the body and 11 μm in post-anal region. Nine lateral, three dorsal and five ventral body pores in the neck region. Lip region slightly expanded, broadly rounded frontally and laterally (Fig. 2D). Amphidial fovea broad and symmetrically bilobed at the base (Fig. 3B). Odontostyle long and slender with simple base, odontophore slightly swollen at the base (Fig. 3A), approx. 1/3 of the odontostyle length. Guide ring located far posterior from oral aperture (Fig. 4A–B). Pharynx dorylaimoid with anterior part more or less coiled, pharyngeal bulb comparatively short measuring 107–138 × 23–28 μm (Fig. 1O). Arrangement of pharyngeal glands normal, dorsal gland nucleus located at 23–34 μm and ventrosublateral gland nuclei at 48–54 μm from the beginning of pharyngeal bulb. Pharyngo-intestinal valve (cardia) hemispherical (Fig. 1P). Tail short dorsally convex and terminus bluntly conoid with two pairs of caudal pores (Fig. 2I). Vulva a transverse slit located slightly anterior from mid body (V = 40–48 %), vagina well developed extending nearly half of body diameter (Fig. 3D, E). Reproductive system amphidelphic with anterior and posterior branches almost equally developed (Fig. 3C). Sperms observed in the uteri of most females (Fig. 3F).

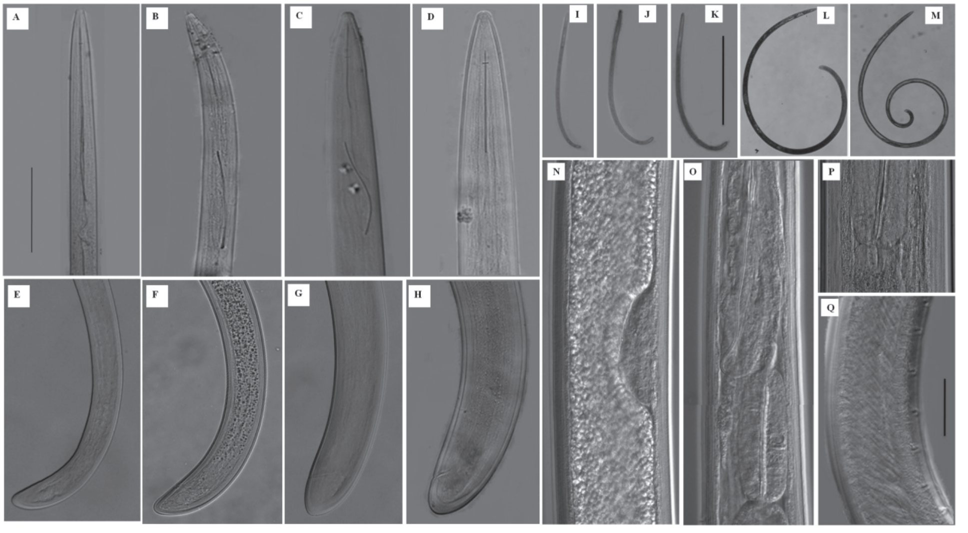

Figure 1. *Longidorus cheni* sp. n. *Juveniles*: **A–C** Anterior region of first-, second- and third-stage **E–G** Posterior end of first-, second- and third-stage **I–K** Habitus of first-, second- and third-stage juvenile **N** developing gonad in a second stage juvenile. *Female*: **D** Anterior end **H** Tail **L** Habitus **O** Pharyngeal bulb region **P** Cardia *Male*: **M** Habitus **Q** Ventromedian supplements. Scale-bars: 60 µm (**A–H**); 100 µm (**I–M**); 15 µm (**N–Q**).

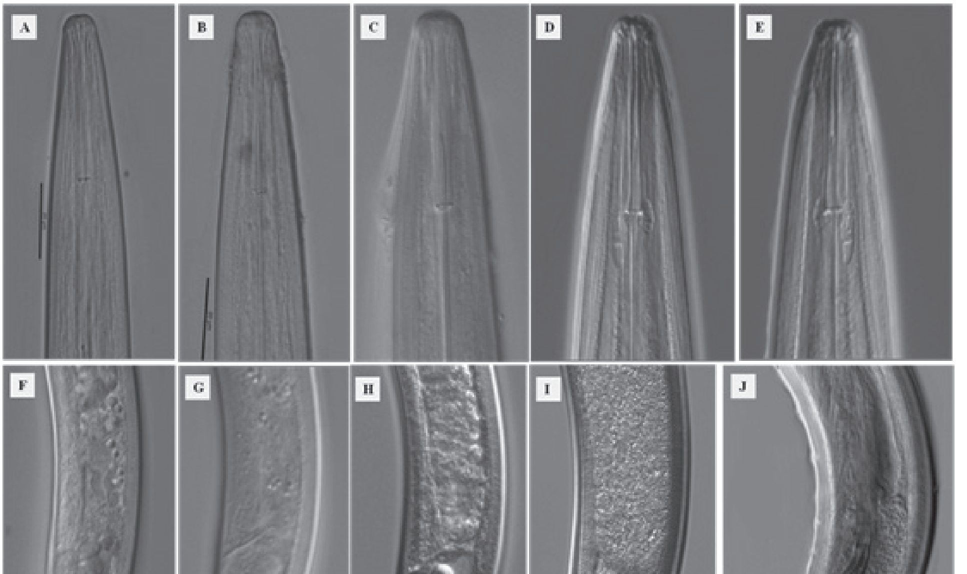

Figure 2. *Longidorus cheni* sp. n. *Juveniles*: **A–C** Head region of first-, second- and third-stage **F–H** Head region of first-, second- and third-stage. *Female*: **D** Head end **I** Tail end; *Male*: **E** Head end **J** Tail end. Scale bar: 20 µm (**A–J**).

Table 1. Measurements (in μm and in the form, mean ± standard deviation and range) of females and males of *Longidorus cheni* sp. n. from two provinces in China.

Origin	Holotype	Shanxi		Beijing	
		Paratypes		Paratypes	
Host		*Larix principis-rupprechtii*		*Pyracantha fortuneana*	
	Female	Females	Males	Females	Males
N		12	12	10	4
L	6606	5778.1 ± 740.7 (4924–6645)	5334.7 ± 731.05 (4553–6709)	5675 ± 687.2 (4125–5678)	5109±686.4 (4153–6548)
a	63.1	51.98 ± 4.6 (47.8–63.1)	61.4 ± 5.6 (52.7–69.1)	49.8 ± 4.1 (45.7–59.0)	58.7±7.9 (46.2–69.0)
b	10.2	9.68 ± 1.79 (7.5–12.4)	9.1 ± 1.5 (7.4–12.2)	9.2 ± 1.79 (7.5–12.2)	8.7±1.3 (7.1–11.4)
c	153.3	133.13 ± 15.04 (115.9–153.3)	108.53 ± 6.56 (100.8–120.1)	135 ± 14.4 (118.0–149.0)	103.1±10.4 (86.1–120.1)
c’	0.68	0.74 ± 0.08 (0.63–0.86)	0.8 ± 0.09 (0.64–0.97)	0.78 ± 0.09 (0.62–0.86)	0.81 ± 0.1 (0.68–0.99)
V	43.2	44.07 ± 3.39 (40.6–49.4)	–	46.4 ± 2.89 (40–48.3)	–
Odontostyle	168	155.7 ± 6.6 (143–168)	156.8 ± 8.85 (142–172)	153.2 ± 5.03 (142–166)	156.3 ± 9.3 (142–173)
Odontophore	103	90.5 ± 7.0 (81.5–103)	88.8 ± 4.9 (8.6–99)	90.0± 6.04 (82–102)	83.3 ± 5.1 (73–86)
Guide ring to anterior end	85	77.6 ± 5.9 (70–91)	78.5 ± 3.4 (74–85)	78.5±3.6 (74–84)	79.3 ± 6.7 (72–93)
Lip width	20	19.7 ± 1.2 (18–22)	19.6 ± 1.2 (17–21)	18.6 ± 2.2 (17.5–23)	19.7 ± 1.3 (17–21)
Width at guide ring	55	49.0 ± 5.2 (42–57)	46.9 ± 4.7 (40–55)	46 ± 4.2 (42–55)	46.5 ± 4.5 (39–55)
Width at anus	63	60.3 ± 7.6 (49–72)	61.9 ± 5.7 (54.5–70)	60 ± 7.4 (48–70)	61.2 ± 5.5 (55–70)
Tail length	33	26.4 ± 7.8 (24–33)	29.1 ±3.1 (27.6–32.2)	26.1±7.7 (25–34)	29.8 ± 4.2 (28–34)
Spicule	112	–	112.3 ± 7.8 (101–124)	–	111.3 ± 7.2 (101–121)

Male. Morphologically similar to female. Body G to spiral shape (Fig. 1M). Testes paired and fully developed. Sperms abundant and irregularly shaped (Fig. 3K). Spicules robust (Fig. 3J). Lateral guiding piece 32–35 μm. Two ad-cloacal pairs of supplements preceded by row of 10–14 ventromedian supplements (Fig. 3H). Tail ventrally curved bluntly conoid to hemispherical, 2–3 lateral pores on each side (Fig. 3H).

Juveniles. Three juvenile stages (J1-J3) distinctly separated by differences in the body length, odontostyle and replacement odontostyle length (Fig 1A–C). In the first stage juvenile, the anterior part of replacement odontostyle is inserted in the wall of odontophore (Fig 3A). Morphologically, juveniles resemble adults except for the smaller size and not developed reproductive system. Habitus assuming J shape does not change with the stage (Fig. 1I–K). Tail length does not change while anal width

Table 2. Measurements (in µm and in the form, mean ± standard deviation and range) of juvenile stages of *Longidorus cheni* sp. n. from two provinces in China.

Origin	Shanxi			Beijing	
	Paratypes			Paratypes	
Stages	J1	J2	J3	J2	J3
N	17	15	20	12	18
L	1582 ± 150. 6 (1390–1929)	2822 ± 390.3 (2413–3539)	3711.5 ± 380.3 (3205–4269.5)	2489 ± 132.5 (2375–3529)	3787.5 ±298.3 (3339–4909)
a	39.8 ± 3.6 (34.6–48.6)	50.54 ± 5.7 (42.9–62.7)	54.3 ± 7.0 (43.3–69.7)	47.7 ± 2.4 (44–59)	57 ± 4.71 (43–67)
b	4.6 ± 0.5 (4.0–5.8)	6.7 ± 1.1 (5.1–8.9)	7.9 ± 1.5 (6.2–11.3)	6.2 ± 0.8 (5.9–8.5)	7.9 ± 2.1 (5.9–10.6)
c	44.2 ± 4.6 (38.2–54.0)	69.03 ± 10.2 (54.8–89.4)	84.9 ± 8.1 (74.45–103.3)	63.9 ± 4.2 (48.0–75.0)	78.3 ± 9.2 (65.1–103.0)
c’	1.25 ± 0.12 (1.02–1.46)	0.99 ± 0.16 (0.75–1.33)	0.82 ± 0.09 (0.68–1.02)	0.9 ± 0.12 (0.8–1.5)	0.81 ± 0.1 (0.65–1.25)
Total stylet	148.9 ± 10.4 (137–174)	180.5 ± 12.0 (165–200.5)	220.8 ± 13.0 (198–246)	178.9± 10.7 (167–195)	212.0 ± 10.2 (193–247)
Odontostyle	96.8 ± 4.2 (91–109)	109.8 ± 6.4 (100–118.5)	133.2 ± 11.7 (121–157)	107 ± 3.3 (101–116)	131.0 ± 5.2 (120–146)
Odontophore	52.2 ± 7.0 (44–66)	70.7 ± 7.2 (64–85)	87.6 ± 3.3 (83–94)	71.9 ± 6.7 (65–89)	81.0 ± 8.1 (83–89)
Replacement odontostyle	103.9 ± 4.3 (96–110.5)	130.9 ± 5.3 (125–141)	150.63 ± 6.48 (143–164)	132 ± 3.4 (129–146)	152.0 ± 4.35 (146–160)
Guide ring to anterior end	43.1 ± 4.0 (39–55)	55.5 ± 6.6 (44.5–65)	65.8 ± 6.1 (57–78)	52.9 ± 3.9 (47–69)	64.0 ± 5.25 (53–75)
Lip width	11.1 ± 0.8 (9–12)	14.6 ± 1.9 (11–18)	15.6 ± 1.8 (13–19)	13.9 ± 0.67 (10–18)	15.0 ± 1.1 (12–19)
Body width at guide ring	26.3 ± 2.9 (22.5–33)	34.1 ± 6.4 (25–46.5)	42.8 ± 9.6 (33–67)	26.3 ± 2.9 (22.5–33)	44.08 ± 6.39 (35–67)
Anal body width	28.9 ± 3.9 (22–38)	42.4 ± 5.4 (33–52)	54.3 ± 8.09 (45–68)	43.2 ± 3.9 (43–56)	52.4 ± 5.4 (43–72)
Tail length	35.9 ± 3.1 (31- 39)	33.17 ± 1.3 (28–34)	32.3 ± 3.3 (30–35.5)	33.8 ± 0.9 (29–35)	31.87 ± 3.3 (29–35)

increases (Fig. 1E-G) thus **c’** ratio decreases (Table 2), guide ring position becoming more posterior during successive stages (Fig. 2A–C). First stage juvenile is characterized by a conoid tail becoming bluntly conoid in second to third stages (Fig. 2F–H).

Sequences and phylogenetic analyses. The length of PCR products based on gel images of the amplification of partial 18S and D2–D3 region of 28S RNA genes of *L. cheni* sp. n. (LDT235 and BJ07) was 844 bps and 856 bps, respectively. The sequences of both populations were identical. The phylogenetic relationships of *L. cheni* sp. n. with the closest species inferred from analyses of the partial 18S rDNA and D2–D3 expansion segments of 28S rDNA sequences using BI are presented in Figs 6 and 7, respectively. In general, the new species grouped with other *Longidorus* species of predominantly Asiatic origin in both phylogenetic reconstructions. In D2–D3 rDNA phylogenetic tree, *L. cheni* clustered in a

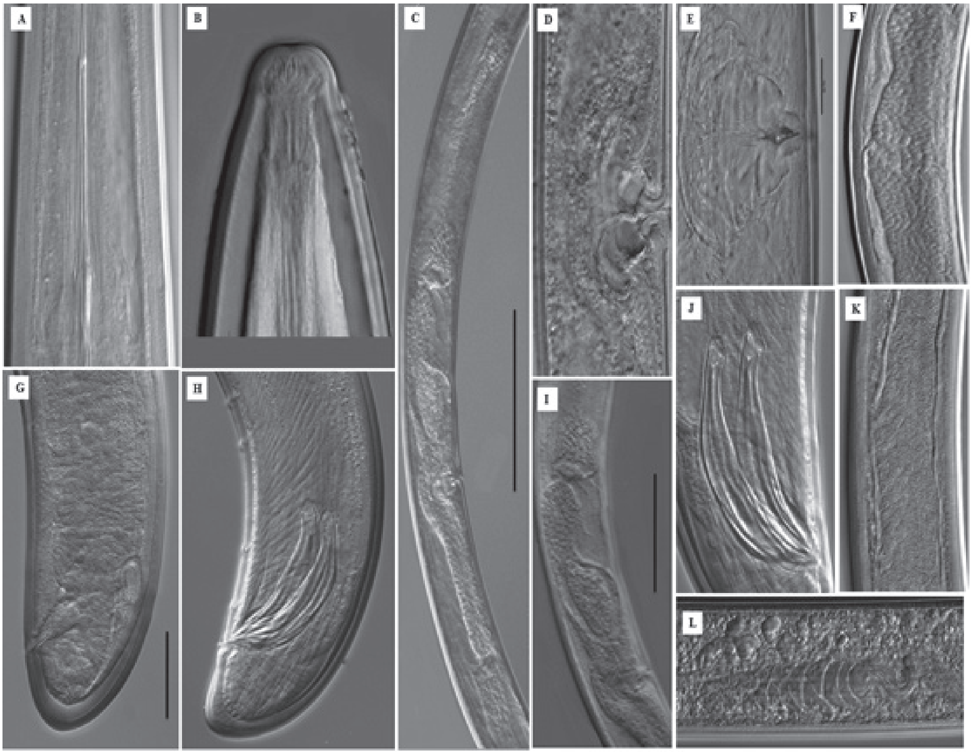

Figure 3. *Longidorus cheni* sp. n. *Female*: **A** Odontophore region **B** Amphidial fovea shape **C** Reproductive system **D–E** Vulval region **F** Sperms inside uteri **I** Oviduct separated by sphincter **G** Tail region **L** Ovary. *Male*: **H** Tail end **J** Spicule **K** Testis with sperms. Scale bars: 20 µm (**A, B, E, G, H, J**); 100 µm (**C**); 50 µm (**D, F, I, K, L**).

well-supported clade comprising four species from China (*L. juglans* (MF318878), *L. fangi* (MF318883-84), *Longidorus* sp. (KF280150); one from Japan (*L. jonesi* (KF552069) and two species from North America, USA (*L. diadecturus* (AY601584) and *Longidorus* sp. (KF242342-43)). With exception of the species for which there are no descriptions, all mentioned species have a guide ring at mid-odontostyle area. Similarly, in the 18S rDNA phylogenetic reconstruction *L. cheni* sp. n. clustered with the same group of species (*L. jonesi*, *L. fangi*, and *L. diadecturus*) and *L. litchii* (AY687996) that has no D2–D3 rDNA sequence deposited in GenBank. The percentage dissimilarities of *L. cheni* to the closest species *L. litchii*, *L. fangi*, and *L. juglans* in 18S rRNA gene were 1.5 %, 1.8 %, and 1.8 %, respectively (a total of 955 positions in the final dataset). Much higher were the pairwise percentage distances of *L. cheni* sp. n. to the closest species in D2–D3 28S rRNA gene ranging from 16.8–16.9 % (*L. fangi* and *L. jonesi*) to 18.3 % (*L. juglans*).

Type habitat and locality. Specimens were recovered from soil around the roots of a conifer (*L. principis-rupprechtii*) and Chinese firethorn (*P. fortuneana*) in mountainous region of Shanxi and botanic garden in Beijing, China, GPS coordinates 37°50'815"N, 111°27'253"E and 30°34'54.7"N, 114°15'40.9"E, respectively.

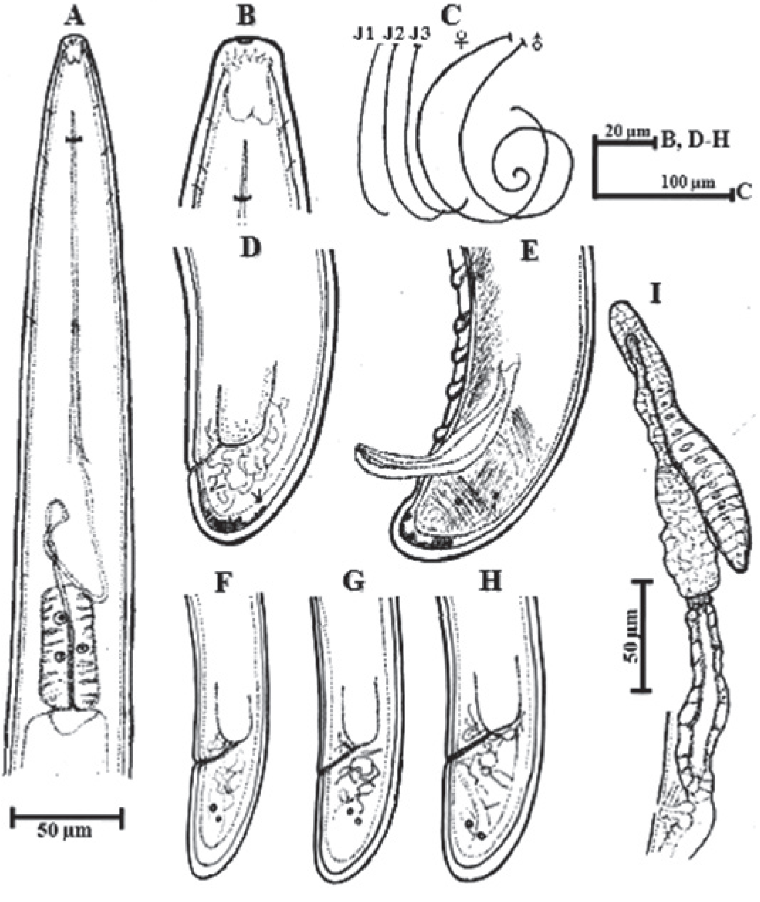

Figure 4. *Longidorus cheni* sp. n. *Female*: **A** Anterior region **B** Amphidial fovea shape **C** habitus **D** Tail region **I** Anterior genital branch. *Male*: **C** Habitus **E** Tail end. *Juveniles*: **C** Habitus **F–H** Posterior end of first-, second- and third- stage.

Type material. Holotype. Female slide no. LS5313 and paratypes (slides no. LS 5301–5312, LS 5314–5350) includes 12 females, 12 males and 52 juveniles deposited in the Nematode collection C602 Nematology laboratory of Zhejiang University, Hangzhou, China. One female, one male, three juveniles deposited at the nematode collection of the Institute of Biodiversity and Ecosystem Research, Bulgarian Academy of Sciences, Sofia, Bulgaria.

Etymology. The species is named after Prof. Pinsan Chen, Institute of Plant Protection, Chinese Academy of Agricultural Sciences, one of the pioneer plant nematologists in China.

Diagnosis and relationship. *Longidorus cheni* sp. n. is an amphimictic species characterized by females with medium body size (L = 4.1–6.6 mm), assuming G-shape, lip region 16–23 µm wide, posteriorly situated guide ring (at 70–93 µm from

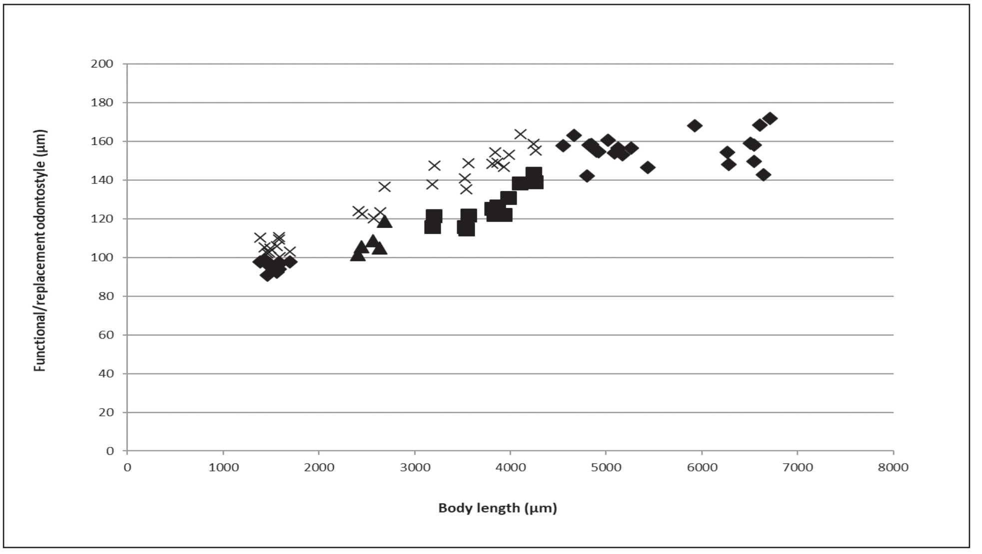

Figure 5. Scatter plot of odontostyle (◆, ▲, ■) and replacement odontostyle (×) against body length of *Longidorus cheni* sp. n. juveniles (J1 to J3) and (◆) adults.

anterior end), long odontostyle (142–168 μm), odontophore base slightly swollen, tail short (24–33 μm) and bluntly conoid to rounded. Males abundant, spicules 111–123 μm long, ventromedian supplements 10–14. Three juvenile stages present. The tail of the first stage juvenile conoid, tail shape in the second and third stage juveniles gradually becoming rounded. Finally, the species have specific ribosomal sequences KY284157 and KF270638 for D2–D3 expansion domains of 28S rDNA, KF261570 and MG656980 for the 18S rDNA region. The identification codes of *L. cheni* sp. n. based on the polytomous key by Chen et al. (1997) and additional codes (Peneva et al. 2013) are: A6-B3-C5-D12-E2-F3-G1-H1-I2-J2-K2.

Longidorus cheni sp. n. belongs to a group of species (*L. jonesi*-group) having guide ring at mid-odontostyle area (Xu et al. 2017) which consists of *L. diadecturus* Eveleigh & Allen, 1982, *L. fursti* Heyns, Coomans, Hutsebaut & Swart, 1987, *L. himalayensis* (Khan, 1986) Xu & Hooper, 1990, *L. ishigakiensis* Hirata, 2002, *L. jagerae* Heyns & Swart, 1998, *L. jonesi* Siddiqi, 1962, *L. juglans*, *L. laricis* Hirata, 1995, *L. litchii*, *L. macromucronatus* Siddiqi, 1962, *L. martini* Merny, 1966, *L. naganensis* Hirata, 1995, *L. orongorongensis* Yeates, Van Etteger & Hooper, 1992, and *L. waikouaitii* Yeates, Boag & Brown, 1997 (See Tables 3 and 4).

Longidorus cheni sp. n. morphologically is most similar to *L. naganensis* from which it can be distinguished by having different first stage juvenile tail (broadly rounded *vs* digitate with mucro (**c'** = 1.02–1.46 *vs* **c'** = 2.0–2.5), males abundant *vs* males absent (Hirata 1995). Furthermore, it can be differentiated from all other species belonging to this group. It differs from:

L. juglans by females having a longer odontostyle (143–168 *vs* 107–120 μm), different amphidial fovea shape (bilobed *vs* non-bilobed) (Xu et al. 2017);

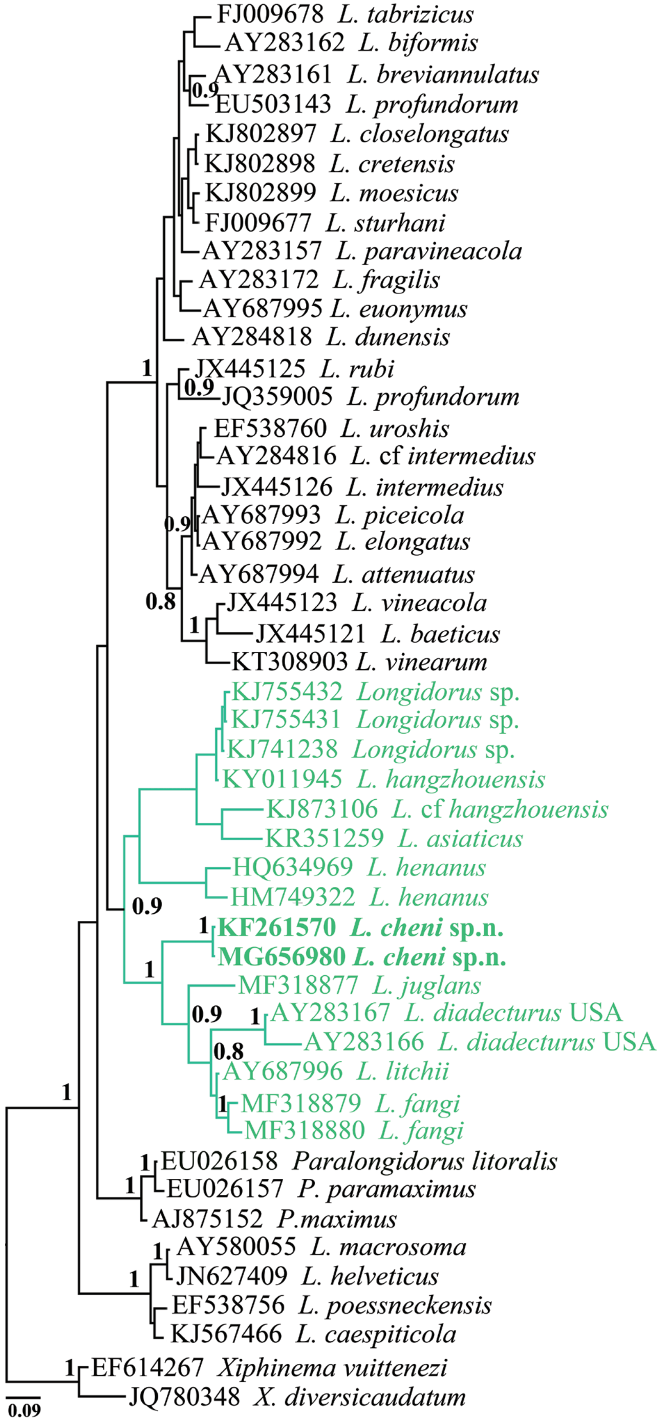

Figure 6. Phylogenetic tree using 18S rDNA and inferred from a Bayesian analysis with GTR+G model and *Xiphinema* spp. as an outgroup. Posterior probabilities ≥ than 0.8 are presented.

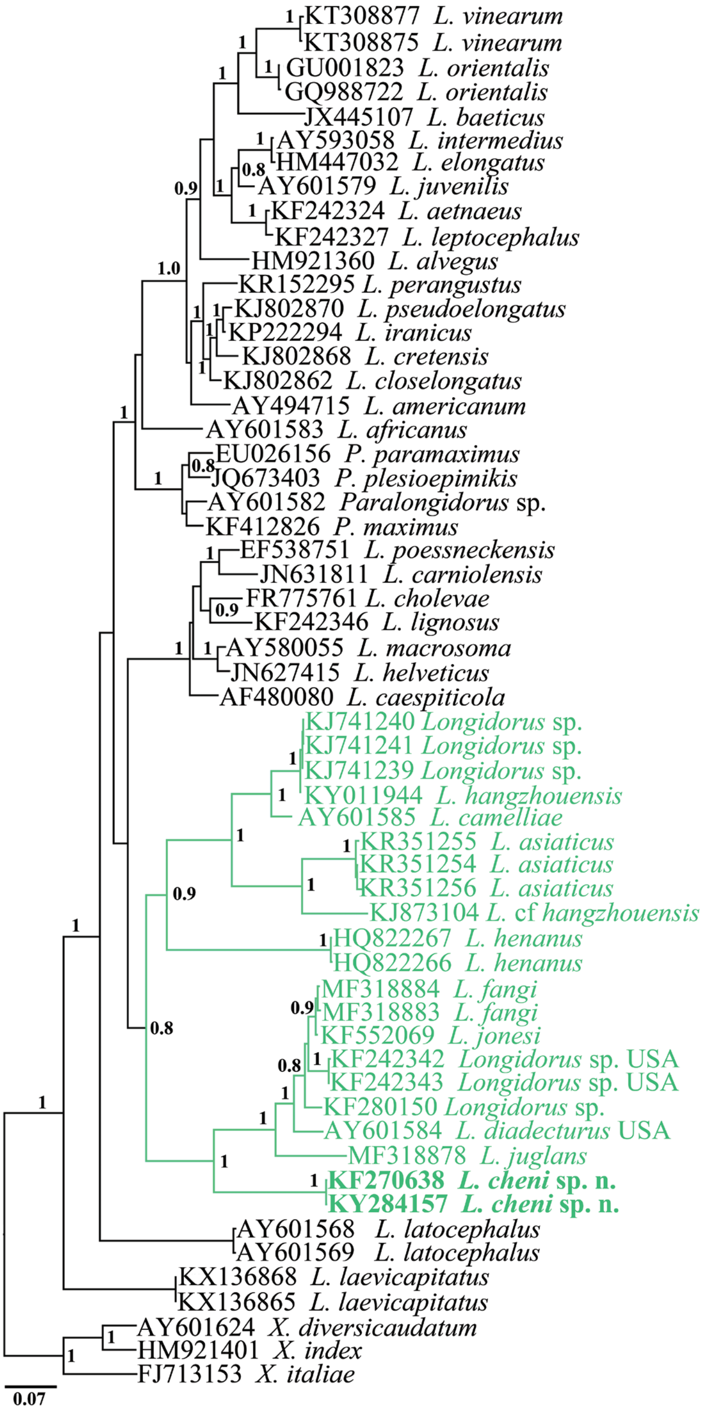

Figure 7. Phylogenetic tree using D2–D3 28S rDNA and inferred from a Bayesian analysis with GTR+G model and *Xiphinema* spp. as an outgroup. Posterior probabilities ≥ than 0.8 are presented.

Table 3. Partial polytomous key of *Longidorus* species with guide ring at mid-odontostyle area including *Longidorus cheni* sp. n. based on polydomous key of Chen et al. (1997), Loof and Chen (1999) and Peneva et al. (2013).

***Longidorus* species**	**A**	**B**	**C**	**D**	**E**	**F**	**G**	**H**	**I**	**J**	**K**
***L. cheni* sp. n.**	6	3	5	12	2	3	1	1	2	2	2
L. laricis	7	3	5	4	2	23	2	1	2	2	7
L. ishigakiensis	7	2	5	1	1	3	23	12	1	2	3
L. litchii	567	2	5	2	2	23	12	1	2	1	7
L. orongorongensis	67	4	5	1	4	34	2	1	2	1	12
L. naganensis	6	3	5	2	2	2(3)	1	1	1	2	7
L. fangi	56	3	5	23	5	23	2	12	1	1	56
L. juglans	5	23	5	1	1	23	1	1	2	2	23
L. jonesi	45	2	5	1	1	2	1	1	1	2	?
L. himalayensis	45	2	5	2	2	2	2	1	1	?	?
L. macromucronatus	45	3	5	3	1	2	2	1	1	1	56
L. waikouaitii	4	3	5	1	4	3	12	1	1	?	?
L. fursti	4	23	5	4	5	2	23	12	1	1	6
L. diadecturus	4	23	5	2	5	2	12	1	1	?	?
L. jagerae	34	2	5	4	1	2	2	12	1	?	?
L. martini	3	12	5	4	1	2	23	12	1	?	?

Note: A – odontostyle length; B – lip region diameter; C – distance of guide ring to anterior body length; D – shape of anterior region; E – amphidial fovea shape; F – body length; G – index "**a**"; H – tail shape; I – presence/absence of male; J – number of juvenile stages; K – tail shape in first stage juvenile.

Table 4. Morphometric comparisons of *Longidorus cheni* sp. n. and related *Longidorus* spp. with close morphological similarities based on polytomous key for identification of species (Cheng et al. 1997).

Species	**L (mm)**	**c'**	**Odontostyle length (μm)**	**Lip region width (μm)**	**Guide ring position (μm)**	**V**
L. cheni	**4.12–6.64**	**0.62–0.86**	**142–173**	**16–23**	**70–94**	**40–49.4**
L. laricis	4.65–5.97	0.64–0.9	160–183	16–18	84–100.5	45.8–51.2
L. ishigakiensis	5.31–6.85	1.0–1.2	158–181	13–14	83–95	45.4–51
L. litchii	4.14–5.29	0.61–0.79	138–171	12.5–14	82.5–96.5	49–54
L. orongorongensis	6.03–7.99	0.61–0.73	152–166	22–23	63–73	49–54
L. naganensis	3.83–5.18	0.69–0.89	141–160	16–18	77–89	47.1–54.3
L. fangi	4.6–5.52	0.75–1.12	124–144	16–18	69.5–87	48–55
L. juglans	3.90–5.25	0.6–0.9	125–140	14–18	69–78	47.1–50.7
L. macromucronatus	4–4.9	0.63–0.8	117–128	14*	58–68	43–47.8
L. himalayensis	3.42–3.9	0.7–0.8	115–125	15	55–60	47.4–50.1
L diadecturus	3.32–4.02	0.77–0.94	109–121	15–16	50–64	44–48
L. jonesi	3.17–3.8	0.6–0.87	107–120	23*	57–66	50.0–52.4
L. waikouaitii	6.44–7.17	0.51–0.74	113–117	16.5–17	56.5–59.5	48.6–53.1
L. jagerae	3.10–3.87	0.8–1.02	95–109	11.5–12.5	62–81	51.5–56.3
L. fursti	3.93–5.08	0.9–1.14	99.5–108	14.5–16	64–73	51.5–53.6
L. martini	2.9–4.5	1.3	83–96	11–13	51–66	52–56

*calculated from the original drawings.

L. laricis by females having a smaller **a** ratio (45.7–63.1 *vs* 83–108), males abundant *vs* males rare, longer spicules (101–124 *vs* 66.2 µm), different tail shape in J1 (conoid, **c'** = 1.02–1.46 *vs* elongate conoid with a digitate tip, **c'** = 1.8–2.4) (Hirata 1995);

L. litchii by females having a smaller **a** ratio (45.7–63.1 *vs* 72–84), wider lip region (17.5–23 *vs* 12.5–14 µm), smaller **V** ratio (40–49.4 *vs* 49–54), longer spicules (101–124 *vs* 68.5–71 µm), number of ventromedian supplements (10–14 *vs* 6–7), number of stages (3 *vs* 4), different tail shape in J1 (bluntly conoid, **c'** = 1.02–1.46 *vs* elongate conoid with a long digitate tip, **c'** = 2.72–3.42) (Xu and Cheng 1992), odontophore base (slightly *vs* strongly flanged (Zheng et al. 2002);

L. fangi by females having a smaller **a** ratio (45.7–63.1 *vs* 81–98), amphidial fovea shape (bilobed *vs* non-bilobed), longer odontostyle (142–168 *vs* 124–144 µm), lower **c'** ratio in J1 (**c'** = 1.02–1.46 *vs* **c'** = 1.58–2.2) (Xu and Cheng 1991);

L. fursti by females having a smaller **a** ratio (45.7–63.1 *vs* 105–137), wider lip region (17.5–23 *vs* 14.5–16 µm), different amphidial pouch shape (bilobed *vs* non-bilobed), longer odontostyle (142–168 *vs* 99.5–108 µm), smaller **V** ratio (40–49.4 *vs* 51.5–53.6), lower **c'** ratio in J1 (**c'** = 1.02–1.46 *vs* **c'** = 2.84–2.93) (Heyns et al. 1987);

L. himalayensis by females having a longer (L = 4.1–6.6 mm *vs* L = 3.42–3.9) and more plump body (**a** = 45.7–63.1 *vs* **a** = 97.8–112), a wider lip region (18–23 *vs* 14–15 µm), longer odontostyle (142–168 *vs* 115–125 µm), more posteriorly situated guide ring (70–91 *vs* 55–60 µm) (Khan 1986);

L. ishigakiensis by females having a smaller **a** ratio (45.7–63.1 *vs* 106–130), wider lip region (18–23 *vs* 13–14 µm), different amphidial pouch shape (bilobed *vs* non-bilobed), smaller **c'** ratio (**c'** = 0.62–0.86 *vs* **c'** = 1.0–1.2), different tail shape in J1 (bluntly conoid, **c'** = 1.02–1.46 *vs* rounded, **c'** = 1.9–2.5), males abundant *vs* males absent (Hirata 2002);

L. jagerae by females having a differently shaped lip region (not expanded *vs* expanded), more plump body (**a** = 45.7–63.1 *vs* **a** = 89–107), longer odontostyle (142–168 *vs* 95–109 µm), more anteriorly situated vulva (**V** = 40.0–49.4 *vs* **V** = 51.5–56.3), prerectal inclusions (absent *vs* present) (Heyns and Swart, 1998);

L. jonesi by females having a longer body (L = 4.1–6.6 *vs* L = 3.17–3.8 mm) and odontostyle (142–168 *vs* 107–120 µm), more posteriorly situated guide ring (70–91 *vs* 57–66 µm), more anteriorly situated vulva (**V** = 40.0–49.4 *vs* **V** = 50–52.4) (Siddiqi 1962);

L. martini by females having a longer body (L = 4.1–6.6 *vs* L = 3.18–4.29 mm) and odontostyle (142–168 *vs* 83–96 µm), more posteriorly situated guide ring (70–91 *vs* 51–66 µm), more anteriorly situated vulva (**V** = 40.0–49.4 *vs* **V** = 52–56) (Merny 1966);

L. diadecturus by females having a longer body (L = 4.1–6.6 *vs* L = 3.32–4.02 mm), odontostyle (143–168 *vs* 109–121 µm) and pharyngeal bulb (107–138 *vs* 62–83 µm), more posteriorly situated guide ring (70–91 *vs* 50–64 µm) (Eveleigh and Allen 1982);

L. orongorongensis by females having a shorter and more plump body (L = 4.1–6.6, **a** = 45.7–63.1 *vs* L = 6.0–8 mm, **a** = 81–106), more posterior guide ring position (70–91 *vs* 63–73 µm), smaller **V** ratio (40–49.4 *vs* 49–54), longer spicule (101–104 *vs* 84–87 µm) (Yeates et al. 1992);

L. macromucronatus by females having a plumper body (**a** = 45.7–63.1 *vs* **a** = 94–105), a wider lip region (17.5–23 *vs* 14 µm), longer odontostyle (142–173 *vs* 117–128 µm), 3 *vs* 4 juvenile stages, differently shaped tail in J1 (broadly conoid *vs* sub-digitate **c'** = 1.02–1.46 *vs* **c'** = 0.63–0.8) (Siddiqi 1962);

L. waikouaitii by having differently shaped amphidial fovea (pocket shaped, bilobed at the base *vs* funnel shaped), a longer odontostyle (142–173 *vs* 113–117 µm), more posterior position of the guide ring (70–91 *vs* 56.5–59.5 µm), males abundant *vs* males absent (Yeates et al. 1997).

Discussion

Our findings on the morphology and genetics of *L. cheni* sp. n. are in agreement with the hypothesis about the common origin of *Longidorus* species having a guide ring at the mid-odontostyle area (Xu et al. 2017); furthermore, these species have the odontophore base slightly or strongly flanged (with exception of the species from New Zealand) and bluntly rounded to a hemispherical tail (code H1(2)). More than half of the species of this group with known juveniles develops through three stages (the only exception is *L. litchii*), all of them occurring in South East Asia (Table 4). This shows a characteristic biogeographical pattern of *Longidorus jonesi*-group being spread in South East Asia (China and Japan, eight species), North India (three), New Zealand (two), South Africa (SA, Rhodesia, three), North America (Canada, USA, two), and only one species (*L. jonesi*) reported from two regions (India, Japan). The highest number of species in South East Asia suggests this region as a probable centre of origin of *Longidorus jonesi*-group.

Acknowledgements

This research was supported by the National Natural Science Foundation of China (No 31772137) and Sino-Bulgaria government cooperation project (No. 14-7 and ДНТС Китай 01/03). The authors are grateful to the reviewers for their thorough revision, useful comments, and remarks.

References

Archidona-Yuste A, Navas-Cortes JA, Cantalapieda-Navarette C, Palomares-Ruis JE, Castillo P (2016) Unravelling the biodiversity and molecular phylogeny of needle nematodes of the genus *Longidorus* (Nematoda:Longidoridae) in olive and description of six new species. PloS ONE 11. https://doi.org/10.1371/journal.pone.0147689

Chen Q, Hooper D, Loof PAA, Xu J (1997) A revised polytomous key for the identification of species of the genus *Longidorus* Micoletzky, 1922 (Nematoda: Dorylaimoidea). Fundamental and Applied Nematology 20: 15–28.

De Grisse AT (1969) Redescription ou modification de quelques techniques utilisées dans l'étude des nematodes phytoparasitaires. Mededelingen van de Rijksfaculteit der Landbouwwetenschappen Gent 34: 351–369.

De Ley P, Félix M-A, Frisse LM, Nadler SA, Sternberg PW, Thomas WK (1999) Molecular and morphological characterisation of two reproductively isolated species with mirror-image anatomy (Nematoda: Cephalobidae). Nematology 1: 519–612.

De Man JG (1876) Onderzoekingenover vrij in de aardelevnde Nematoden. Tijdschrift der Nederlandsche dierkundige Vereeniging 2: 78–196.

Eveleigh ES, Allen WR (1982) Description of *Longidorus diadecturus* (Nematoda: Longidoridae), a vector of the peach rosette mosaic virus in peach orchards in southwestern Ontario, Canada. Canadian Journal of Zoology 60: 112–115. https://doi.org/10.1139/z82-014

Guo K, Shi HL, Liu K, Zheng JW (2011) Past and present distribution and host of *Longidorus* (Nematoda: Dorylaimida) in mainland China. Zootaxa 3088: 27–38.

Gutiérrez-Gutiérrez C, Palomares-Rius JE, Cantalapiedra-Navarrete C, Landa BB, Castillo P (2011). Prevalence, polyphasic identification, and molecular phylogeny of dagger and needle nematodes infesting vineyards in southern Spain. European Journal of Plant Pathology 129: 427–453. https://doi.org/10.1007/s10658-010-9705-y

Gutiérrez-Gutiérrez C, Cantalapiedra-Navarrete C, Monte-Borrego M, Palomares-Rius JE, Castillo P (2013) Molecular phylogeny of the nematode genus *Longidorus* (Nematoda: Longidoridae) with description of three new species. Zoological Journal of the Linnean Society 167: 473–500. https://doi.org/10.1111/zoj.12019

Heyns J, Coomans A, Hutsebaut M, Swart A (1987) *Longidorus fursti* n. sp. from South Africa with a discussion of its relationships (Nematoda: Longidoridae). Revue de Nématologie 10: 381–385.

Heyns J, Swart A (1998) *Longidorus jagerae* sp. n., another longidorid specie with globular inclusions in the prerectum (Nematoda: Longidoridae). Koedoe 41: 31–36. https://doi.org/10.4102/koedoe.v41i1.243

Hirata K (1995) Descriptions of Two New Species of *Longidorus* (Dorylaimida: Longidoridae) from Nagano, Japan. Japanese Journal of Nematology 25: 33–43. https://doi.org/10.3725/jjn1993.25.1_33

Hirata K (2002) Description of a new species of *Longidorus* (Dorylaimida: Longidoridae) from Ishigaki Is., Japan. Japanese Journal of Nematology 32: 1–6. https://doi.org/10.3725/jjn1993.32.1_1

Huelsenbeck JP, Ronquist F (2001) MRBAYES: Bayesian inference of phylogenetic trees. Bioinformatics 17: 754–755. https://doi.org/10.1093/bioinformatics/17.8.754

Khan E (1986) One new genus and four new species in the superfamily Longidoroidea (Nematoda). Indian Journal of Nematology 16: 195–193.

Kumar S, Stecher G, Tamura K (2016) MEGA7: Molecular Evolutionary Genetics Analysis version 7.0 for bigger datasets. Molecular Biology and Evolution 33: 1870-1874. https://doi.org/10.1093/molbev/msw054

Lazarova S, Peneva V, Kumari S (2016) Morphological and molecular characterisation, and phylogenetic position of *X. browni* sp. n., *X. penevi* sp. n. and two known species of *Xiphinema americanum*-group (Nematoda, Longidoridae). ZooKeys 574: 1–42. https://doi.org/10.3897/zookeys.574.8037

Loof PAA, Chen Q (1999) A revised polytomous key for the identification of species of the genus *Longidorus* Micoletzky, 1922 (Nematoda: Dorylaimoidea). Supplement 1. Nematology 1 (1): 55–59. https://doi.org/10.1163/156854199507974

Merny G (1966) Nématodes d'Afrique tropicale: un nouveau *Paratylenchus* (Criconematidae), deux nouveaux *Longidorus* et observations sur *Longidorus laevicapitatus* Williams, 1959 (Dorylaimidae). Nematologica 12: 385–395. https://doi.org/10.1163/187529266X00860

Peneva V, Lazarova S, De Luca F, Brown DJF (2013) Description of *Longidorus cholevae* sp. n. (Nematoda, Dorylaimida) from riparian habitat in the Rila Mountains, Bulgaria. ZooKeys 330: 1–26. https://doi.org/10.3897/zookeys.330.5750

Ronquist F, Teslenko M, van der Mark P, Ayres DL, Darling A, Höhna S, Larget B, Liu L, Suchard MA, Huelsenbeck JP (2012) MrBayes 3.2: Efficient Bayesian Phylogenetic Inference and Model Choice across a Large Model Space. Systematic Biology 61: 539–542. https://doi.org/10.1093/sysbio/sys029

Sela I, Ashkenazy H, Katoh K, Pupko T (2015) GUIDANCE2: accurate detection of unreliable alignment regions accounting for the uncertainty of multiple parameters. Nucleic Acids Research 43 (Web Server issue): W7–W14. https://doi.org/10.1093/nar/gkq443

Seinhorst W (1959) A rapid method for the transfer of nematodes from fixative to anhydrous glycerin. Nematologica 4: 67–69.

Siddiqi MR (1962) Studies on the genus *Longidorus* Micoletzky, 1922 (Nematoda: Dorylaimoidea), with descriptions of three new species. Proceeding of the Helminthological Society of Washington 29: 177–188.

Sturhan D (2014) Plant-parasitic nematodes in Germany – an annotated checklist. Soil organisms 86: 177–198.

Tanha Maafi Z, Subbotin SA, Sturhan D, Baroti Sh, Taher ZM (2015) Characterisation of *Longidorus iranicus* Sturhan & Barooti, 1983 (Nematoda: Longidoridae) from Iran and synonymisation of *L. moesicus* Lamberti, Choleva & Agostinelli, 1983 Russian. Journal of Nematology 23: 21–28.

Triscuizzi N, Archidona-Yuste A, Troccoli A, Fanelli E, De Luca F, Vovlas N, Castillo P (2015) Description of new needle nematode *Longidorus asiaticus* n. sp. (Nematoda: Longidoridae) from rhizosphere of crape myrtle (*Lagerstroemia indica*) bonsai trees imported into Italy from China. European Journal of Plant Pathology 143: 567–580. https://doi.org/10.1007/s10658-015-0710-z

Xu J, Cheng H (1991) A new species of *Longidorus* (Nematoda: Longidoridae). Journal of Nanjing Agriculture University 14: 38–42.

Xu J, Cheng H (1992) *Longidorus litchii* n. sp. and *L. henanus* n. sp. (Nemata: Longidoridae) from China. Fundamental and Applied Nematology 15: 517–523.

Xu J, Hooper DJ (1990) Observations on some species of *Longidorus* (Nematoda: Longidoridae) from Jiangsu Province, China, with a description of *Longidorus jiangsuensis* n. sp. Revue de Nématologie 13: 323–330.

Xu Y, Guo K, Ye W, Wang J, Zheng J, Zhao Z (2017) Morphological and molecular characterization of *Longidorus juglans* sp. nov. and a sister species *L. fangi* Xu & Cheng, 1991 from China. Nematology 19: 951–970. http://dx.doi.org/10.1163/15685411-00003099

Yeates GW, Van Etteger M, Hooper D (1992) *Longidorus orongorongensis* n. sp. (Nematoda: Dorylaimida) from subsoil of conifer/broadleaved forest. New Zealand Journal of Zoology 19: 25–31. http://dx.doi.org/10.1080/03014223.1992.10423248

Zheng J, Pan C, Furlanetto C, Neilson R, Brown DJF (2002) The morphology of odontophore of *Longidorus litchii* Xu & Cheng, 1992 (Nematoda; Longidoridae). Russian Journal of Nematology 10: 123–126.

Zheng J, Peneva V, Brown DJF (2000) *Longidorus camelliae* n. sp. (Nematoda: Longidoridae) associated with ornamental cultivars of *Camellia japonica* L. growing in a nursery at Fuyang, Zhejiang Province, Eastern China. Systematic Parasitology 47: 119–125. https://doi.org/10.1023/A:1006482322716

Zheng J, Peng D, Robbins RT, BrownDJF (2001) Description of *Longidorus hangzhouensis* sp. n. (Nemata: Longidoridae) from Zhejiang province, new geographical records of *L. henanus* Xu & Cheng, 1992, and an identification key for *Longidorus* species occurring in China. Nematology 3: 219–227. http://dx.doi.org/10.1163/156854101750413298

ZooKeys 744: 19–41 (2018)
doi: 10.3897/zookeys.744.22970
http://zookeys.pensoft.net

RESEARCH ARTICLE

A peer-reviewed open-access journal
ZooKeys
Launched to accelerate biodiversity research

The genus *Paleosepharia* Laboissière, 1936 in Taiwan: review and nomenclatural changes (Coleoptera, Chrysomelidae, Galerucinae)

Chi-Feng Lee[1]

1 *Applied Zoology Division, Taiwan Agricultural Research Institute, 189 Chung-Cheng Road, Wufeng, Taichung 413, Taiwan*

Corresponding author: *Chi-Feng Lee* (chifeng@tari.gov.tw)

Academic editor: *A. Eben* | Received 13 December 2017 | Accepted 1 March 2018 | Published 19 March 2018

*http://zoobank.org/*0676B41B-F28B-4206-8B88-FC39B0F2A196

Citation: Lee C-F (2018) The genus *Paleosepharia* Laboissière, 1936 in Taiwan: review and nomenclatural changes (Coleoptera, Chrysomelidae, Galerucinae). ZooKeys 744: 19–41. https://doi.org/10.3897/zookeys.744.22970

Abstract
Taxonomic study of species of the genus *Monolepta* Chevrolat, 1836 with subscutellar incised ridges in males and occurring in Taiwan resulted in the transfer of all species to *Paleosepharia* Laboissière, 1936: *P. amiana* (Chûjô, 1962), **comb. n.,** *P. formosana* (Chûjô, 1935), **comb. n.,** *P. nantouensis* (Kimoto, 1996) **comb. n.**, and *P. yasumatsui* (Kimoto, 1969), **comb. n.** The position of *M. excavata* Chûjô, 1938 in *Paleosepharia* is confirmed. Lectotypes are designated for *M. excavata* Chûjô, 1938 and *M. formosana* Chûjô, 1935. Generic characters of *Paleosepharia* are re-evaluated in the context of these nomenclatural changes.

Keywords
Food plants, leaf beetles, new combination, taxonomic revision

Introduction

Members of the genus *Paleosepharia* Laboissière resemble those of *Monolepta* Chevrolat, but both genera can be separated externally by specific structures of the elytral epipleuron and the sexually dimorphic elytra. The epipleuron is abbreviated or suddenly narrowed before the middle, and subscutellar bulges or incised ridges are absent from the elytra in both sexes of *Monolepta*. In contrast the epipleuron continues to the apex, and subscutellar bulges or incised ridges are present on the elytra in males of *Paleose-*

pharia (Mohamedsaid 1996; Wagner and Bieneck 2012; Medvedev 2014; Rizki et al. 2014, 2016). In addition, some additional genitalic characters were proposed for *Paleosepharia* by Rizki et al. (2016). Taxonomic status of some species of *Monolepta* should be re-evaluated in cases where they were described based only on female specimens because important sexually dimorphic diagnostic characters may have been excluded. *Paleosepharia* comprises 76 species and one subspecies in the Oriental and Palaearctic regions (Nie et al. 2017)

Among the 30 species of *Monolepta* described from Taiwan so far (Kimoto and Takizawa 1997), *M. excavata* Chûjô, 1938 was transferred *Paleosepharia* by Gressitt and Kimoto (1963), but that transfer was not followed by subsequent taxonomists except Beenen (2010). Some species of *Monolepta* in Taiwan could be members of *Paleosepharia* but their diagnostic characters are unclear due to insufficient material. Extensive collections have been conducted by the Taiwan Chrysomelid Research Team (TCRT) since 2007, resulting in the publication of several books and many taxonomic and nomenclatural changes, including the study reported here (Lee and Cheng 2007, 2010; Lee et al. 2016). Five Taiwanese species of *Monolepta* possess subscutellar incised ridges in males, including *M. amiana* Chûjô, 1962, *M. excavata* Chûjô, 1938, *M. formosana* Chûjô, 1935, *M. nantouensis* Kimoto, 1996, and *M. yasumatsui* Kimoto, 1969. In the study reported here, the status of these species are revaluated and genitalic characters proposed by Rizki et al. (2016) are compared with other members of the genus and those of *Paleosepharia*.

Materials and methods

The abdomens of adults were separated from the forebody and boiled in 10 % KOH solution, followed by washing in distilled water to prepare genitalia for illustrations. The genitalia were then dissected from the abdomen, mounted on slides in glycerin, and studied and drawn using a Leica M165 stereomicroscope. For detailed examinations a Nikon ECLIPSE 50i microscope was used.

At least three pairs from each species were examined to delimit variability of diagnostic characters. For species collected from more than one locality, at least one pair from each locality was examined. Length was measured from the anterior margin of the eye to the elytral apex, and width at the greatest width of the elytra.

Specimens studied herein are deposited at the following institutes and collections:

KMNH Kitakyushu Museum of Natural History and Human History, Kitakyushu, Japan [Yûsuke Minoshima];
KUEC Faculty of Agriculture, Kyushu University, Fukuoka, Japan [Osamu Tadauchi];
NMNS National Museum of Natural Science, Taichung, Taiwan [Ming-Luen Jeng];
SDEI Senckenberg Deutsches Entomologisches Institut, Müncheberg, Germany [Kostantin S. Nadein];
TARI Taiwan Agricultural Research Institute, Taichung, Taiwan

Exact label data are cited for all type specimens of described species; a double slash (//) divides the data on different labels and a single slash (/) divides the data in different rows. Other comments and remarks are in square brackets: [p] – preceding data are printed, [h] – preceding data are handwritten, [w] – white label, [y] – yellow label, [b] – blue label, and [r] – red label.

Systematics

***Paleosepharia amiana* (Chûjô), comb. n.**
Figs 1A–1C, 2

Monolepta amiana Chûjô, 1962: 136 (Taitung); Kimoto 1969: 47 (Nantou); Kimoto 1991: 13 (Kaohsiung); Kimoto and Chu 1996: 78 (catalogue); Kimoto and Takizawa 1997: 385 (catalogue); Beenen 2010: 482 (catalogue); Yang et al. 2015: 266 (catalogue); Lee et al. 2016: 108 (food plants).

Type material. Depository of the single female holotype is unknown. Chûjô (1962) indicated that most specimens were deposited at the TARI except for some in his collection. Although some specimens were found at the KUEC, the type of this species was not among them.

Other material examined (n = 82). Pingtung: 1♀ (TARI), Jinshuiying [浸水營], 12.VIII.2010, leg. J.-C. Chen; 1♀, Tahanshan [大漢山], 4.X.2010, leg. J.-C. Chen; 6♀♀ (TARI), same locality, 22.IX.2011, leg. J.-C. Chen; 3♂♂, 11♀♀ (TARI), same locality, 3.IX.2012, leg. Y.-T. Chung; 1♂ (TARI), same locality, 13.IX.2012, leg. J.-C. Chen; 1♂, 1♀ (TARI), same locality, 14.IX.2012, leg. Y.-T. Chung; 1♂ (TARI), same locality, 30.VII.2013, leg. B.-X. Guo; 1♀ (TARI), same locality, 17.VIII.2013, leg. J.-C. Chen; 1♂, 2♀♀ (TARI), same locality, 3.IX.2013, leg. Y.-T. Chung; 7♀♀ (TARI), same locality, 11.IX.2013, leg. Y.-T. Chung; 2♂♂, 8♀♀ (TARI), same locality, 24.IX.2013, leg. Y.-T. Chung; 2♂♂, 3♀♀ (TARI), same locality, 1.X.2013, leg. Y.-T. Chung; 1♀ (TARI), same locality, 8.X.2013, leg. Y-T. Chung; 4♀♀ (TARI), same locality, 25.X.2013, leg. Y.-T. Chung; 1♀ (TARI), same locality, 16.XII.2013, leg. Y.-T. Chung; 2♂♂ (TARI), same locality, 19.VII.2014, leg. W.-C. Liao; 2♀♀ (TARI), same locality, 17.VI.2016, leg. Y.-T. Chung; 1♂ (TARI), same locality, 6.VIII.2016, leg. Y.-T. Chung; **Taipei**: 2♀♀ (TARI), Manyuehyuan [滿月圓], 3.VII.2010, leg. H. Lee; 1♀ (TARI), same but with "8.VII.2010"; 1♀ (TARI), same but with "8.IV.2010"; 1♀ (TARI), same but with "7.VIII.2014"; **Taitung**: 2♀♀ (TARI), Lichia trail [利嘉林道], 15.VII.2014, leg. Y.-T. Chung; 1♂ (TARI), same locality, 17.VII.2014, leg. Y.-T. Wang; 1♀ (TARI), same locality, 25.VII.2015, leg. Y.-T. Chung, P.-H. Kuo & S.-P. Wu; 1♂ (TARI), same locality, 1.VII.2016, B.-X. Guo; **Taoyuan**: 2♀♀ (TARI), Hsiaowulai [小烏來], 29.IX.2009, leg. M.-H. Tsou; 4♀♀ (TARI), same locality, 10.X.2009, leg. M.-H. Tsou; 1♂, 1♀ (TARI), Sankuang [三光], 14.VII.2010, leg. H. Lee.

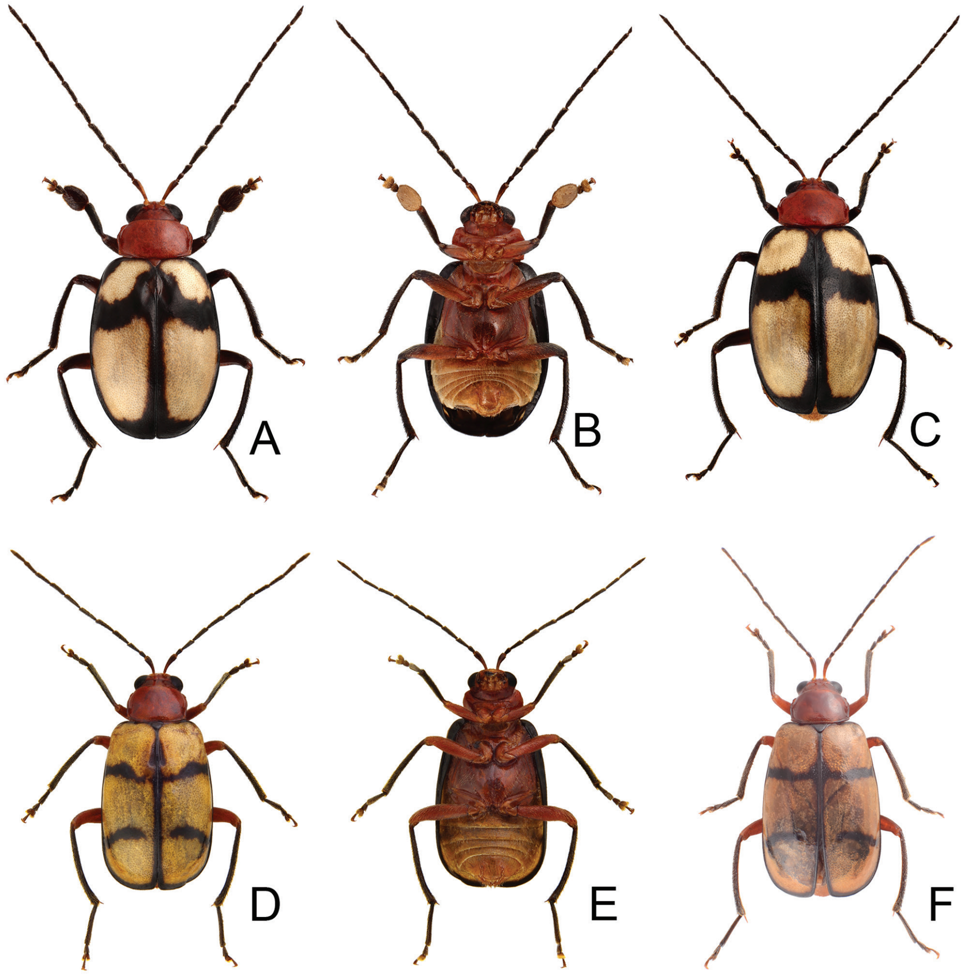

Figures 1. Habitus of *Paleosepharia* species. **A** *P. amiana* (Chûjô), male, dorsal view **B** Ditto, ventral view **C** *P. amiana* (Chûjô), female, color variation, dorsal view **D** *P. excavata* (Chûjô), male, dorsal view **E** Ditto, ventral view **F** *P. excavata* (Chûjô), female, dorsal view.

Diagnosis. Members of *Paleosepharia* amiana are similar to those of *P. excavata*, *P. formosana*, and *P. yasumatsui* with black stripes along the outer margins of yellow elytra. However, this species is easily recognized by the presence of only one transverse black band on the elytra (two transverse bands in others). The aedeagus of male *P. amiana* is similar to that of *P. nantouensis* in possessing a relatively narrow penis (more than 6.5 times longer than wide; less than 6.0 times in other species), acute apex of tectum (bifurcate apex in other species), and one pair of elongate and apically curved spiculae (lacking such spiculae in other species). It differs by the broader tectum (broader than penis; narrower than penis in *P. nantouensis*) and different sizes of the two pairs of hooked spiculae (same sizes in *P. nantouensis*).

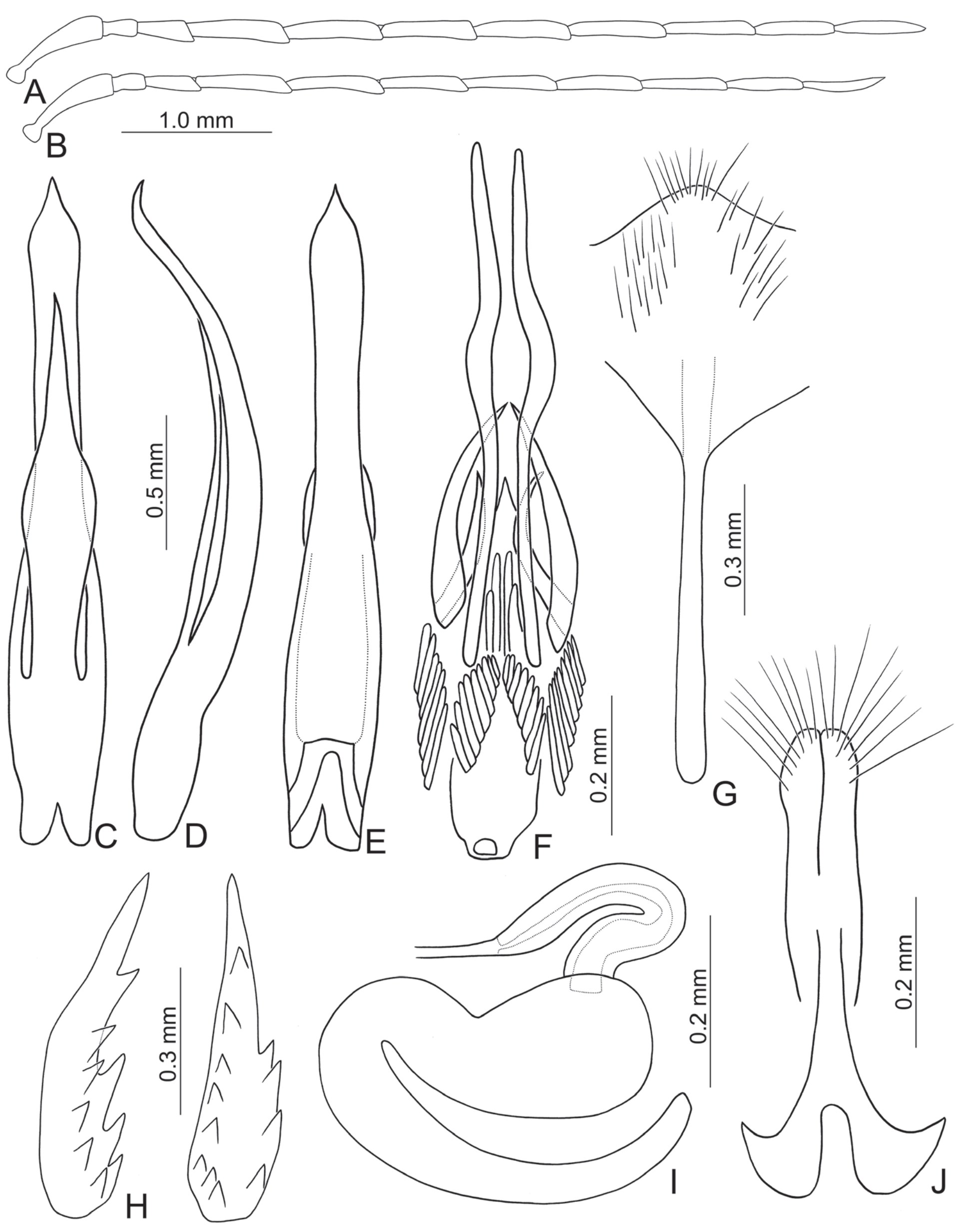

Figures 2. Diagnostic characters of *Paleosepharia amiana* (Chûjô). **A** Antenna, male **B** Antenna, female **C** Penis, dorsal view **D** Penis, lateral view **E** Penis, ventral view **F** Endophallic spiculae **G** Abdominal ventrite VIII **H** Bursa sclerites, left sclerite in lateral view, right sclerite in dorsal view **I** Spermatheca **J** Gonocoxae.

Description. Males. Length 6.0–6.5 mm, width 3.3–3.4 mm. General color reddish brown (Fig. 1A–1B); antennae except two basal antennomeres, scutellum, tibiae, and tarsi black; elytra yellow, with wide black stripe along lateral margins and suture extending to apex, and one transverse, wide black band at basal 2/3. Antenna (Fig. 2A) filiform, ratio of length of antennomeres I to XI 1.0 : 0.3 : 0.5 : 0.9 : 0.9 : 0.9 : 0.9 : 0.9 : 0.8 : 0.7 : 0.8; ratio of length to width from antennomere I to XI 4.6 : 1.9 : 2.8 : 5.0 : 5.1 : 5.1 : 5.7 : 6.0 : 6.5 : 5.7 : 7.1. Pronotum 1.86–1.97 times wider than long; lateral margins slightly curved, basal margin slightly curved, apical margin slightly concave; disc with reticulate microsculpture and dense, minute punctures. Elytra 1.34–1.45 times longer than wide; lateral margins curved, widest behind middle; disc with one pair of oblique depressions starting from suture at scutellum, longitudinal ridge present inside each depression and along suture; disc with dense, minute punctures; apex truncate. First tarsomeres of front legs strongly swollen and dorso-ventrally flattened. Penis (Fig. 2C–E) extremely slender, 7.3 times longer than wide; parallel-sided, basally widened from middle, apically tapering; tectum elongate from basal 1/4 to apical 1/5, widest at midpoint and wider than penis, apically tapering, apex acute; moderately recurved at middle and near apex in lateral view; ventral surface with lateral areas membranous. Endophallic spiculae complex (Fig. 2F) with one pair of extremely elongate spiculae, apices curved at middle; two pairs of elongate hooked spiculae, one pair longer and curved inwards, the other pair shorter and curved outwards; one pair of longitudinal rows of elongate, apically curved setae near base; one row of elongate, apically tapering setae at sides behind middle.

Females. Length 5.6–6.5 mm, width 3.3–3.5 mm. Similar to male (Fig. 1C) but elytra lacking oblique depressions; first tarsomeres of front legs normal; ratio of length of antennomeres I to XI (Fig. 2B) 1.0 : 0.3 : 0.5 : 0.9 : 0.9 : 0.8 : 0.9 : 0.8 : 0.8 : 0.7 : 0.7; ratio of length to width from antennomere I to XI 4.8 : 2.0 : 3.7 : 5.6 : 5.6 : 5.9 : 6.7 : 6.2 : 7.2 : 6.4 : 6.7. Gonocoxae (Fig. 2J) slender, tightly conjunct from apical 1/3 to base; each gonocoxa with eight setae from apical 1/6 to apex, apex truncate. Ventrite VIII (Fig. 2G) weakly sclerotized except apex, with several short setae at apex, and several long setae at sides, spiculum elongate. Spermathecal receptaculum (Fig. 2I) swollen; pump extremely slender and curved; sclerotized spermathecal duct slender. Bursa sclerites (Fig. 2H) elongate and apically tapering, with stout teeth along lateral margin at base; slightly curved in lateral view.

Food plants. Melastomataceae: *Blastus cochinchinensis* Lour.; Sapindaceae: *Koelreuteria henryi* Dummer; Fagaceae: *Castanopsis formosana* (Skan) Hayata (Lee et al. 2016).

Distribution. Endemic to Taiwan.

***Paleosepharia excavata* (Chûjô)**

Figs 1D–F, 3

Monolepta excavata Chûjô, 1938 (Taiwan: Ilan, Nantou, Hualien): 144; Chûjô 1962: 114 (redescription); Chûjô 1965: 96 (Nantou); Kimoto 1969: 47 (Taichung, Nantou); Kimoto 1986: 58 (Nantou); Kimoto 1989: 254 (Taitung); Kimoto 1991: 14 (Taoyuan); Kimoto and Chu 1996: 79 (catalogue); Kimoto and Takizawa 1997: 385 (catalogue); Lee and Cheng 2010: 101 (food plants); Yang et al. 2015: 268 (catalogue).

Paleosepharia excavata: Gressitt and Kimoto 1963: 646; Beenen 2010: 485 (catalogue).
Paleosepharia polychroma Laboissière, 1938: 8 (China: Jiangsu, Jiangxi); Gressitt and Kimoto 1963: 646 (as synonym of *P. excavata*).

Type material. *Monolepta excavata*. Lecotype ♂ (TARI), here designated, labeled: "Taiheizan [= Taipingshan, 太平山] / 23-V-1931 / Col. R. Takahashi [p, w] // CO / Type [p, y, circular label with yellow border] // *Monolepta* / *excavata* / Chûjô [h] // DET. M. CHUJO [p, w] // 2193 [p, w]". Paralectotypes. 1♂ (TARI): "Horisha [= Puli, 埔里] / 12/V/1913 [h] / Col. M. Maki [p, w] // CO / Type [p, y, circular label with yellow border] // *Monolepta* / *excavata* / Chûjô [h] // DET. M. CHUJO [p, w] // 2194 [p, w]"; 1♂, 1♀ (TARI): "Kuaru [h] [unknown] / FORMOSA [p] / 20.VI.1937 [h] / COL. M. CHUJO [p, w] // CO / Type [p, y, circular label with yellow border] // *Monolepta* / *excavata* / Chûjô [h] // DET. M. CHUJO [p, w] // No. 1640 or 1346 [p, w]"; 1♀ (TARI): "Formosa / Musha, [= Wushe, 霧社] 1919 / V.18-VI.15. / T. Okuni [p, w] // CO / Type [p, y, circular label with yellow border] // *Monolepta* / *excavata* / Chûjô [h] // DET. M. CHUJO [p, w] // 1396 [p, w]"; 1♀ (TARI): "18/IV/1910 / Kanmon [h] [= Kuangman, 關門] / Col. I. Nitobe [p, w] // CO / Type [p, y, circular label with yellow border] // *Monolepta* / *excavata* / Chûjô [h] // DET. M. CHUJO [p, w] // 1973 [p, w]"; 1♀ (SDEI): "Formosa / Karenko [= Hualien, 花蓮], -19. / VII 20-VIII 4. / T. Okuni [p, w] // *Monolepta* / *excavata* / Chûjô [h] // DET. M. CHUJO [p, w] // 1973 [p, w] // Syntypus [p, r]".

Paleosepharia polychroma. The syntypes at the Institute Royal des Sciences Naturelles de Belgique, Bruxelles, and the Naturhistoriska Riksmuseet, Stockholm were not studied. *Paleosepharia* polychroma could be a distinct species because of slight difference of color patterns on the elytra between both species. Correctly assessing the status of this species requires further study.

Other material examined (n = 72). Chiayi: 1♂ (TARI), Alishan [阿里山], 5–9.VII.1981, leg. L. Y. Chou & S. C. Lin; **Hsinchu**: 1♂ (TARI), Kuanwu [觀霧], 6.IV.2010, leg. L.-H. Sun; 1♂ (TARI), same locality, 30.IV.2010, leg. M.-H. Tsou; 1♀ (TARI), Litungshan [李棟山], 6.VI.2010, leg. Y.-L. Lin; 1♂ (TARI), Mamei [馬美], 4.V.2008, leg. S.-F. Yu; 3♀♀ (TARI), same locality, 18.V.2008, leg. M.-H. Tsou; 1♂ (TARI), Talu trail [大鹿林道], 19.VI.2010, leg. Y.-L. Lin; 1♀ (TARI), same locality, 11.VII.2016, leg. H. Lee; **Hualien**: 1♂, 1♀ (TARI), Hsinpaiyang [新白陽], 15–20.X.2007, leg. Y.-F. Hsu; 1♀ (TARI), Huitouwan [迴頭灣], 10.VII.2007, leg. C.-F. Lee; 1♂, 1♀ (TARI), Wanjung [萬榮], 11.VI.2011, leg. M.-H. Tsou; **Ilan**: 1♀ (TARI), Chinyang [金洋], 23.X.2011, leg. C.-H. Hsieh; 1♀ (NMNS), Tsuifenghu [翠峰湖], 21.VI.1992, leg. C. Y. Li; 1♂ (NMNS), Taipingshan [太平山], 8.III.1989, leg. K. W. Huang; 1♂, 3♀♀ (TARI), same locality, 17.VIII.2007, leg. Y.-C. Chang; **Nantou**: 1♂ (NMNS), Aowanta [奧萬大], 9.IX.2008, leg. C. C. Lai; 1♂ (TARI), Fenghuangshan [鳳凰山], 10.V.2010, leg. Y.-T. Wang; 1♀ (TARI), Hoshe [和社], 23.I.2014, leg. H.-T. Yeh; 1♂ (TARI), Huakang [華岡], 13.IX.2010, leg. C.-F. Lee; 1♀ (TARI), Meifeng [梅峰], 20–22.VI.1979, leg. K. S. Lin & B. H. Chen; 1♀ (NMNS), same locality, 24.IX.1997, leg. W. T. Yang; 1♂ (NMNS), Oiwake [= Tsuifeng, 翠

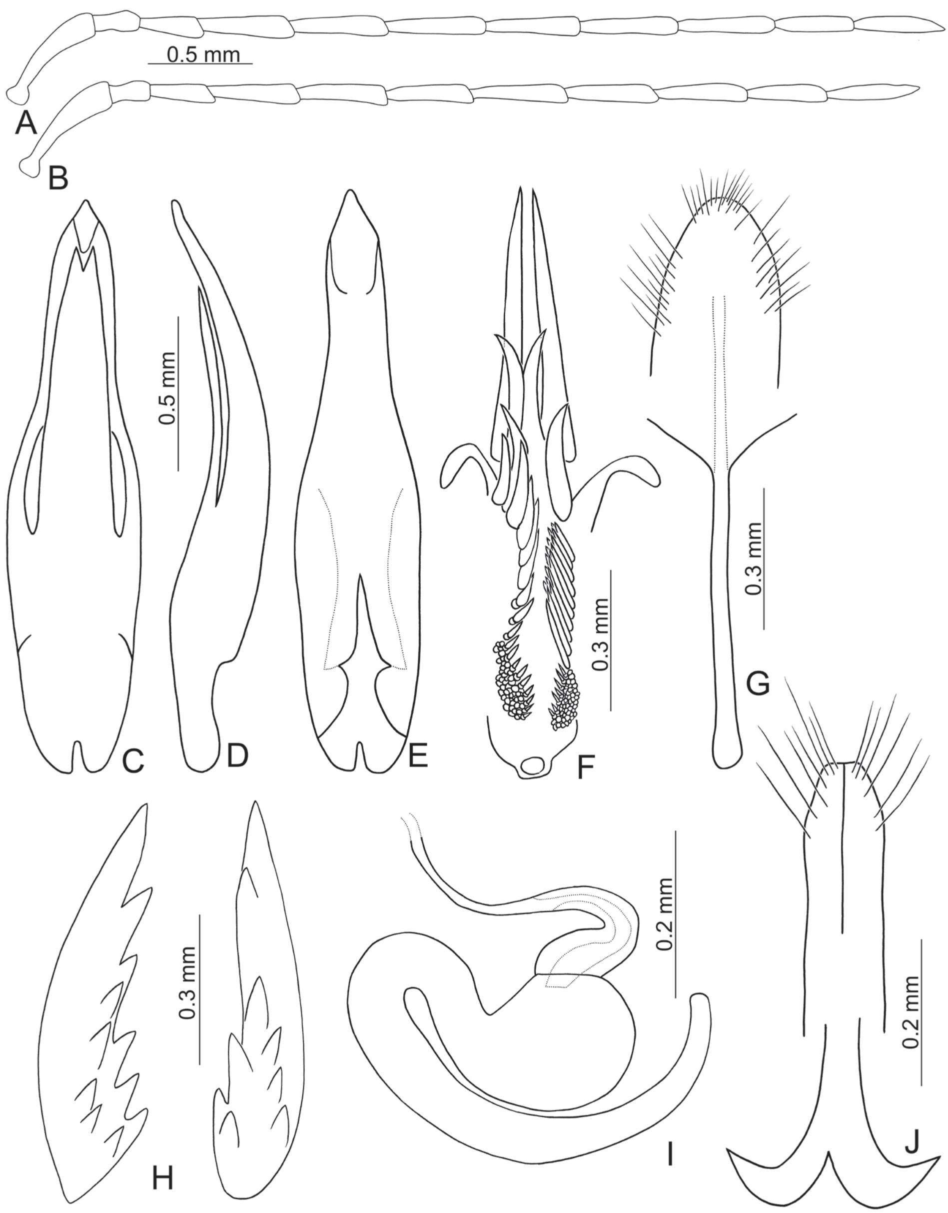

Figures 3. Diagnostic characters of *Paleosepharia excavata* (Chûjô). **A** Antenna, male **B** Antenna, female **C** Penis, dorsal view **D** Penis, lateral view **E** Penis, ventral view **F** Endophallic spiculae, hooked spiculae removed at right side **G** Abdominal ventrite VIII **H** Bursa sclerites, left sclerite in lateral view, right sclerite in dorsal view **I** Spermatheca **J** Gonocoxae.

峰]-Tattaka [= Sungkang, 松崗], 24.VI.1961, leg. T. Shirozu; 1♂ (TARI), Tsuifeng [翠峰], 21.VI.1979, leg. K. S. Lin & B. H. Chen; 1♂ (TARI), same locality, 25–27.VI.1981, leg. K. S. Lin & W. S. Tang; 1♂ (TARI), Tungfu [同富], 8.V.2011, leg. C.-

F. Lee; **Taichung**: 3♂♂, 3♀♀ (TARI), Anmashan [鞍馬山], 21.IV.2010, leg. C.-F. Lee; **Taitung**: 1♂ (TARI), Hsiangyang [向陽], 9.V.2013, leg. J.-C. Chen; 1♂ (TARI), Lichia [利嘉], 19.V.2009, leg. U. Ong; 3♀♀ (TARI), same locality, 15.VII.2014, leg. Y.-T. Chung; 1♀ (TARI), Litao [利稻], 23.VI.2010, leg. M.-H. Tsou; 4♀♀ (TARI), Liyuan [栗園], 29.III.2011, leg. C.-F. Lee; 1♀ (TARI), same locality, 24.VII.2013, leg. C.-F. Lee; 1♂ (TARI), same locality, 24.II.2014, leg. J.-C. Chen; 1♂ (TARI), same locality, 14.III.2014, leg. W.-C. Huang; 2♀♀, same locality, 28.III.2014, leg. W.-C. Huang; 1♀ (TARI), Motien [摩天], 23.VI.2010, leg. M.-H. Tsou; 1♀ (TARI), Wulu [霧鹿], 24.VI.2010, leg. M.-H. Tsou; 1♀ (TARI), same locality, 5.X.2010, leg. M.-H. Tsou; 1♂, 5♀♀ (TARI), same locality, 29.III.2011, leg. C.-F. Lee; 1♂ (NMNS), Yenping [延平], 30.VII.1992, leg. W. T. Yang; **Taoyuan**: 3♂♂, 1♀ (TARI), Hsuanyuan [萱源], 16.XII2008, leg. S.-F. Yu; 1♀ (TARI), Lalashan [拉拉山], 10.X.2009, leg. H. Lee; 2♂♂, 6♀♀ (TARI), Paling [巴陵], 8.XI.2009, leg. M.-H. Tsou; 1♀ (TARI), Tungyanshan [東眼山], 15.V.2010, leg. H. Lee; 1♂ (TARI), same locality, 5.XI.2011, leg. H. Lee.

Diagnosis. Adults of *Paleosepharia* excavata are similar to those of *P. formosana* and *P. yasumatsui* in possessing two transverse black bands on yellow elytra, but this species is easily recognized by its slender, indistinctly margined transverse black bands (broad and distinctly margined bands in others). Males of these species are also similar in possessing a broader penis (less than 6.0 times longer than wide; more than 6.5 times in other species), bifurcate apex of tectum (acute apex in other species), and lacking a pair of elongate and apically curved spiculae (such spiculae present in other species). Males of *P. excavata* differ in possessing a shallow notch in the apex of the tectum (deep notch in apex of tectum in *P. yasumatsui*), recurved apex of penis (not recurved in *P. yasumatsui*), short hooked spiculae 1/2 lengths of longer spiculae (1/6 lengths of longer spiculae in *P. formosana*, 4/5 lengths of longer spiculae in *P. yasumatsui*).

Description. Males. Length 4.8–6.1 mm, width 2.5–3.0 mm. General color reddish brown (Fig. 1D–E); antennae, scutellum, tibiae, and tarsi black; elytra yellow, with slender black stripes along each lateral margin and suture extending from base to apex, and two transverse, slender, indistinctly defined black bands at basal 1/3 and 2/3, usually abbreviated near suture and lateral margins. Antenna (Fig. 3A) filiform, ratio of length of antennomeres I to XI 1.0 : 0.4 : 0.6 : 0.9 : 0.9 : 0.9 : 0.8 : 0.8 : 0.8 : 0.7 : 0.8; ratio of length to width from antennomere I-XI 4.6 : 2.1 : 3.1 : 4.8 : 4.8 : 5.6 : 5.4 : 5.5 : 5.5 : 5.0 : 5.7. Pronotum 1.58–1.59 times wider than long; lateral margins slightly curved, basal margin slightly curved, apical margin slightly concave; disc with lateral fovea and dense minute punctures. Elytra parallel-sided; 1.49–1.56 times longer than wide; with one pair of oblique dark depressions at suture behind scutellum; disc with dense, minute punctures; apex truncate. Penis (Fig. 3C–E) elongate, 4.5 times longer than wide; parallel-sided, abruptly widened at apical 1/3, apically tapering; tectum elongate from middle to near apex, basally broadened, apex bifurcate; moderately recurved at basal 1/4 in lateral view; ventral surface with lateral areas membranous, apical membranous area short. Endophallic spiculae complex (Fig. 3F) with longest pair directed anteriorly, one pair of hooked spiculae 1/2 lengths of the longest spiculae;

one pair of longitudinal rows of hooked setae starting from bases of longest spiculae, smaller near base; one row of elongate, apically tapering setae covering surface behind hook-like setae; and one paired cluster of short, hooked setae near base.

Females. Length 5.4–6.3 mm, width 2.8–3.3 mm. Similar to male (Fig. 1F); but elytra lacking oblique depressions, anterior transverse black band extending to suture; ratio of length of antennomeres I to XI (Fig. 3B) 1.0 : 0.3 : 0.6 : 0.8 : 0.7 : 0.7 : 0.8 : 0.8 : 0.8 : 0.7 : 0.8; ratio of length to width from antennomere I to XI 4.1 : 1.9 : 3.3 : 4.5 : 4.4 : 4.4 : 5.1 : 4.9 : 5.5 : 4.8 : 6.0. Gonocoxae (Fig. 3J) slender, tightly conjunct from apical 1/3 to base; each gonocoxa with six or seven setae from apical 1/6 to apex, apex truncate. Ventrite VIII (Fig. 3G) weakly sclerotized medially, with several short setae at apex, and two rows of long setae at sides, spiculum extremely elongate. Spermathecal receptaculum (Fig. 3I) swollen; pump extremely slender and curved; sclerotized spermathecal duct slender. Bursa sclerites (Fig. 3H) elongate and apically tapering, with stout teeth along lateral margin at base; slightly curved in lateral view.

Food plant. Betulaceae: *Alnus formosana* (Burkill ex Forbes & Hemsl.) Makino (Lee and Cheng 2010).

Distribution. Taiwan, China.

Paleosepharia formosana (Chûjô), comb. n.

Figs 4A–C, 5

Monolepta formosana Chûjô, 1935: 172 (Taipei, Nantou); Chûjô 1938: 143 (Chiayi); Chûjô 1962: 135 (redescription; Taitung); Chûjô 1965: 97 (Taipei, Nantou); Kimoto 1965: 488 (Nantou); Kimoto 1966: 32 (Chiayi, Nantou); Kimoto 1969: 48 (Taipei, Taichung, Nantou); Kimoto 1986: 58 (Nantou); Kimoto 1989: 254 (Taipei, Kaohsiung); Kimoto and Chu 1996: 79 (catalogue); Kimoto and Takizawa 1997: 385 (catalogue); Lee and Cheng 2007: 112 (food plants); Beenen 2010: 483 (catalogue); Yang et al. 2015: 268 (catalogue).

Type material. Lectotype ♂ (TARI), here designated, labeled: "Sôzan [h] [= Yangmingshan, 陽明山] / FORMOSA [p] / 24.IX.1932 [h] / COL. M. CHUJO [P] // CO / Type [p, y, circular label with yellow border] // *Monolepta* / *formosana* / Chûjô [h] // DET. M. CHUJO [p, w] // No. 1341 [p, w]". Paralectotypes. 3♂♂, 1♀ (TARI), same data as lectotype, but with "1342, 1343, 1901, or 1902; 1♂ (SDEI): "Fuhosho [= Wucheng, 五城] / Formosa / Sauter [p] VIII [h] 07–09 [p, w] // *Monolepta* / *formosana* / Chûjô [h] // DET. M. CHUJO [p, w] // Syntypus [p, r]".

Other material examined (n = 90). Hsinchu: 1♀ (TARI), Litungshan [李棟山], 6.VI.2010, leg. Y.-L. Lin; 2♂♂ (TARI), Lupi [魯壁], 26.VII.2008, leg. M.-H. Tsou; **Hualien**: 1♂ (TARI), Huitouwan [迴頭灣], 10.VII.2007, leg. C.-F. Lee; 1♀ (TARI), Huojanting [豁然亭], 7–14.IV.2007, leg. Y.-F. Hsu; 1♀ (TARI), Wanjung [萬榮], 11.VI.2011, leg. M.-H. Tsou; **Ilan**: 1♂, 1♀ (NMNS), Fushan Botanical Garden [福山植物園], 26–27.VIII.2003, leg. M. L. Chan; 2♀♀ (TARI), same locality,

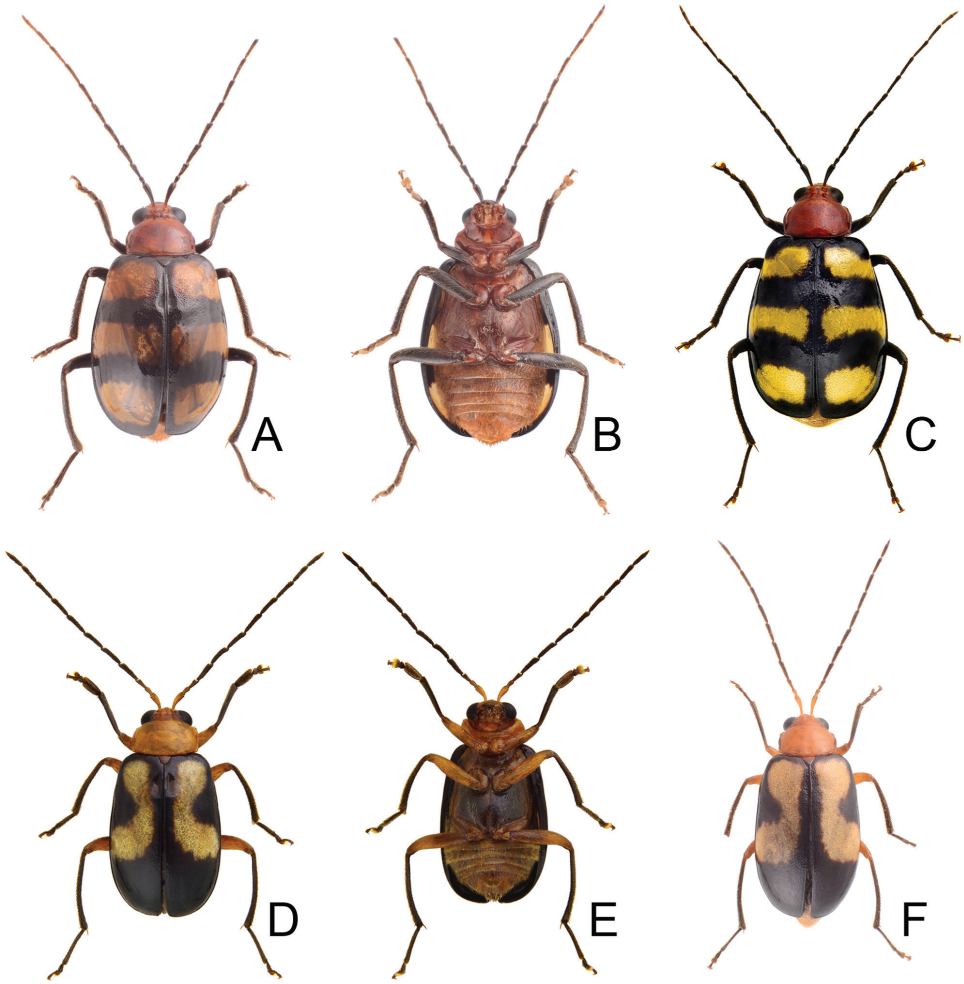

Figures 4. Habitus of *Paleosepharia* species. **A** *P. formosan*a (Chûjô), male, dorsal view **B** Ditto, ventral view **C** *P. formosana*(Chûjô), female, color variation, dorsal view **D** *P. nantouensis*(Kimoto), male, dorsal view **E** Ditto, ventral view **F** nantouensis (Kimoto), female, dorsal view.

2.IV.2008, leg. M.-H. Tsou; 2♀♀ (TARI), same locality, 8.V.2008, leg. S.-F. Yu; 1♀ (TARI), same locality, 8.VII.2013, leg. Y.-T. Wang; 1♀ (TARI), Yingtzuling [鶯仔嶺], 7.IV.2012, leg. Y.-L. Lin; **Kaoshiung**: 1♂ (TARI), Tengchih [藤枝], 7.IX.2012, leg. W.-C. Liao; 1♀ (TARI), Tona trail [多納林道], 3.II.2013, leg. B.-X. Guo; **Nantou**: 1♂ (NMNS), Huisun Forest [惠蓀林場], 12–13.XI.1998, leg. C. S. Lin & W. T. Yang; 1♂ (TARI), 17.XI.2008, same locality, leg. M.-H. Tsou; 1♀ (NMNS), Lake Candidius [= Jihyuehtan, 日月潭], 26.VI.1961, leg. T. Shirozu; 3♀♀ (TARI), Lienhuachih [蓮華池], 23–26.V.1980, leg. K. S. Lin & B. H. Chen; 1♀ (TARI), same locality, 26.VII.1984, leg. K. S. Lin; 1♀ (NMNS), same locality, 12.VII.-9.VIII.2004, leg. C. S. Lin & W. T. Yang; 1♂ (NMNS), same locality, 4.X.-15.XI.2004, leg. C. S.

Lin & W. T. Yang; 1♂ (TARI), same locality, 22.III.2009, leg. U. Ong; 3♂♂, 3♀♀ (TARI), Lushan［盧山］, 27–31.V.1980, leg. K. S. Lin & L. Y. Chou; 1♂ (TARI), same locality, 28.VI.1981, leg. K. S. Lin & W. S. Tang; 1♂ (NMNS), Nanshanchi [南山溪], 21.VI.1965, leg. B. S. Chang; 1♂ (TARI), same locality, 11.VII.2007, leg. M.-H. Tsou; 1♀ (TARI), Sungchuankang [松泉崗], 25.VII.2010, leg. T.-Y. Liu; 1♂ (TARI), Sunglintsun [松林村], 9.VII.2007, leg. M.-H. Tsou; 2♂♂ (TARI), Tungpu [東埔], 25–29.IX.1980, leg. L. Y. Chou & T. Lin; 1♀ (TARI), same locality, 28.IV.-2.V.1981, leg. T. Lin & C. J. Lee; 1♂, 1♀ (TARI), same locality, 5–8.X.1981, leg. T. Lin & W. S. Tang; 2♂♂, 2♀♀ (TARI), same locality, 19–23.VII.1982, leg. L. Y. Chou & T. Lin; 2♂♂ (TARI), same locality, 22–25.XI.1982, leg. K. C. Chou & S. P. Huang; 1♀ (TARI), same locality, 20–24.VI.1983, leg. K. C. Chou & C. Y. Wong; 2♂♂, 4♀♀ (TARI), same locality, 23–27.VII.1984, K. C. Chou & C. H. Yang; 1♀ (TARI), Wanfengtsun [萬豐村], 4.X.2007, leg. W.-T. Liu; 3♂♂, 1♀ (TARI), same locality, 8.VII.2008, leg. W.-T. Liu; 1♂ (TARI), Wushe [霧社], 4.VIII.1981, leg. T. Lin & W. S. Tang; **Pingtung**: 2♀♀ (TARI), Ali [阿禮], 17.II.2016, leg. Y.-T. Chung; 1♀ (TARI), Lilungshan [里龍山], 17.VIII.2014, leg. Y.-T. Chung; 1♀ (TARI), Kenting [墾丁], 5–9.XII.1982, leg. S. C. Lin & S. P. Huang; 1♀ (TARI), Nanjenhu [南仁湖], 15.III.2010, leg. M.-H. Tsou; 1♂ (TARI), Tahanshan [大漢山], 20.VII.2007, leg. S.-F. Yu; 1♂ (TARI), same locality, 6.II.2008, leg. M.-H. Tsou; 2♂♂ (TARI), 13–14.VIII.2011, leg. Y.-T. Wang; 1♀ (TARI), same locality, 20.X.2012, leg. W.-C. Liao; 1♂ (TARI), same locality, 15.XII.2012, leg. W.-C. Liao; 1♂ (TARI), same locality, 10.VII.2013, leg. Y.-T. Chung; 1♀ (TARI), 10.IV.2017, leg. Y.-T. Chung; 3♀♀ (TARI), Wutai [霧台], 15–16.III.2009, leg. Y.-F. Hsu; 1♀ (TARI), same locality, 12.IV.2009, U. Ong; **Taipei**: 1♂, 1♀ (NMNS), Fushan [福山], 28–29.V.2004, leg. C. S. Lin & W. T. Yang; 1♂, 1♀ (NMNS), Rimogan [= Fushan, 福山]-Magan, 10.VII.1961, leg. T. Shirozu; 1♀ (TARI), Wulai [烏來], 4.III.2007, leg. S.-F. Yu; 1♂ (TARI), same locality, 30.III.2007, leg. C.-F. Lee; **Taichung**: 1♂, 1♀ (NMNS), Bojinjiashan [波津加山], 8.X.1987, leg. I. C. Hsu; 2♂♂, 1♀ (TARI), Chiapaotai [佳保台], 14–18.X.1980, leg. K. S. Lin & C. H. Wang; 1♀ (NMNS), Kukuan [谷關], 11–12.IV.1986, leg. C. S. Lin; **Taitung**: 1♂ (TARI), Lichia [利嘉], 24.IV.2008, leg. C.-L. Hsiao; 1♀ (TARI), Liyuan [栗園], 29.III.2011, leg. C.-F. Lee; 1♂ (TARI), Shouka [壽卡], 13.VI.2013, leg. Y.-T. Chung; 2♂♂ (TARI), same locality, 27.X.2013, leg. W.-C. Liao; 1♀ (TARI), same locality, 19.IV.2015, leg. W.-C. Liao; 1♂, 1♀ (TARI), Tulanshan [都蘭山], 14.IX.2014, leg. Y.-T. Chung; 1♂ (TARI), Wulu [霧鹿], 5.X.2010, leg. M.-H. Tsou; **Taoyuan**: 1♀ (TARI), Hsiaowulai [小烏來], 29.IX.2009, leg. M.-H. Tsou; 1♂, 2♀♀ (TARI), Paling [巴陵], 3–5.V.1983, leg. K. C. Chou & C. C. Pan; 1♂ (TARI), Tungyanshan [東眼山], 12.IV.2007, leg. M.-H. Tsou; 1♂ (TARI), same locality, 20.IX.2007, leg. S.-F. Yu.

Diagnosis. Adults of *Paleosepharia formosana* are similar to those of *P. yasumatsui* in possessing two broad, well-defined transverse black bands on the elytra. However, males of *P. yasumatsui* are easily separated from those of *P. formosana* by the absence of anterior transverse black bands near the suture (present in *P. formosana*), and presence of clusters of stout setae behind the scutellum (lacking stout setae in *P. formosana*).

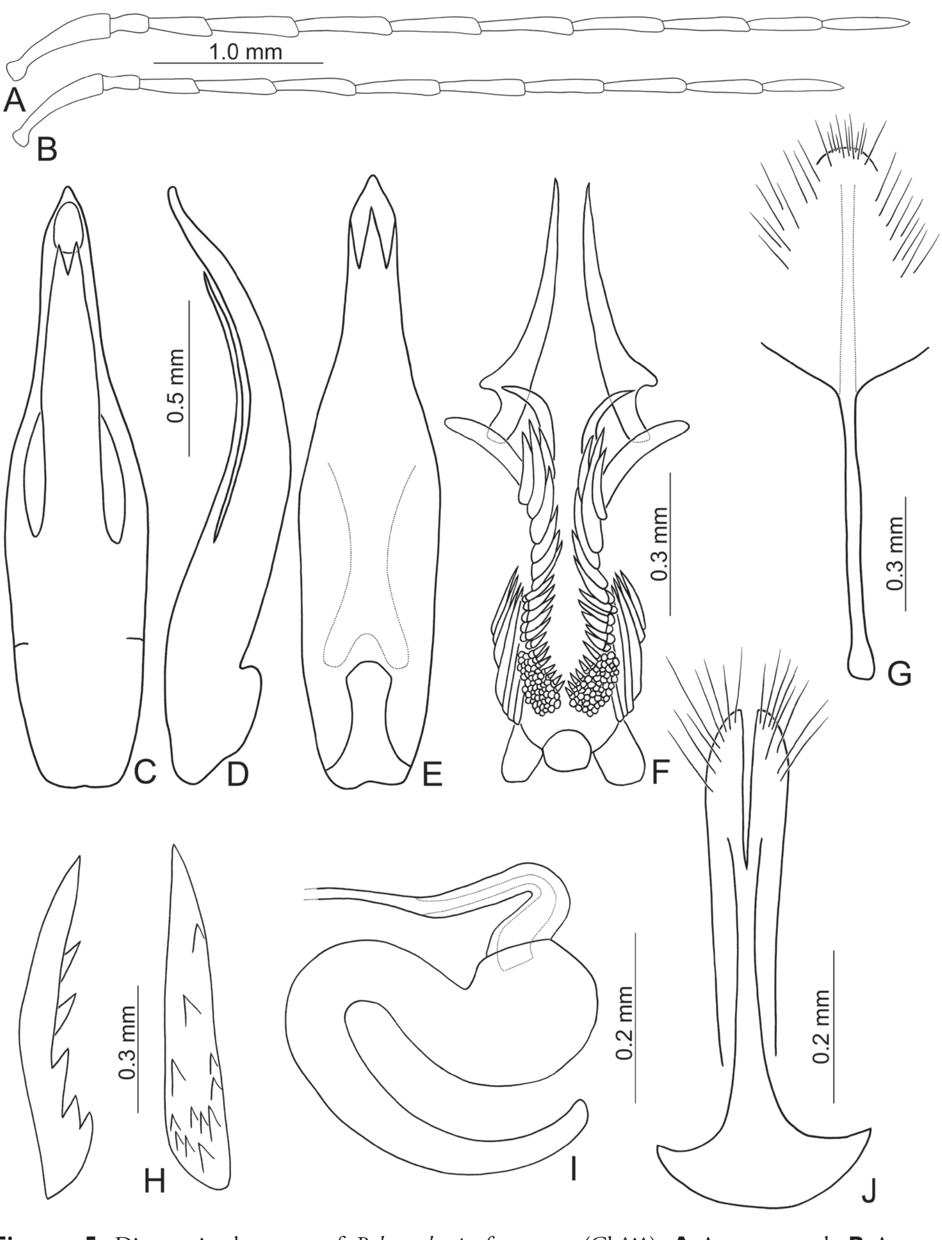

Figures 5. Diagnostic characters of *Paleosepharia formosana* (Chûjô). **A** Antenna, male **B** Antenna, female **C** Penis, dorsal view **D** Penis, lateral view **E** Penis, ventral view **F** Endophallic spiculae **G** Abdominal ventrite VIII **H** Bursa sclerites, left sclerite in lateral view, right sclerite in dorsal view **I** Spermatheca **J** Gonocoxae.

Females of *P. yasumatsui* are similar to those of *P. formosana* but differ by their straight lateral margins of the elytra and continuously arcuate posterior black stripes (rounded elytra and independently arcuate black stripes in *P. formosana*). Males of *P. formosana*, *P. excavata*, and *P. yasumatsui* are similar in possessing a broad penis (less than 6.0 times longer than wide; more than 6.5 times in other species), bifurcate apex of tectum (acute apex in other species), lacking a pair of elongate, apically curved spiculae (such spiculae present in other species). They differ in possessing a shallow notch of the apex of the tectum (deep notch in *P. yasumatsui*), recurved apex of the penis (not recurved in *P. yasumatsui*), short hooked spiculae 1/6 the lengths of longer spiculae (1/2 length of longer spiculae in *P. excavata*, 4/5 length of longer spiculae in *P. yasumatsui*).

Description. Males. Length 5.6–6.3 mm, width 3.2–3.5 mm. General color reddish brown (Fig. 4A–B); antennae and legs black; scutellum reddish brown; elytra yellow, with wide black stripe along lateral margins and suture, extending from base to apex, and two transverse, wide black bands at basal 1/3 and 2/3. Antenna (Fig. 5A) filiform, ratio of length of antennomeres I to XI 1.0 : 0.3 : 0.6 : 0.8 : 0.9 : 0.8 : 0.8 : 0.8 : 0.8 : 0.7 : 0.8; ratio of length to width from antennomere I to XI 4.4 : 2.0 : 3.2 : 4.7 : 5.3 : 5.7 : 5.7 : 6.5 : 6.2 : 5.8 : 6.8. Pronotum 1.76–1.78 times wider than long; lateral margins straight; basal margin slightly curved, apical margin slightly concave; disc evenly convex, with reticulate microsculpture and dense, minute punctures. Elytra widest at apical 1/3; 1.34–1.35 times longer than wide; with one pair of longitudinal depressions near suture, behind scutellum; disc with dense, minute punctures; apex truncate. Penis (Fig. 5C–E) elongate, 4.4 times longer than wide; parallel-sided, abruptly widened at apical 1/3, apically tapering; tectum elongate from middle to near apex, parallel-sided; apex bifurcate; moderately recurved at basal 1/4 in lateral view; ventral surface with lateral areas membranous, apical membranous area short and with tapering process from lower part of membranous area. Endophallic spiculae (Fig. 5F) with longest pair directed anteriorly, another pair of shorter, hooked spiculae curved outside near apex; one pair of longitudinal rows of hooked setae originating from bases of longest setae and reaching near base, smaller near base; one paired cluster of short hooked setae covering surface near base; one row of long, apically tapering setae on side, smaller near apex.

Females. Length 5.7–6.7 mm, width 3.4–3.6 mm. Similar to male (Fig. 4C); but elytra lacking longitudinal depressions; ratio of length of antennomeres I to XI (Fig. 5B) 1.0 : 0.3 : 0.6 : 0.8 : 0.7 : 0.8 : 0.8 : 0.8 : 0.8 : 0.7 : 0.8; ratio of length to width from antennomere I to XI 5.3 : 2.4 : 4.1 : 5.2 : 4.9 : 5.3 : 5.3 : 5.8 : 5.9 : 5.5 : 6.5. Gonocoxae (Fig. 5J) slender, tightly conjunct from apical 1/3 to base; each gonocoxa with eight setae from apical 1/6 to apex, apex curved. Ventrite VIII (Fig. 5G) weakly sclerotized apically, apical margin curved, with several short setae and several long setae at sides, spiculum extremely elongate. Spermathecal receptaculum (Fig. 5I) swollen; pump extremely slender and curved; sclerotized spermathecal duct slender. Bursa sclerites (Fig. 5H) elongate and apically tapering, with dense, stout teeth near base; slightly curved in lateral view.

Food plants. Saxifragaceae: *Itea parviflora* Hemsl.; Hamamelidaceae: *Liquidambar formosana* Hance; Myrsinaceae: *Ardisia sieboldii* Miq (Lee and Cheng 2007).

Remarks. Lee and Cheng (2007) misidentified males of *Paleosepharia formosana*; they are re-identified as belonging to females of *P. yasumatsui*.

Distribution. Endemic to Taiwan.

Paleosepharia nantouensis **(Kimoto), comb. n.**
Figs 4D–F, 6

Monolepta nantouensis Kimoto, 1996: 38; Kimoto and Takizawa 1997: 386 (catalogue); Beenen 2010: 484 (catalogue); Lee and Cheng 2010: 102 (food plant); Yang et al. 2015: 270 (catalogue).

Type material. Paratype 1♀ (KMNH): “Baibara [h, w] // C. TAIWAN, / End of 1950’s [p, w] // *Monolepta* / *nantouensis* / Kimoto, n. sp. [h] / Det. S. Kimoto. 19 [p, w] // PHOTO [p, r] // PARATYPE [p, b]”.

Other material examined (n = 22). Hsinchu: 2♀♀ (TARI), Chenhsipao [鎮西堡], 26.VII.2014, leg. Y.-L. Lin; 4♂♂ (TARI), Chienshih [尖石], 12.VII.2009, leg. M.-H. Tsou; 1♀ (TARI), Lupi [魯壁], 20.VII.2008, leg. M.-H. Tsou; 1♀ (TARI), same locality, 26.VII.2008, leg. M.-H. Tsou; **Ilan**: 1♀ (TARI), Suyuan [思源], 23.VII.2008, leg. H.-Y. Lee; 1♀ (TARI), same locality, 8.VIII.2014, leg. S.-F. Yu; **Kaoshiung**: 1♂ (TARI), Meilungshan [美瓏山], 15.VI.2016, leg. B.-X. Guo; Taichung: 1♂ (NMNS), Anmashan [鞍馬山], 18.VII.2005, leg. Y.-L. Chen; **Taitung**: 2♂♂, 3♀♀ (TARI), Liyuan [栗園], 24.VII.2013, leg. C.-F. Lee; **Taoyuan**: 1♂, 1♀ (TARI), Lalashan [拉拉山], 2.VIII.2008, leg. M.-H. Tsou; 1♂ (TARI), same locality, 7.VIII.2008, leg. H.-J. Chen; 1♀ (TARI), same locality, 30.VIII.2008, leg. M.-H. Tsou; 1♀ (NMNS), Shanpaling [上巴陵], 26.VIII.1987, leg. I. C. Hsu; 1♂ (TARI), Tamanshan [塔曼山], 3.VIII.2008, leg. M.-H. Tsou; 1♀ (TARI), same but with “leg. S.-F. Yu”.

Description. Males. Length 4.7–5.2 mm, width 2.4–2.6 mm. General color yellowish brown (Fig. 4D–E); antennae, except two basal antennomeres, tibiae, tarsi, and metaventrite blackish brown; scutellum yellowish brown; elytra black, with one pair of broad, curved white stripes from near base to middle, curved inwards at middle. Antenna (Fig. 6A) filiform, ratio of length of antennomeres I to XI 1.0 : 0.3 : 0.5 : 0.9 : 0.9 : 0.9 : 0.9 : 0.9 : 0.9 : 0.8 : 0.9; ratio of length to width from antennomere I to XI 3.7 : 2.0 : 2.9 : 5.1 : 5.1 : 4.9 : 5.0 : 4.9 : 5.2 : 4.9 : 5.6. Pronotum 1.69–1.81 times wider than long; lateral margins slightly curved, basal margin slightly curved, apical margin slightly concave; disc evenly convex, with reticulate microsculpture and dense, minute punctures and one pair of weak fovea at sides. Elytra parallel-sided; 1.51–1.57 times longer than wide; with one pair of depressions near suture in basal 1/3; disc with dense, minute punctures; apex truncate. First tarsomeres of front legs dorso-ventrally flattened. Penis (Fig. 6C–E) extremely slender, 6.8 times longer than wide; parallel-sided, posterior widened at middle, apically tapering; tectum elongate from basal 1/5 to apical 1/6, widest at middle and as wide as penis, apically tapering, apex acute; moderately recurved at middle and near apex in lateral view; ventral surface without membranous areas. Endophallic spiculae complex (Fig. 6F) with the longest pair apically curved; also possessing two pairs of long hooked spiculae of equal length, one pair curved inwards, the other curved outwards; a pair of longitudinal rows of hook-like setae distal to bases of longest spiculae; one longitudinal pair of long, apically tapering setae along sides distal to bases of longest spiculae.

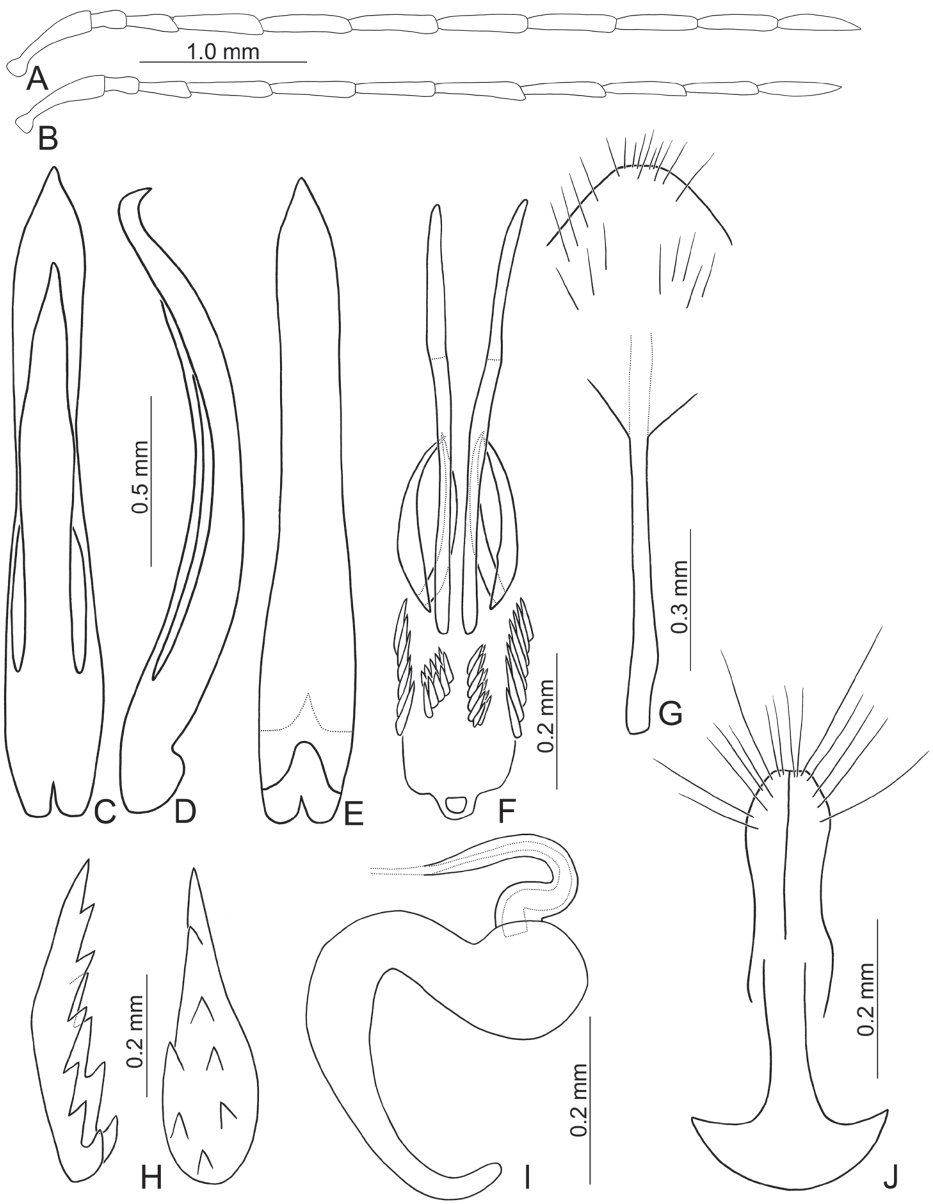

Figures 6. Diagnostic characters of *Paleosepharia nantouensis* (Kimoto). **A** Antenna, male **B** Antenna, female **C** Penis, dorsal view **D** Penis, lateral view **E** Penis, ventral view **F** Endophallic spiculae **G** Abdominal ventrite VIII **H** Bursa sclerites, left sclerite in lateral view, right sclerite in dorsal view **I** Spermatheca **J** Gonocoxae.

Females. Length 5.3–6.3 mm, width 2.6–3.3 mm. Similar to males (Fig. 4F); but elytra lacking oblique depressions; first tarsomeres of front legs normal; ratio of length of antennomeres I to XI (Fig. 6B) 1.0 : 0.3 : 0.5 : 0.9 : 0.9 : 0.8 : 0.9 : 0.8 : 0.8 : 0.7

: 0.7; ratio of length to width from antennomere I-XI 4.8 : 2.0 : 3.7 : 5.6 : 5.6 : 5.9 : 6.7 : 6.2 : 7.2 : 6.4 : 6.7. Gonocoxae (Fig. 6J) slender, tightly conjunct from apical 1/3 to base; each gonocoxa with eight setae from apical 1/6 to apex, apex truncate. Ventrite VIII (Fig. 6G) weakly sclerotized except apex, with several short setae at apex, and several long setae at sides, spiculum elongate. Spermathecal receptaculum (Fig. 6I) swollen; pump extremely slender and curved; sclerotized spermathecal duct slender. Bursa sclerites (Fig. 6H) elongate and apically tapering, with stout teeth along lateral margin at base; slightly curved in lateral view.

Food plant. Fagaceae: *Castanopsis carlesii* (Hemsl.) Hayata (Lee and Cheng 2010).

Distribution. Endemic to Taiwan.

Paleosepharia yasumatsui (Kimoto), comb. n.

Figs 7, 8

Monolepta yasumatsui Kimoto, 1969: 51 (Nantou, Ilan); Kimoto 1991: 15 (Kaohsiung); Kimoto and Chu 1996: 83 (catalogue); Kimoto and Takizawa 1997: 387 (catalogue); Beenen 2010: 485 (catalogue); Lee and Cheng 2010: 103 (food plants); Yang et al. 2015: 274 (catalogue).

Type material. Holotype ♂ (KUEC), labeled: "(Taiwan) / Nanshanchi [南山溪] / Nantou Hsien [p, w] // 30[h].vi.1965 / S. Kimoto [p, w] // Japan-U. S. / Co-op. Sic. / Programme [p, y] // *Monolepta* / *yasumatsui* / Kimoto, n. sp. [h, w] // HOLOTYPE [p, r]". Paratypes. 1♂ (KMNH): "(TAIWAN) / Penpuchi [本部溪] / Nontou Hsien / 13. VII. 1966 / H. Kamiya leg. [p, w] // *Monolepta* / *yasumatsui* / Kimoto, n. sp. [h, w] // PARATYPE [p, b]"; 1♂ (KMNH): "(Taiwan) [p] / (Taipinshan [太平山]) / Ilan [h] Hsien [p, w] // 5.viii.1967 [h] / B. S. Chang [p, w] // *Monolepta* / *yasumatsui* / Kimoto, n. sp. [h, w] // PARATYPE [p, b]".

Other material examined (n = 68). Hsinchu: 1♂, 1♀ (TARI), Mamei [馬美], 18.V.2008, leg. S.-F. Yu; 1♀ (TARI), Talu trail [大鹿林道], 17.III.2012, leg. Y.-L. Lin; **Hualien**: 1♂ (TARI), Wanjung [萬榮], 11.VI.2011, leg. M.-H. Tsou; **Ilan**: 2♀♀ (TARI), Fushan Botanical Park [福山植物園], 1.IV.2008, leg. M.-H. Tsou; 1♀ (TARI), same but with "leg. H.-J. Chen; 1♂ (TARI), same locality, 13.IV.2011, leg. C.-F. Lee; 1♂ (TARI), same locality, 3.VII.2013, leg. Y.-T. Wang; 1♂, 1♀ (NMNS), Mingchi [明池], 18.II.2000, leg. M. L. Chan; 1♂ (TARI), 17.III.2007, leg. M.-H. Tsou; 2♂♂ (TARI), same locality, 16.VIII.2008, leg. M.-H. Tsou; 1♂ (TARI), same locality, 5.IV.2009, leg. M.-H. Tsou; 1♂ (TARI), Shenmihu [神秘湖], 17.IV.2010, leg. M.-H. Tsou; 1♂ (TARI), Taipingshan [太平山], 15.XI.2007, leg. S.-S. Li; 2♀♀ (TARI), Tungshan [銅山], 6.IX.2010, leg. Y.-F. Hsu; **Kaoshiung**: 1♂ (TARI), Chungchihkuan [中之關], 10–13.X.2012, leg. L.-P. Hsu; 1♂ (TARI), Tengchih [藤枝], 27.IX.2013, leg. W.-C. Liao; 2♀♀ (TARI), same locality, 30.VIII.2014, leg. B.-X. Guo; 1♂, 1♀ (TARI), same locality, 2.IV.2016, leg. W.-C. Liao; 1♀ (TARI), Tianchih [天池], 11.X.2012, leg. L.-P. Hsu; 1♂ (NMNS), Tona trail [多納林道], 30.IV.1998, leg. M. L Chan; 1♀

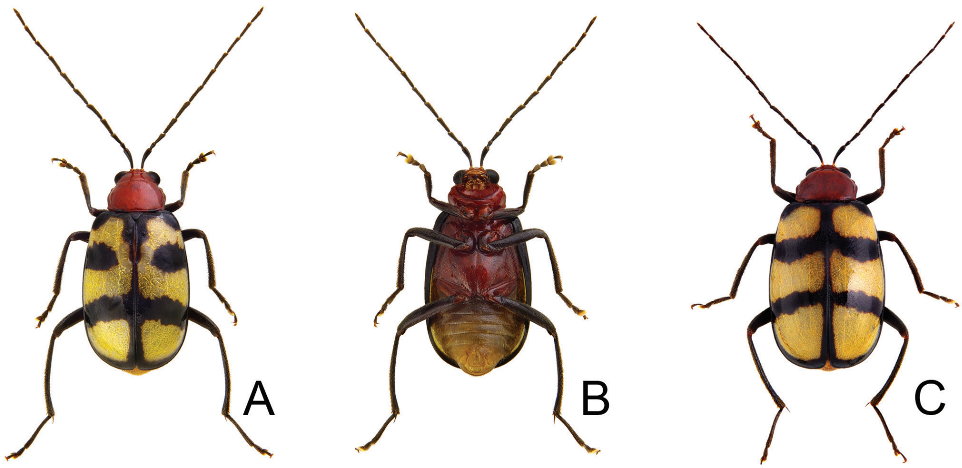

Figures 7. Habitus of *Paleosepharia yasumatsui* (Kimoto). **A** Male, dorsal view **B** Ditto, ventral view **C** Female, dorsal view.

(TARI), 20.III.2010, leg. U. Ong; **Nantou**: 1♂ (TARI), Huisunlinchang [惠蓀林場], 26.IV.2014, leg. B.-X. Guo; 1♂ (TARI), same locality, 23.IV.2015, leg. Y.-T. Chung; 2♀♀ (NMNS), Lienhuachih [蓮華池], 21.IV.1998, leg. M. M. Yang & H. T. Chan; 1♂ (TARI), Nanshanchi [南山溪], 25.VII.2008, leg. W.-T. Liu; 1♀ (TARI), same locality, 7.IV.2010, leg. Y.-T. Wang; 1♂ (NMNS), Peitungyenshan [北東眼山], 23–25. IX.1998, leg. W. T. Yang; 1♂ (TARI), Pihu [碧湖], 27.IX.2011, leg. J.-C. Chen; **Pingtung**: 2♂♂ (TARI), Jinshuiying [浸水營], 19.XI.2009, leg. J.-C. Chen; 1♂ (TARI), same locality, 12.IX.2011, leg. J.-C. Chen; 1♂ (TARI), same locality, 12.IV.2012, leg. C.-F. Lee; 1♀ (TARI), same locality, 27.IV.2014, leg. J.-C. Chen; 1♂ (TARI), Tahanshan [大漢山], 6.VIII.2013, leg. Y.-T. Chung; 1♂ (TARI), Wutai [霧台], 12.IV.2009, leg. U. Ong; 2♀♀ (TARI), same locality, 17.V.2009, leg. U. Ong; **Taipei**: 1♀ (TARI), Wulai [烏來], 4.III.2007, leg. S.-F. Yu; 1♂ (TARI), same locality, 17.V.2008, leg. M.-H. Tsou; **Taichung**: 1♂ (TARI), Anmashan [鞍馬山], 22.III.2011, leg. C.-F. Lee; 1♂ (TARI), same locality, 19.X.2011, leg. C.-F. Lee; 1♂ (NMNS), Chiapaotai [佳保台], 6.XII.1991, leg. Y. C. Shiau; 1♀ (TARI), Kukuan [谷關], 19.III.2014, leg. C.-F. Lee; Tainan: 1♀ (TARI), Kantoushan [崁頭山], 20.X.2013, leg. W.-C. Liao; **Taitung**: 3♀♀ (TARI), Lichia [利嘉], 9.IV.2016, S.-P. Wu; 2♂♂, 1♀ (TARI), Motien [摩天], 5.X.2010, leg. C.-F. Lee; 1♂, 1♀ (TARI), Wulu [霧鹿], 5.X.2010, leg. M.-H. Tsou; **Taoyuan**: 1♂ (TARI), Fuhsing [復興], 12.IV.2009, leg. M.-H. Tsou; 2♂♂ (TARI), Hsiaowulai [小烏來], 29.IX.2009, leg. M.-H. Tsou; 8♂♂ (TARI), same locality, 10.X.2009, leg. M.-H. Tsou; 1♂ (TARI), Lalashan [拉拉山], 26.X.2008, leg. M.-H. Tsou; 1♂ (TARI), Paling [巴陵], 8.XI.2009, leg. M.-H. Tsou; 1♂ (TARI), Sankuang [三光], 17.X.2009, leg. Y.-L. Lin; 2♂♂ (NMNS), Shanpaling [上巴陵], 26.VIII.1987, leg. I. C. Hsu; 1♀ (TARI), Tungyanshan [東眼山], 20.IX.2007, leg. S.-F. Yu.

Diagnosis. Adults of *P. yasumatsui* are similar to those of *P. formosana* in possessing two broad, distinctly margined transverse black bands on the elytra. However, males of

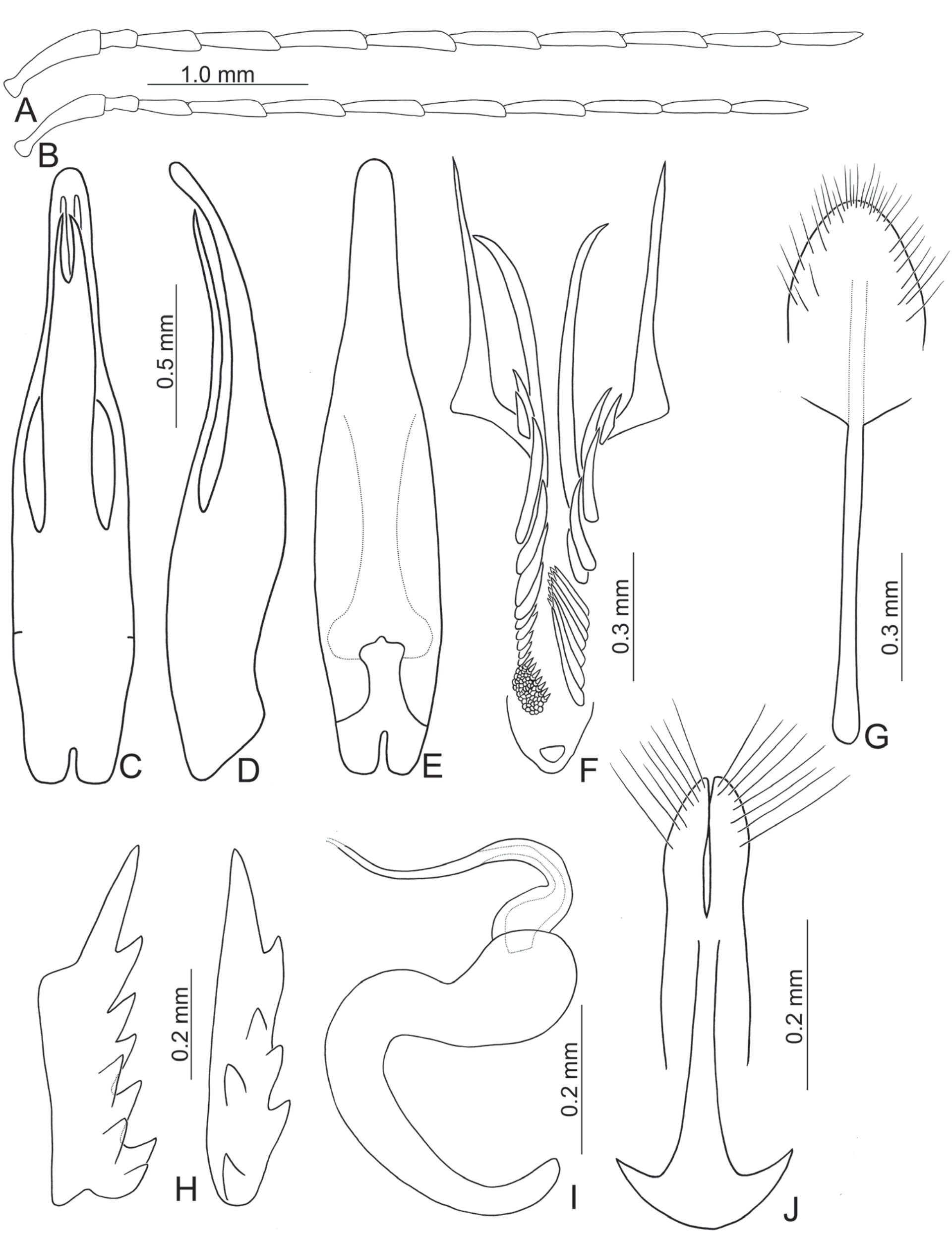

Figures 8. Diagnostic characters of *Paleosepharia yasumatsui* (Kimoto). **A** Antenna, male **B** Antenna, female **C** Penis, dorsal view **D** Penis, lateral view **E** Penis, ventral view **F** Endophallic spiculae, hooked spiculae removed at right side **G** Abdominal ventrite VIII **H** Bursa sclerites, left sclerite in lateral view, right sclerite in dorsal view **I** Spermatheca **J** Gonocoxae.

P. yasumatsui are easily separated from those of *P. formosana* by the absence of an anterior, transverse black band near the suture (present in *P. formosana*), and presence of clusters of stout setae behind the scutellum (lacking stout setae in *P. formosana*). Females of *P. yasumatsui* are similar to those of *P. formosana* but differ in the straight lateral margin of the elytra and continuously arcuate, posterior black stripes (rounded elytra and separated arcuate black stripes in *P. formosana*). Males of *P. formosana*, *P. excavata*, and *P. yasumatsui* are similar in possessing a broader penis (less than 6.0 times longer than wide; more than 6.5 times in other species), bifurcate apex of tectum (acute apex in other species), and lacking a pair of elongate, apically curved spiculae (such spiculae present in other species). Males of *P. yasumatsui* differ in having a deep notch at the apex of the tectum (shallow notch at apex of tectum in other species), curved apex of penis (recurved in other species), short, hooked spiculae 4/5 sizes of long spiculae (1/2 sizes of long spiculae in *P. excavata*, 1/6 sizes of long spiculae in *P. formosana*).

Description. Males. Length 5.2–6.0 mm, width 2.7–3.3 mm. General color reddish brown (Fig. 7A–B); antennae and legs black; scutellum reddish brown; elytra yellow, with wide black stripe along lateral margins and suture extending from base to apex; two transverse wide black bands at basal 1/3 and 2/3, anterior band abbreviated near suture. Antenna (Fig. 8A) filiform, ratio of length of antennomeres I to XI 1.0 : 0.3 : 0.6 : 0.8 : 0.9 : 0.9 : 0.9 : 0.8 : 0.8 : 0.7 : 0.8; ratio of length to width from antennomere I-XI 4.2 : 2.0 : 3.2 : 4.2 : 5.1 : 5.1 : 5.1 : 5.5 : 5.4 : 5.1 : 6.7. Pronotum 1.44–1.51 times wider than long; lateral margins slightly curved, basal margin slightly curved, apical margin slightly concave; disc evenly convex, with reticulate microsculpture and dense, minute punctures, and with one pair weak fovea at sides. Elytra subparallel, gradually broadened towards apices; 1.45–1.49 times longer than wide; with one pair of weak depressions near suture at basal 1/3; with paired clusters of long setae behind scutellum; disc with dense, minute punctures; apex truncate. Penis (Fig. 8C–E) elongate, 5.5 times longer than wide; parallel-sided, strongly widened at apical 1/3, apically curved; tectum elongate from middle to near apex, parallel-sided; apex deeply bifurcate; slightly recurved at basal 1/4 in lateral view; ventral surface with lateral areas membranous. Endophallic spiculae complex (Fig. 8F) with one longest pair directed anteriorly, another shorter pair of hooked spiculae; one pair of elongate rows of hooked setae distal to base of longest spiculae, smaller near base; one paired cluster of short and apically tapering setae near base; one pair of elongate rows of long, apically tapering setae covered by hooked setae.

Females. Length 4.6–5.7 mm, width 2.6–3.1 mm. Similar to male (Fig. 7C); but elytra lacking depressions and clusters of long setae, and anterior black band extending to suture, ratio of length of antennomeres I to XI (Fig. 8B) 1.0 : 0.3 : 0.5 : 0.9 : 0.9 : 0.8 : 0.9 : 0.9 : 0.8 : 0.7 : 0.9; ratio of length to width from antennomere I to XI 4.7 : 2.1 : 3.4 : 5.4 : 5.3 : 5.3 : 6.1 : 5.6 : 6.3 : 5.4 : 6.0. Gonocoxae (Fig. 8J) slender, tightly conjunct from apical 1/3 to base; each gonocoxa with seven to eight setae from apical 1/6 to apex, apex truncate. Ventrite VIII (Fig. 8G) medially and weakly sclerotized with apical margin curved, with dense, short setae at apex, and several long setae at sides, spiculum extremely elongate. Spermathecal receptaculum (Fig. 8I) swollen; pump extremely slender and curved; sclerotized spermathecal duct slender. Bursa sclerites (Fig. 8H) elongate and apically tapering, two elongate rows of stout setae at sides; slightly curved in lateral view.

Food plants. Saxifragaceae: *Itea parviflora* Hemsl.; Betulaceae: *Alnus formosana* (Burkill ex Forbes & Hemsl.) Makino; Symplocaceae: *Symplocos wikstroemiifolia* Hayata (Lee and Cheng 2010).

Distribution. Endemic to Taiwan.

Key to Taiwanese species of the genus *Paleosepharia*

1	Elytra black, with one pair of inwardly curved white stripes (Fig. 4D, F)	***P. nantouensis***
–	Elytra yellow, with black stripes along outer margins and transverse black bands	**2**
2	Only one transverse black band on elytra (Fig. 1A, 1C)	***P. amiana***
–	Two transverse black bands on elytra	**3**
3	Transverse black bands on elytra slender and weakly margined; tibiae reddish brown (Fig. 1D, F)	***P. excavata***
–	Transverse black bands on elytra broad and distinctly margined; tibiae black	**4**
4	Anterior transverse black bands reduced near suture, cluster of stout setae behind scutellum present in males (Fig. 7A); elytra straight, with posterior transverse black band continuously arcuate (Fig. 7A, C)	***P. yasumatsui***
–	Anterior transverse black bands connected and lacking cluster of stout setae behind scutellum in males (Fig. 4A); elytra rounded, with posterior transverse black bands separately arcuate by suture (Fig. 4A, C)	***P. formosana***

Discussion

All species considered in this study definitely belong within *Paleosepharia*. This conclusion is based on the presence of subscutellar incised ridges on the elytra in males and the continuous elytral epipleurae and truncate apices. In males, the aedeagi of all species possess one paired cluster of short, basally hooked setae and one pair of elongate rows of slender and apically tapering lateral setae. Additionally, they possess two pairs of strongly sclerotized spiculae as Rizki et al. (2016) stated. An additional pair of elongate rows of large hooked spiculae from the apex to midpoint of the spiculae complex are found in males of *P. formosana*, *P. excavata*, and *P. yasumatsui*. An additional pair of extremely long, slender and apically curved speculae are found in males of *P. amiana* and *P. nantouensis*. However, the two moveable spines formed by the eighth tergites are not found in these Taiwanese species. Wagner and Bieneck (2012) speculated that the apically incised tectum is good character to separate *Paleosepharia* from other genera, but in Taiwanese species part of them (*P. excavata*, *P. formosana*, and *P. yasumatsui*) share this character. This character is not special for *Paleosepharia*. Additionally, the shapes of male aedeagi in *Paleosepharia* are characteristic: they recurve dorsally, not ventrally as in members of *Monolepta*. Female genitalic characters are similar and less diagnostic for species identification. However, the shape and number of bursal sclerites are unique and may prove to be synapomorphic for the genus.

Acknowledgements

I am grateful to the Taiwan Chrysomelid Research Team (TCRT) for assistance in collecting material, including Hou-Jay Chen, Jung-Chang Chen, Yi-Ting Chung, Bo-Xin Guo, Hsueh Lee, Wen-Chuan Liao, Mei-Hua Tsou, and Su-Fang Yu. I especially thank Chi-Lung Lee, and Hsing-Tzung Cheng for photos of specimens, and Chih-Kai Yang for identification of host plants. This study was supported by the Ministry of Science and Technology MOST 105-2313-B-055-001-MY2. I am grateful to Prof. Christopher Carlton (Louisiana State Arthropod Museum, USA) for reviewing the manuscript.

References

Beenen R (2010) Galerucinae. In: Löbl I, Smetana A (Eds) Catalogue of Palaearctic Coleoptera, Vol. 6. Apollo Books, Stenstrup, 443–491.

Chûjô M (1935) H. Sauter's. Formosa-Ausbeute: Subfamily Galerucinae (Coleoptera: Chrysomelidae). Arbeiten über Morphologische und Taxonomische Entomologie 2: 160–174.

Chûjô M (1938) H. Sauter's Formosa-Collection: subfamily Galerucinae (Coleoptera: Chrysomelidae). Arbeiten über Morphologische und Taxonomische Entomologie 5: 135–152.

Chûjô M (1962) A taxonomic study on the Chrysomelidae (Insecta: Coleoptera) from Formosa Part XI. Subfamily Galerucinae. The Philippine Journal of Science 91: 1–239.

Chûjô M (1965) Chrysomelid-beetles of Formosa (I). Special Bulletin of Lepidopterological Society Japan 1: 88–104.

Gressitt JL, Kimoto S (1963) The Chrysomelidae (Coleopt.) of China and Korea. Pacific Insects Monograph 1B: 301–1026.

Kimoto S (1965) A list of specimens of Chrysomelidae from Taiwan preserved in the Naturhistorisches Museum / Wien (Insecta: Coleoptera). Annalen des Naturhistorischen Museums in Wien 68: 485–490.

Kimoto S (1966) A list of the chrysomelid specimens of Taiwan preserved in the Zoological Museum, Berlin. Esakia 5: 21–38.

Kimoto S (1969) Motes on the Chryosmelidae from Taiwan II. Esakia 7: 1–68.

Kimoto S (1986) The Chrysomelidae (Insecta: Coleoptera) collected by the Nagoya University Scientific Expedition to Taiwan in 1984. Kurume University Journal 35: 53–62.

Kimoto S (1989) The Taiwanese Chrysomelidae (Insecta: Coleoptera) collected by Dr. Kintaro Baba, on the occasion of his entomological survey in 1983 and 1986. Kurume University Journal 38: 237–272.

Kimoto S (1991) The Taiwanese Chrysomelidae (Insecta: Coleoptera) collected by Dr. Kintaro Baba, on the occasion of his entomological survey in 1987, 1988 and 1989. Kurume University Journal 40: 1–27.

Kimoto S (1996) Notes on the Chrysomelidae from Taiwan, China. XIII. Entomologial Review of Japan, 51: 27–51.

Kimoto S, Chu YI (1996) Systematic catalog of Chrysomelidae of Taiwan (Insecta: Coleoptera). Bulletin of the Institute of Comparative Studies of International Cultures and Societies 16: 1–152.

Kimoto S, Takizawa H (1997) Leaf beetles (Chrysomelidae) of Taiwan. Tokai University Press, Tokyo, 581 pp.

Laboissière V (1938) Galerucinae (Col.) de la Chine. Du musée Stockholm. Arkiv för Zoologi 30 A: 1–9.

Lee C-F, Cheng H-T (2007) The Chrysomelidae of Taiwan 1. Sishou-Hills Insect Observation Network, New Taipei City, 199 pp. [In Chinese]

Lee C-F, Cheng H-T (2010) The Chrysomelidae of Taiwan 2. Sishou-Hills Insect Observation Network and Taiwan Agricultural Research Institute, COA, New Taipei City and Taichung City, 191 pp. [In Chinese]

Lee C-F, Tsou M-H, Cheng H-T (2016) The Chrysomelidae of Taiwan 3. Sishou-Hills Insect Observation Network, New Taipei City, 199 pp. [In Chinese]

Medvedev LN (2014) Revision of the genus *Paleosepharia* Laboissiere, 1936 (Coleoptera: Chrysomelidae) from Indochina. Russian Entomological Journal 23: 45–51.

Mohamedsaid MS (1996) *Paleosepharia* of Peninsular Malaysia (Coleoptera: Chrysomelidae: Galerucinae). Serangga 1: 7–21.

Nie R-E, Bezděk J, Yang X-K (2017) How many genera and species of Galerucinae s. str. do we know? Updated statistics (Coleoptera, Chrysomelidae). ZooKeys 720: 91–102. https://doi.org/10.3897/zookeys.720.13517

Rizki A, Hazmi IR, Ruslan MY, Idris AB (2014) Redescription of *Paleosepharia* azlani (Mohamedsaid, 1998) (Coleoptera: Chrysomelidae: Galerucinae). Serangga 19: 31–38.

Rizki A, Hazmi IR, Wagner T, Idris AB (2016) Redescription of *Paleosepharia* trunctata Laboissière, 1936, type species of the genus *Paleosepharia* Laboissière, 1936 (Coleoptera: Chrysomelidae: Galerucinae). The Coleopterists Bulletin 70: 395–398. https://doi.org/10.1649/0010-065X-70.2.395

Wagner T, Bieneck S (2012) Galerucine type material described by Victor Motschulsky in 1858 and 1866 from the Zoological Museum Moscow (Coleoptera: Chrysomelidae, Galerucinae). Entomologische Zeitschrift 122: 205–216.

Yang X-K, Ge S, Nie R, Ruan Y, Li W (2015) Chinese leaf beetles. Science Press, Beijing, 507 pp.

ZooKeys 744: 43–47 (2018)
doi: 10.3897/zookeys.744.23318
http://zookeys.pensoft.net

RESEARCH ARTICLE

A peer-reviewed open-access journal
ZooKeys
Launched to accelerate biodiversity research

First record of *Arthromelodes* Jeannel in China, with description of a new species (Coleoptera, Staphylinidae, Pselaphinae)

Zi-Wei Yin[1]

1 *Department of Biology, College of Life and Environmental Sciences, Shanghai Normal University, Shanghai, China*

Corresponding author: *Zi-Wei Yin* (pselaphinae@gmail.com)

Academic editor: *A. Brunke* | Received 29 December 2017 | Accepted 28 February 2018 | Published 19 March 2018

http://zoobank.org/A150F9F7-2EDF-42C8-96D6-03FD0193C03C

Citation: Yin Z-W (2018) First record of *Arthromelodes* Jeannel in China, with description of a new species (Coleoptera, Staphylinidae, Pselaphinae). ZooKeys 744: 43–47. https://doi.org/10.3897/zookeys.744.23318

Abstract
A new species of *Arthromelodes* Jeannel, *A. choui* **sp. n.**, is described from northern Taitung, Taiwan, representing the first record of the genus in China. The species is distinctive, and may be readily separated from its congeners by the unique structures of male tergite 1(IV), and the aedeagus.

Keywords
Arthromelodes, China, new species, Pselaphinae, Taiwan, taxonomy

Introduction

The genus *Arthromelodes* Jeannel of the pselaphine tribe Batrisini is a group of modest size containing 21 species and subspecies distributed in Japan (20 spp.) and Vietnam (1 sp.) (Jeannel 1954, 1957–1958; Nomura 1991; Arai 2002). This genus was included in Jeannel's fifth division of the Batrisina (Jeannel 1958, 1959) and Nomura's '*Batrisocenus* complex of genera' (Nomura 1991) of Asian Batrisini, where members share a median and a pair of lateral longitudinal sulci, and a complete transverse antebasal sulcus on the pronotum, the lack of lateral or discal spines on the pronotum, the presence of two basal foveae on each elytron, and an elongate abdominal tergite 1(IV). *Arthromelodes* resembles *Batrisocenus* Raffray (also *Physomerinus* Jeannel and *Batriscenaulax* Jeannel) and *Batrisceniola* Jeannel in most external features (probably due to extensive homoplasy of characters), and under current definition may be separated from the former only by the aedeagus with a moderately developed basal capsule (capsule is strongly reduced in *Batrisocenus*; *e.g.*, Chandler 2001: 264), and from the latter by the lack of a median bunch of erect setae on tergite 4(VII) (bunched setae are present on tergite 4 in both sexes of *Batrisceniola*; *e.g.*, Yin and Li 2014). Within *Arthromelodes*, species are usually easy to determine thanks to the distinct sexual modifications of the male metatibiae (usually present), and of abdominal tergites 1(IV) and 4(VII).

A large series of pselaphine beetles collected in Taiwan by Dr. Wen-I Chou was recently sent to me for identification. A majority of the specimens belong to four species: *Cratna abdominalis* Löbl (347 specimens), *Taiwanophodes minor* Hlaváč (282 specimens), *Pselaphodes linae* Yin & Li (123 specimens), and *Batraxis splendida* Nomura (31 specimens); the rest include a *Labomimus* sp. (36 specimens), a *Batrisoschema* sp. (2 specimens), and a new species of *Arthromelodes* (8 specimens), representing the first record of this genus in China, which is described and compared to similar congeners here.

Materials and methods

The type series is deposited in the Insect Collection of the Shanghai Normal University, Shanghai, China (**SNUC**), and the National Museum of Natural Science, Taichung, Taiwan (**NMNS**). The collecting data of the material are quoted verbatim; information not included on the label is placed in parentheses. Following Chandler (2001), the abdominal tergites and sternites are given Arabic numerals for visible sclerites, and Roman numerals indicate the morphological position. Habitus image (Fig. 1A) was taken using a Canon 5D Mark III camera in conjunction with a Canon MP-E 65 mm f/2.8 1–5× Macro Lens, and a Canon MT-24EX Macro Twin Lite Flash was used as light source. Images of the morphological details (Fig. 1B–G) were produced using a Canon G9 camera mounted on an Olympus CX31 microscope under transmitted or reflected light. Zerene Stacker version 1.04 was used for image stacking. All images were edited and grouped in Adobe Photoshop CS5 Extended.

Taxonomy

Arthromelodes choui **sp. n.**
http://zoobank.org/619D8A25-690D-472A-9346-82C1E465F684
Fig. 1

Type material (8 specimens)**. Holotype: CHINA:** ♂: 'Taiwan, Taitung County (台东县), Haiduan Township (海端乡), Lidao (利稻), 23°10'55"N, 120°57'53"E, 1150 m,

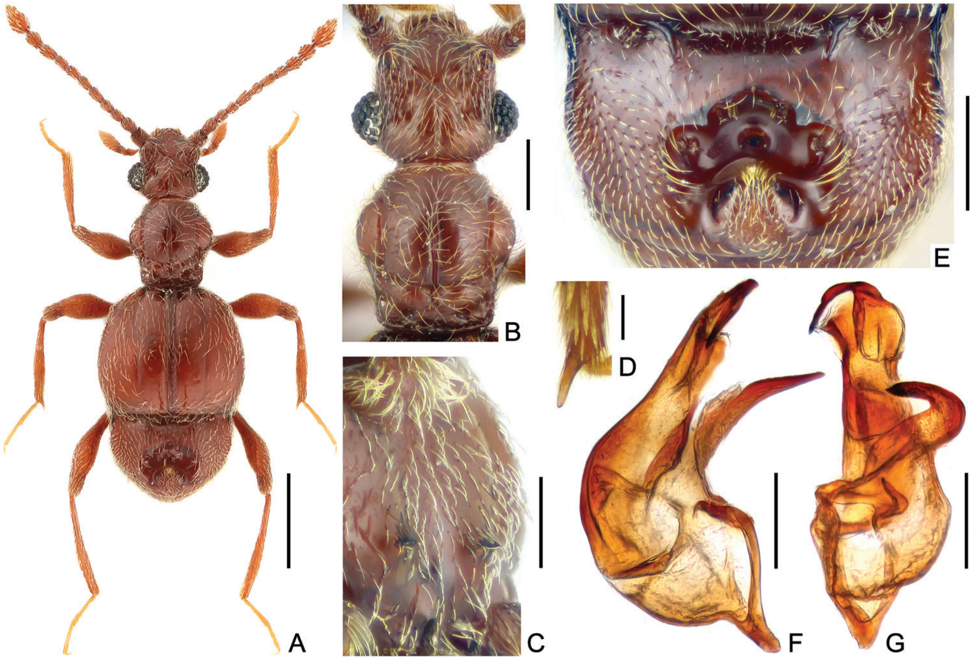

Figure 1. *Arthromelodes choui* sp. n., male. **A** habitus **B** head and pronotum **C** metaventrite, showing laminar projections at the middle **D** apex of mesotibia **E** tergite 1(IV), showing abdominal modification **F–G** Aedeagus, in lateral (**F**), and ventral (**G**) view. Scale bars: 0.5 mm (**A**); 0.2 mm (**B, E**); 0.1 mm (**C, F–G**); 0.05 mm (**D**).

24.iii.2017, light trap, Chou Wen-I leg.' (in SNUC). **Paratype: CHINA:** 7 ♂♂, same collecting data as the holotype (5 in SNUC, 2 in NMNS).

Diagnosis of male. Body length slightly more than 2 mm; metaventrite with pair of laminar projections; abdominal tergite 1(IV) with large cavity at posterior half, lateral setiferous patches composed of short setae and weakly demarcated; legs lacking modifications, except mesotibia with distinct apical spur; aedeagus with median lobe strongly curved rightwards apically, dorsal lobe erect, and strongly narrowed and curved downwards at apex.

Description. Male (Fig. 1A). Length 2.09–2.22 mm; body reddish-brown, maxillary palpi and tarsi lighter. Head and pronotum (Fig. 1B) sparsely punctate. Head slightly wider than long, length from anterior margin of clypeus to head base 0.40–0.42 mm, width across compound eyes 0.44–0.47 mm; each eye composed of about 30 facets. Antennal clubs loosely formed by apical three antennomeres. Pronotum about as long as wide, length along midline 0.46–0.48 mm, maximum width 0.44–0.48 mm; lateral margins rounded at middle, constricted and nearly parallel at basal 1/3. Elytra wider than long, length along suture 0.66–0.72 mm, maximum width 0.77–0.83 mm; shallow discal striae reaching past 3/4 of elytral length; marginal sulcus complete; with slight denticle at humeral angle. Metaventrite with one pair of laminar projections (Fig. 1C) at middle. Mesotrochanter slightly protuberant at ventral margin; mesotibia with distinct apical spur (Fig. 1D). Abdomen slightly narrower than elytra, length of dorsally visible part posterior to elytra along midline 0.57–0.60 mm, maximum width 0.65–0.68 mm; tergite 1(IV) (Fig. 1E) much longer than 2–4 (V–VII) combined, deeply and broadly concaved at posteromedian portion, anterior margin of cavity angularly protruding posteriorly, with two pairs of secretory setae, elongate setae along lateral margins pointed posteromedially, bottom of cavity glabrous, with two pairs of secretory setae at middle and at sides, with one large nodule located posterior of cavity, setiferous lateral patches composed of short setae and weakly demarcated. Aedeagus (Fig. 1F–G) asymmetric, length 0.37 mm; median lobe strongly curved rightwards apically, capsule with distinct basoventral projection; parameres fused and reduced to ventral membrane; dorsal lobe erect, strongly narrowed and curved downwards at apex.

Female. Unknown.

Comments. Using the key in Nomura (1991), *Arthromelodes choui* would key out at couplet 9 with *A. sinuatipes* Nomura and *A. aizuanus* Nomura. These three species share the presence of a cavity on male tergite 1(IV), a nodule placed posterior to the cavity, as well as a pair of setiferous patches lateral to the cavity. *Arthromelodes choui* may be readily separated from *A. sinuatipes* by the less laterally expanded margins of tergite 1, the less demarcated setiferous patches, the sinuate anterior margin of tergal cavity, and the much less transverse basal capsule of the aedeagus; and from *A. aizuanus* by the much larger abdominal cavity, the broader and less demarcated setiferous patches, and much shorter basoventral projection of the aedeagus. A similar tergal cavity and nodule are also present in *A. dilatatus* (Raffray) (with four subspecies), but this species can be easily characterized by the distinct lateral expansions at sides of tergite 1(IV), while the new species lacks such structures. Arai (2002) described *A. watanabei* Arai from Honshu, Japan, and this species may be separated from *A. choui* by the cavity on tergite 1 being much smaller and shallower, and by the form of the aedeagus (Arai, 2002: figs 1, 6–7). According to the description and figures in Jeannel (1954: 249), *A. choui* may be well-separated from *A. carieri* Jeannel (type species of *Arthromelodes*) from Vietnam again by the different structures of the male tergal cavity and aedeagus.

Distribution. Southern China: Taiwan.

Etymology. The specific epithet is dedicated to my friend Wen-I Chou, a Taiwanese specialist of Cerambycidae, who collected the type series of the new species.

Acknowledgments

I am grateful to Wen-I Chou for collecting and donation of the material used in this paper. Donald Chandler (University of New Hampshire, Durham, USA) and Shûhei Nomura (National Museum of Nature and Science, Tsukuba, Japan) read a previous draft and provided helpful comments. The present study was supported by the National Science Foundation of China (No. 31501874).

References

Arai S (2002) A new species of the genus *Arthromelodes* (Coleoptera, Staphylinidae, Pselaphinae) from Kanto District, central Japan. Special Bulletin of the Japanese Society of Coleopterology 5: 275–279.

Chandler DS (2001) Biology, morphology and systematics of the ant-like litter beetles of Australia (Coleoptera: Staphylinidae: Pselaphinae). Memoirs on Entomology, International 15: 1– 560.

Jeannel R (1954) Les Psélaphides de Madagascar. Mémoires de l'Institut Scientifique de Madagascar (E: Entomologie) 4: 139–344.

Jeannel R (1957) Sur quelques Psélaphides du Tonkin recueillis par le Père A. de Cooman. Revue Française d'Entomologie 24(1): 5–32.

Jeannel R (1958) Révision des Psélaphides du Japon. Mémoires du Muséum National d'Histoire Naturelle (A: Zoologie) 18: 1–138.

Jeannel R (1959) Révision des Psélaphides de l'Afrique intertropicale. Annales du Musée Royal du Congo Belge, Tervuren (Série 8: Sciences Zoologiques) 75: 1–742.

Nomura S (1991) Systematic study on the genus *Batrisoplisus* and its allied genera from Japan (Coleoptera, Pselaphidae). Esakia 30: 1–462.

Yin ZW, Li LZ (2014) *Batrisceniola fengtingae* sp. nov., the first record of the genus in China (Coleoptera: Staphylinidae: Pselaphinae). Acta Entomologica Musei Nationalis Pragae 54: 233–236.

ZooKeys 744: 49–65 (2018)
doi: 10.3897/zookeys.744.22421
http://zookeys.pensoft.net

RESEARCH ARTICLE

A peer-reviewed open-access journal
ZooKeys
Launched to accelerate biodiversity research

The leaf-mining genus *Antispila* Hübner, 1825 feeding on Vitaceae in Shandong Peninsula, China with one new species (Lepidoptera, Heliozelidae)

Nan Wang[1], Tengteng Liu[1], Jiasheng Xu[2], Bin Jiang[3,4]

1 *Shandong Provincial Key Laboratory of Animal Resistance Biology, College of Life Sciences, Shandong Normal University, Jinan 250014, P. R. China* **2** *School of Life and Environmental Science, Gannan Normal University, Ganzhou 341000, P. R. China* **3** *Kunyushan Forest Farm, Yantai 264002, P. R. China* **4** *Kunyushan National Nature Reverse, Yantai 264002, P. R. China*

Corresponding author: *Tengteng Liu* (liutt@sdnu.edu.cn)

Academic editor: *E. van Nieukerken* | Received 21 November 2017 | Accepted 7 March 2018 | Published 19 March 2018

http://zoobank.org/40FD3262-DCB4-45A3-82AC-8474D3E7026A

Citation: Wang N, Liu T, Xu J, Jiang B (2018) The leaf-mining genus *Antispila* Hübner, 1825 feeding on Vitaceae in Shandong Peninsula, China with one new species (Lepidoptera, Heliozelidae). ZooKeys 744: 49–65. https://doi.org/10.3897/zookeys.744.22421

Abstract

The *Antispila* species feeding on Vitaceae from Shandong Peninsula, China are treated. *Antispila kunyuensis* Liu, **sp. n.**, feeding on *Ampelopsis humulifolia*, is described as new to science, and *A. uenoi* Kuroko, 1987, feeding on *Vitis amurensis*, is recorded as new for China. *Vitis amurensis* is documented as a new host plant for *A. uenoi*. The adult male and female, host plant and typical patterns of leaf-mines of both species are illustrated, as are male and female genitalia and venation. The venation and the paired tufts of scales on the 7th abdominal segment in male are illustrated for *A. uenoi* for the first time. DNA barcodes of both species are also provided, together with a neighbor-joining tree for facilitating species delimitation.

Keywords

Ampelopsis, *Antispila*, China, DNA barcode, Heliozelidae, Lepidoptera, new species, Shandong Peninsula, *Vitis*

Introduction

The family Heliozelidae comprises 126 described species in 12 genera (van Nieukerken et al. 2011, 2012, van Nieukerken and Geertsema 2015, Liu and Wang 2017), with the largest diversity in North America and Australia. The Heliozelidae were only recently recorded as new for China, with one formally published species (Liu and Wang 2017), but also several database records in BOLD (http://www.boldsystems.org). However, the knowledge of Chinese Heliozelidae is slowly increasing, and two more species feeding on Vitaceae are described in the present paper. Vitaceae comprises an important group of hosts for Heliozelidae, especially for the genus *Antispila* Hübner, 1825 (van Nieukerken et al. 2012). Eleven out of the 20 Palearctic and Oriental species of *Antispila* feed on Vitaceae (Meyrick 1926, Kuroko 1961, 1987, van Nieukerken et al. 2012, van Nieukerken and Geertsema 2015).

Shandong Peninsula is located in the east of China, facing the Korean Peninsula across the Yellow Sea. Although located in a relatively developed region, the arthropod diversity is still rather poorly known and lacks systematic work, so new species, especially small-sized ones, can still be discovered. Here, we discovered two species of the leaf-mining genus *Antispila* during an ongoing biodiversity exploration in Shandong Peninsula. One of these is a new species, the other one, *A. uenoi* Kuroko, 1987 is new for China. Both are described here in detail, increasing the number of known species of the genus *Antispila* in China to three.

Material and methods

Leaves with active mines were placed in small plastic bags for rearing. After the shields had been exscinded and the larvae had left the mines, leaves with vacant leaf-mines were dried in a plant press. The larval shields, the corresponding adults, and the vacant leaf-mines were identically coded.

Genitalia and wings were dissected and mounted according to the methods introduced by Li (2002), but stained with Eosin Y and/or Chlorazol Black. Illustrations were prepared by using a Leica DM1000 microscope. Adult photographs were taken with a Leica S6D stereo microscope. Photographs of the host plants and leaf-mines were taken in the field using a Canon EOS 650D camera plus a Macro Lens, and enlarged photographs of leaf-mines were taken with the Leica S6D stereo microscope.

DNA was extracted from adult specimens preserved in 95% ethanol in Shandong Normal University, Jinan, China, with the whole body skeleton including genitalia and wings preserved as vouchers (Knölke et al. 2005). Protocols for total DNA extraction and mitochondrial COI gene amplification followed that described in our previous study (Liu and Wang 2017). The sequence data used in this study have been deposited in GenBank and in the BOLD database, a public dataset "DS-ANTIVIT" (https://doi.org/10.5883/DS-ANTIVIT). Sequences were aligned using the MUSCLE model and genetic distance estimation was analyzed using the Kimura 2-Parameter model in BOLD.

Terminology for adults follows van Nieukerken et al. (2012); the term canalis spiralis of female genitalia follows Kuroko (1987). The classification of the host plants is based on APG (2016), and plant scientific names follow The Plant List (2013).

All the specimens examined, including the holotype of the new species, are deposited in the Zoological Collection of Shandong Normal University (**SDNU**). The type depository of *A. uenoi* Kuroko, 1987, collection of the Entomological Laboratory, University of Osaka Prefecture, is abbreviated as **UOP**.

Taxonomy

Antispila kunyuensis **Liu, sp. n.**
http://zoobank.org/25296AE0-2076-4A19-913B-617825812FF4
Figs 1, 2, 6, 9, 11–15, 26–29, 34–38

Type material. Holotype. ♂, China, Shandong Province, Yantai, Mt. Kunyu National Nature Reverse, 121.740°E, 37.292°N, 400 m, larva coll. 2017.vi.28, mine on *Ampelopsis humulifolia*, emerged viii.06, collector Bin Jiang, genitalia no. SDNU. LIU0014, registered no. SDNU.YT170601.2. **Paratypes**. 3♂, 3♀, genitalia nos. SDNU.LIU0009♂, SDNU.LIU0016♀, SDNU.LIU0044♂, DNA voucher slide no. SDNU.LIU0013♀ (whole body on one slide), registered nos. SDNU.YT170601.1, SDNU.YT170601.3–6, other data same as holotype.

Other material. Leaf-mine. Shandong Province: Yantai, Mt. Kunyu National Nature Reverse, 121.740°E, 37.292°N, 400 m, vacant mine coll. 2016.vii.31, on *Ampelopsis humulifolia*, collector Tengteng Liu & Encui Wang, registered no. SDNU. YT160761–7, YT160785.

Diagnosis. Two *Antispila* species, *A. ampelopsia* Kuroko, 1961 and *A. orbiculella* Kuroko, 1961, are known to feed on *Ampelopsis*, and both associate with the same species, *A. brevipedunculata*. *Antispila kunyuensis* can easily be distinguished from *A. ampelopsia* by the fine features of the phallus and the ovipositor, and from *A. orbiculella* by the two separate basal spots that are joined forming a transverse fascia in the forewing.

Description. Adult (Figs 1, 2, 6). Forewing length 1.7–2.1 mm. Head silvery gray, with reddish reflection, more apparent on front. Antennae dark fuscous, silvery gray on distal two segments. Labial palpus silvery gray, pointed apically. Thorax and tegula dark fuscous. Legs gray, with blackish gray pigmentation outer surface. Forewing dark fuscous, with strong reddish reflection; two pairs of opposite triangular silvery spots on costa and dorsum, the inner pair with costal spot before middle, dorsal spot at basal 1/4, the outer pair with costal spot at 3/4, dorsal spot largest, near tornus; cilia unicolorous with forewing on basal 3/4, whitish gray on distal 1/4. Hind wing dark gray, cilia darker. Abdomen dark gray dorsally, yellowish gray ventrally.

Venation (Fig. 9). Forewing with Sc reaching before middle on costa; R_1 from 2/5 on upper margin of cell to costal 3/5, Rs_1 from distal 1/7 on upper margin of cell to costal 3/4, Rs_2 from beyond distal end of cell, Rs_{3+4} reaching costa before apex; cell tri-

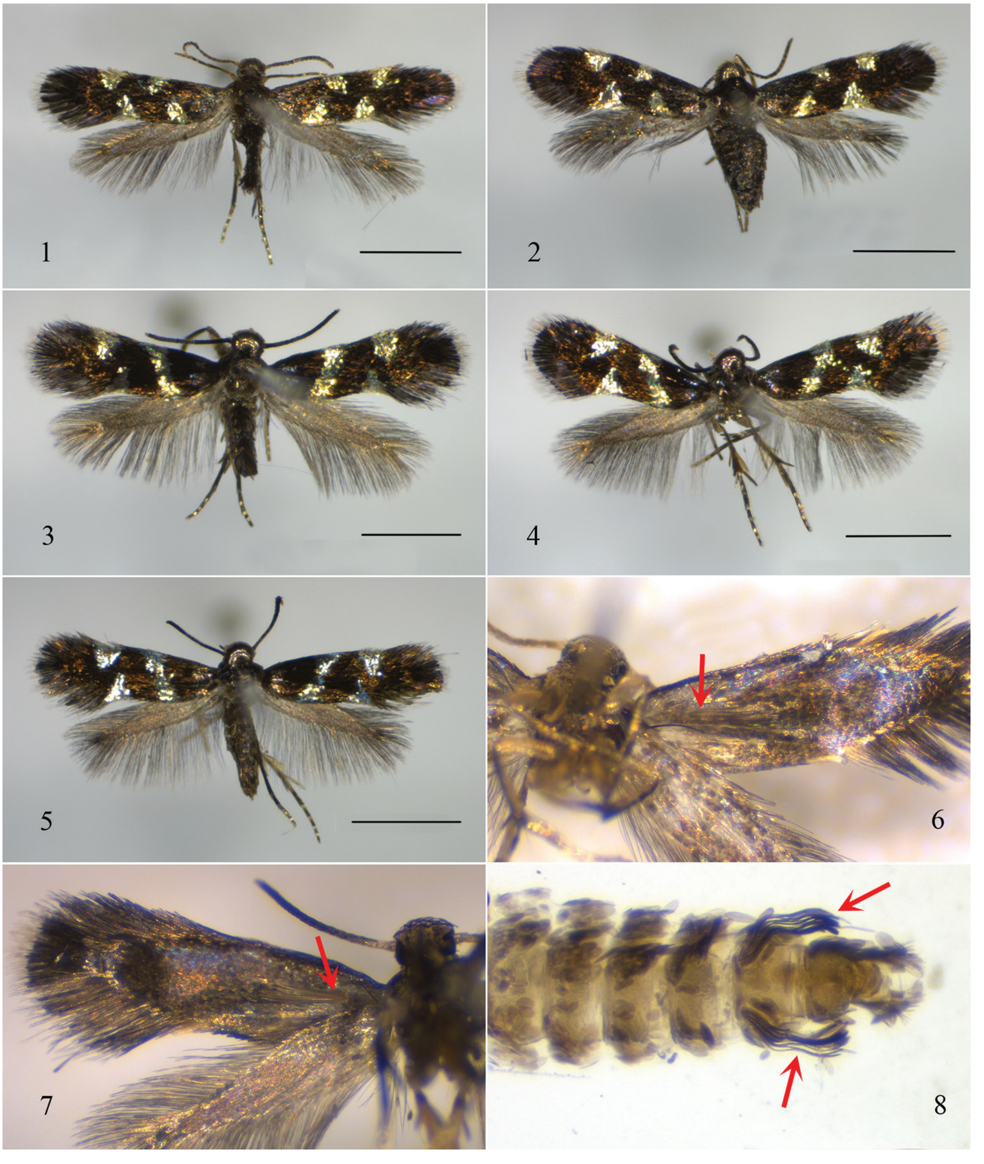

Figures 1–8. Adult of *Antispila* species. **1** *A. kunyuensis*, holotype, male, SDNU.QD170705.1 **2** *A. kunyuensis* sp. n., paratype, female, SDNU.YT170601.4 **3** *A. uenoi*, male, SDNU.QD170705.1 **4** *A. uenoi*, female, SDNU.QD170705.3 **5** *A. uenoi*, female, SDNU.QD170707 **6** *A. kunyuensis*, male, paratype, ventral view of forewing indicating bristles of retinaculum, SDNU.YT170601.3 **7** *A. uenoi*, ventral view of forewing indicating bristles of retinaculum **8** *A. uenoi*, male, indicating paired tufts of slender scales on the 7th abdominal segment, photographed during dissection in water, SDNU.QD170705.1. Scale bars: 1.0 mm.

angular distally; M_1 stalked with Rs_{3+4}, to termen near apex, M_{2+3} from near distal end of cell; CuA from distal 1/6 of lower margin of cell; A_{1+2} to beyond middle of dorsum. Hindwing with Sc to costal 3/5, R+M ending in 3 branches: Rs to costa near apex, M_2

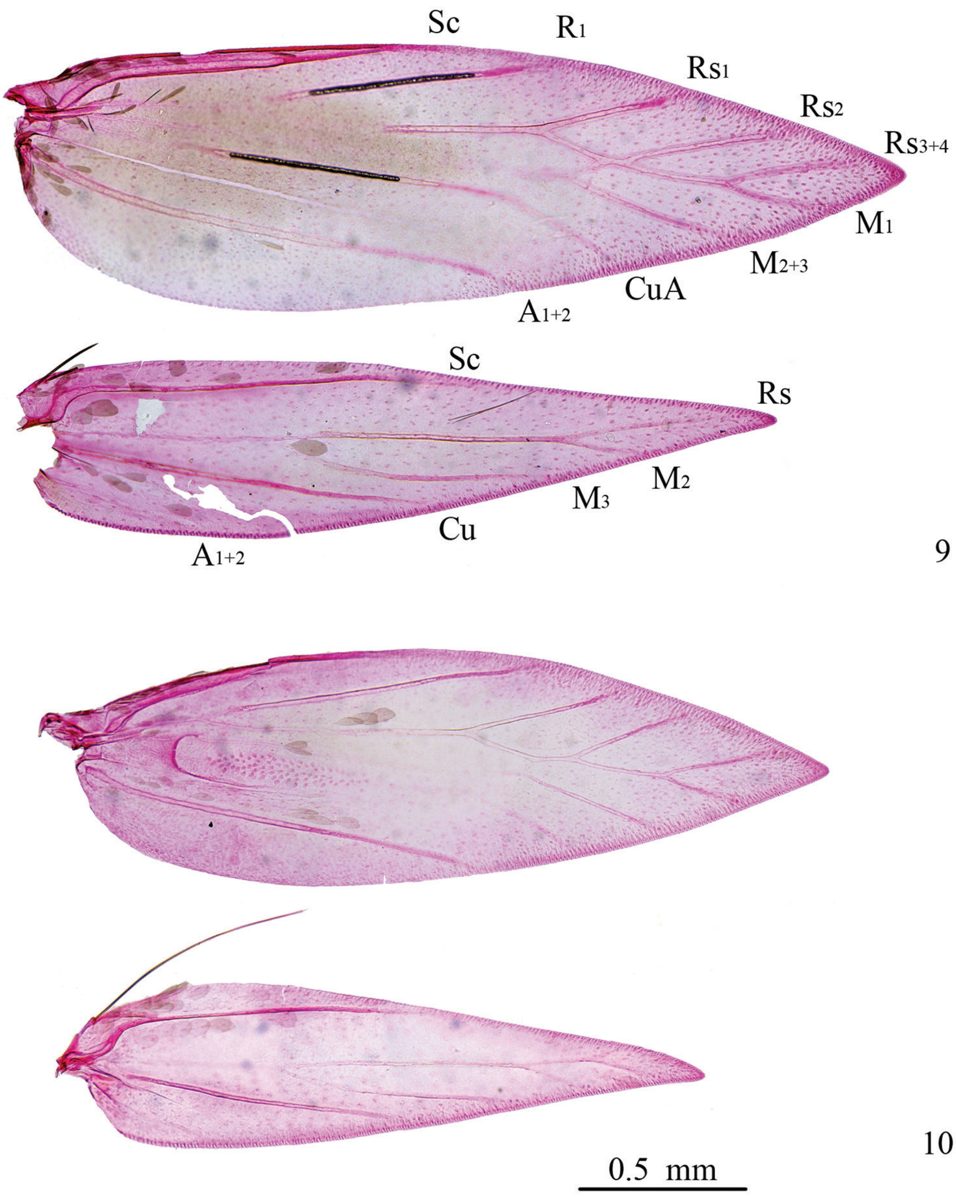

Figures 9–10. Wing venation of *Antispila* species. **9** *A. kunyuensis*, paratype, female, SDNU.LIU0013 **10** *A. uenoi*, male, SDNU.LIU0012.

and M_3 to dorsum; Cu to middle of dorsum; A_{1+2} weak. Male with one long frenulum, female bearing two shorter frenular bristles.

Male genitalia (Figs 11–15). Tuba analis developed (Fig. 12). Uncus bar-shaped, protruded towards posteriorly at middle. Vinculum shorter than phallus, slightly rectangular on anterior margin. Valva more or less triangular, digital process long and

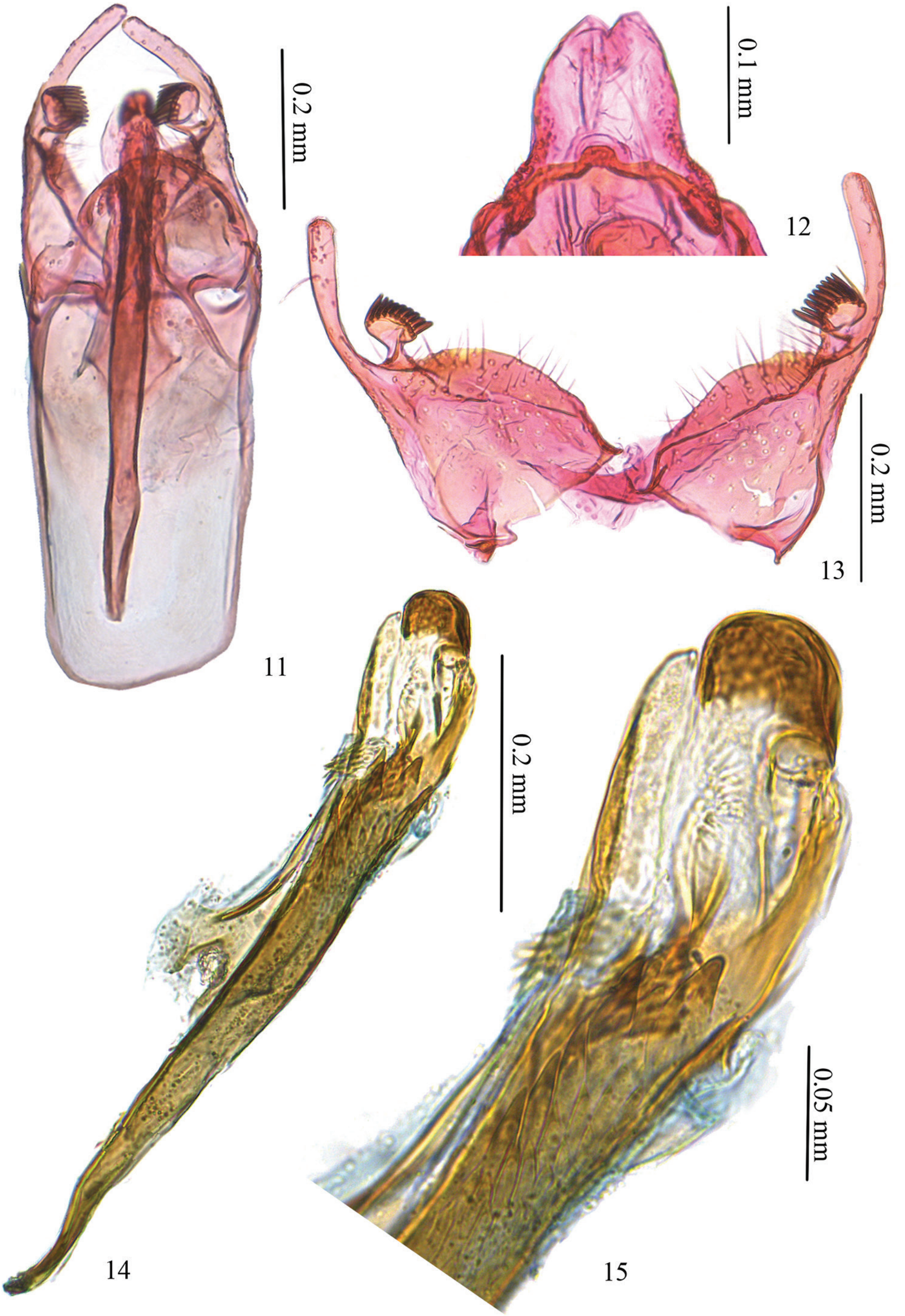

Figures 11–15. Male genitalia of *Antispila kunyuensis*. **11** whole genitalia, SDNU.LIU0014 **12** tegumen, SDNU.LIU0009 **13** valva, same slide as 12 **14** phallus, lateral view, SDNU.LIU0044 **15** enlarged distal part of phallus, same slide as 14.

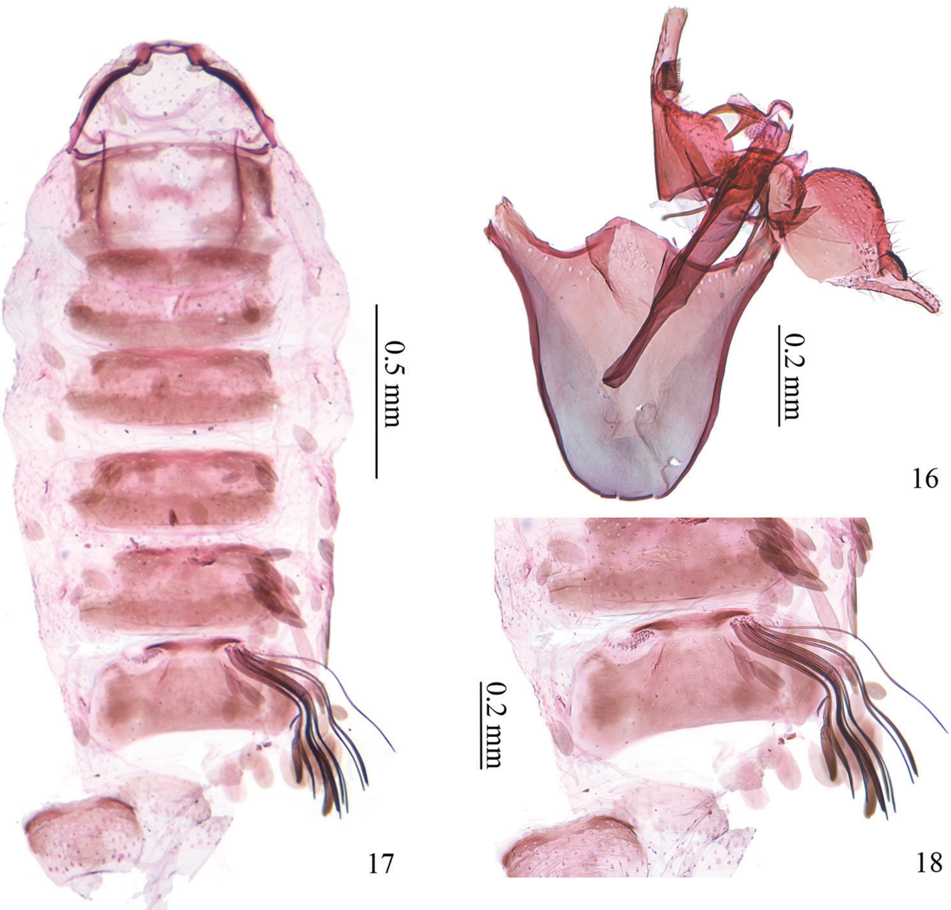

Figures 16–18. Male genitalia and abdomen of *Antispila uenoi*. **16** whole male genitalia, unrolled, SDNU.LIU0015 **17** abdomen, ventral view, notice the tuft of slender scales on the 7th segment, left tuft detached, same slide as 16 **18** enlarged view of tuft of slender scales, same slide as 16.

narrow, almost same length as valva, pecten on pedicel, with nine comb teeth (Fig. 13). Juxta half as long as phallus, densely covered with small teeth on basal 2/5, anterior arrow pointed on basal corners. Phallus nearly as long as length of vinculum + tegumen, narrowed anteriorly (Fig. 11); phallotheca with five to six strong teeth and a group of smaller sharp-pointed teeth, with a cluster of smaller spines at base of juxta; distal part with a mushroom-shaped process and a straight process ventrally (Figs 14, 15).

Female genitalia (Figs 26–29). Ovipositor with three cusps at either side, with basal one largest and middle one smallest (Fig. 28). Vestibulum round, more or less sclerotized (Fig. 29). Corpus bursae membranous.

DNA barcode. One DNA barcode from a paratype was obtained. A neighbor-joining tree, covering most Asian *Antispila* species and other Vitaceae-feeding species, was generated for facilitating species delimitation (Fig. 33).

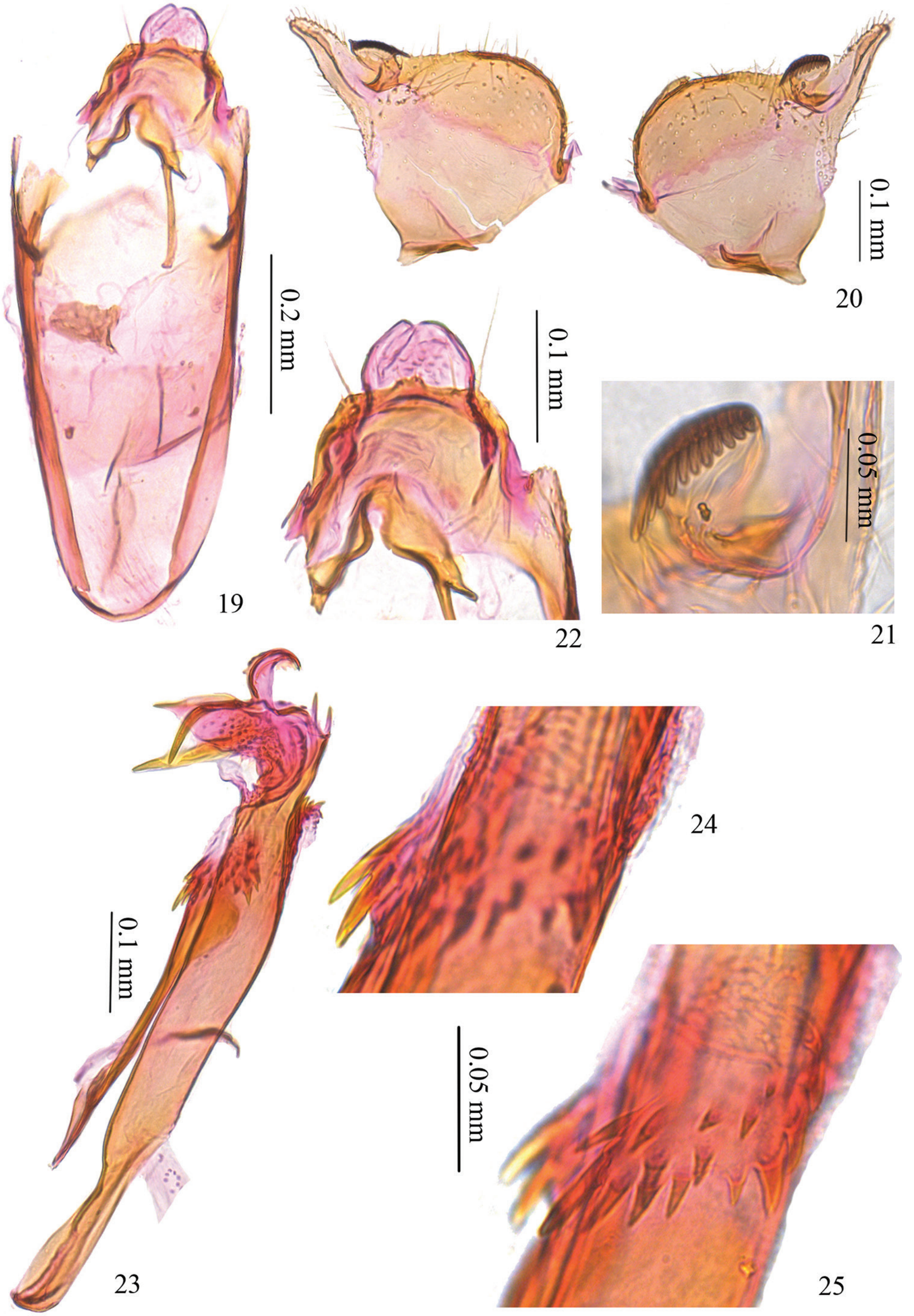

Figures 19–25. Male genitalia of *Antispila uenoi*. **19–23** SDNU.LIU0011 **19** tegumen and vinculum, **20** valva **21** enlarged view of comb **22** tegumen **23** phallus, lateral view **24** enlarged view of spines on base of juxta, SDNU.LIU0012 **25** same part as 24 under a shallow focus.

Host plant. *Ampelopsis humulifolia* Bunge (Figs 34, 35). The placement of the leaf-mines is variable (Figs 36–38), from the base to the apex of a leaf, from absolutely along veins to between but not touching veins. This results in variably-shaped blotch mines, but the majority of blotches are more or less round (Figs 38, 42–45). Frass primarily occupies the opposite side of the cut-out in round blotch mines, or occasionally disperses throughout the mine (Fig. 37), but always in a broad medial band in wide gallery mines (Fig. 38). This species overwinters as a prepupa in the shield. A single generation per year was observed at the type locality.

Distribution. China (Shandong).

Etymology. The specific name is derived from the type locality of the new species, Mt. Kunyu, representing the most famous nature reserve in Shandong Peninsula, focusing on forest ecosystem conservation.

Antispila uenoi Kuroko, 1987

Figs 3–5, 7, 8, 10, 16–25, 30–31, 39–41, 46–49

Antispila uenoi Kuroko, 1987: 113. TL: Japan (Iwate Prefecture). TD: UOP.

Material examined. China: 2♂, 3♀, Mt. Laoshan, Qingdao, Shandong Province, 120.609°E, 36.204°N, 400 m, larva coll. 2017.vii.01, mine on leaf serration of *Vitis amurensis*, case made vii.03, emerged vii.15, collectors Tengteng Liu and Nan Wang, genitalia no. SDNU.LIU0008♀, SDNU.LIU0015♂, DNA voucher slide no. SDNU.LIU0011♂ (whole body on one slide), registered no. SDNU.QD170705.1–3; 2♂, 2♀, Mt. Laoshan, Qingdao, Shandong Province, 120.609°E, 36.204°N, 400 m, larva coll. 2017.vii.01, mine on leaf basal area, case made vii.03, emerged vii.15, genitalia no. SDNU.LIU0043♀, DNA voucher slide no. SDNU.LIU0012♂ (whole body on one slide), collectors Tengteng Liu and Zhenquan Gao, registered nos. SDNU.QD170707, SDNU.QD1707.1–2.

Diagnosis. Kuroko (1987) gave a detailed diagnosis to distinguish *A. uenoi* from *A. ampelopsia*.

Description. *Adult* (Figs 3–5, 7). Forewing length 1.6–1.8 mm. Head silvery gray, with reddish and purple reflection. Antennae dark fuscous, silvery on distal two segments. Labial palpus silvery gray, pointed apically. Thorax and tegula dark fuscous. Legs black, with whitish gray pigmentation on distal part of tarsomeres. Forewing blackish fuscous, with strong purple reflection; an oblique silvery fascia from before middle on costa to basal 1/4 on dorsum, a triangular silvery spot on costal 3/4, with a similar one opposite to it near tornus; cilia unicolorous with forewing on basal 3/4, whitish gray on distal 1/4. Hind wing gray, cilia darker. Abdomen dark gray dorsally, gray ventrally.

Female with forewing patterns more distinct (Figs 4, 5).

Venation (Fig. 10). Forewing with Sc reaching before middle on costa; R_1 from 2/5 on upper margin of cell to costal 3/5, Rs_1 from distal 1/7 on upper margin of cell to costal 3/4, Rs_2 from well beyond distal end of cell, Rs_{3+4} reaching costa before apex; cell

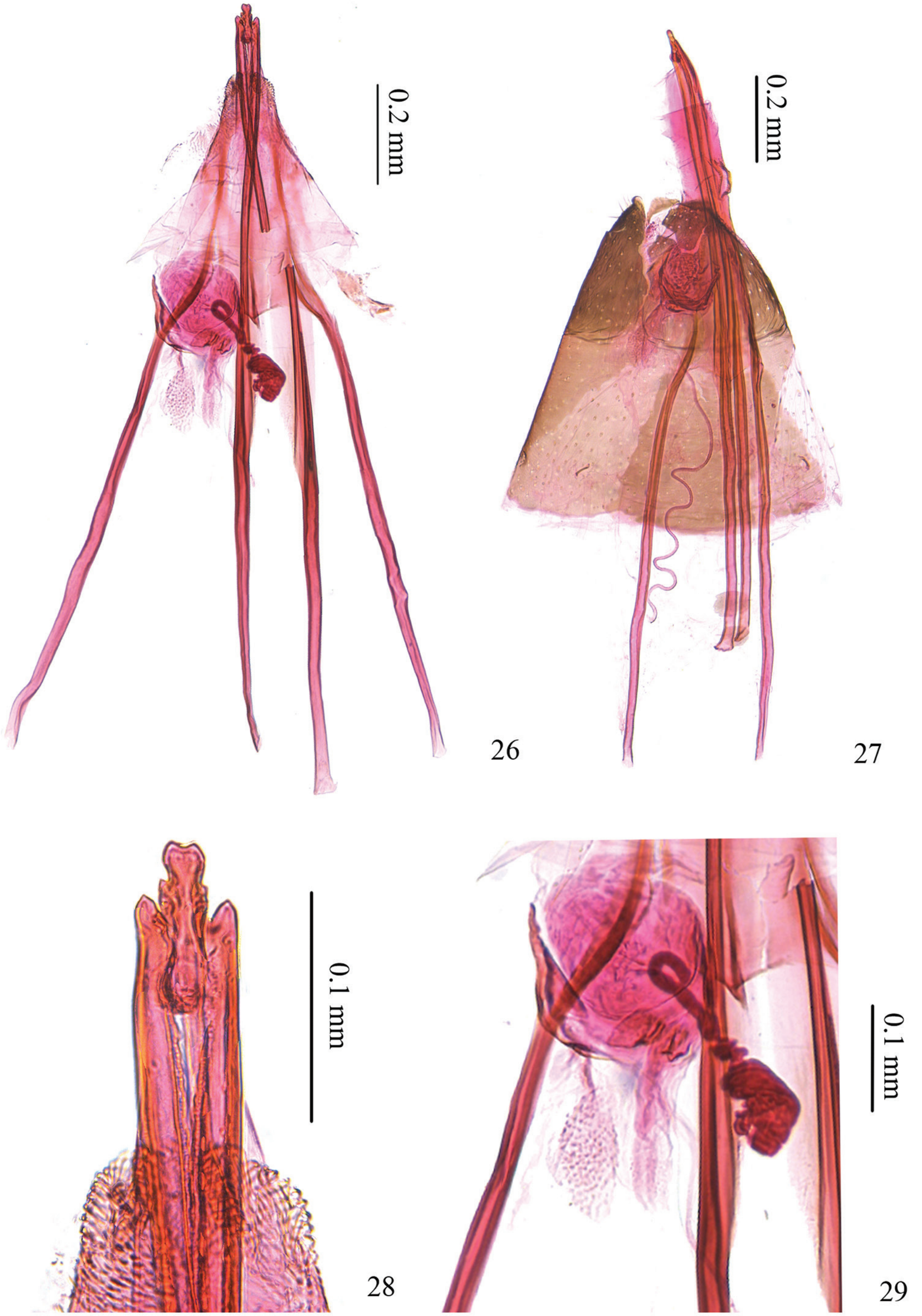

Figures 26–29. Female genitalia of *Antispila kunyuensis*. **26** female genitalia, SDNU.LIU0016 **27** female genitalia, SDNU.LIU0013 **28** detail of ovipositor tip, same slide as 26 **29** detail of vestibulum, same slide as 26.

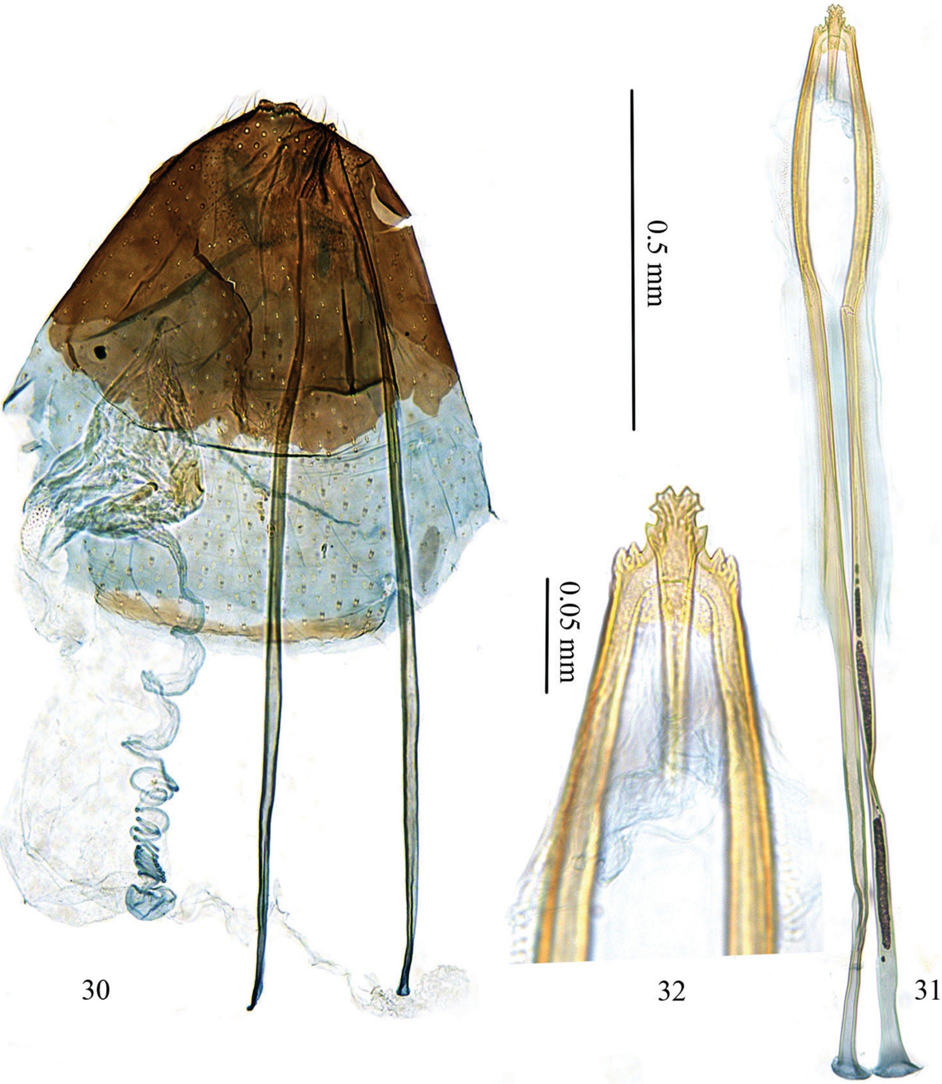

Figures 30–32. Female genitalia of *Antispila uenoi*. **30** female genitalia, SDNU.LIU0043 **31** posterior apophyses and ovipositor tip, same slide as 30 **32** detail of ovipositor tip, same slide as 30.

truncated distally; M_1 stalked with Rs_{3+4}, to termen near apex, M_{2+3} from lower corner of distal end of cell; CuA from distal 1/7 of lower margin of cell; A_{1+2} to beyond middle of dorsum. Hindwing with Sc to beyond middle of costa, R+M ending in 4 branches: Rs to costa, M_1 to dorsum near apex, M_2 and M_3 to dorsum; Cu to middle of dorsum; A_{1+2} weak. Male with one long frenulum, female bearing two shorter frenular bristles.

Male genitalia (Figs 16–25). Tuba analis developed. Uncus bar-shaped, with two papillae bearing two short setae each at middle, bearing one long and a few shorter setae laterally (Fig. 22). Vinculum shorter than phallus, rounded on anterior margin. Valva

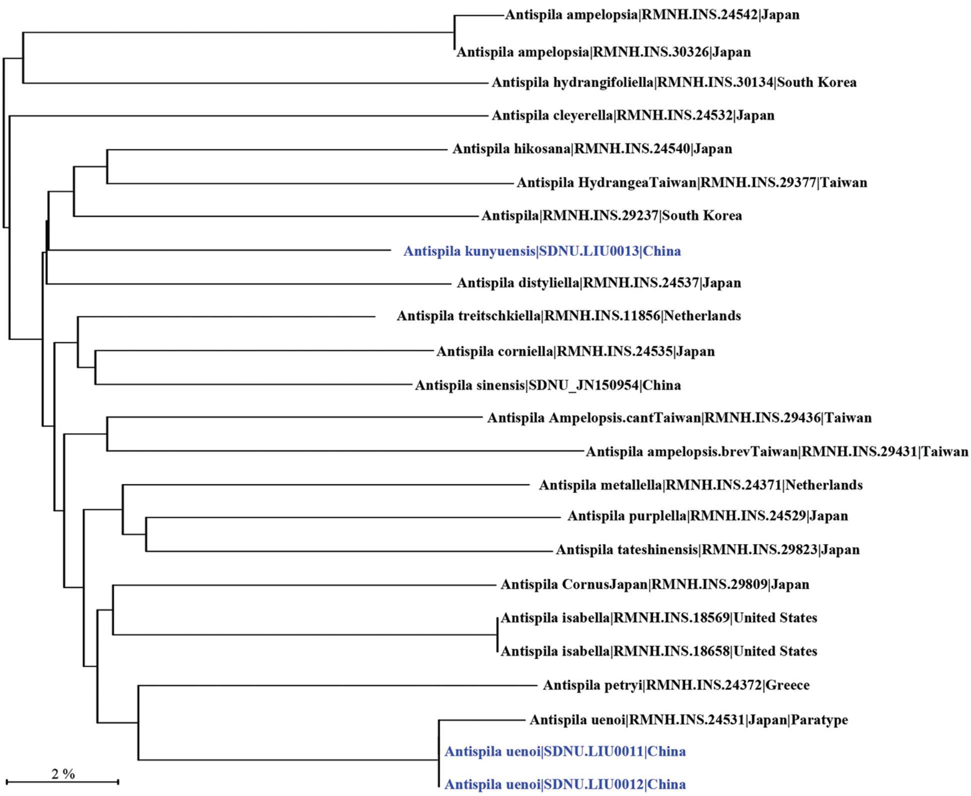

Figure 33. Neighbor Joining Tree, based on DNA barcodes of *Antispila* species, especially Vitaceae-feeding and Asian species.

semicircular on ventral margin, digital process about half the width of valva, pecten with 12 comb teeth (Figs 20, 21). Juxta longer than half length of phallus, anterior arrow broad and almost semicircular. Phallus as long as length of vinculum + tegumen, narrowed anteriorly; phallotheca with groups of spines, more concentrated and larger ventrally (Figs 24, 25); distal part with two processes ventrally, one large and curved, the other V-shaped with one branch larger than the other, two smaller similar processes dorso-apically, one less sclerotized and curved process at apex with several membranous teeth ventrally (Fig. 23). Paired tufts of slender scales on the 7th abdominal segment (Figs 8, 17, 18).

Female genitalia (Figs 30–32). Ovipositor with six cusps at either side, with apical three smaller, tip distinctly indented (Fig. 32). Vestibulum membranous, with a sclerotized granule and a weak circular ring surrounding opening of canalis spiralis (Fig. 30). Corpus bursae membranous.

DNA barcode. Two DNA barcodes were obtained (Fig. 33). A partial DNA barcode of 268 bp generated from a paratype of *A. uenoi* (RMNH.INS.24531) was used for identification of the Chinese specimens. The genetic distance between the Chinese specimens and the paratype is 1.53%.

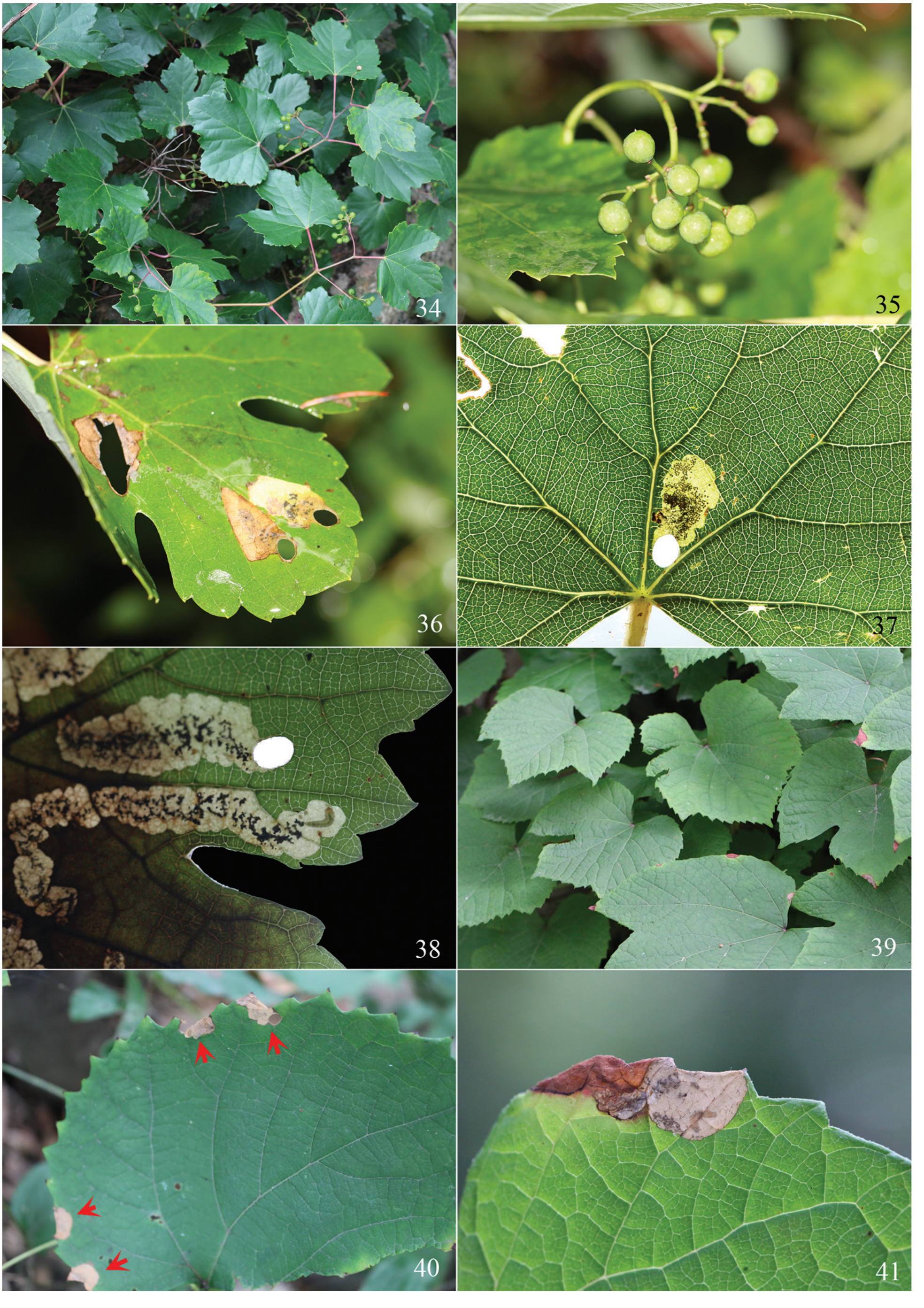

Figures 34–41. Host plant and leaf-mines of *Antispila* species. **34–38** *A. kunyuensis* **34** Host plant, *Ampelopsis humulifolia* **35** unripe fruits of *A. humulifolia* **36–38** leaf-mines **39–41** *A. uenoi* **39** Host plant, *Vitis amurensis* **40** leaf-mines along leaf margin, indicated by red arrows **41** leaf-mine with a dead larva.

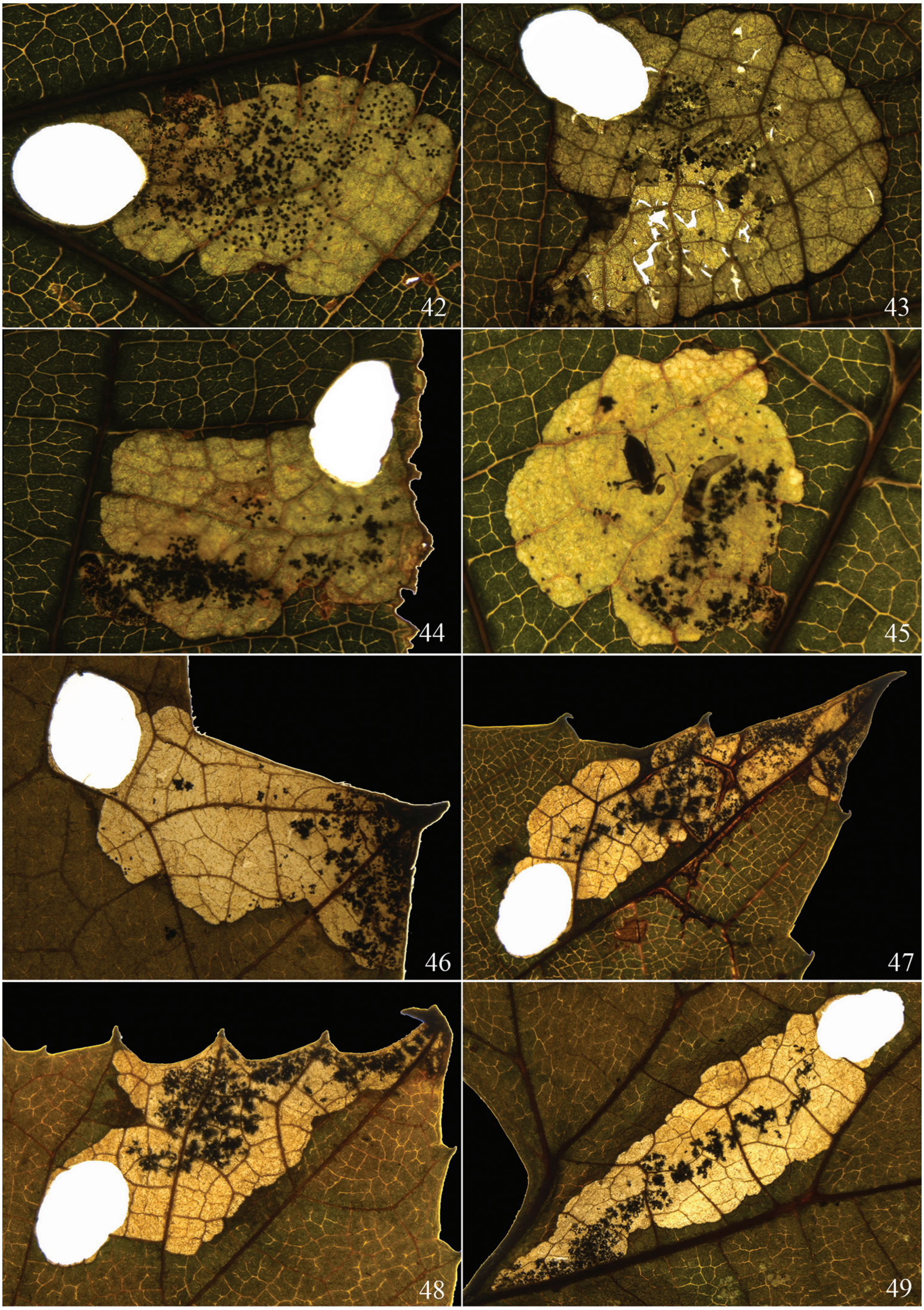

Figures 42–49. Leaf-mines of *Antispila* species. **42–45** *A. kunyuensis*, fig. **42** is the identical mine to Fig. 37, one dead larva and a parasitoid, most likely a species of Eulophidae in Figure 45 **46–49** *A. uenoi*, leaf-mines occupying leaf serration and apical area in Figures 46–48, leaf-mine occupying leaf basal area in Figure 49.

Host plants. *Vitis amurensis* Rupr. (Fig. 39), *V. coignetiae* Pulliat ex Planch. and *V. labruscana* L.H. Bailey (Kuroko 1987). *Vitis amurensis* is recorded here as a new host.

Biology. Leaf-mines on *Vitis amurensis* can occupy serrations along the leaf margin (Figs 40, 41, 46–48) or the leaf basal area (Fig. 49) in an almost equal proportion, calculated from our rearing data (5 : 4); no other placements (e. g. leaf central area) of mines were observed, although in Japan the majority of mines occupy the apical or marginal area of the leaves on other hosts (Kuroko 1987). Frass often dispersed along mines (Figs 47–49). This species overwinters as a prepupa in the shield. Two generations probably occur in Shandong Peninsula.

Distribution. China (Shandong), Japan: Honshu. The host plant *Vitis amurensis* is widespread in the northeast and eastern parts of China (Chen et al. 2007), Eastern Russia (Afonin et al. 2008), Japan: Honshu and Korea (Ohwi 1965). A much wider distribution of the moth is expected, where its host plants occur.

Remarks. This species is newly recorded in China. The venation and the paired tufts of scales on the 7th abdominal segment in male are illustrated for *A. uenoi* for the first time.

Discussion

In the Miocene, the arthropod diversity of Shandong Peninsula was quite rich, which is well documented by numerous fossil records from Shanwang, Shandong province (Zhang 1989, 1994). During the last centuries, the Yellow River shifted its mouth a number of times and finally diverted to the Bohai Sea in 1855 (Cheng and Xue 1997, Wang et al. 2010). Both long-term historical and recent regional processes may have significantly influenced the species richness of Shandong Peninsula, which makes this peninsula an interesting region for biogeographical and biodiversity studies (e.g., Zheng et al. 2009). Heliozelidae, together with other small-sized Lepidoptera species, are expected to experience an increase in species richness upon a deeper exploration of this region, as will be the case for all of China. For instance, in Argyresthiidae, the number of species increased from 14 to 64 after the study by Liu et al. (2017). This would be true when considering the host preference of the heliozelids and the rich diversity of Vitaceae and many other host families in China. Take Vitaceae for example. A majority of *Antispila* species show a specific host preferences for Vitaceae and Cornaceae (Milla et al. 2017, van Nieukerken et al. 2018), and there are 146 species of Vitaceae distributed in eight genera in China, with 87 endemic species, which are mostly native to central, south, and southwest China (Chen et al. 2007).

Acknowledgements

We thank the staff of the Kunyu National Nature Reserve for their support during the field work. We thank reviewers Toshiya Hirowatari and Erik J. van Nieukerken for their insightful comments and corrections which greatly improved the manuscript. This study is supported by the Shandong Provincial Natural Science Foundation, China (No. ZR2017BC051).

References

Afonin AN, Greene SL, Dzyubenko NI, Frolov AN (2008) Interactive agricultural ecological atlas of Russia and neighboring countries. Economic plants and their diseases, pests and weeds. http://www.agroatlas.ru [accessed 6 March 2018]

APG (2016) An update of the Angiosperm Phylogeny Group classification for the orders and families of flowering plants: APG IV. Botanical Journal of the Linnean Society 181: 1–20. https://doi.org/10.1111/boj.12385

Chen ZD, Ren H, Wen J (2007) Vitaceae. Flora of China 12: 173–222. http://foc.eflora.cn/content.aspx?TaxonId=10946 [Accessed 21 November 2017]

Cheng GD, Xue CT (1997) Sedimentary Geology of the Yellow River Delta. Geological Press, Beijing, 153 pp. [In Chinese]

Knölke S, Erlacher S, Hausmann A, Miller MA, Segerer AH (2005) A procedure for combined genitalia dissection and DNA extraction in Lepidoptera. Insect systematics & evolution 35: 401–409. https://doi.org/10.1163/187631204788912463

Kuroko H (1961) The genus *Antispila* from Japan, with descriptions of seven new species (Lepidoptera, Heliozelidae). Esakia 3: 11–24. http://hdl.handle.net/2324/2347

Kuroko H (1987) Three new species of the genus *Antispila* (Lepidoptera: Heliozelidae) from Japan. Tinea 12, Supplement: 109–117.

Li HH (2002) The Gelechiidae of China (I) (Lepidoptera: Gelechioidea). Nankai University Press, Tianjin, China, 504 pp. [In Chinese]

Liu TT, Wang SX (2017) First report of the leaf-mining genus *Antispila* Hübner, [1825] from mainland China, with the description of a new species feeding on *Cornus* (Lepidoptera, Heliozelidae). ZooKeys 686: 95–107. https://doi.org/10.3897/zookeys.686.13680

Liu TT, Wang SX, Li HH (2017) Review of the genus *Argyresthia* Hübner, [1825] (Lepidoptera: Yponomeutoidea: Argyresthiidae) from China, with descriptions of forty-three new species. Zootaxa 4292: 1–135. https://doi.org/10.11646/zootaxa.4292.1.1

Meyrick E (1923–1930) Exotic Microlepidoptera. Thornhanger, Marlborough, Wilts, 640 pp.

Milla L, Nieukerken EJ van, Vijverberg R, Doorenweerd C, Wilcox SA, Halsey M, Young DA, Jones TM, Kallies A, Hilton DJ (2017) A preliminary molecular phylogeny of shield-bearer moths (Lepidoptera: Adeloidea: Heliozelidae) highlights rich undescribed diversity. Molecular Phylogenetics and Evolution 120: 129–143. https://doi.org/10.1016/j.ympev.2017.12.004

Nieukerken EJ van, Geertsema H (2015) A new leafminer on grapevine and *Rhoicissus* (Vitaceae) in South Africa within an expanded generic concept of *Holocacista* (Insecta, Lepidoptera, Heliozelidae). ZooKeys 507: 41–97. https://doi.org/10.3897/zookeys.507.9536

Nieukerken EJ van, Kaila L, Kitching IJ, Kristensen NP, Lees DC, Minet J, Mitter C, Mutanen M, Regier JC, Simonsen TJ, Wahlberg N, Yen S-H, Zahiri R, Adamski D, Baixeras J, Bartsch D, Bengtsson BÅ, Brown JW, Bucheli SR, Davis DR, De Prins J, De Prins W, Epstein ME, Gentili-Poole P, Gielis C, Hättenschwiler P, Hausmann A, Holloway JD, Kallies A, Karsholt O, Kawahara AY, Koster SJC, Kozlov M, Lafontaine JD, Lamas G, Landry J-F, Lee S, Nuss M, Park K-T, Penz C, Rota J, Schintlmeister A, Schmidt BC, Sohn J-C, Solis MA, Tarmann GM, Warren AD, Weller S, Yakovlev RV, Zolotuhin VV, Zwick A (2011) Order Lepidoptera Linnaeus, 1758. Animal biodiversity: An outline of higher-level classification and survey of taxonomic richness. Zootaxa 3148: 212–221. http://www.mapress.com/zootaxa/2011/f/zt03148p221.pdf

Nieukerken EJ van, Wagner DL, Baldessari M, Mazzon L, Angeli G, Girolami V, Duso C, Doorenweerd C (2012) *Antispila oinophylla* new species (Lepidoptera, Heliozelidae), a new North American grapevine leafminer invading Italian vineyards: taxonomy, DNA barcodes and life cycle. ZooKeys 170: 29–77. https://doi.org/10.3897/zookeys.170.2617

Nieukerken EJ van, Lees DC, Doorenweerd C, Koster S, Bryner R, Schreurs A, Timmermans MJTN, Sattler K (2018) Two European *Cornus* L. feeding leafmining moths, *Antispila petryi* Martini, 1899, sp. rev. and *A. treitschkiella* (Fischer von Röslerstamm, 1843) (Lepidoptera, Heliozelidae): an unjustified synonymy and overlooked range expansion. Nota Lepidopterologica 41: 39–86. https://doi.org/10.3897/nl.41.22264

Ohwi J (1965) Flora of Japan. Smithsonian Institution, Washington, D.C., 1110 pp. https://doi.org/10.5962/bhl.title.43786

The Plant List (2013) The Plant List, a working list of all plant species. Version 1.1. http://www.theplantlist.org/ [Accessed 21 November 2017]

Wang H, Bi N, Saito Y, Wang Y, Sun X, Zhang J, Yang Z (2010) Recent changes in sediment delivery by the Huanghe (Yellow River) to the sea: Causes and environmental implications in its estuary. Journal of Hydrology 391: 302–313. https://doi.org/10.1016/j.jhydrol.2010.07.030

Zhang JF (1989) Fossil Insects from Shanwang, Shandong, China. Shandong Science and Technology Publishing House, Jinan, 459 pp. [In Chinese]

Zhang JF, Sun B, Zhang XY (1994) Miocene insects and spiders from ShanWang, Shandong. Science Press, Beijing, 298 pp. [In Chinese]

Zheng Y, Fu J, Li SQ (2009) Toward understanding the distribution of Laurasian frogs: A test of Savage's biogeographical hypothesis using the genus *Bombina*. Molecular Phylogenetics and Evolution 52: 70–83. https://doi.org/10.1016/j.ympev.2009.03.026

ZooKeys 744: 67–77 (2018)
doi: 10.3897/zookeys.744.21742
http://zookeys.pensoft.net

RESEARCH ARTICLE

A peer-reviewed open-access journal
ZooKeys
Launched to accelerate biodiversity research

Triplophysa anshuiensis, a new species of blind loach from the Xijiang River, China (Teleostei, Nemacheilidae)

Tie-Jun Wu[1], Mu-Lan Wei[2], Jia-Hu Lan[2], Li-Na Du[3]

1 *Guangxi Institute of Fisheries, Nanning 530021, China* **2** *Du'an Fishery Technique Popularization Station, Du'an 530700, China* **3** *Kunming Institute of Zoology, Chinese Academy of Sciences, Kunming 650223, China*

Corresponding author: *Li-Na Du* (duln04@mail.kiz.ac.cn)

Academic editor: *N. Bogutskaya* | Received 18 October 2017 | Accepted 29 January 2018 | Published 20 March 2018

http://zoobank.org/106098F3-E7C3-4442-99EC-C9F772122222

Citation: Wu T-J, Wei M-L, Lan J-H, Du L-N (2018) *Triplophysa anshuiensis*, a new species of blind loach from the Xijiang River, China (Teleostei, Nemacheilidae). ZooKeys 744: 67–77. https://doi.org/10.3897/zookeys.744.21742

Abstract

A new cave-dwelling fish, *Triplophysa anshuiensis*, is described here based on specimens collected from a karst cave in Guangxi Zhuang Autonomous Region, China, interconnected with the Hongshui River system, a tributary of the Xijiang River in the Pearl River (Zhu Jiang) Drainage. The species can be distinguished from its congeners by a combination of morphological characters. A key to the cave-dwelling species of *Triplophysa* in the Xijiang River is provided.

Keywords

cave fish, Guangxi, new species, *Triplophysa*

Introduction

Triplophysa is an ecologically important and taxonomically challenging genus, distributed in lakes, rivers, and streams of the Qinghai-Tibet Plateau and adjacent region. The genus is diagnosed by a marked sexual dimorphism. In males the dorsal surface of the outer pectoral-fin rays are thickened, broadened, and covered by breeding tubercles; breeding tubercles are also present on the sides of the head, extending from the eye almost to the insertion of the maxillary barbels. Even though *Barbatula* species share the same sexual dimorphism, *Triplophysa* can be distinguished by close together nostrils in contrast to widely separated nostrils *in Barbatula* (Bănărescu and Nalbant 1968, Zhu 1989, Ren et al. 2012).

The distribution area of the genus extends westward to the Aral Sea Basin and interior drainages of Baluchistan and north-westward to western Mongolia and Republic of Tuva in Russia (Zhu 1989). In China, in addition to the Qinghai-Tibetan Plateau and Inner Mongolia, *Triplophysa* also occurs in Beijing, Shanxi, Sichuan, Yunnan, Chongqing, Hunan, Hubei, Guizhou, and Guangxi (Chen et al. 2009). The Guangxi Zhuang Autonomous Region lies in southern China where karst caves and subterranean streams are a dominant geological feature. The diversity of species is very high in many isolated rivers, especially in caves. So far, 27 cave-dwelling species in the genus *Triplophysa* have been described in China (Romero et al. 2009, Kottelat 2012, Lan et al. 2013, Yang et al. 2016, Li and Li 2017, Li and Lan 2017, Liu et al. 2017). According to Lan et al. (2013), these species can be placed into three groups according to their eye development, viz. normal eyes, reduced eyes, or no eyes. Of the 27 species, 23 are recorded from Xijiang River. Among them, ten species belong to the group with normal eyes, including *T. aluensis* Li & Zhu, 2000, *T. flavicorpus* Yang, Chen & Lan, 2004, *T. huapingensis* Zheng, Chen & Yang, 2012, *T. longipectoralis* Zheng, Du, Chen & Yang, 2009, *T. nandanensis* Lan, Yang & Chen, *T. nasobarbatula* Wang & Li, 2001, *T. tianxingensis* Yang, Li & Chen, 2016, *T. xiangshuingensis* Li, 2004, *T. yunnanensis* Yang, 1990, and *T. zhenfengensis* Wang & Li, 2001. Five species belong to the group with reduced eyes, namely *T. langpingensis* Yang, 2013, *T. luochengensis* Li, Lan, Chen & Du, 2017, *T. macrocephala* Yang, Wu & Yang, 2012, *T. tianeensis* Chen, Cui & Yang, 2004, and *T. tianlinensis* Li, Li & Lan, 2017. The group without eyes includes eight species, namely, *T. dongganensis* Yang, 2013, *T. fengshanensis* Lan, 2013, *T. gejiuensis* Chu & Chen, 1979, *T. huanjiangensis* Yang, Wu & Lan, 2011, *T. lihuensis* Wu, Yang & Lan, 2012, *T. longibarbata* Chen, Yang, Sket & Aljancic, 1998, *T. qiubeiensis* Li & Yang, 2008, and *T. shilinensis* Chen & Yang, 1992 (Zheng et al. 2012, Lan et al. 2013, Zhang and Zhao 2016, Li and Li 2017, Li and Lan 2017). In May 2012, two specimens of nemacheiline loach were collected from a karst cave in Anshui Village, Lingyun County, Guangxi Zhuang Autonomous Region, China. These specimens represent a new species of *Triplophysa*, which is described herein.

Materials and methods

Specimens were preserved in 8 % formalin and are maintained at the Kunming Natural History Museum of Zoology, Kunming Institute of Zoology (KIZ), Chinese Academy of Sciences. Counts and measurements follow Kottelat (1990), except for the median caudal-fin length, which is the length of the shortest branched caudal-fin ray. Measurements were made point-to-point with digital calipers recorded to 0.1 mm. Abbreviations: P_L-A, distance between pelvic-fin origin and anal-fin origin; P_T-P_L, distance between pectoral-fin origin and pelvic-fin origin.

Data on *T. huanjiangensis*, *T. fengshanensis*, and *T. dongganensis* are cited from Lan et al. (2013). Data on *T. xiangshuingensis* and *T. zhenfengensis* are from Li (2004) and Wang and Li (2001), respectively. Other comparative species were measured at KIZ, Chinese Academy of Sciences.

Results

***Triplophysa anshuiensis* sp. n.**
http://zoobank.org/4E1C8A91-8F51-46F2-B66D-99B9F7C98EAB
Figures 1–3; Table 1

Type specimens. *Holotype*. Kunming Natural History Museum of Zoology, Kunming Institute of Zoology, Chinese Academy of Sciences, Kunming, KIZ2012005747, 65.2 mm standard length, Anshui Village, Lingyun County, Guangxi Zhuang Autonomous Region, China; 24.3632N, 106.7412E, Altitude 719 m; collected by J. H. Lan, 12 May 2012. ***Paratypes.*** Kunming Natural History Museum of Zoology, KIZ 2012005746, 68.5 mm SL; collected with holotype.

Diagnosis. *Triplophysa anshuiensis* can be distinguished from all species of *Triplophysa* by the following combination of characters: eyes absent, gill rakers absent in outer row and eight gill rakers in inner row on first gill arch, 14 branched caudal-fin rays, body scaleless, tips of depressed pectoral fins not reaching pelvic-fin origin, 12–13 preoperculo-mandibular pores, lateral line complete, posterior chamber of air bladder developed.

Description. Morphometric data of type specimens of *Triplophysa anshuiensis* are given in Table 1. D, 4/7–8; A, 2/6; P, 1/10; V, 1/6, C, 14; 8 inner gill rakers in inner row on first gill arch (n=1). Cephalic lateral-line canals with 2+2 supra-temporal, 8 supraorbital, 4+8–9 infraorbital, and 12–13 preoperculo-mandibular pores. Lateral line complete, with 52–54 pores.

Body elongated, slightly compressed anteriorly, more strongly compressed posteriorly. Deepest point of body in front of dorsal-fin origin, body depth 12–16% of SL. Head compressed, maximum width greater than depth. Anterior and posterior nostrils adjacent, anterior nostril in short tube with elongated barbel-like tip, tip of nostril barbel reaching posterior margin of posterior nostrils. Eyes absent. Mouth inferior, mouth corner situated below anterior nostril. Lips thick with shallow furrows; lower lip with a “V” type median notch. Upper and lower jaw arched, processus dentiformis on upper jaw absent and no corresponding notch on lower jaw. Three pairs of barbels; inner rostral barbel 50–54 % of lateral head length; outer rostral barbel 20–26 % of lateral head length; maxillary barbel 36–39 % of lateral head length. Body scaleless. Intestine straight. Posterior chamber of air bladder developed, reaching dorsal-fin origin (Fig. 3).

Dorsal fin distally truncate, origin anterior to pelvic-fin insertion, situated slightly anterior to midpoint between tip of snout and caudal-fin base; first branched ray longest, reaching anus when adpressed vertically. Anal fin distally truncate. Pectoral fins moderately developed, 60–67 % of distance between pectoral and pelvic fins. Tip of

Figure 1. Lateral and ventral views of *Triplophysa anshuiensis* sp. n., holotype KIZ 2012005747, 65.2 mm SL. Scale = 1 cm.

Figure 2. Type locality of *Triplophysa anshuiensis* sp. n., a cave in Anshui Village, Guangxi, China.

depressed pelvic fin reaching anus. Anus short distance from anal-fin origin. Caudal fin forked, tips pointed.

Coloration. Fixation in 8 % formalin, body yellowish. Black pigments irregularly present on dorsum of body.

Sexual dimorphism. No sexual dimorphism was observed in the two specimens.

Table 1. Morphometric data of type specimens of *Triplophysa anshuiensis* sp. n.

Measurements	**Paratype**	**Holotype**
	2012005746	**201005747**
Standard length	68.5	65.2
Lateral head length	14.5	13.8
Percent of SL		
Body depth	15.7	12.2
Lateral head length	21.1	21.1
Predorsal length	52.6	47.5
Prepelvic length	55.1	52.0
Preanal length	79.2	72.5
Preanus length	71.4	66.9
Caudal-peduncle length	15.1	14.6
Caudal-peduncle depth	9.0	9.8
Percent of HL		
Maximum head depth	50.7	47.7
Maximum head width	53.1	52.0
Pectoral fin length/Pt-Pl	66.4	59.8
Pelvic fin length/Pl-A	77.2	63.6
CPD/CPL	59.2	67.3

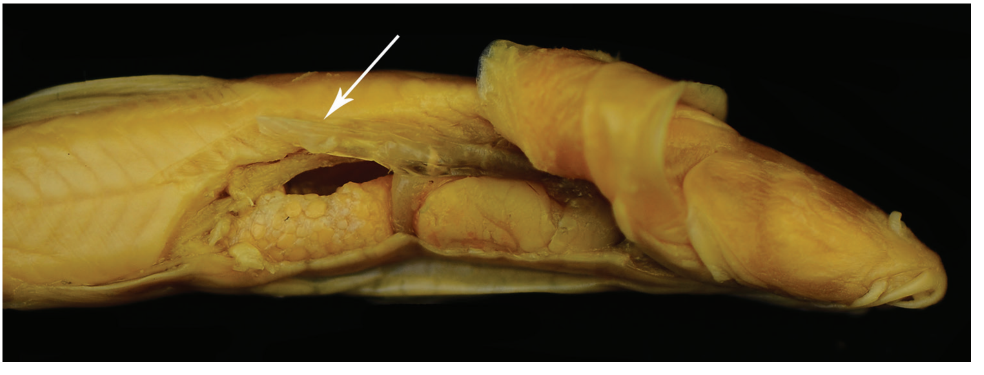

Figure 3. Posterior chamber of air bladder of *Triplophysa anshuiensis* sp. n.

Distribution. A karst cave in Anshui Village, Lingyun County, Guangxi Zhuang Autonomous Region, China, whichis interconnected with the Hongshui River system, a tributary of the Xijiang River in the Pearl River (Zhu Jiang) Drainage.

Habitat and ecology. An underground stream was found about 40 m from and 10 m below the entrance to a cave. *Triplophysa anshuiensis* inhabits pools in which the substratum is mud and cobblestones (Fig. 2). Pools are interconnected by underwater channels. No other species were recorded in this cave.

Etymology. The specific name, *anshuiensis*, is derived from the village Anshui, the type locality of the species.

Discussion

Thirteen *Triplophysa* species have been recorded in karst caves and subterranean streams in the Guangxi Zhuang Autonomous Region (Yang et al. 2004, Lan et al. 2013): *T. dongganensis*, *T. fengshanensis*, *T. flavicorpus*, *T. huanjiangensis*, *T. huapingensis*, *T. langpingensis*, *T. lihuensis*, *T. longipectoralis*, *T. luochengensis*, *T. macrocephala*, *T. nandanensis*, *T. tianeensis*, and *T. tianlinensis*. In morphology, the new species can be distinguished from *T. huapingensis*, *T. longipectoralis*, *T. nandanensis*, and *T. flavicorpus* by the eyes absent (vs. normally developed). Furthermore, *T. anshuiensis* can be easily distinguished from *T. flavicorpus* by the gill rakers absent in outer row on first gill arch (vs. 5–6). The new species can be distinguished from *T. nandanensis* by the posterior chamber of the air bladder developed (vs. reduced). *Triplophysa anshuiensis* differs from *T. huapingensis* and *T. longipectoralis* by 8 gill rakers in inner row on first gill arch (vs. 13), 14 branched caudal-fin rays (vs. 16 in *T. huapingensis*), the tip of the pectoral fin when depressed not reaching pelvic-fin origin (vs. exceeding the pelvic-fin origin in *T. longipectoralis*). Among the Guangxi species with the eyes degenerated or absent, the new species can be distinguished from *T. langpingensis*, *T. luochengensis*, *T. macrocephala*, *T. tianeensis*, and *T. tianlinensis* by the eyes absent (vs. degenerated, with black pigment). From *T. luochengensis,* it can be further distinguished by 14 branched caudal-fin rays (vs. 15–17) and a scaleless body (vs. scaled), from *T. tianeensis* by 14 branched caudal-fin rays (vs. 15–17), 8 gill rakers in inner row on first gill arch (vs. 10–11), and posterior chamber of air bladder developed (vs. reduced), from *T. macrocephala* and *T. tianlinensis* by 14 branched caudal-fin rays (vs. 15–17), and from *T. langpingensis* by a complete lateral line (vs. incomplete).

In the group of Guangxi species with completely reduced eyes, *T. anshuiensis* is similar to *T. lihuensis*, *T. huanjiangensis*, *T. fengshanensis*, and *T. dongganensis* in having no scales on the whole body. The new species can be distinguished from *T. lihuensis* and *T. huanjiangensis* by 8 gill rakers in inner row on first gill arch (vs. 10–13 in *T. lihuensis* and *T. huanjiangensis*, whereas unknown in *T. dongganensis* and *T. fengshanensis*), from *T. fengshanensis* by 14 branched caudal-fin rays (vs. 16), and caudal peduncle depth 6.6–6.9 times in standard length (vs. 5.0–5.3), and from *T. dongganensis* by caudal peduncle depth 10.2–11.2 times in standard length (vs. 11.4–16.9), and caudal peduncle depth 1.5–1.7 times in its length (vs. 1.8–2.9). In addition to the species of *Triplophysa* from Guangxi, there are ten more troglobitic *Triplophysa* species recorded in the Xijiang River, including *T. aluensis*, *T. gejiuensis*, *T. longibarbata*, *T. nasobarbatula*, *T. qiubeiensis*, *T. shilinensis*, *T. xiangshuingensis*, *T. yunnanensis*, and *T. zhenfengensis* (Chen 1992, Chu and Chen 1979, Wang and Li 2001, Chen and Yang 2005, Yang et al. 2016, Liu et al. 2017). *Triplophysa anshuiensis* can be easily distinguished from *T. nasobarbatula*, *T. xiangshuingensis*, *T. yunnanensis*, and *T. zhenfengensis* by eyes absent (vs. normal), body colorless (vs. body with color pattern), scaleless (vs. scaled in *T. nasobarbatula*, *T. xiangshuingensis*, *T. yunnanensis*, and *T. zhenfengensis*), and 14 branched caudal-fin rays. *Triplophysa anshuiensis* can be distinguished from other species by the following characters: eyes absent (vs. degenerated, with black pigment in *T. aluensis*), 8 supraorbital pores (vs. 5 in *T. gejiuensis* and absent in *T. shilinensis*), 12–13 preoperculo-mandibular pores (vs. 7 in *T. gejiuensis* and absent in *T. shilinensis*), and caudal peduncle length 1.5–1.7 times in its length (vs. more than two times in *T. qiubeiensis* and *T. longibarbata*).

Key to cave-dwelling species of *Triplophysa* in Xijiang Drainage

1	Eyes normal	**2**
–	Eyes reduced or absent	**10**
2	Body scaleless	**3**
–	Body covered by scales	**4**
3	Fourteen branched caudal-fin rays	***T. xiangshuingensis***
–	Sixteen branched caudal-fin rays	***T. aluensis***
4	Processus dentiformis present in upper jaw	***T. zhenfengensis***
–	Processus dentiformis absent in upper jaw	**5**
5	Tip of pectoral fin exceeding pelvic fin origin	***T. longipectoralis***
–	Tip of pectoral fin not reaching pelvic fin origin	**6**
6	Tip of depressed pelvic fin exceeding anus	***T. flavicorpus***
–	Tip of depressed pelvic fin not reaching anus	**7**
7	Eye diameter / lateral head length < 10 %	***T. yunnanensis***
–	Eye diameter / lateral head length > 10 %	**8**
8	Caudal peduncle length/depth 1.8–2.1	***T. nasobarbatula***
–	Caudal peduncle length/depth 1.2–1.7	**9**
9	Pectoral fin length / P_T-P_L 58–69 %	***T. huapingensis***
–	Pectoral fin length / P_T-P_L 78–82 %	***T. nandanensis***
10	Eyes reduced	**11**
–	Eyes absent	**15**
11	Lateral line incomplete	***T. langpingensis***
–	Lateral line complete	**12**
12	Body covered by scales	***T. luochengensis***
–	Body scaleless	**13**
13	Nine gill rakers in inner row on the first gill arch…	***T. macrocephala***
–	Ten–11 gill rakers in inner row on the first gill arch	**14**
14	Eight–9 branched pectoral-fin rays	***T. tianeensis***
–	Ten branched pectoral-fin rays	***T. tianlinensis***
15	Lateral-line absent	**16**
–	Lateral-line complete	**17**
16	Posterior chamber of air bladder developed	***T. huanjiangensis***
–	Posterior chamber of air bladder reduced	***T. lihuensis***
17	Six branched dorsal-fin rays	***T. shilinensis***
–	Seven branched dorsal-fin rays	**18**

18 Five branched pelvic-fin rays .... ***T. qiubeiensis***
– Seven branched pelvic-fin rays **19**
19 Sixteen branched caudal-fin rays .... ***T. fengshanensis***
– Thirteen–15 branched caudal-fin rays **20**
20 Caudal peduncle length/depth 3–3.1 .... ***T. longibarbata***
– Caudal peduncle length/depth less than 3 .... **21**
21 Standard length/caudal peduncle depth more than 14 .... ***T. dongganensis***
– Standard length/ caudal peduncle depth less than 12 .... **22**
22 Cephalic lateral-line canals with 8 supraorbital and 12–13 preoperculo-mandibular pores .... ***T. anshuiensis* sp. n.**
– Cephalic lateral-line canals with 5 supraorbital and 7 preoperculo-mandibular pores .... ***T. gejiuensis***

Comparative material

All specimens from Pearl River.

Triplophysa gejiuensis: KIZ 7803001, holotype, 44.0 mm SL, 7803002–005, paratypes, 4 ex., 42.7–46.3 mm SL, Gejiu County, Yunnan Province.

T. huapingensis: KIZ 2008007607, holotype, 62.3 mm SL; KIZ 2008007606, 2008007608–610, paratypes, 4 ex, 44.5–59.3 mm SL, Huaping Town, Leye County, Guangxi Zhuang Autonomous Region.

T. macrocephala: KIZ 04100631, holotype, 55.7 mm SL; KIZ 04100618–619, paratypes, 3 ex, 49.3–53.8 mm SL, Lihu County, Nadan City, Guangxi Zhuang Autonomous Region.

T. shilinensis: KIZ 2004013853–854, 2 ex, 41.5–46.7 mm SL, Shilin County, Yunnan Province.

T. tianeensis: KIZ 200301003, holotype, 57.9 mm SL; KIZ 200301001–002, KIZ 200301004–006, paratypes, 5 ex, 35.5–59.1 mm SL, Tian'e County, Guangxi Zhuang Autonomous Region.

T. nandanensis: KIZ 911911, holotype, 58.2 mm SL, KIZ 911008–009, 9110012–017, paratypes, 9 ex, 36.9–81.3 mm SL, Liuzai County, Nandan City, Guangxi Zhuang Autonomous Region.

T. longipectoralis: KIZ 01050218, holotype, 50.7 mm SL; KIZ 01050219–221, 01050223–224, paratypes, 5 ex, 36.9–52.0 mm SL, Huanjiang County, Hechi City, Guangxi Zhuang Autonomous Region.

T. lihuensis: KIZ 2010003082, holotype, 59.3 mm SL; KIZ 2010003083–084, paratypes, 2 ex, 55.6–58.3 mm SL, Renguang Village, Lihu Town, Nandan County, Guangxi Zhuang Autonomous Region.

T. langpingensis: uncat. 3 ex, 44.7–70.9 mm SL, Langping County, Guangxi Zhuang Autonomous Region.

T. aluensis: KIZ 20006005–007, 3 ex, 43.2–82.6 mm SL, A'lu County, Yunnan.

T. yunnanensis: KIZ 874200, holotype, 59.8 mm SL, KIZ 874197, KIZ 874199, paratypes, 2 ex, 48.1–62.2 mm SL, Jiuxiang Town, Yiliang County, Yunnan Province.

T. nasobarbatula: KIZ 2005001276, KIZ 2005001325, 2 ex, 34.2–40.5 mm SL, Libo County, Guizhou Province.

Acknowledgements

The study was funded by the Special Funds for Young Scholars of Taxonomy of the Chinese Academy of Sciences (ZSBR-011), National Natural Science Foundation of China (31460556), and Guangxi Natural Science Foundation (2017GXNSFFA198010). We are grateful to Dr Christine Watts for polishing this manuscript before submission.

References

Bănărescu P, Nalbant T (1968) Cobitidae (Pisces, Cypriniformes) collected by the German India Expedition. Mitteilungenausdem Hamburgischen Zoologischen Museum und Institut 65: 327–351.

Chen XY, Yang JX (2005) *Triplophysa rosa* sp. nov.: a new blind loach from China. Journal of Fish Biology 66: 599–608. https://doi.org/10.1111/j.0022-1112.2005.00622.x

Chen XY, Cui GH, Yang JX (2004) A new cave-dwelling fish species of genus *Triplophysa* (Balitoridae) from Guangxi, China. Zoological Research 25: 227–231.

Chen YR, Yang JX, Xu GC (1992) A new blind loach of *Triplophysa* from Yunnan Stone Forest with comments on its phylogenetic relationship. Zoological Research 13: 17–23.

Chu XL, Chen YR (1979) A new blind cobitid fish (Pisces, Cypriniformes) from subterranean waters in Yunnan, China. Acta Zoologica Sinica 25: 285–287.

Chen YR, Yang JX, Sket B, Aljancic G (1998) A new blind cave loach of with comment on its characters evolution. Zoological Research 19: 59–63.

Chen ZM, Li WX, Yang JX (2009) A new miniature species of the genus *Triplophysa* (Balitoridae: Nemacheilinae) from Yunnan, China. Zoologischer Anzeiger 248: 85–91. https://doi.org/10.1016/j.jcz.2009.02.001

Eschmeyer W N, Fricke R, Laan R (2016) Catalog of fishes: genera, species, references. Electronic version accessed 2016. http://researcharchive.calacademy.org/research/ichthyology/catalog/fishcatmain.asp

Kottelat M (1990) Indochinese Nemacheilinaes. A revision of Nemacheilinae loaches (Pisces: Cypriniformes) of Thailand, Burma, Laos, Cambodia and southern Vietnam. Dr. Friedrich Pfeil, VerlagMuchen, Germany, 262 pp.

Kottelat M (2012) Conspectus cobitidum: an inventory of the loaches of the world (Teleostei: Cypriniformes: Cobitoidei). Raffles Bulletin of Zoology 26: 1–199.

Lan JH, Gan X, Wu TJ, Yang J (2013) Cave Fishes of Guangxi, China. Science Press, Beijing, 104–139. [In Chinese]

Lan JH, Yang JX, Chen YR (1995) Two new species of the subfamily Nemacheilinae from Guangxi, China (Cypriniformes: Cobitidae). Acta Zootaxonomica Sinica 20: 366–372.

Li J, Lan JH, Chen XY, Du LN (2017) Description of *Triplophysa luochengensis* sp. nov. (Teleostei: Nemacheilidae) from a karst cave in Guangxi, China. Journal of Fish Biology 91: 1009–1017. https://doi.org/10.1111/jfb.13364

Li J, Li XH, Lan JH, Du LN (2016) Description of a new troglobitic loach, *Triplophysa tianlinensis*, from Guangxi, China (Teleostei: Nemacheilidae). Ichthyological Research 64: 295–300. https://doi.org/10.1007/s10228-016-0565-0

Li WX, Zhu ZG (2000) A new species of *Triplophysa* from cave Yunnan. Journal of Yunnan University 22: 396–398.

Li WX (2004) The three new species of Cobitidae from Yunnan, China. Journal of Jishou University (Natural Science Edition) 25: 3–96.

Li WX, Yang HF, Chen H, Tao CP, Qi SQ, Han F (2008) A new blind underground species of the genus *Triplophysa* (Balitoridae) from Yunnan, China. Zoological Research 29: 674–678. https://doi.org/10.3724/SP.J.1141.2008.06674

Liu SW, Pan XF, Yang JX, Chen XY (2017) A new cave-dwelling loach, *Triplophysa xichouensis* sp. nov. (Teleostei: Nemacheilidae) from Yunnan, China. Journal of Fish Biology 90: 834–846. https://doi.org/10.1111/jfb.13201

Prokofiev AM (2010) Morphological classification of loaches (Nemacheilinae). Journal of Ichthyology 50: 827–913. https://doi.org/10.1134/S0032945210100012

Ren Q, Yang JX, Chen XY (2012) A new species of the genus *Triplophysa* (Cypriniformes: Nemacheilidae), *Triplophysa longliensis* sp. nov, from Guizhou, China. Zootaxa 3586: 187–194.

Romero A, Zhao YH, Chen XY (2009) The hypogean fishes of China. Environmental Biology of Fishes 86: 211–278. https://doi.org/10.1007/s10641-009-9441-3

Wang DZ, Li DJ (2001) Two new species of the genus *Triplophysa* from Guizhou, China (Cypriniformes: Cobitidae). Acta Zootaxonomica Sinica 26: 98–101.

Wu TJ, Yang J, Lan JH (2012) A new blind loach, *Triplophysa lihuensis* (Teleostei: Balitoridae), from Guangxi, China. Zoological Studies 51: 874–880.

Yang GY, Yuan FX, Liao YM (1986) A new blind Cobitidae fish from the subterranean water in Xiangxi, China. Journal of Huazhong Agricultural University 5: 219–223.

Yang HF, Li WX, Chen ZM (2016) A new cave species of the genus *Triplophysa* from Yunnan, China. Zoological Research 37: 296–300.

Yang J (2013) In: Lan JH, Gan X, Wu TJ, Yang J (Ed.) Cave Fishes of Guangxi, China. Science Press, Beijing, 131–144.

Yang JX (1990) In: Chu XL, Chen YR (Ed.) The fishes of Yunnan, China. Part 2. Science Press, Beijing,. 313 pp. [In Chinese]

Yang JX, Chen XY, Lan JH (2004) Occurrence of two new plateau-indicator loaches of Nemacheilinae (Balitoridae) in Guangxi with reference to zoogeographical significance. Zoological Research 25: 111–116.

Yang J, Wu TJ, Lan JH (2011) A new blind loach species, *Triplophysa huanjiangensis* (Teleostei: Balitoridae), from Guangxi, China. Zoological Research 32: 566–571.

Yang J, Wu TJ, Yang JX (2012) A new cave-dwelling loach, *Triplophysa macrocephala* (Teleostei: Cypriniformes: Balitoridae), from Guangxi, China. Environmental Biology of Fish 93: 169–175. https://doi.org/10.1007/s10641-011-9901-4

Zhang CG, Zhao YH (2016) Species Diversity and Distribution of Inland Fishes in China. Science Press, Beijing, 133 pp.

Zheng LP, Du LN, Chen XY, Yang JX (2009) A new species of genus *Triplophysa* (Nemacheilinae: Balitoridae), *Triplophysa longipectoralis* sp. nov. from Guangxi, China. Environmental Biology of Fish 85: 221–227. https://doi.org/10.1007/s10641-009-9485-4

Zheng LP, Yang JX, Chen XY (2012) A new species of *Triplophysa* (Nemacheilidae: Cypriniformes), from Guangxi, southern China. Journal of Fish Biology 80: 831–841. https://doi.org/10.1111/j.1095-8649.2012.03227.x

Zhu SQ (1989) The loaches of the subfamily Nemacheilinae in China (Cypriniformes: Cobitidae). Jiangsu Science and Technology Publishing House, Nanjing, 68–129. [In Chinese]

ZooKeys 744: 79–138 (2018)
doi: 10.3897/zookeys.744.22766
http://zookeys.pensoft.net

RESEARCH ARTICLE

A peer-reviewed open-access journal
ZooKeys
Launched to accelerate biodiversity research

Andersonoplatus, a new, remarkable leaf litter inhabiting genus of Monoplatina (Coleoptera, Chrysomelidae, Galerucinae, Alticini)

Adelita M. Linzmeier[1], Alexander S. Konstantinov[2]

1 *Universidade Federal da Fronteira Sul – UFFS, Rua Edmundo Gaievski, 1000, sala 211, 85.770-000, Realeza – PR, Brazil* **2** *Systematic Entomology Laboratory, USDA, Smithsonian Institution, P.O. Box 37012, National Museum of Natural History, Washington, DC 20013-7012, USA*

Corresponding author: *Alexander S. Konstantinov* (alex.konstantinov@ars.usda.gov)

Academic editor: *Ron Beenen* | Received 5 December 2017 | Accepted 19 February 2018 | Published 20 March 2018

http://zoobank.org/D55E1848-1E7B-4F22-A1A7-AF2434EAB243

Citation: Linzmeier AM, Konstantinov AS (2018) *Andersonoplatus*, a new, remarkable leaf litter inhabiting genus of Monoplatina (Coleoptera, Chrysomelidae, Galerucinae, Alticini). ZooKeys 744: 79–138. https://doi.org/10.3897/zookeys.744.22766

Abstract

Andersonoplatus, a new genus with 16 new species from Venezuela (*A. andersoni*, *A. bechyneorum*, *A. castaneus*, *A. flavus*, *A. jolyi*, *A. laculata*, *A. lagunanegra*, *A. macubaji*, *A. merga*, *A. merida*, *A. microoculus*, *A. peck*, *A. rosalesi*, *A. sanare*, *A. saviniae*) and Panama (*A. baru*), is described and illustrated. All the specimens were collected in leaf litter by R. Anderson and S. and J. Peck. *Andersonoplatus* is compared to *Andersonaltica* Linzmeier & Konstantinov, *Apleuraltica* Bechyne, *Distigmoptera* Blake and *Ulrica* Scherer.

Keywords

Alticini, flightless, leaf litter, Neotropical region, new genus, new species

Introduction

The Monoplatina (Chrysomelidae, Galerucinae, Alticini) was established by Chapuis (1875) to group 42 genera described by Clark (1860). Monoplatina currently contains 47 genera and more than 560 species being mainly distributed in the Neotropical region, mostly in South America (Linzmeier and Konstantinov 2009, 2012). Monoplatina flea beetles can be diagnosed within Alticini by the globose fourth visible metatarsomere (Fig. 1E), the closed or very narrowly open procoxal cavities, and by a very thick metafemur, usually as wide as long and most of the times longer than the metatibia.

Recent collecting of leaf litter inhabiting beetles in Central America (Anderson 2010) revealed an entirely new fauna of flea beetles. The first group of this fauna was described recently (Linzmeier and Konstantinov 2012). The second group is being described below.

Materials and methods

Most specimens described in this paper were collected by R. Anderson of the Canadian Museum of Nature as part of his long term studies of weevils (and other beetles) from leaf litter in the New World.

Dissecting techniques and terminology used follow Konstantinov (1998). Specimen observations were made with a Zeiss Stemi SV11 Apo microscope. Digital photographs were taken with Axio Zoom V16 microscope and AxioCam HRC digital camera attached to it. The holotypes will be deposited in Museo del Instituto de Zoologia, UCV, Maracay, Venezuela (**MIZA**), currently and temporarily they are in the National Museum of Natural History, Smithsonian Institution, Washington DC, USA (**USNM**). Paratypes are split between collection of the Canadian Museum of Nature, Ottawa, Canada (**CMNC**) and USNM.

Taxonomy

Andersonoplatus **gen. n.**
http://zoobank.org/AEF0385C-245F-4A58-8EF3-BC1CD3E5EF5F
Figs 1–35

Description. Body length 1.62–4.00 mm, width 0.81–1.78 mm, sparsely pilose to pilose, elliptical, moderately flat to convex in lateral view. Color yellow to pale brown to dark. Apterous.

Head: hypognathous, flat to slightly convex in lateral view, generally smooth or reticulated, sparsely pubescent. Frons and vertex flat or forming a 135° angle in lateral view. Supraorbital pore small, almost indistinguishable to large, generally among other pores, bearing a seta. Antennal callus generally longer than wide, rounded to quadrate separated by long midfrontal sulcus, delineated from vertex by a shallow or deep, straight or inclined sulcus, entering interantennal space. Suprantennal sulcus well developed. Orbit narrow. Antennal socket elongatew or rounded. Frontal ridge short, wider at middle or V-shaped, usually poorly defined laterally. Anterofrontal ridge generally long, relatively tall, oblique, poorly defined. Eyes large to very small generally rounded. Clypeus long. Labrum slightly notched in middle, with six setiferous pores, four with log setae and two with short setae. First maxillary palpomere as wide as long, as wide as the second. Second maxillary palpomere twice as long as first, globose in some species. Third maxillary palpomere thinner, conical, and as long as the first. First labial palpomeres quadrate, second longer than first and, third smaller, thinner and conical. Antenna with eleven antennomeres, filiform to moniliform.

Thorax: pronotum trapezoidal, narrower than elytra, anterior margin straight, wider than posterior; posterior margin nearly straight to slightly convex; lateral margin sinuated. Anterior and posterior angle generally bearing seta, anterior angles in some species pointed outward. Surface shiny to dull, generally reticulated and with punctuation shallow and disperse to deep and well defined; pilosity short and sparse to dense. Post basal impression present, generally absent in middle, but represented by two generally shallow, rounded impressions laterally. Some species have lateral margin notched near middle. Pronotal disc flat to weakly raised. Scutellum rounded to triangular, wider than long, setose. Prosternal surface reticulated to punctuated. Prosternal intercoxal process narrow or thin, generally margined, extended posteriorly beyond coxa ending in a triangular form. Posterior end nearly twice as wide as middle. Procoxae globose. Procoxal cavities closed to narrowly open posteriorly. Mesosternum as long as prosternal process, T-shaped, straight posteriorly. Metasternum smooth, with sparse pilosity, convex in lateral view, shorter than pro- and mesosternum together; posterior margin with deep furrow medially that runs longitudinally along 1/3 of metasternum. Elytra elliptical, generally fused, truncate at apex. Elytral surface shiny, with sparse to dense semi-erect hairs. Punctures forming seven or nine striae (excluding short scutellar and marginal striae). Interspaces flat to convex. Humeral and basal calli generally absent. Epipleura wide, sinuous, nearly vertical or nearly horizontal, narrowing at elytral apex, reaching it.

Fore- and midlegs with femora slightly dilated and thickened toward apex; tibiae subcylindrical, somewhat enlarged toward apex; apex of tibiae with row of denticles; pubescence sparsely distributed. First and second pro- and mesotarsomeres similar in size, as wide as long; third tarsomere varies in length; fourth visible tarsomere as long as the first and second together. In males the first pro- and mesotarsomeres more globose. Metafemur greatly enlarged, longer than wide and longer than metatibia. Metatibia nearly straight in lateral view, curved or nearly straight in dorsal view. Outer lateral dorsal ridge ending in an apical tooth followed by numerous denticles. Inner lateral dorsal with some denticles at end, in some species ending in an apical tooth. Metatibial spur generally short. Metatarsomeres one to three variable in length, generally similar in size; third metatarsomere not bilobed; visible globose, swollen with its base elongate. Claws simple or appendiculate and long.

Abdomen: sparsely pubescent, reticulated, sparsely punctured, with five visible ventrites. Fifth ventrite variable in length, with distinct sexual dimorphism: males with small salient lobe located centrally on posterior margin and perpendicular line; females with last ventrite evenly conical at apex. Posterior margin of fourth ventrite straight to concave. Abdominal pleurites as sclerotized as ventrites.

Male genitalia: median lobe simple, convex in lateral view; in ventral view, with lateral margins almost parallel, apex subtriangular, slightly protruding into more or less differentiated denticle, in some species round on top. Basal part long and bent ventrally in lateral view.

Female genitalia: eighth tergite with rounded anterior margin, more sclerotized laterally, bearing many moderately long setae. Tignum long, narrow, with central canal; posterior and anterior sclerotization variable in shape. Vaginal palpi elongate, posteriorly and anteriorly strongly sclerotized, each with approximately eight setae at apex. Palpi narrowly rounded at apex, enlarged at last third but thinned at apex, situated close together and merged anteriorly for more than half of their length. Spermatheca curved, with receptacle and pump not differentiated from each other. Apex of pump with spoon-like projection. Spermathecal duct long, not forming coils.

Type species. *Andersonoplatus microoculus* Linzmeier & Konstantinov, sp. n.

Etymology. We dedicate this new genus to R. Anderson for his remarkable discoveries of leaf litter flea beetles in the New World. The name is masculine.

Differential diagnosis. *Andersonoplatus* differs from all other known genera of Monoplatina in having the dorsoventrally flat, elliptical elytra and the pronotum being trapezoidal, usually anteriorly wider than posteriorly, much narrower than elytra with sinuate lateral margin. All the *Andersonoplatus* species are apterous with mostly fused elytra, lacking wings. Flightlessness is a common feature of leaf litter or other substrate living leaf beetles. Other apterous Monoplatina species are placed in *Andersonaltica* Linzmeier & Konstantinov, 2012, *Apleuraltica* Bechyne, 1986, *Distigmoptera* Blake, 1943 and *Ulrica* Scherer, 1962. *Andersonoplatus* can be easily differentiated from *Andersonaltica* in having mostly filiform antennae. Antennae in *Andersonaltica* are clubbed. *Andersonoplatus* can be differentiated from *Apleuraltica* and *Distigmoptera* based on having pronotum laterally margined with distinct border and mostly flat disc. In *Apleuraltica* and *Distigmoptera* the lateral margin of pronotum is lacking distinct border (or with very faint one in *Distigmoptera*) and the disc is with two noticeable bumps separated by a longitudinal impression. *Andersonoplatus* can be differentiated from *Ulrica* by a body thinner in lateral view and the pronotum being anteriorly wider than posteriorly. In *Ulrica* the body is thicker in lateral view and the pronotum being anteriorly narrower than posteriorly.

Andersonoplatus andersoni **sp. n.**

http://zoobank.org/0603250A-C52E-4017-BF6E-85E506F3E4AD

Figs 1, 2

Description. Body length 2.43–3.02 mm, width 1.24–1.72 mm, pronotum and elytra with sparse, semi-erect hairs, shiny, moderately convex in lateral view. Color pale brown to dark brown.

Head (Fig. 1D): slightly convex in lateral view, generally smooth with fine reticulation and few punctures of different size and shape above antennal callus, gena shiny, with

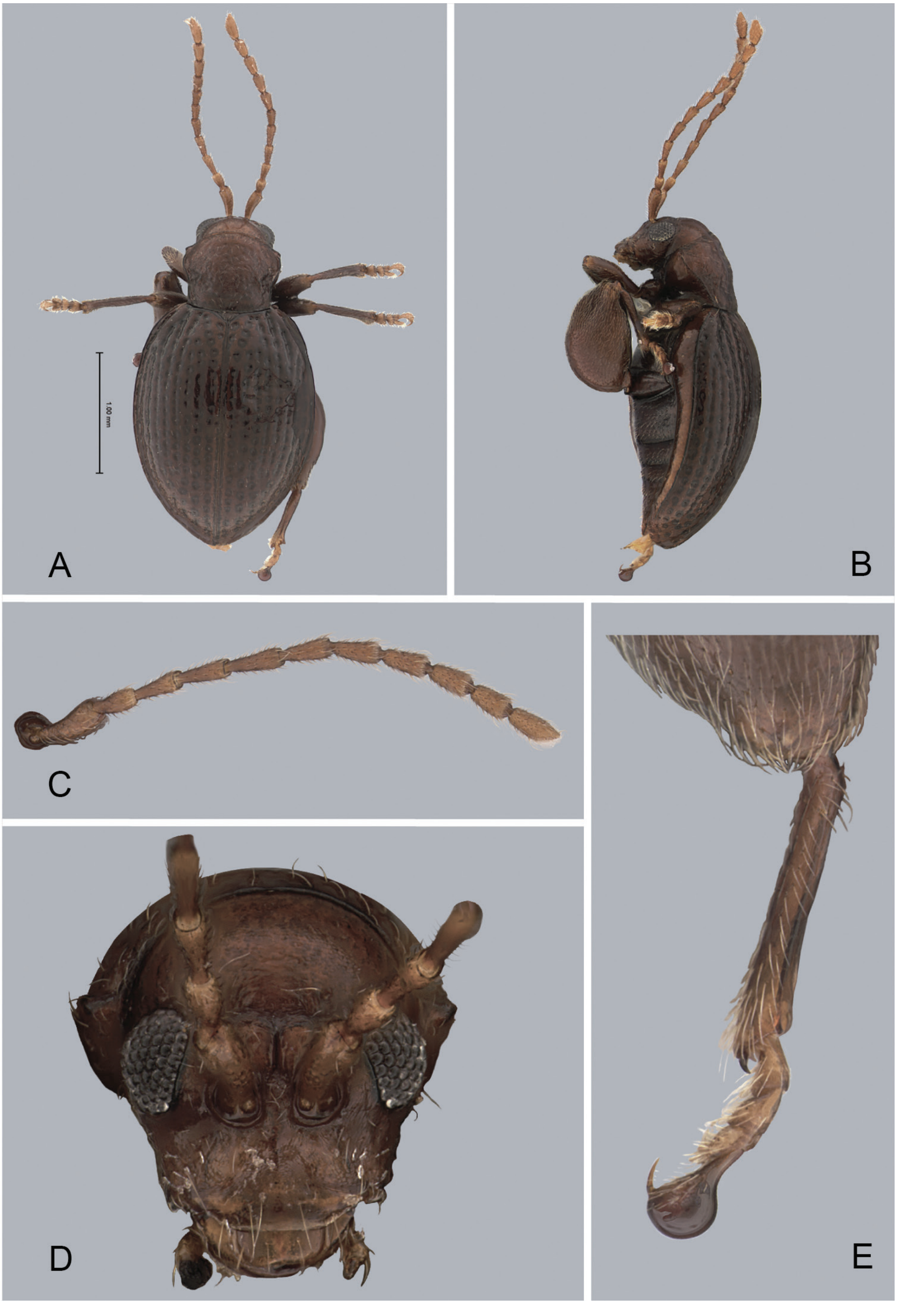

Figure 1. *Andersonoplatus andersoni*. **A** Habitus dorsal **B** Habitus lateral **C** Antenna **D** Head, frontal view **E** Hind leg.

few sparse punctures and sparse pilosity. Frons and vertex forming almost a 135° angle in lateral view. Antennal callus delineate from vertex by deep and straight supracallinal sulcus. Antennal callus elevated above vertex; surface even, with no or two punctures, if bearing setae, they are short. Orbital sulcus deep. Supraorbital sulcus represented by few deep punctures near antennal socket, absent near supracallinal sulcus. Supraorbital and supracallinal sulci not connected. Suprafrontal sulcus shallow. Frontolateral sulcus deep. Frontogenal suture deep. Frontal ridge short and narrow, widest in middle. Anterofrontal ridge long, relatively tall, oblique. Antennae filiform. The last five antennomeres slightly wider and shorter than antennomeres III-VI; antennomere II shortest.

Thorax: pronotum (Fig. 1A, B) much narrower than elytra, notched laterally near middle. Anterior margin straight, wider than posterior, posterior margin nearly straight, lateral margin slightly sinuated. Surface reticulated, granulated, with very short and sparse pilosity and two vague impressions below middle, sparsely covered with variously defined punctures, diameter of which smaller than distance between punctures. Prosternal surface densely punctate. Elytra fused. Elytral surface shiny, with sparse, white, semi-erect hairs. Punctures (Fig. 1A) forming nine striae, ninth stria merge with marginal one. Interspaces convex. Punctures at base of fifth and sixth striae deeper than other having fold-like appearance. Second and third striae not reaching elytral base. Epipleura nearly vertical. Metafemur longer than wide and 1.46 times longer than metatibia. Claws appendiculate and long.

Male genitalia (Fig. 2F): median lobe simple, convex in lateral view; in ventral view, with lateral margins lightly concave, apex subtriangular, slightly protruding, and rounded on top. Ventral side with shallow longitudinal impression bottom of which covered with transverse wrinkles, sides of impression not forming ridges. Basal part long and bent ventrally in lateral view.

Female genitalia (Fig. 2A–E): eighth tergite with rounded posterior margin, more sclerotized laterally, bearing many moderately long setae (Fig. 2D). Tignum long, narrow, with central canal; posterior area broad, truncate; anterior area spatulate (Fig. 2C). Vaginal palpi elongate, basally strongly sclerotized, each with approximately eight setae at apex (Fig. 2B). Palpi rounded at apex, enlarged at last third but thinned at apex, situated close together and merged anteriorly for more than half of their length. Spermatheca curved, with receptacle and pump not differentiated from each other. Apex of pump with spoon-like projection. Spermathecal duct long, widest at base, without coils, making relatively long loop (Fig. 2E).

Type material. Holotype, ♂. VENEZUELA: Trujillo/ camino viejo a Trujillo, Paramo/ La Cristalina, km 9.7, 2400m/ 09°21'21"N, 70°17'51"W/ 20.V.1998-022F/ R.Anderson, elfin for. Litter (MIZA). **Paratypes** (7♂ 4♀ USNM). (2♂ USNM) same label as holotype except: (1♂ USNM) "022A"; (3♂1♀ CMNC) "022E"; (1♂3♀ USNM) "022J".

Etymology. We name this species after R. Anderson. Regardless how many taxa we name after him, his remarkable discoveries of leaf litter flea beetles in the New World would warrant many more.

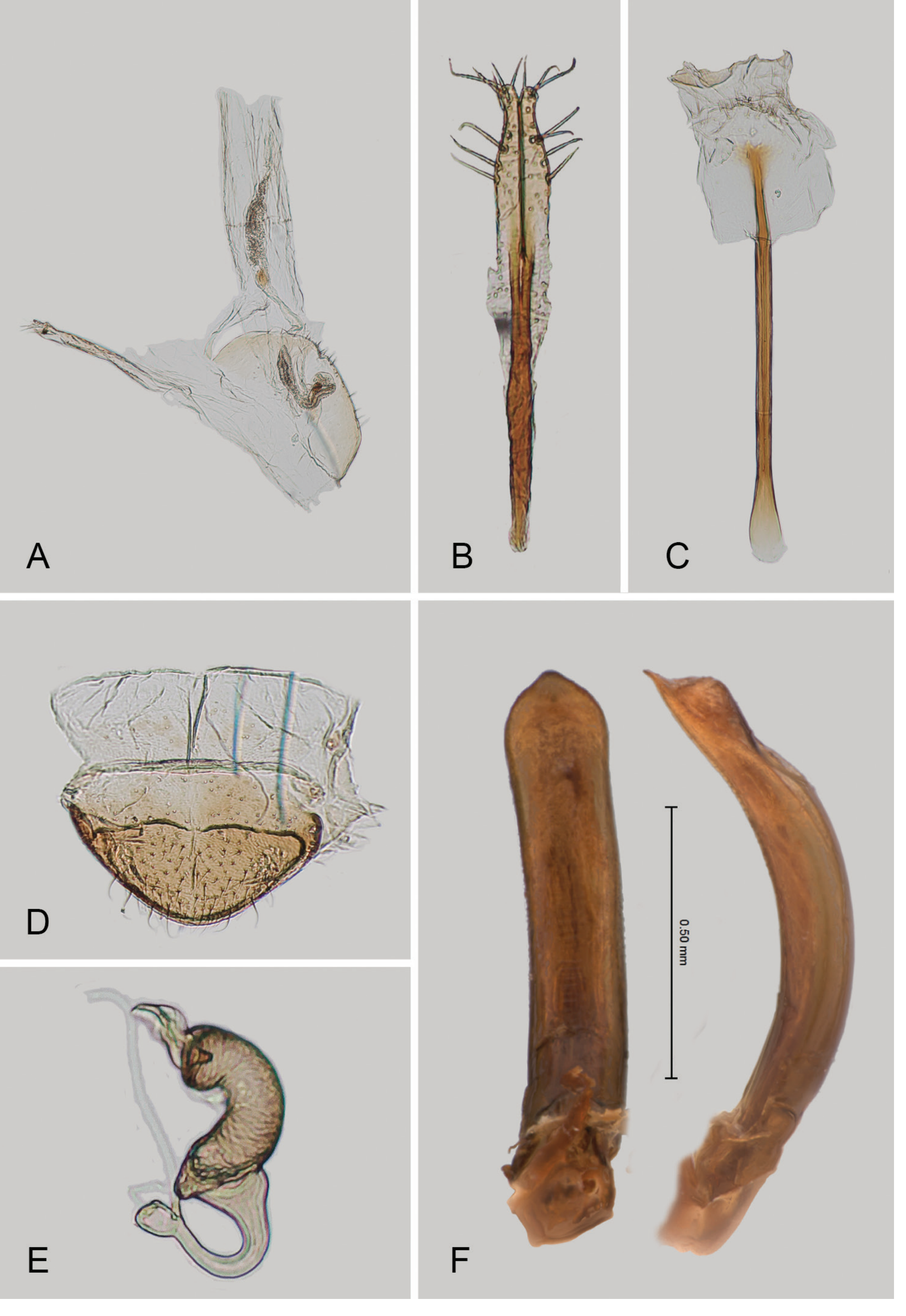

Figure 2. *Andersonoplatus andersoni*. **A** Female genitalia, lateral view **B** Vaginal palpi **C** Tignum **D** Last abdominal tergite of female **E** Spermatheca **F** Median lobe of aedeagus, ventral and lateral views.

Differential diagnosis. *Andersonoplatus andersoni* is similar to *A. sanare* but can be differentiated from it based on the following characters: ventral side of median lobe with shallow longitudinal impression bottom of which covered with transverse wrinkles (Fig. 2F) and spermathecal duct making relatively long loop (Fig. 2E). In *A. sanare*: ventral side of median lobe without longitudinal impression (Fig. 33A) and spermathecal duct making relatively short loop (Fig. 33E).

Andersonoplatus baru **sp. n.**
http://zoobank.org/41C61682-A5A2-4231-9DF7-96D4BDA2F57D
Figs 3, 4

Description. Body length 3.39–3.40 mm, width 1.62–1.67 mm, moderately shiny, densely pilose, with semi-erect hairs, flat in lateral view. Uniform yellow with antennae and legs slightly lighter than body.

Head (Fig. 3B, D): slightly convex in lateral view, moderately shiny, generally reticulated, and densely pilose. Frons and vertex forming near a 135° angle in lateral view. Antennal callus delimited from vertex by straight sulcus; slightly elevated above vertex; surface uneven, with more than two punctures, some of them bearing setae. Orbital sulcus shallow. Supraorbital sulcus deep not connected with supracallinal. Suprafrontal and frontolateral sulcus absent. Frontogenal suture shallow. Orbit narrower than transverse diameter of antennal socket. Interantennal space narrower than transverse diameter of eye and as wide as transverse diameter of antennal socket. Frontal ridge short and narrow. Anterofrontal ridge short, relatively tall, oblique. Last five antennomeres shorter and wider than second.

Thorax: pronotum (Fig. 3A, B) slightly trapezoidal, narrower than elytra. Anterior margin wider than the posterior, posterior margin straight, lateral margin slightly sinuated. Surface reticulated, densely punctate, densely pilose. Pronotal disc dull. Scutellum triangular, wider than long, reticulated. Prosternal surface reticulated. Posterior end nearly twice as wide as middle. Elytra fused. Elytral surface dull, pilose, with semi-erect hairs, deeply punctate (Fig. 3A). Punctures forming nine striae. Interspaces convex, with small punctures. Marginal elytral stria consisting of two punctures. Second and third striae reaching elytral base. Epipleura nearly vertical. Metafemur longer than wide and 1.57 times longer than metatibia. Metatibia almost straight in lateral view, slightly curved in dorsal view. Claws simple and long. Posterior margin of fourth ventrite nearly straight. Males unknown.

Female genitalia (Fig. 4A–C): tignum long, narrow, with central canal; posterior area broad, sclerotization poorly delineated; anterior area spatulate (Fig. 4B). Vaginal palpi elongate, basally strongly sclerotized, each with approximately eight setae at apex (Fig. 4C). Palpi rounded at apex, enlarged at last third but thinned at apex, situated close together and merged anteriorly for more than half of their length. Posterior sclerotization of vaginal palpi with convex sides. Spermatheca curved, with receptacle and

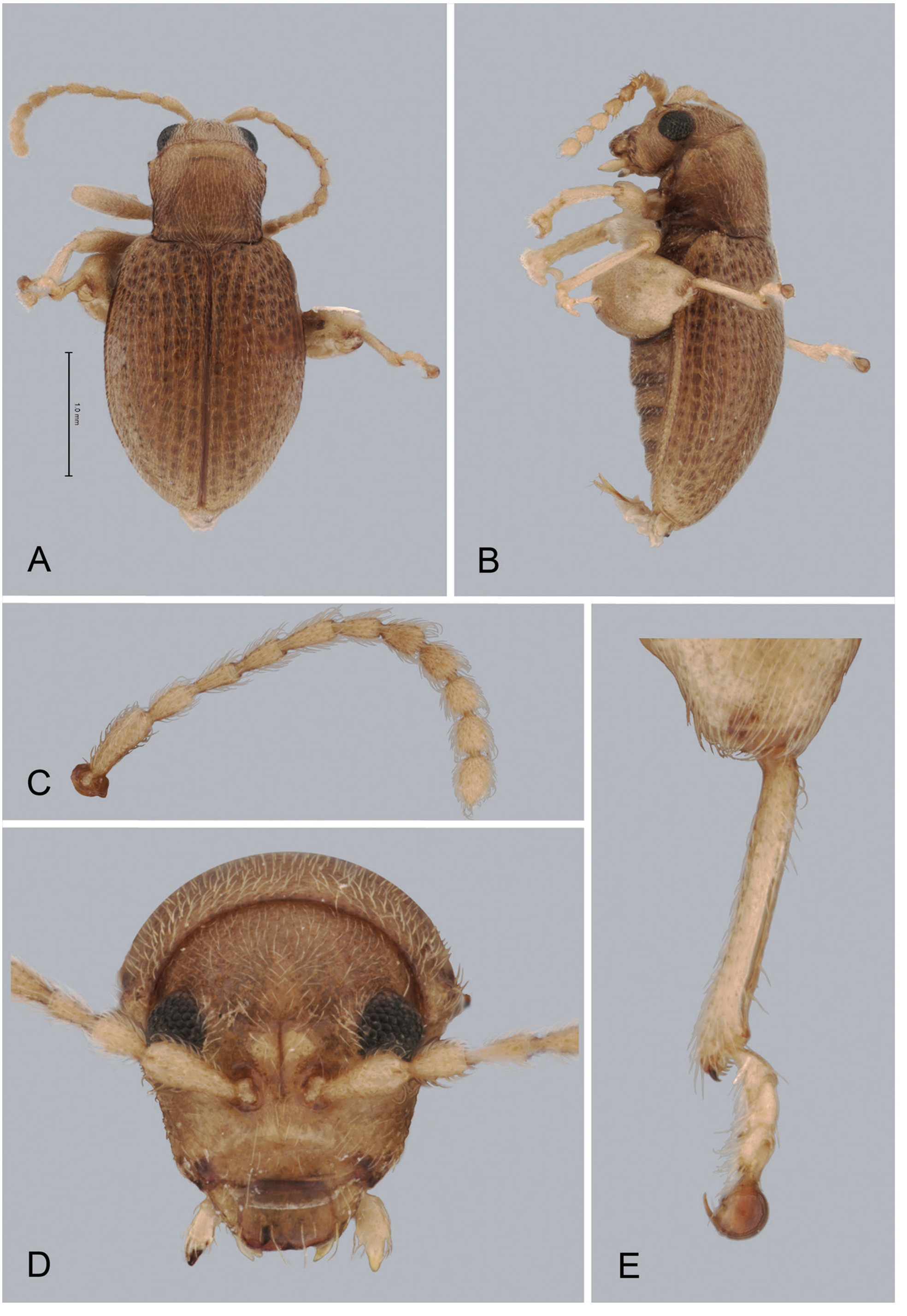

Figure 3. *Andersonoplatus baru*. **A** Habitus dorsal **B** Habitus lateral **C** Antenna **D** Head, frontal view **E** Hind leg.

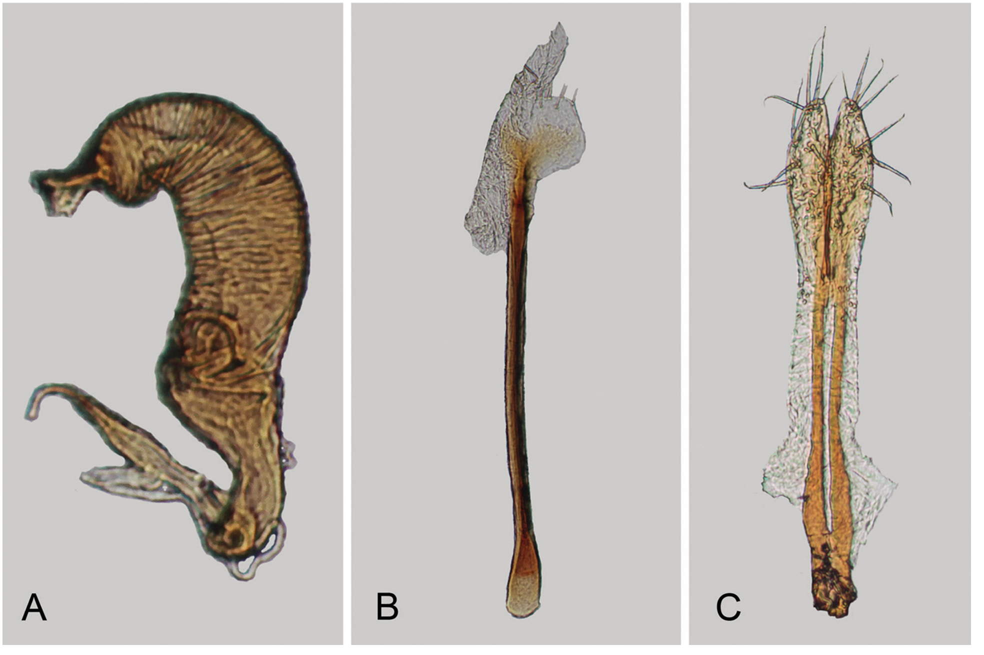

Figure 4. *Andersonoplatus baru*. **A** Spermatheca **B** Tignum **C** Vaginal palpi.

pump not differentiated from each other. Apex of pump with spoon-like projection. Spermathecal duct long, widest at base, without coils (Fig. 4A).

Type material. Holotype, ♀. PANAMA: Chiriquí/ P.Nac. Volcan Baru, 5.9/ km E. Cerro Punta, 2400m/ 14.VI.1995-21B, R.S. Ander-/ son, oak ridge bamboo for. litt. (MIZA). **Paratype** (1♀ USNM). Same label as holotype except “21G”.

Etymology. This species is a noun in apposition based on the type locality, volcano Baru in Chiriqui mountains where it was collected.

Diagnosis. Dorsal surface densely covered with hairs, light straw color, second and third elytral striae reaching elytral base.

Andersonoplatus bechyneorum sp. n.

http://zoobank.org/A103349B-1412-4E92-AF34-96FEC964836C

Figs 5, 6

Description. Body length 2.32–2.64 mm, width 1.29–1.40 mm, pronotum and elytra with sparse, semi-erect hairs, shiny, elliptical, moderately convex in lateral view. Color castaneous.

Head (Fig. 5B, D): slightly convex in lateral view, generally smooth, gena and frons shiny with sparse pilosity. Frons and vertex forming an angle of approximately 135° in lateral view. Antennal callus delineate from vertex by shallow and straight supracallinal

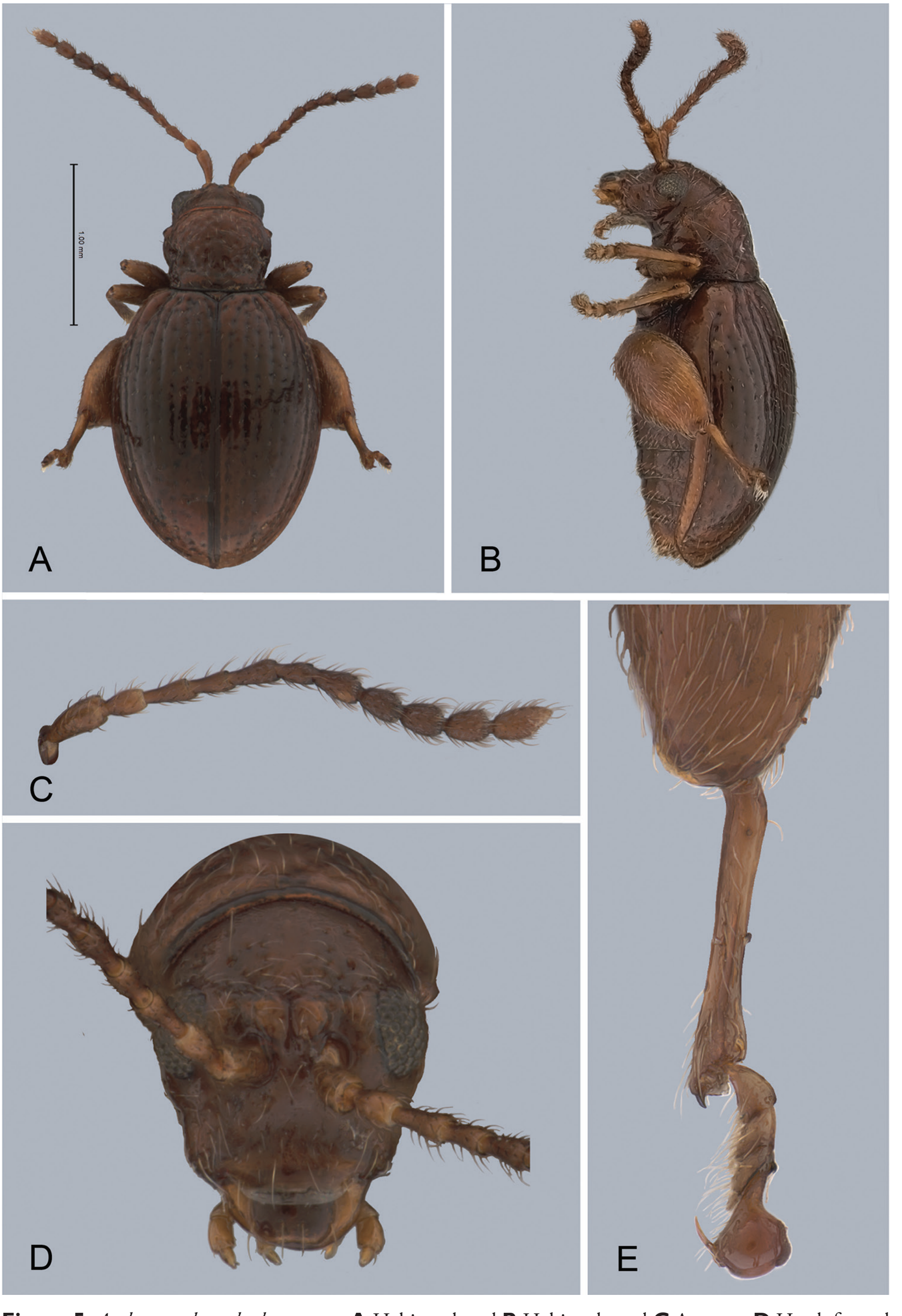

Figure 5. *Andersonoplatus bechyneorum*. **A** Habitus dorsal **B** Habitus lateral **C** Antenna **D** Head, frontal view **E** Hind leg.

sulcus. Antennal callus slightly elevated above vertex, surface even, with no or two punctures, if bearing setae, they are short. Orbital sulcus shallow. Supraorbital sulcus represented by few deep punctures near antennal socket, absent near supracallinal sulcus. Supraorbital and supracallinal sulcus not connected. Suprafrontal sulcus absent. Frontolateral sulcus shallow. Frontogenal suture indistinguishable. Interantennal space narrower than transverse diameter of eye and as wide as transverse diameter of antennal socket. Frontal ridge short and narrow. Last five antennomeres slightly wider than preceding ones.

Thorax: pronotum (Fig. 5A, B) much narrower than elytra, notched laterally below middle. Anterior margin straight, wider than posterior, posterior margin nearly straight, lateral margin sinuated. Anterior angles acute. Surface deeply granulate, with pilosity very short and very sparse. Pronotal disc weakly raised. Post basal impression present, with deeper rounded impressions laterally. Scutellum rounded, much shorter than wide, setose. Prosternal surface reticulated. Posterior end of intercoxal process nearly twice as wide as middle. Elytra fused. Elytral surface shiny, with very sparse, white, semi-erect hairs, deeply punctated (Fig. 5A). Punctures forming nine striae, the ninth stria overlapping with marginal one. Each punctation bears one very short setae (some setae can be found on the interspaces). Interspaces very convex. Punctures at base of fifth and sixth striae deeper than other having fold-like appearance. Marginal line of elytra interrupted at base. Second and third striae not reaching elytral base. Epipleura slightly convex, nearly vertical. Metafemur longer than wide and 1.60 times longer than metatibia. Claws simple and long.

Male genitalia (Fig. 6D): ventral side with deep longitudinal impression with bottom lacking transverse wrinkles, sides of impression form high ridges. Apical denticle sharply bent ventrally.

Female genitalia (Fig. 6A–C): tignum long, narrow, with central canal; posterior area broad, sclerotization relatively well delineated; anterior area spatulate (Fig. 6B). Vaginal palpi elongate, basally strongly sclerotized, each with approximately eight setae at apex (Fig. 6A). Palpi pointed at apex, enlarged at last third but thinned at apex, situated close together and merged anteriorly for more than half of their length. Spermatheca curved, with receptacle and pump not differentiated from each other. Apex of pump with spoon-like projection. Spermathecal duct short, widest at base, without coils (Fig. 6C).

Type material. Holotype, ♂. VENEZUELA: Trujillo/ camino viejo a Trujillo, Paramo/ La Cristalina, km 9.7, 2400m/ 09°21'21"N, 70°17'51"W/20.V.1998-022B/ R.Anderson, elfin for. litter (MIZA). **Paratypes** (5♂ USNM, 1♀ CMNC). Same label as holotype.

Etymology. We name this species after Mila and Jan Bechyne who together made large contribution to our knowledge of mostly Neotropical leaf beetles describing 143 genera and 2290 species.

Differential diagnosis. *Andersonoplatus bechyneorum* can be differentiated from most *Andersonoplatus* species by the following characters: pronotal surface uneven, covered with relatively large but poorly defined punctures (Fig. 5A) and median lobe of aedeagus ventrally with two ridges and deep grove between them (Fig. 6D).

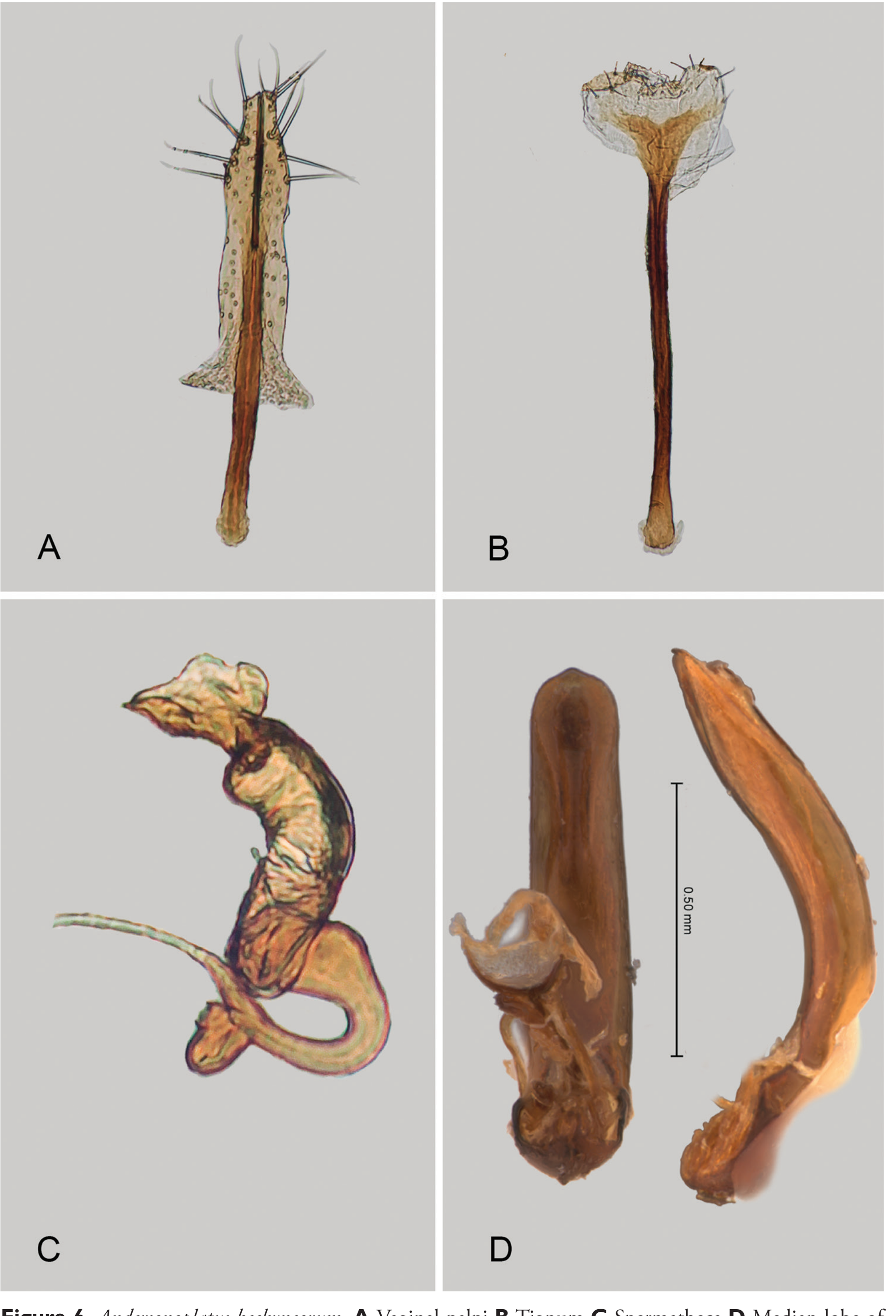

Figure 6. *Andersonoplatus bechyneorum*. **A** Vaginal palpi **B** Tignum **C** Spermatheca **D** Median lobe of aedeagus, ventral and lateral views.

***Andersonoplatus castaneus* sp. n.**
http://zoobank.org/49729921-C29A-4A50-B370-623232423114
Figs 7, 8, 9

Description. Body length 2.59–3.29 mm, width 1.45–1.78 mm, pronotum and elytra with very sparse, semi-erect hair, shiny, moderately convex in lateral view. Color brown to chestnut brown with a pearl luster; antennae and legs much lighter.

Head (Fig. 7B, D): slightly convex in lateral view, generally smooth with fine reticulation, gena with sparse pilosity. Frons and vertex forming nearly a 135° angle in lateral view. Antennal callus delimited from vertex by deep and slightly inclined supracallinal sulcus. Antennal callus raised, surface even, with no or two punctures, if bearing setae, they are short. Orbital sulcus deep. Supraorbital sulcus absent. Supraantennal sulcus deep. Suprafrontal sulcus absent. Frontolateral sulcus shallow. Frontogenal suture well developed. Subgenal suture well developed along base of mandible. Orbit narrower than transverse diameter of antennal socket. Interantennal space narrower than transverse diameter of eye and as wide as transverse diameter of antennal socket. Frontal ridge short and narrow. Eyes with nearly more than 20, small ommatidia. The last five antennomeres as long as sixth, slightly wider than preceding ones; second antennomere shortest (Fig. 7C).

Thorax: pronotum (Fig. 7A, B) much narrower than elytra, notched laterally below middle. Anterior margin wider than posterior, posterior margin slightly concave, lateral margin sinuated. Anterior angles pointed outward. Surface reticulated, with pilosity very short and sparse, lacking punctures. Pronotal disc weakly raised. Scutellum triangular. Prosternal surface reticulated. Prosternal intercoxal process narrow. Posterior end twice as wide as middle. Elytra weakly fused. Elytral surface shiny, with very sparse, white, semi-erect hairs, and a pearl luster. Punctures (Fig. 7A) forming nine striae (marginal stria consisting of one or two punctures). Elytral interspaces flat. Second and third striae reaching elytral base. Epipleura nearly vertical. Metafemur greatly enlarged, longer than wide and 1.76 times longer than metatibia. Claws simple and long.

Male genitalia (Fig. 8A): ventral side with longitudinal impression with bottom lacking transverse wrinkles, sides of impression form ridges. Apical denticle not developed in ventral view, apex bent ventrally.

Female genitalia (Fig. 8B–G): tignum long, narrow, bent, with central canal; posterior area broad, sclerotization relatively well delineated; anterior area weakly widened (Fig. 8B). Vaginal palpi elongate, basally strongly sclerotized, each with approximately eight setae at apex (Fig. 8C). Palpi pointed at apex, enlarged at last third but thinned at apex, situated close together and merged anteriorly for more than half of their length. Spermatheca curved, with receptacle and pump not differentiated from each other. Apex of pump with spoon-like projection. Spermathecal duct short, widest at base, without coils (Fig. 8E).

Type material. Holotype, ♂. VENEZUELA: Trujillo/ camino Viejo a Trujillo, Paramo/ La Cristalina, km 9.7, 2400m/ 09°21'21"N, 70°17'51"W/ 20.V.1998-022C (MIZA). **Paratypes** (6♂ 5♀ USNM). Same label as holotype except: (1♂1♀ CMNC)

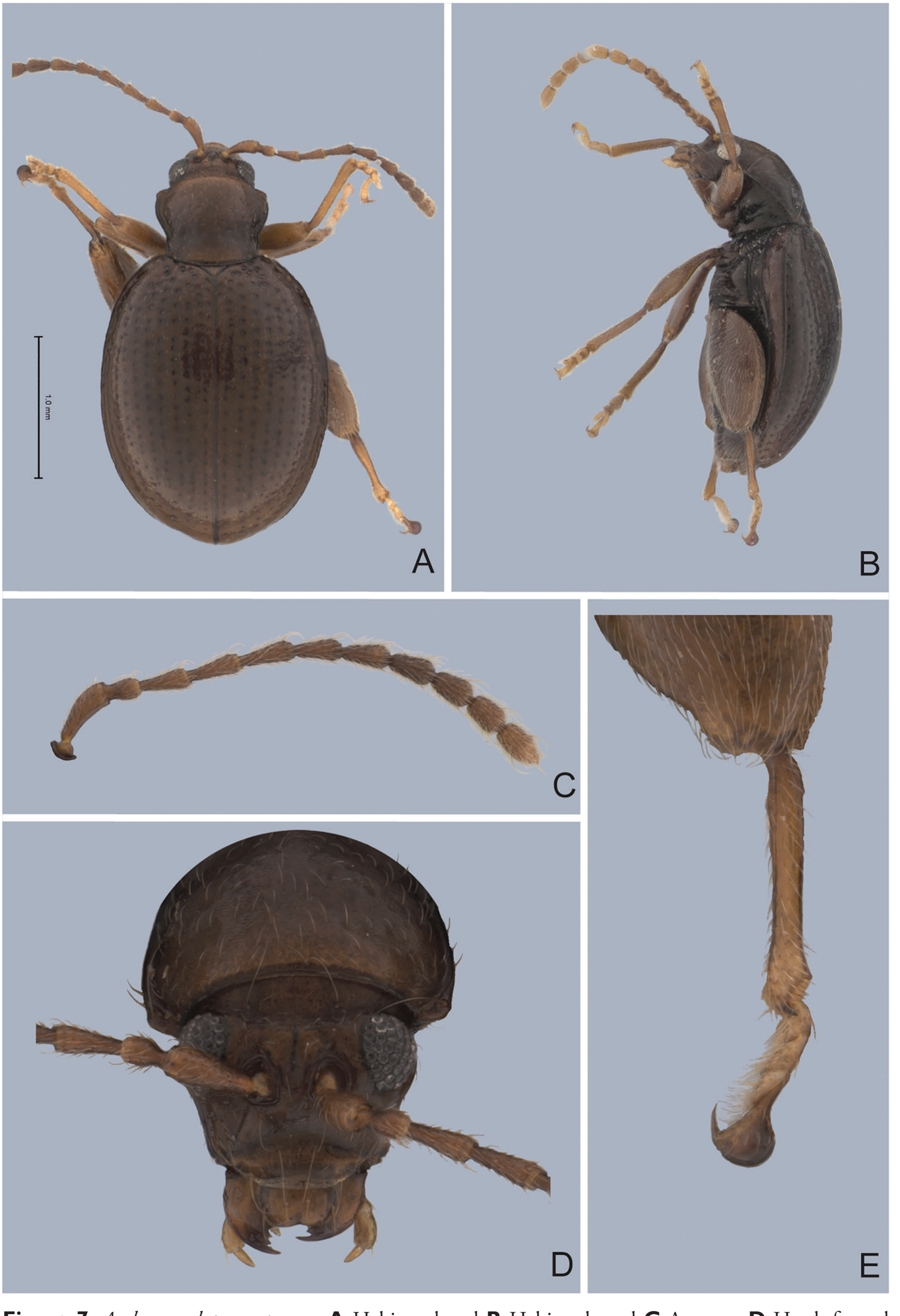

Figure 7. *Andersonoplatus castaneus*. **A** Habitus dorsal **B** Habitus lateral **C** Antenna **D** Head, frontal view **E** Hind leg.

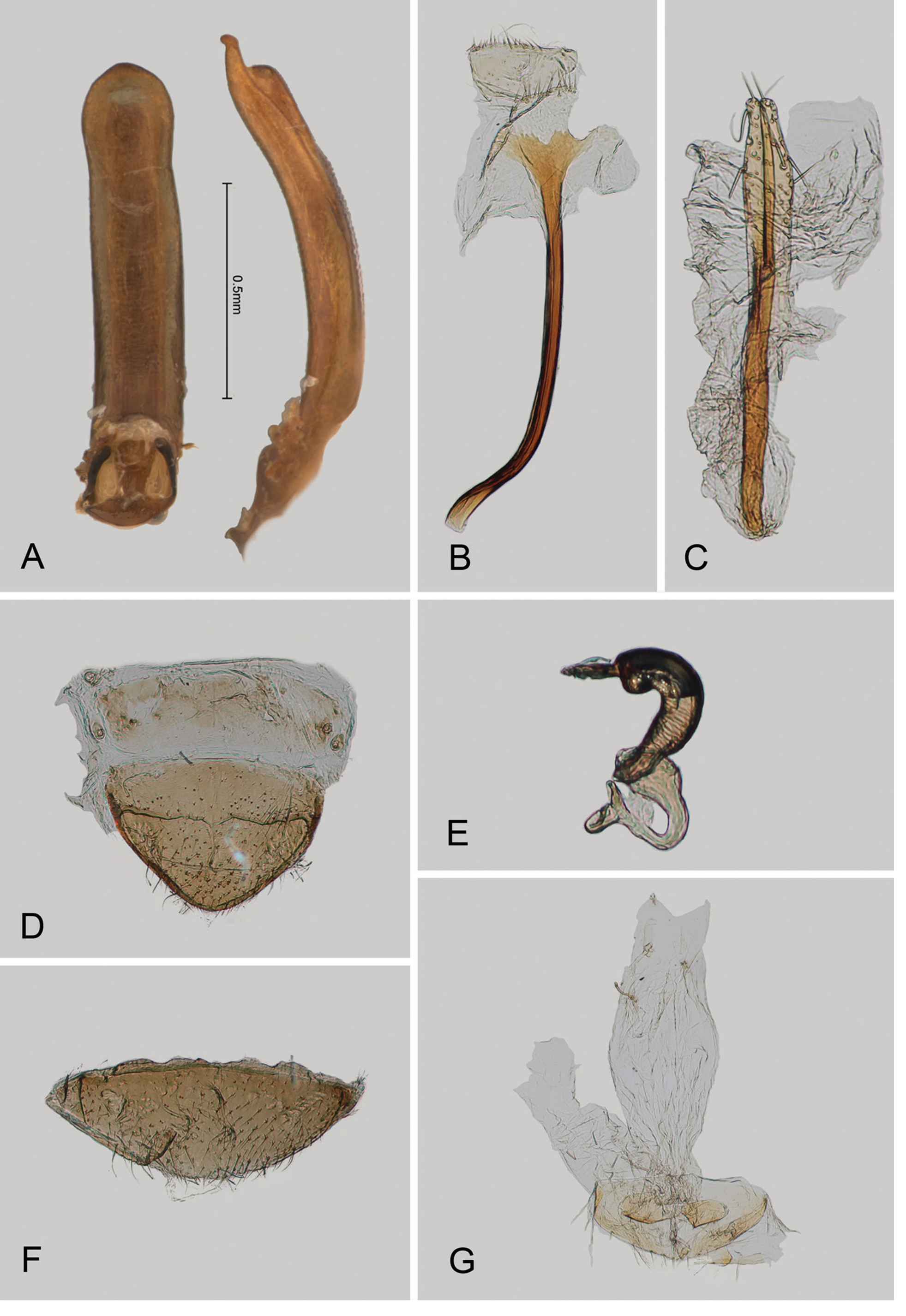

Figure 8. *Andersonoplatus castaneus*. **A** Median lobe of aedeagus, ventral and lateral views **B** Tignum **C** Vaginal palpi **D** Last abdominal tergite of female **E** Spermatheca **F** Last abdominal sternite of female **G** Female genitalia, ventral view.

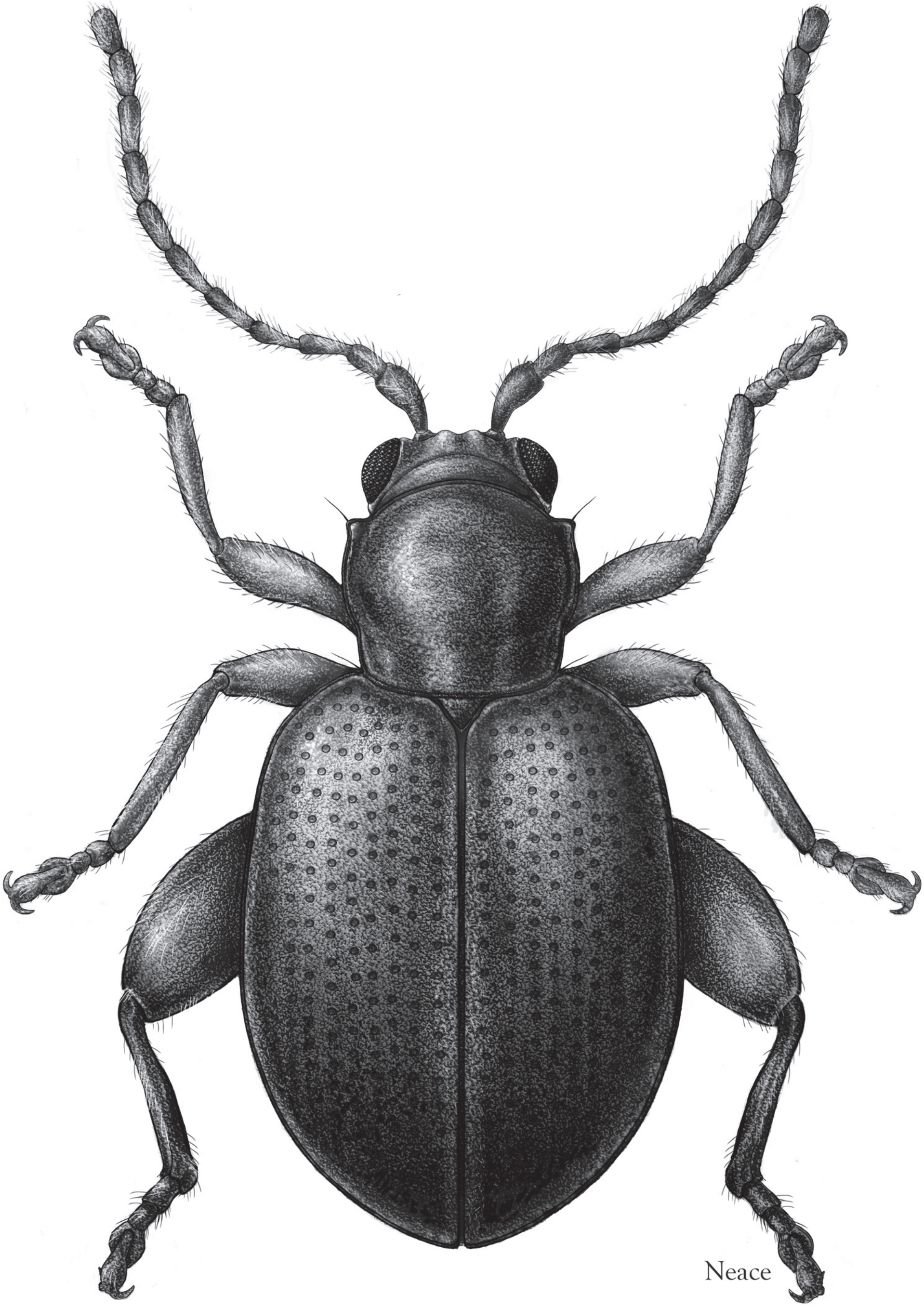

Figure 9. *Andersonoplatus castaneus*. Dorsal habitus, illustration by Meghan Neace.

“022D”; (1♂1♀ USNM) “022F”; (3♂2♀ USNM) “022J”; (1♀ CMNC) “022E”; (1♂ CMNC) “camino viejo a Trujillo/ km 6.0, 2240m/ 09°21'03"N, 70°17'36"W/ E.Anderson, cloud for. litter”.

Etymology. The specific epithet is a noun in apposition based on the color of the beetles.

Differential diagnosis. *Andersonoplatus castaneus* is similar to *A. jolyi* and can be differentiated from it based on the following characters: supracallinal sulci well developed, deep (Fig. 7D); apex of median lobe of aedeagus bent ventrally in lateral view (Fig. 8A).

Andersonoplatus flavus sp. n.

http://zoobank.org/2361E43C-6838-4339-A589-128B453FAA84

Figs 10, 11

Description. Body length 2.70–2.91 mm, width 1.40–1.51 mm, pronotum and elytra with sparse, semi-erect hairs, shiny, moderately convex in lateral view. Color yellow.

Head (Fig. 10B, D): slightly convex in lateral view, vertex smooth with a fine reticulation, gena shiny, slightly punctuated with sparse pilosity. Frons and vertex forming nearly a 135° angle in lateral view. Antennal callus delineated from vertex by deep and inclined supracallinal sulcus. Antennal callus elevated above vertex, surface even, with no or two punctures, if bearing setae, they are short. Orbital sulcus deep. Supraorbital sulcus shallow, almost connected with supracallinal sulcus. Suprafrontal and frontolateral sulci deep. Frontogenal suture well developed. Orbit narrower than transverse diameter of antennal socket. Interantennal space narrower than transverse diameter of eye and transverse diameter of antennal socket separately. Frontal ridge short and narrow. Antennae filiform; antennomeres three to eleven similar in length with last five ones slightly wider; second antennomere shortest (Fig. 10C).

Thorax: pronotum (Fig. 10A) much narrower than elytra, notched laterally nearly at middle. Anterior margin wider than posterior, posterior margin nearly straight, lateral margin slightly sinuated. Anterior angles pointed outward. Surface reticulated, sparsely covered with large punctures, with very short and very sparse hairs, sparsely covered with variously defined punctures, diameter of which smaller than distance between punctures. Pronotal disc weakly raised. Scutellum triangular, much shorter than wide. Prosternal surface reticulated. Prosternal intercoxal process narrow. Posterior end twice as wide as middle. Elytra fused. Elytral surface shiny, with sparse, white, semi-erect hairs. Punctures forming nine striae, ninth stria merge with marginal one. Interspaces slightly convex. Punctures at base of fifth and sixth striae deeper than others. Second and third striae not reaching elytral base. Epipleura nearly vertical, with a line of punctation along internal margin. Metafemur greatly enlarged, 1.59 times longer than metatibia. Claws appendiculate, long.

Male genitalia (Fig. 11A): apical denticle well developed, wide in ventral view, apex straight, not bent ventrally.

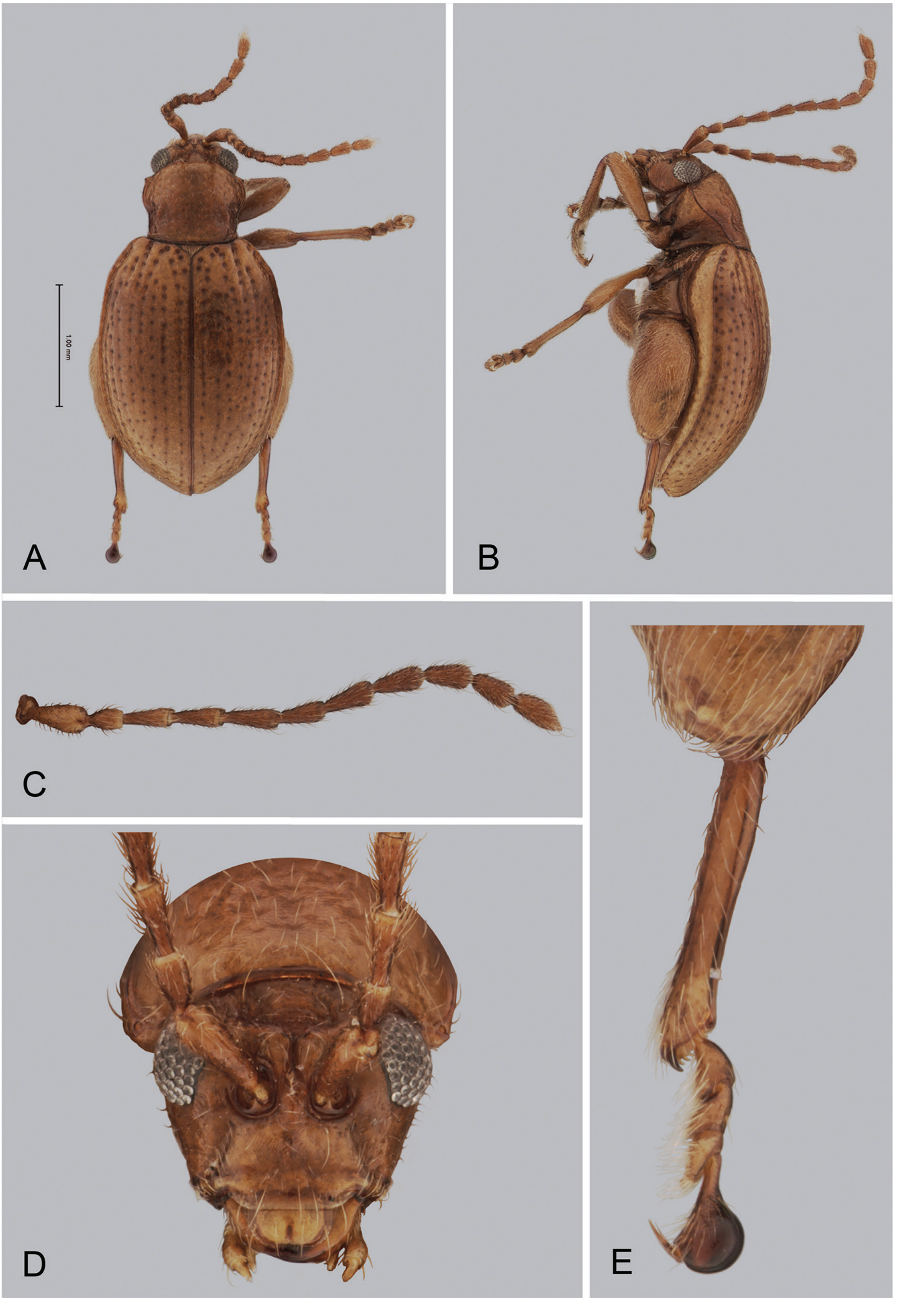

Figure 10. *Andersonoplatus flavus*. **A** Habitus dorsal **B** Habitus lateral **C** Antenna **D** Head, frontal view **E** Hind leg.

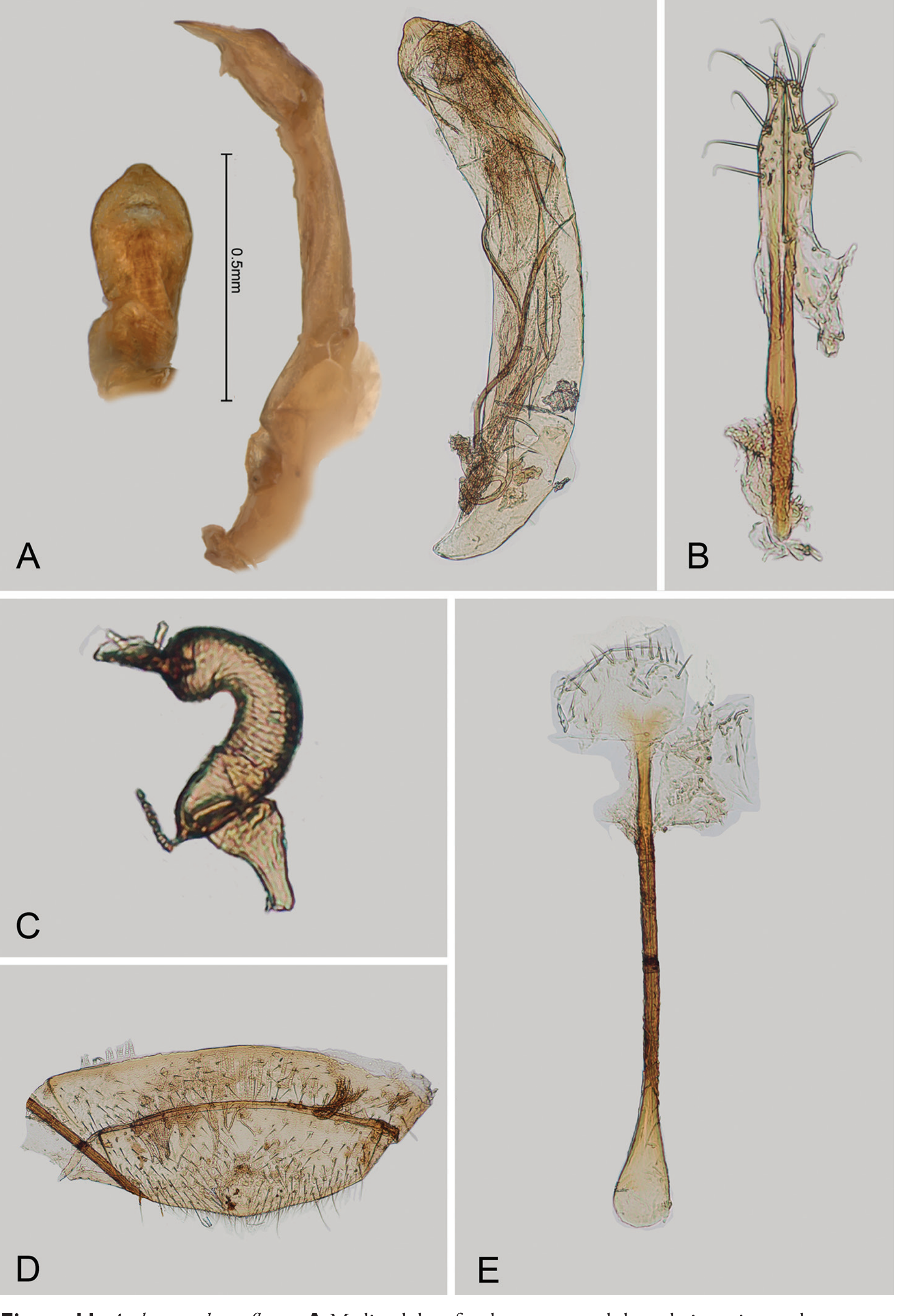

Figure 11. *Andersonoplatus flavus*. **A** Median lobe of aedeagus, ventral, lateral views, internal structures under compound scope **B** Vaginal palpi **C** Spermatheca **D** Last abdominal sternite of female **E** Tignum.

Female genitalia (Fig. 11B–E): tignum long, narrow, slightly bent, with central canal; posterior area broad, sclerotization poorly delineated, anterior area weakly spatulate (Fig. 11E). Vaginal palpi elongate, basally strongly sclerotized, each with approximately eight setae at apex (Fig. 11B). Palpi pointed at apex, enlarged at last third but thinned at apex, situated close together and merged anteriorly for more than half of their length. Spermatheca curved, with receptacle and pump not differentiated from each other. Apex of pump with spoon-like projection. Spermathecal duct short, widest at base, without coils (Fig. 11C).

Type material. Holotype, ♂. VENEZUELA: Trujillo/ camino viejo a Trujillo, Paramo/ La Cristalina, km 9.7, 2400m/ 09°21'21"N, 70°17'51"W/ 20.V.1998-022F/ R.Anderson, elfin for. litter (MIZA). **Paratypes** (1♂ 1♀ USNM) same label as holotype. (1♀ CMNC) same label as holotype data except: "022C" and "22E".

Etymology. The specific epithet is a noun in apposition based on the color of the beetles.

Differential diagnosis. *Andersonoplatus flavus* can be differentiated from most *Andersonoplatus* species based on the following characters: body color yellow; pronotal surface sparsely covered with variously defined punctures, diameter of which smaller than distance between punctures; second elytral stria not reaching base; supracallinal sulci very deep; antennomeres longer than in most species of genus.

Andersonoplatus jolyi sp. n.

http://zoobank.org/D60F429D-7A7E-4EAA-B9B2-1E33156800D1
Figs 12, 13

Description. Body length 2.59–2.97 mm, width 1.29–1.40 mm, shiny, pilose, slightly flat in lateral view. Color light brown to dark brown.

Head (Fig. 12B, D): slightly convex in lateral view, generally reticulate, pilose. Supracallinal sulci poorly developed, barely perceptible, or marked with few punctures. Antennal callus not raised entering interantennal space, surface even, with no or two punctures, if bearing setae, they are short. Orbital sulcus shallow, represented by a line of punctures. Supraorbital sulcus absent. Suprafrontal sulcus deep. Frontolateral sulcus absent. Frontogenal suture shallow. Orbit narrow, punctated. Interantennal space slightly wider than transverse diameter of eye and twice as wide as transverse diameter of antennal socket. Frontal ridge wide and short. Anterofrontal ridge short and shallow. Eyes with more than 20, small ommatidia. Antenna (Fig. 12C) with antennomere two similar in length to three, the last five ones moniliform, with denser setae.

Thorax: pronotum (Fig. 12A, B) narrower than elytra. Anterior margin, wider than posterior; posterior margin nearly straight, lateral margin sinuated. Surface reticulate, punctuate, with sparse, well visible pilosity. Pronotal disc not raised. Scutellum rounded, much shorter than wide. Prosternal surface reticulated. Prosternal intercoxal process thin. Posterior end nearly twice as wide as middle. Procoxae very close to each other. Elytra fused. Elytral surface shiny, with short, white, semi-erect hairs. Punctures

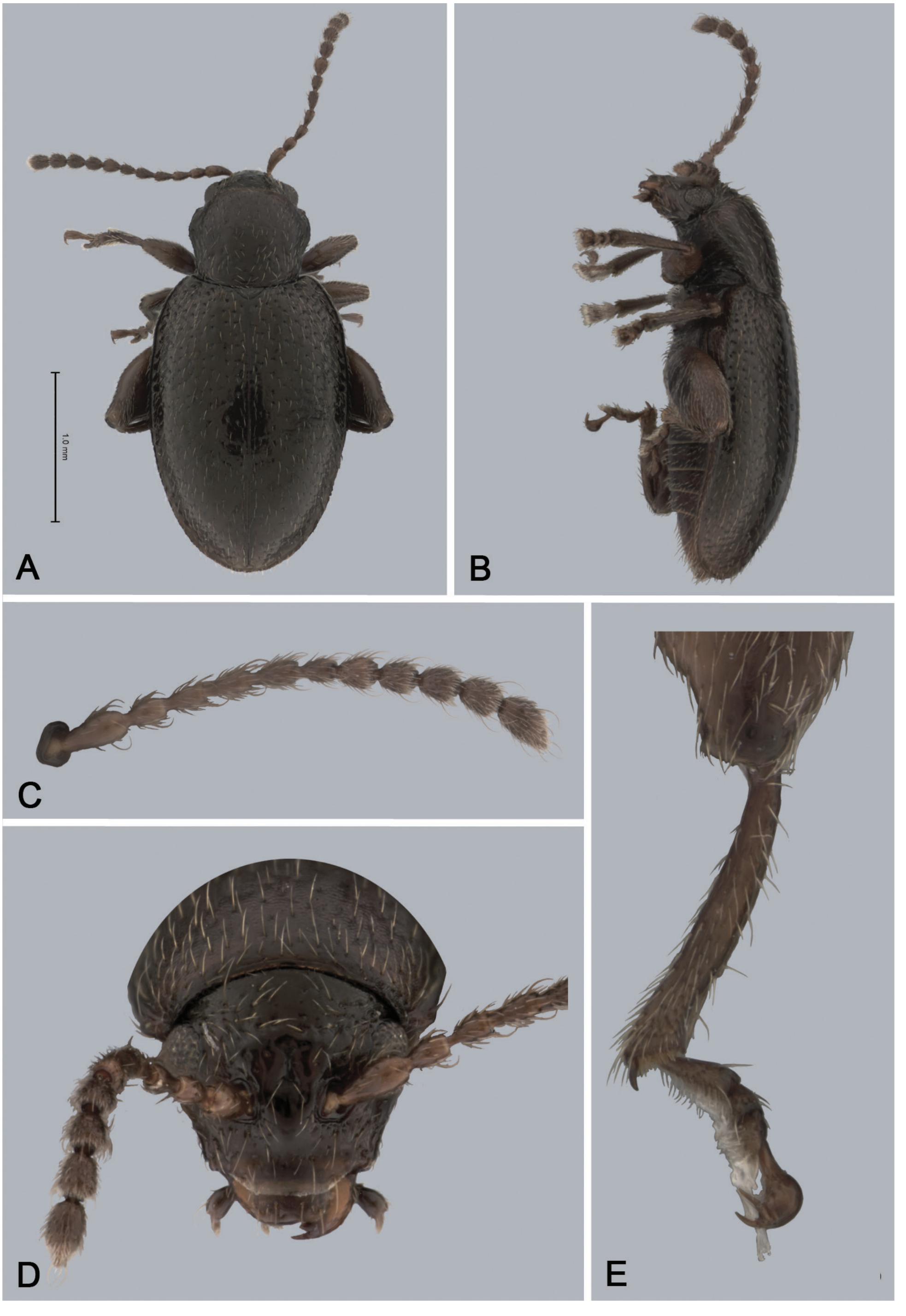

Figure 12. *Andersonoplatus jolyi*. **A** Habitus dorsal **B** Habitus lateral **C** Antenna **D** Head, frontal view **E** Hind leg.

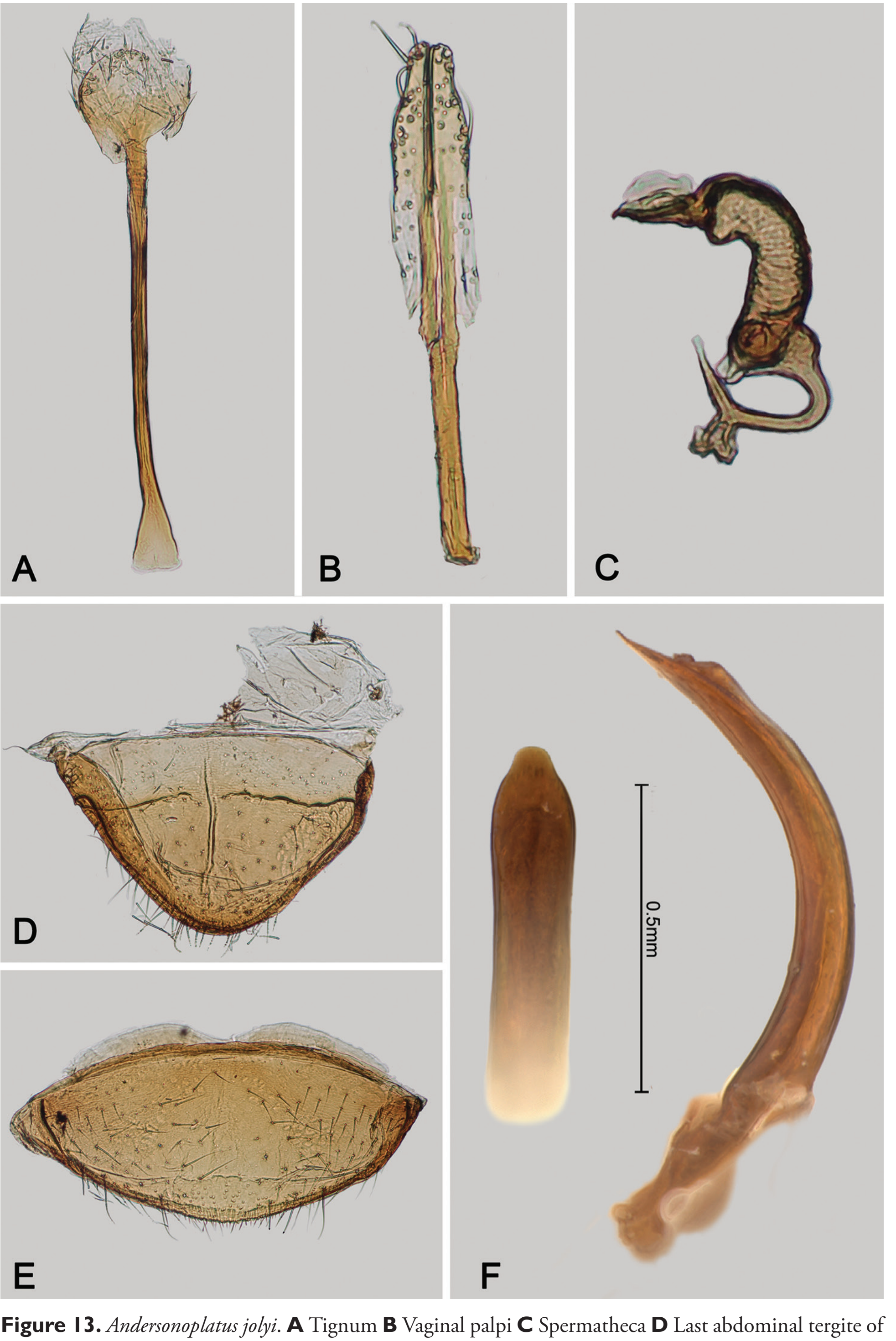

Figure 13. *Andersonoplatus jolyi*. **A** Tignum **B** Vaginal palpi **C** Spermatheca **D** Last abdominal tergite of female **E** Last abdominal sternite of female **F** Median lobe of aedeagus, ventral and lateral views.

(Fig. 12A) forming nine slightly confused lines. Each puncture bears one very short setae. Interspaces flat. Epipleura nearly horizontal. Metafemur elongated, 1.59 times longer than metatibia. Metatibia slightly curved in lateral and dorsal view. Outer and inner lateral dorsal ridge ending in an apical tooth followed by numerous denticles (Fig. 12E). Metatibial spur thin and long. First metatarsomere almost as long as second and third together, second and third as wide as long. Claws appendiculate and long. Fifth ventrite longer than three preceding ones.

Male genitalia (Fig. 13F): ventral side convex, shiny, with few shallow transverse wrinkles; apical denticle wide in ventral view, apex straight, not bent ventrally.

Female genitalia (Fig. 13A–E): tignum long, narrow, slightly bent, with central canal; anterior sclerotization widening abruptly with straight sides and apex, posterior sclerotization poorly delineated, wide, wider than anterior (Fig. 13A). Vaginal palpi elongate, basally strongly sclerotized, each with approximately eight setae at apex (Fig. 13B). Palpi pointed at apex, enlarged at last third but thinned at apex, situated close together and merged anteriorly for more than half of their length. Spermatheca curved, with receptacle and pump not differentiated from each other. Apex of pump with spoon-like projection. Spermathecal duct short, widest at base, without coils (Fig. 13C). Last abdominal sternite and tergite (Fig. 13D, E) evenly sclerotized with evenly placed setae.

Type material. Holotype, ♂. (1) VENEZUELA: Merida/ Paseo de Aguila, Paramo de/ Mucuchies, 3740m/ 08°50'58"N, 70°48'34"W/ 21.V.1998-025B, R.Anderson. (2) dead leaves under *Espeletia timotensis* (MIZA). **Paratypes** (3♂ 7♀ USNM). (1♂2♀ USNM) same label as holotype except: (1♂1♀ CMNC) "025C". (1♂4♀ USNM) VENEZUELA: Merida/ Alto de Timotes, Paramo/ de Mucuchies, 4000m/ 08°51'24"N, 70°49'30"W/ 26.V.1998-042, R.Anderson.

Etymology. We name this species after Luis Jose Joly of Museo del Instituto de Zoologia, UCV, Maracay, Venezuela, a fellow coleopterist who contributed greatly to our knowledge of beetles of Venezuela.

Differential diagnosis. *Andersonoplatus jolyi* is similar to *A. castaneus* and can be differentiated from it based on the following characters: more elongated and flat body (Fig. 12A, B); supracallinal sulci poorly developed, barely perceptible (Fig. 12D); last five antennomeres moniliform (Fig. 12C); apex of median lobe of aedeagus straight in lateral view (Fig. 13F).

***Andersonoplatus laculata* sp. n.**

http://zoobank.org/F7DBE819-E3F6-4B47-B47D-4437B68E330F

Fig. 14

Description. Body length 3.89–4.00 mm, width 1.72–1.78 mm, shiny, glossy, with very sparse semi-erect hairs, almost flat in lateral view. Color black; fore- and middle legs and antennae yellow.

Head (Figs 14A, B, E): slightly convex in lateral view, shiny, generally smooth, with very short hairs. Gena reticulated, punctuated and with sparse pilosity. Frons and

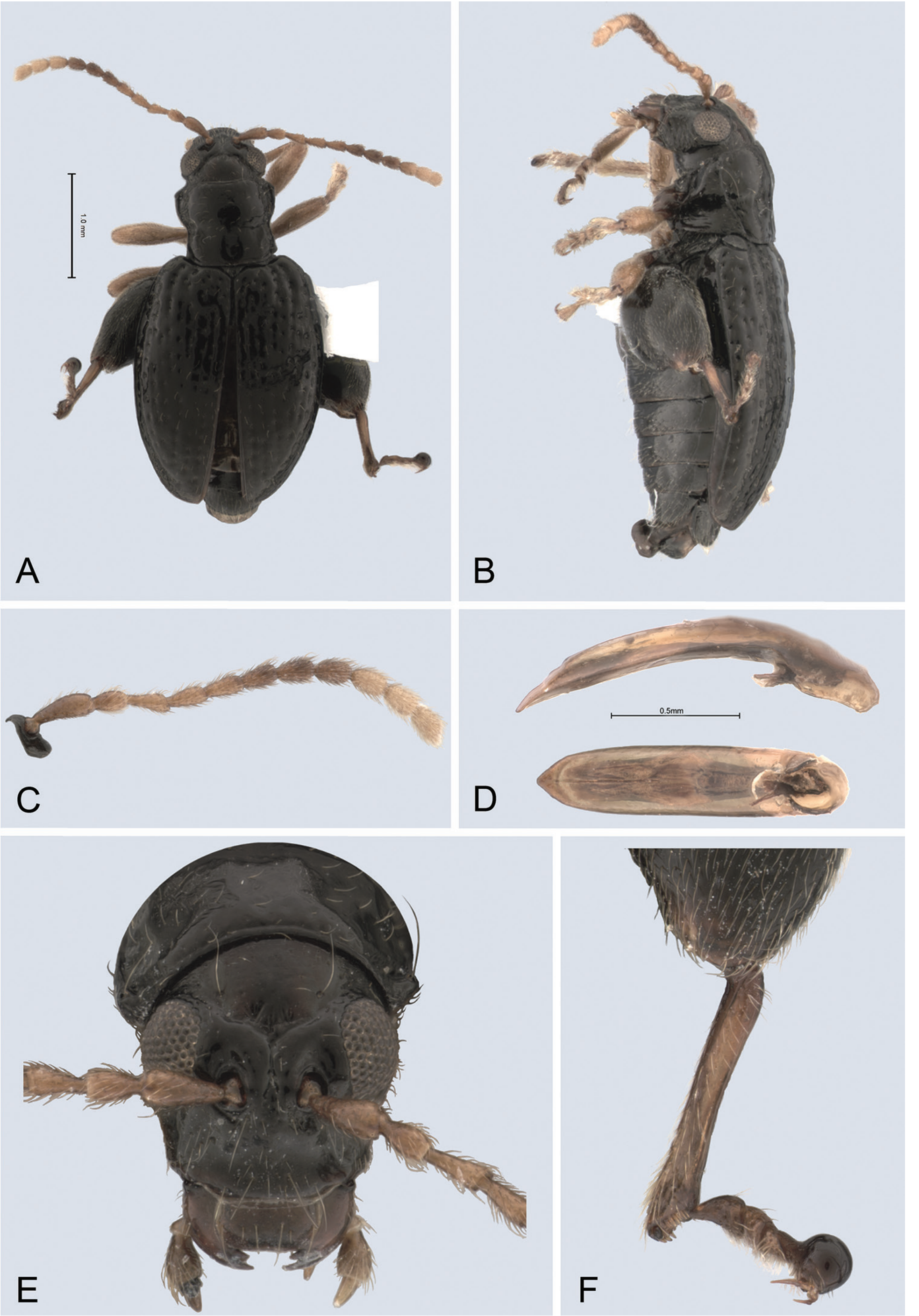

Figure 14. *Andersonoplatus laculata*. **A** Habitus dorsal **B** Habitus lateral **C** Antenna **D** Median lobe of aedeagus, ventral and lateral views **E** Head, frontal view **F** Hind leg.

vertex forming nearly a 135° angle in lateral view. Supraorbital pore small bearing a seta. Antennal callus delimited from vertex by deep and straight supracallinal sulcus, surface even, with no or two punctures, if bearing setae, they are short. Midfrontal sulcus runs from supracallinal sulcus to anterior margin of antennae. Antennal callus slightly raised. Orbital sulcus deep. Supraorbital sulcus deep, not connected with orbital sulcus. Suprafrontal and frontolateral sulcus absent. Frontogenal suture well developed. Orbit as wide as transverse diameter of antennal socket. Interantennal space narrower than transverse diameter of eye and wider than transverse diameter of antennal socket. Antennal socket rounded. Frontal ridge poorly defined, short, antennal calli nearly touching anterofrontal ridge. Anterofrontal ridge long, relatively tall, oblique. First maxillary palpomere longer than wide, shorter than second. Second maxillary palpomere slightly longer than first, globose. Antenna filiform; last six antennomeres slightly shorter and wider than three preceding ones with last three ones light in color.

Thorax: pronotum (Fig. 14A, B) much narrower than elytra, deeply notched at middle. Anterior margin slightly sinuated, wider than posterior, posterior margin slightly convex, lateral margin deeply sinuated. Surface smooth, glossy, with pilosity very short and sparse. Post basal impression represented by three round, shallow impressions, one longitudinally elongated medially and two laterally. Pronotal disc raised. Scutellum triangular, reticulated, wider than long. Prosternal surface reticulated and punctuated. Prosternal intercoxal process as wide as prosternum. Posterior end twice as wide as middle. Procoxal cavity narrowly open. Mesosternum reticulate, punctuate. Elytra not fused. Elytral surface shiny, glossy, with very sparse and short semi-erected hairs, deeply punctate. Punctures forming nine striae, slightly confused. Interspaces slightly convex. Humeral and basal calli shallow. Post basal impression present behind basal callus. Second stria reaching elytral base, third stria missing few punctures before elytral base. Epipleura nearly vertical, slightly narrowed at elytral apex. Metafemur 1.84 times longer than metatibia. Metatibia almost straight in lateral view, curved in dorsal view. Metatarsomeres one and two of similar size, slightly longer than third. Claws simple and long. Ventrites of nearly same length.

Male genitalia (Fig. 14D): ventral side flat with low longitudinal ridge apically; apical denticle poorly developed, apex straight except extreme tip that faces ventrally. Females unknown.

Type material. Holotype, ♂. VENEZUELA: Merida/ Paramo La Culata/ 18.5km N.E. Merida, 2950m/ 08°44'34"N, 71°03'44"W/ 25.V.1998-037C, R. Anderson/ paramo, streamside shrub litter (MIZA). **Paratypes** (2♂). Same label as holotype, except (1) “037F” (USNM), (1) “037A” (CMNC).

Etymology. The specific epithet is a noun in apposition based on the type locality.

Differential diagnosis. *Andersonoplatus laculata* can be differentiated from most *Andersonoplatus* species based on the following characters: pronotal surface shiny, lacking punctures (Figs 14A, B, E); ventral side of aedeagus flat with low longitudinal ridge apically (Fig. 14D).

***Andersonoplatus lagunanegra* sp. n.**
http://zoobank.org/08AE5CD0-D886-4D78-BECB-960EFB4C917B
Figs 15, 16

Description. Body length 2.16–2.32 mm, width 0.97–1.02 mm, shiny, pilose, with semi-erect hairs, flat in lateral view. Color brown to dark.

Head (Fig. 15D): slightly convex in lateral view, shiny, evenly reticulated, with sparse pilosity. Frons and vertex forming nearly a 135° angle in lateral view. Vertex punctuated. Antennal callus delimited from vertex by slightly inclined sulcus; slightly elevated above vertex; surface uneven, with more than two punctures, some of them bearing setae. Orbital sulcus shallow. Supraorbital sulcus absent. Suprafrontal sulcus shallow. Frontolateral sulcus absent. Orbit narrow, punctured, as narrow as transverse diameter of antennal socket. Interantennal space wider than transverse diameter of eye and transverse diameter of antennal socket separately. Frontal ridge short and wide. Anterofrontal ridge short, relatively tall, oblique. Eyes oval. Antenna with antennomeres II-X similar in length, eleventh slightly longer, the last five moniliform; sixth antennomere much smaller than seventh.

Thorax: pronotum (Fig. 15A) narrower than elytra. Anterior margin wider than posterior, posterior margin slightly convex, lateral margin slightly sinuated. Surface reticulated, pilose. Pronotum with shallow, elongated impression anteromedially (absent in female). Pronotal disc not raised. Scutellum rounded, wider than long. Prosternal surface reticulated. Prosternal intercoxal process thin. Posterior end twice as wide as middle. Procoxae very close to each other. Elytra fused. Elytral surface shiny, pilose, with golden, semi-erect hairs, punctate (Fig. 15A); two inclined strips of less dense pilosity. Lines of punctures not well defined, partly confused. Shallow impression running on base of fifth and sixth striae. Epipleura nearly vertical. Metafemur enlarged, 1.38 times longer than metatibia. Metatibia almost straight in lateral and dorsal view. Outer and inner lateral dorsal ridge ending in an apical tooth followed by numerous denticles (Fig. 15E). Claws simple and long.

Male genitalia (Fig. 16A): ventral side with shallow longitudinal impression running deeper basally; in lateral view strongly curved, apical denticle (in ventral view) longer and better pronounced.

Female genitalia (Fig. 16B–G): tignum long, narrow, slightly bent, with central canal; anterior sclerotization narrow, posterior sclerotization poorly delineated, much wider than anterior (Fig. 16B). Vaginal palpi elongate, basally strongly sclerotized, each with approximately eight setae at apex (Fig. 16C). Palpi pointed at apex, enlarged at last third but thinned at apex, situated close together and merged anteriorly for more than half of their length. Spermatheca curved, with receptacle and pump not differentiated from each other, receptacle longer than pump. Apex of pump with spoon-like projection. Spermathecal duct short, widest at base, without coils, making loop (Fig. 16G).

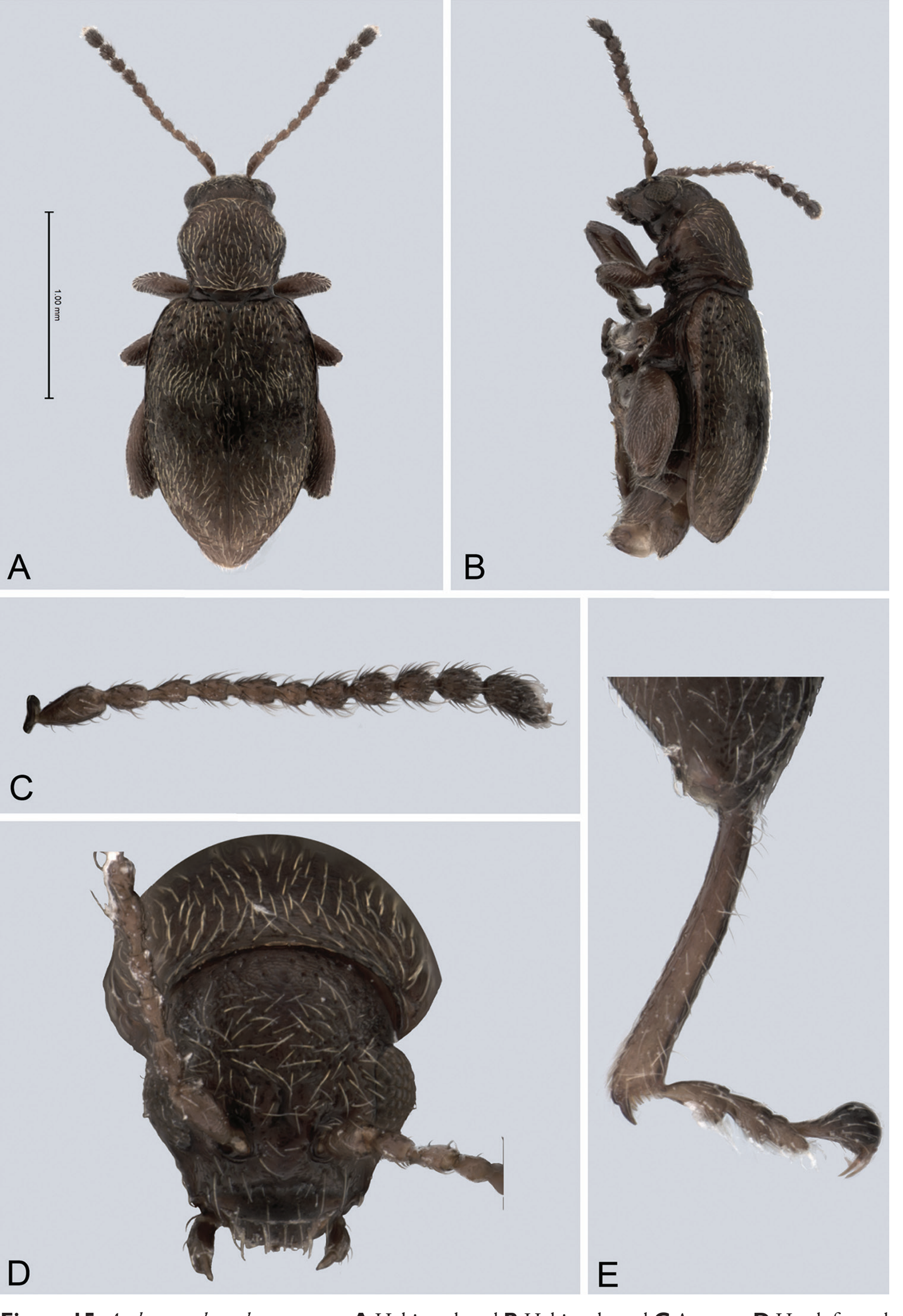

Figure 15. *Andersonoplatus lagunanegra*. **A** Habitus dorsal **B** Habitus lateral **C** Antenna **D** Head, frontal view **E** Hind leg.

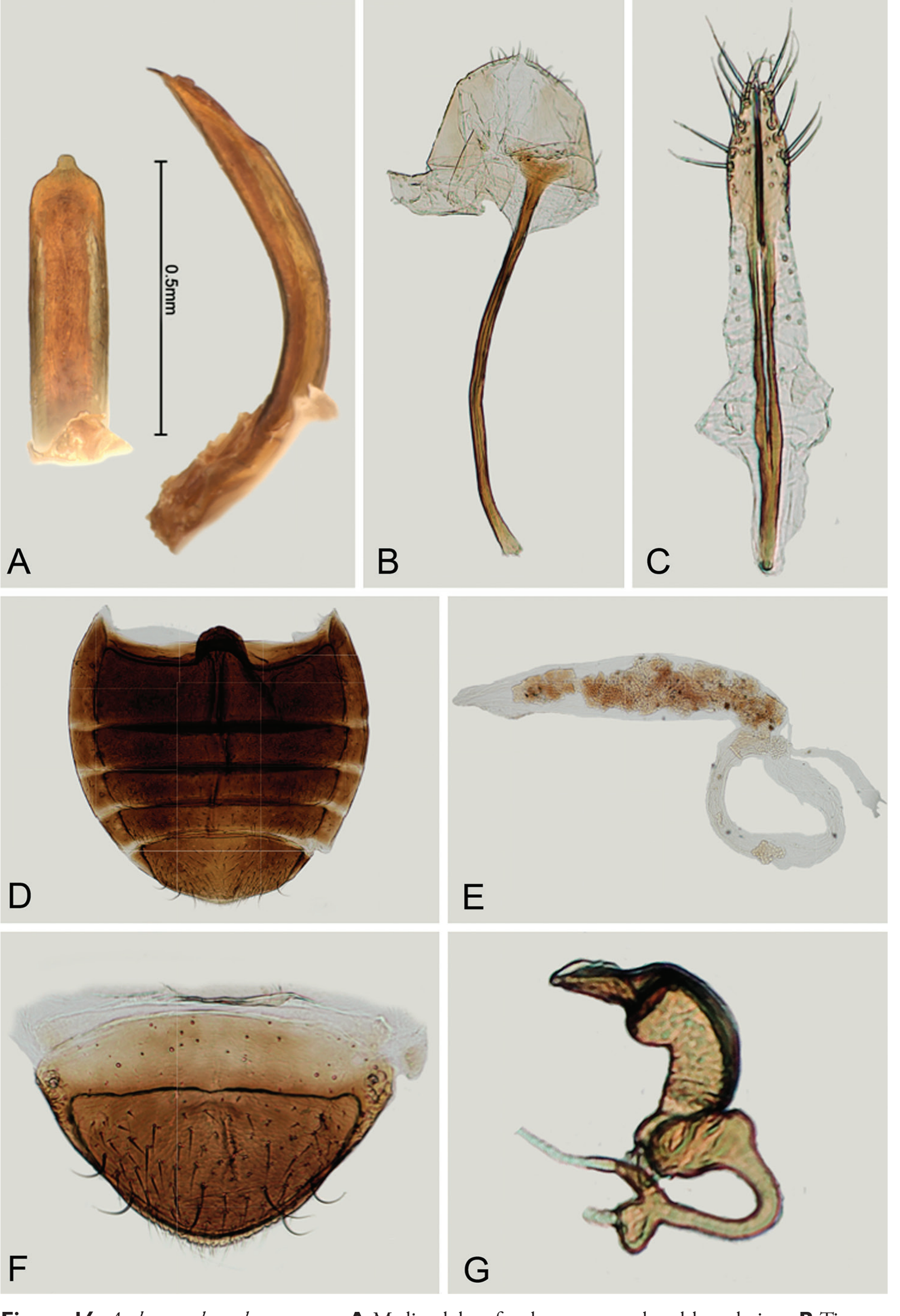

Figure 16. *Andersonoplatus lagunanegra*. **A** Median lobe of aedeagus, ventral and lateral views **B** Tignum **C** Vaginal palpi **D** Female abdomen, ventral view **E** Gut **F** Last abdominal tergite of female **G** Spermatheca.

Type material. Holotype, ♂. VENEZUELA: Merida/ P.N. Sierra Nevada/ Laguna Negra, 3300m/ 08°47'14"N, 70°48'31"W/ 23.V.1998-028B, R.Anderson/ elfin forest litter (MIZA). **Paratypes** (2♀ CMNC, USNM) same label as holotype except "028H".

Etymology. The specific epithet is a noun in apposition based on the type locality.

Differential diagnosis. *Andersonoplatus lagunanegra* is similar to *A. saviniae* and can be separated from it based on the following characters: sixth antennomere much smaller than seventh (Fig. 15C); aedeagus in lateral view strongly curved, apical denticle (in ventral view) longer and better pronounced (Fig. 16A).

Andersonoplatus macubaji sp. n.

http://zoobank.org/3696A919-D7B9-4D6A-8C3C-9FA9EB25A321
Figs 17, 18

Description. Body length 2.86–2.97 mm, width 1.40–1.51 mm, shiny, pilose, flat in lateral view. Color brown.

Head (Fig. 17D): slightly convex in lateral view, shiny, evenly reticulated, vertex punctuated. Frons and vertex forming nearly a 135° angle in lateral view. Antennal callus delimited from vertex by shallow, slightly inclined supracallinal sulcus. Antennal callus slightly raised, covered with punctures bearing setae. Orbital sulcus shallow. Supraorbital sulcus absent. Supracallinal sulcus poorly delimited. Suprafrontal and frontolateral sulcus shallow. Frontogenal and frontolateral sutures well developed. Orbit as wide as transverse diameter of antennal socket. Interantennal space narrower than transverse diameter of eye and wider than transverse diameter of antennal socket. Frontal ridge short, narrow. Anterofrontal ridge short, relatively tall, oblique. Antennae filiform; second antennomere shorter.

Thorax: pronotum (Fig. 17A, B) narrower than elytra. Anterior margin wider than posterior, posterior margin straight, lateral margin slightly sinuated. Surface reticulate, punctate, pilose. Pronotal disc not raised. Scutellum rounded, reticulated, wider than long. Prosternal surface reticulated. Prosternal intercoxal process narrow. Posterior end twice as wide as middle. Elytra fused. Elytral surface shiny, pilose, punctate. Punctures forming nine striae. Interspaces flat. Second and third striae reaching elytral base. Epipleura nearly vertical, pilose. Metafemur 1.74 times longer than metatibia. Metatibia almost straight in lateral view, slightly curved in dorsal view. Outer and inner lateral dorsal ridge ending in an apical tooth followed by numerous denticles (Fig. 17E). Metatarsomeres one and two of similar size, twice as long than third. Claws simple and long.

Male unknown.

Female genitalia (Fig. 18A–C): tignum long, narrow, slightly bent, with central canal; anterior sclerotization narrow, posterior sclerotization poorly delineated, two-pronged pitchfork-like, wider than anterior (Fig. 18B). Vaginal palpi elongate, basally strongly sclerotized, posterior sclerotization concave. Palpi narrowly rounded at apex, enlarged at last third but thinned at apex, separated on one third of their length (Fig. 18C). Spermatheca curved, with receptacle and pump not differentiated from

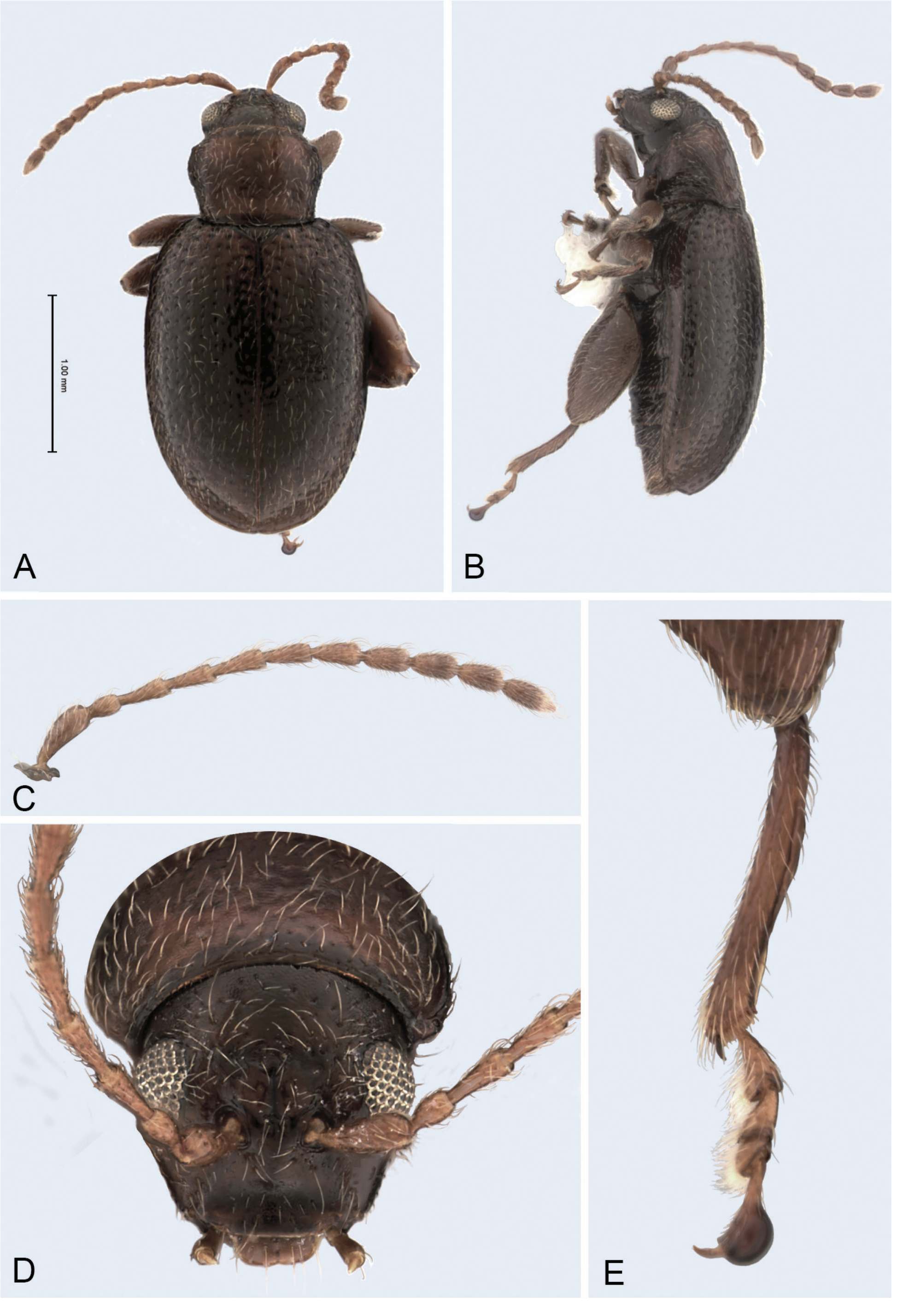

Figure 17. *Andersonoplatus macubaji*. **A** Habitus dorsal **B** Habitus lateral **C** Antenna **D** Head, frontal view **E** Hind leg.

Figure 18. *Andersonoplatus macubaji*. **A** Spermatheca **B** Tignum **C** Vaginal palpi.

each other, receptacle longer than pump. Apex of pump with spoon-like projection relatively thick at base. Spermathecal duct short, widest at base, without coils, making narrow loop (Fig. 18A).

Type material. Holotype, ♀. VENEZUELA: Merida/ Apartaderos, Laguna/ Macubaji, 3500m/ 29.VII.1989, S.&J. Peck/ paramo cushion plant/ litter, 89-285 (MIZA). **Paratype** (1♀ USNM). Same label as holotype.

Etymology. The specific epithet is a noun in apposition based on the type locality.

Differential diagnosis. *Andersonoplatus macubaji* is similar to *A. merida* and can be differentiated from it based on the following characters: vaginal palpi separated on one third of their length (Fig. 18C); posterior sclerotization of vaginal palpi concave on side (Fig. 18C); anterior end of tignum narrow (Fig. 18B).

Andersonoplatus merga **sp. n.**

http://zoobank.org/AC4589C1-AA7A-4325-AF98-7147B95B053B

Figs 19, 20

Description. Body length 3.51–3.67 mm, width 1.78–1.89 mm, shiny, with sparse, semi-erect hairs, slightly convex in lateral view. Color dark brown.

Head (Fig. 19D): slightly convex in lateral view, shiny, evenly reticulated, generally sparsely punctuated. Frons and vertex forming nearly a 135° angle in lateral view. Antennal callus delimited from vertex by poorly delimited supracallinal sulcus. Antennal callus slightly raised, covered with punctures. Vertex with coarse transverse wrinkles most evident near orbital sulci. Orbital sulcus shallow. Supraorbital absent. Suprafrontal sulcus shallow. Frontolateral sulcus deep. Frontogenal suture well developed. Orbit as wide as transverse diameter of antennal socket. Interantennal space narrower than transverse diameter of eye and wider than transverse diameter of antennal socket. Frontal ridge short, V-shaped. Antenna filiform; second antennomere shorter.

Thorax: pronotum (Fig. 19A, B) narrower than elytra. Anterior margin wider than posterior, posterior margin almost straight, lateral margin sinuated. Anterolateral callosities long, pointed, denticle-like. Surface reticulated, punctuated, pilose. Pronotal disc slightly raised. Scutellum triangular, reticulated, wider than long. Prosternal surface reticulated. Posterior end approximately twice as wide as middle. Procoxae globose. Elytra fused. Elytral surface shiny, with very sparse and short hairs, punctate. Punctures forming nine striae. Interspaces slightly convex. Second and third striae reaching elytral base. Epipleura nearly vertical, pilose. Metafemur 1.6 times longer than metatibia. Metatibia almost straight in lateral and slightly curved in dorsal view. Metatarsomeres one and two of similar size, twice as long as third. Claws appendiculate and long.

Male unknown.

Female genitalia (Fig. 20A–C): tignum long, narrow, slightly bent, with central canal; anterior sclerotization narrow, posterior sclerotization well delineated, two-pronged pitchfork-like, wider than anterior (Fig. 20B). Vaginal palpi elongate, basally strongly sclerotized, each with approximately eight setae at apex. Palpi narrowly rounded at apex, enlarged at last third but thinned at apex; separated on one third of their length; posterior sclerotization of vaginal palpi concave on side (Fig. 20C). Spermatheca curved, with receptacle and pump not differentiated from each other, receptacle longer than pump. Apex of pump with spoon-like projection relatively thick at base. Spermathecal duct short, widest at base, without coils, making narrow loop (Fig. 20A).

Type material. Holotype, ♀. VENEZUELA: Merida/ Paramo de La Culata/ 18.5km N.E. Merida, 2950m/ 08°44'34"N, 71°03'44"W/ 25.V.1998-037A, R.Anderson/ paramo, streamside shrub litter (MIZA). **Paratype** (1♀ USNM). Same label as holotype.

Etymology. The specific epithet is a noun in apposition based on a two-pronged pitchfork-like posterior margin of tignum.

Differential diagnosis. *Andersonoplatus merga* is similar to *A. macubaji* and *A. merida*. It can be separated from them based on the following characters: vertex with coarse transverse wrinkles most evident near orbital sulci (Fig. 19D); anterolateral callosity of pronotum long curved denticle-like (Fig. 19A). In *A. macubaji* and *A. merida*: vertex without coarse transverse wrinkles near orbital sulci (Fig. 17B), anterolateral callosity of pronotum short, not denticle-like (Fig. 17A).

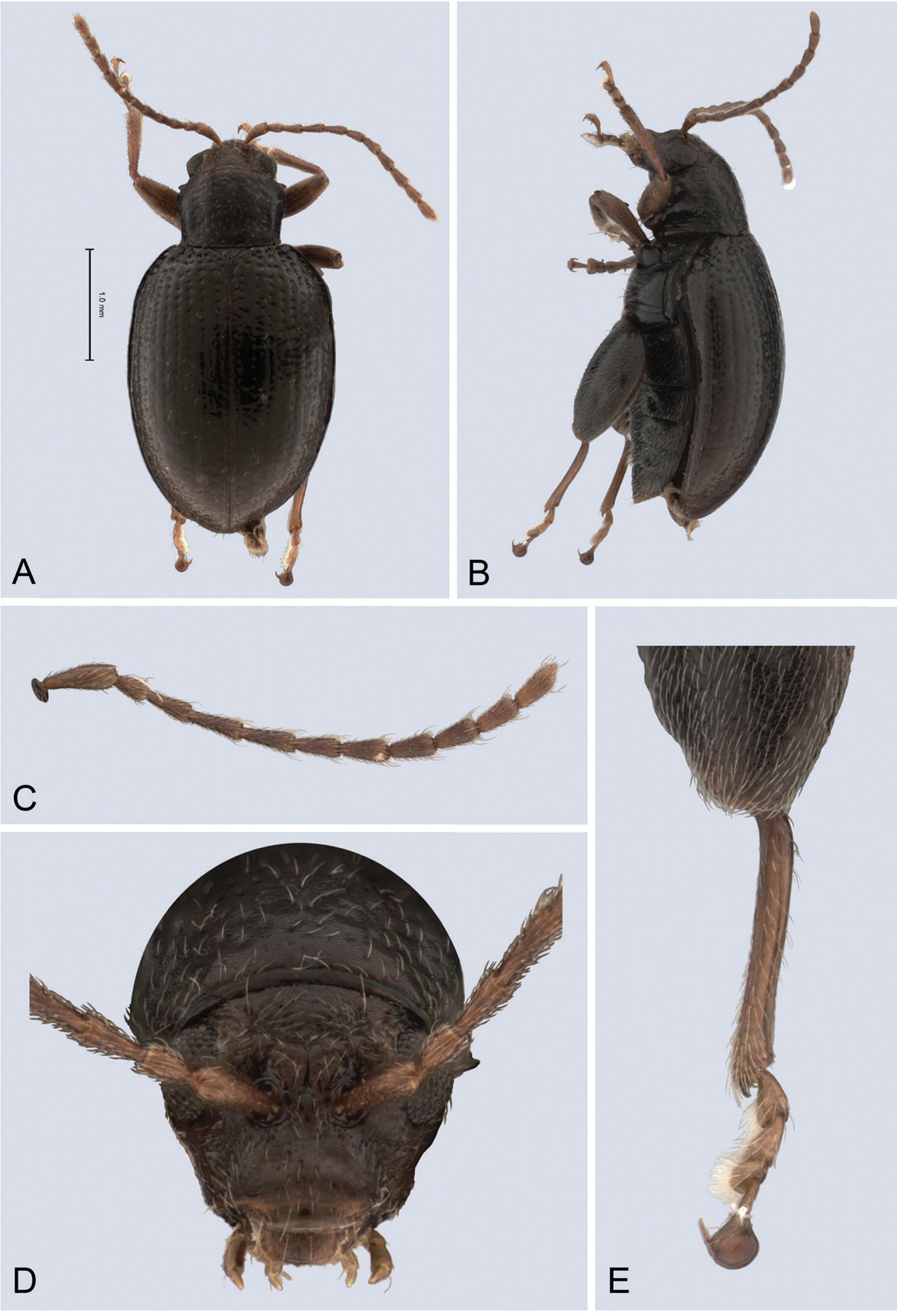

Figure 19. *Andersonoplatus merga*. **A** Habitus dorsal **B** Habitus lateral **C** Antenna **D** Head, frontal view **E** Hind leg.

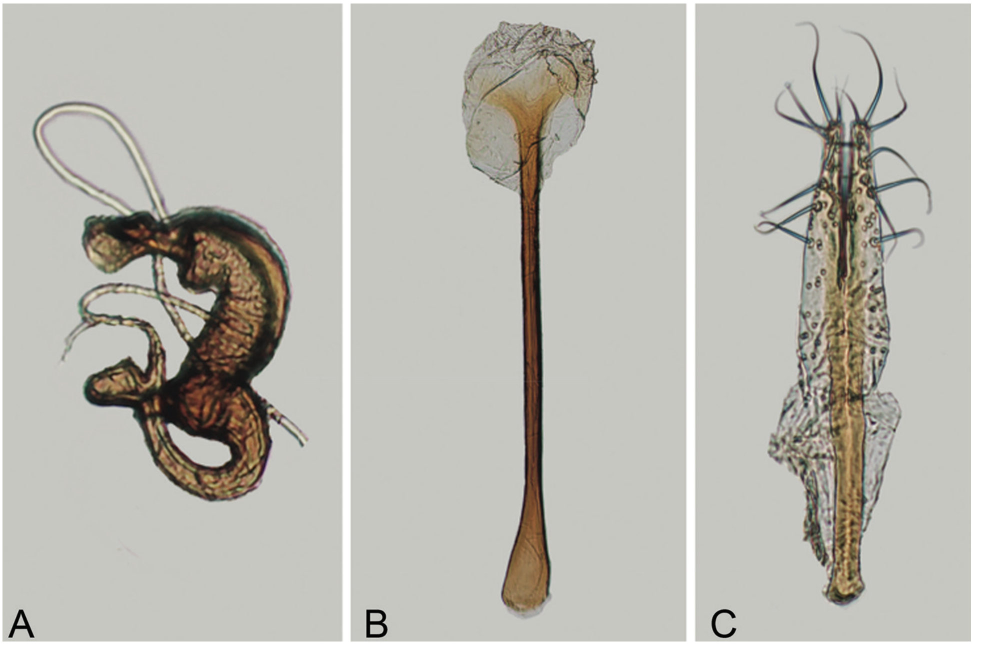

Figure 20. *Andersonoplatus merga*. **A** Spermatheca **B** Tignum **C** Vaginal palpi.

***Andersonoplatus merida* sp. n.**
http://zoobank.org/EBFBEE6A-CB79-4E91-A8E5-849C36407F80
Figs 21, 22

Description. Body length 3.18–3.56 mm, width 1.56–1.89 mm, shiny, pilose, nearly flat in lateral view. Color castaneous.

Head (Fig. 21D): slightly convex in lateral view, shiny, evenly reticulated, generally sparsely punctuated. Frons and vertex forming nearly a 135° angle in lateral view. Antennal callus delimited from vertex by poorly formed, inclined supracallinal sulcus. Antennal callus slightly raised, surface uneven, with more than two punctures, some of them bearing setae. Orbital and supraorbital sulcus absent. Suprafrontal shallow. Frontolateral sulcus absent. Frontogenal suture well developed. Orbit slightly wider than transverse diameter of antennal socket. Interantennal space narrower than transverse diameter of eye and slightly wider than transverse diameter of antennal socket. Antennal socket rounded. Frontal ridge short, V-shaped. Antennae filiform; second antennomere shorter.

Thorax: pronotum (Figs 21A, B) narrower than elytra. Anterior margin wider than posterior, posterior margin nearly straight, lateral margin sinuated. Anterior angles pointed outwards. Surface reticulated, punctuate, pilose. Pronotal disc not raised. Scutellum triangular, reticulated, wider than long. Prosternal surface reticulated. Prosternal intercoxal process thin. Posterior end twice as wide as middle. Procoxae very

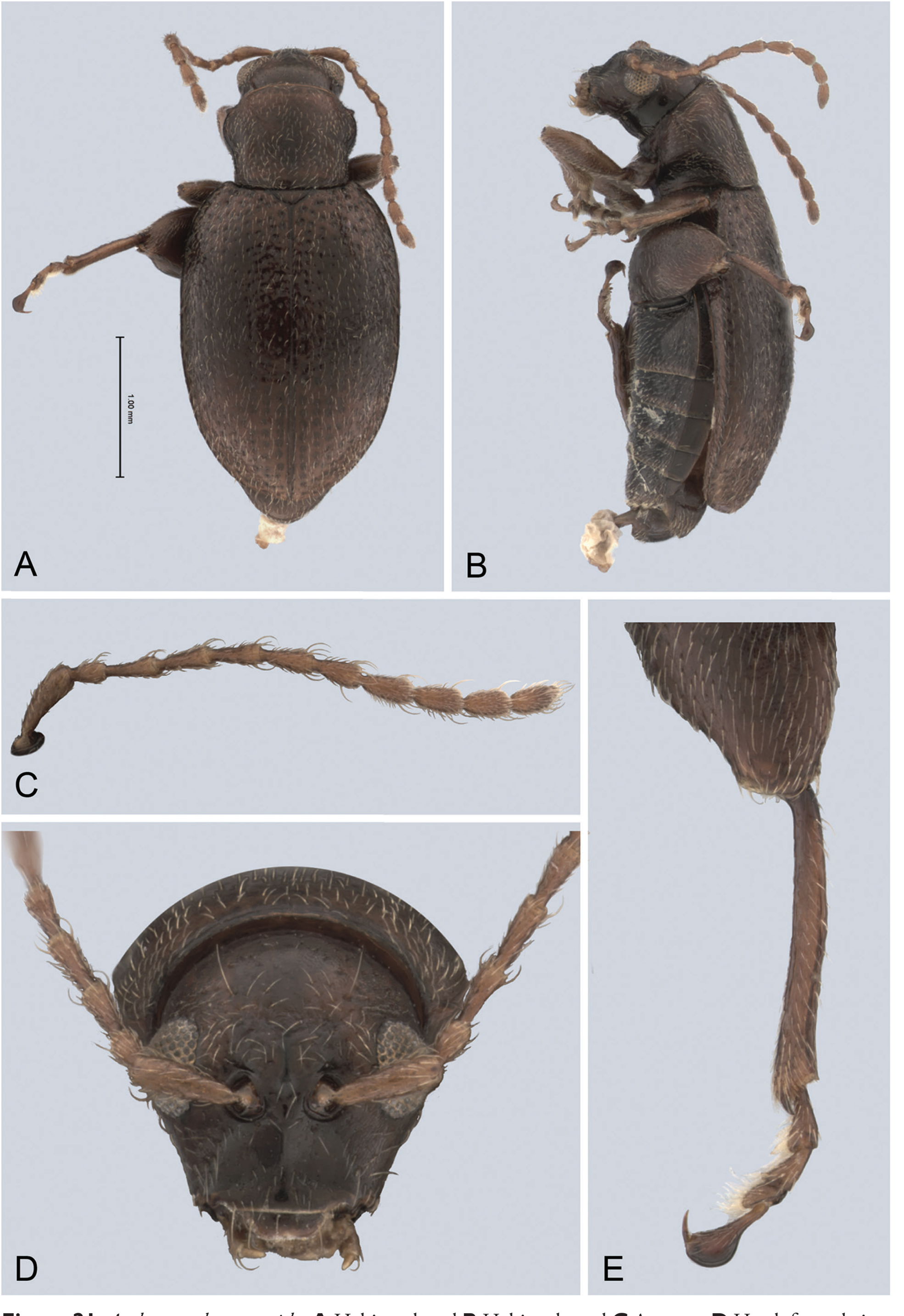

Figure 21. *Andersonoplatus merida*. **A** Habitus dorsal **B** Habitus lateral **C** Antenna **D** Head, frontal view **E** Hind leg.

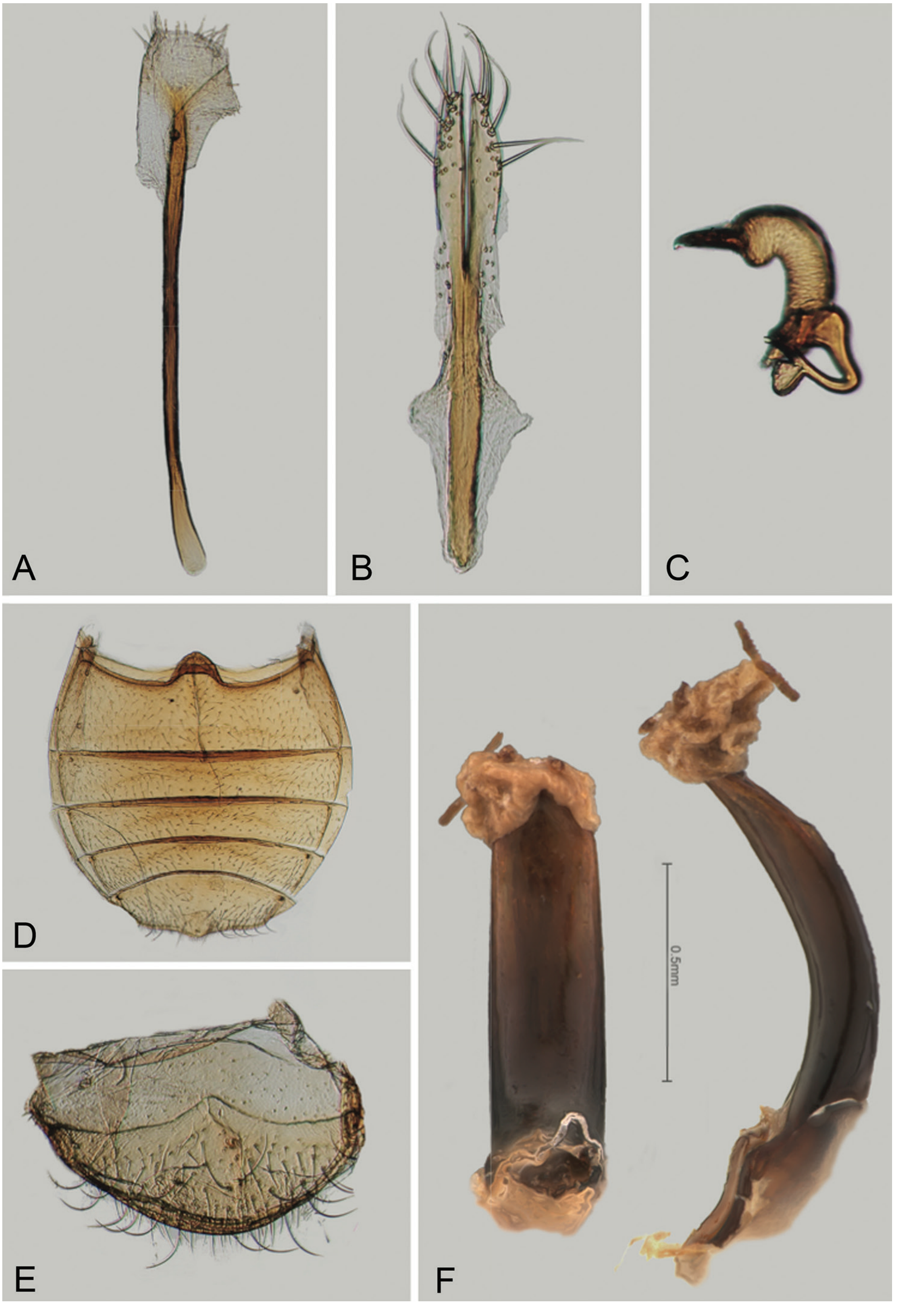

Figure 22. *Andersonoplatus merida*. **A** Tignum **B** Vaginal palpi **C** Spermatheca **D** Female abdomen, ventral view **E** Last abdominal tergite of female **F** Median lobe of aedeagus, ventral and lateral views.

close to each other. Elytra fused. Elytral surface shiny, pilose, punctate (Fig. 21A). Punctures forming nine striae. Interspaces flat. Second and third striae reaching elytral base. Epipleura nearly horizontal. Metafemur 1.37 times longer than metatibia. Metatibia almost straight in lateral and dorsal views. Metatarsomeres one and two of similar size, twice as long as third. Claws appendiculate and long.

Male genitalia (Fig. 22F): ventral side evenly convex without grooves and ridges, flattened apically.

Female genitalia (Fig. 22A–E): tignum long, narrow, slightly bent, with central canal; anterior sclerotization relatively wide, posterior sclerotization well delineated, narrower than anterior (Fig. 22A). Vaginal palpi elongate, basally strongly sclerotized, each with eight setae at apex. Palpi narrowly rounded at apex, posterior sclerotization slightly curved on side (Fig. 22B), separated on more than one third of their length (Fig. 22B). Spermatheca curved, with receptacle and pump not differentiated from each other, receptacle longer than pump. Apex of pump with relatively thick spoon-like projection. Spermathecal duct short, widest at base, without coils, making narrow loop (Fig. 22C).

Type material. Holotype, ♂. (1) VENEZUELA: Merida/ Alto de Timotes, Paramo/ de Mucuchies, 4000m/ 08°51'30"N, 70°49'29"W/ 26.V.1998-043, R.Anderson. (2) dead leaves under /*Espeletia* sp (MIZA). **Paratypes** (2♀ USNM). (1♀ USNM) VENEZUELA: Merida/ P.N.Sierra Nevada/ Laguna Negra, 3300m/ 08°47'14"N, 70°48'31"W/ 23.V.1998-028B, R.Anderson/ elfin forest litter. (1♀ CMNC) VENEZUELA: Merida/ Merida, Telef./ Loma Redonda, 4100m/ 22–29.VI.1989, S.&J. Peck/ paramo, *Polylepsis* grove/ ex: carrion trap.

Etymology. The specific epithet is a noun in apposition based on the type locality.

Differential diagnosis. *Andersonoplatus merida* is similar to *A. macubaji* and can be differentiated from it based on the following characters: vaginal palpi separated on more than one third of their length (Fig. 22B); posterior sclerotization of vaginal palpi slightly curved on side (Fig. 22B); anterior end of tignum relatively wide (Fig. 22A).

***Andersonoplatus microoculus* sp. n.**

http://zoobank.org/146846F8-FD3E-41AD-A8C2-9CF7FC6A9CD0

Figs 23–27

Description. Body length 2.10–2.43 mm, width 0.97–1.18 mm, pronotum and elytra with sparse, semi-erect hairs, shiny, slightly flat in lateral view. Color light brown to almost black; antennae and legs yellow or at least lighter than rest of body.

Head (Figs 23D; 25F; 26A, B, C): flat in lateral view, generally smooth, vertex slightly reticulated; gena shiny, with very sparse pilosity. Antennal callus delimited from vertex by well-developed and straight supracallinal sulcus. Antennal callus elevated above vertex, surface even, with no or two punctures, if bearing setae, they are short. Orbital sulcus shallow. Supraorbital sulcus shallow almost connected with supracallinal sulcus. Suprafrontal sulcus shallow. Frontolateral sulcus absent. Frontogenal suture shallow. Orbit as wide as transverse diameter of antennal socket. Interantennal space wider than transverse diameter of eye and wider than transverse diameter of antennal socket. Antennal socket rounded. Frontal ridge short, V-shaped. Anterofrontal ridge low, oblique. Eyes small, with approximately 12 large ommatidia. Antenna with the last five antennomeres moniliform, with denser and longer setae.

Thorax: pronotum (Fig. 25D, F) longer than wide, much narrower than elytra, notched at middle. Anterior margin nearly straight, wider than posterior; posterior margin slightly convex, lateral margin sinuated. Surface reticulated, with pilosity sparse. Post basal impression absent. Pronotal disc not raised. Scutellum very small and triangular. Prosternal surface reticulated. Prosternal intercoxal process thin in middle. Posterior end more than twice as wide as middle (Fig. 26C). Elytra fused. Elytral surface shiny, with short, white, semi-erect hairs. Punctures forming seven striae. Each punctation bears one very short setae (can be found some setae on the interestriae). Interspaces flat. Second and third striae reaching elytral base. Epipleura nearly vertical. Metafemur greatly enlarged, 1.95 times longer than metatibia. Metatarsomeres one and two similar in size, slightly longer than third. Claws slightly appendiculate and long (Fig. 27C, D).

Male genitalia (Fig. 24A): ventral side convex and shiny, without longitudinal impression, slightly flattened at apex; apical denticle well developed in ventral view, narrow, apex straight and not bent ventrally.

Female genitalia (Fig. 24B–E): tignum long, narrow, slightly bent, with central canal; anterior sclerotization widening gradually with curved sides and convex apex, posterior sclerotization poorly delineated, narrow, as wide as anterior (Fig. 24B). Vaginal palpi elongate, basally strongly sclerotized, each with eight setae at apex (Fig. 24E). Palpi pointed at apex, enlarged at last third but thinned at apex, situated close together and merged anteriorly for more than half of their length. Spermatheca curved, with receptacle and pump not differentiated from each other. Apex of pump with spoon-like projection. Spermathecal duct short, widest at base, without coils (Fig. 24C). Last abdominal sternite (Fig. 24D) evenly sclerotized with evenly placed setae.

Type material. Holotype, ♂. VENEZUELA: Trujillo/ camino viejo a Trujillo, Paramo/ La Cristalina, km 9.7, 2400m/ 09°21'22"N, 70°17'51"W/ 20.V.1998-022B/ R.Anderson, elfin for. Litter (MIZA). **Paratypes** (16♂ 7♀). (5♂1♀) same label as holotype except: (2♂4♀ USNM) “022D”; (3♂1♀ USNM) “022E”; (2♂1♀ CMNC) “022F”; (3♂ USNM) “022G”; (1♂ USNM) “022J”.

Etymology. The specific epithet is a noun in apposition based on relatively small eyes of the beetles.

Differential diagnosis. *Andersonoplatus microoculus* can be identified by the small eyes, with approximately 12 large ommatidia (Figs 23B, D) and pronotum comparatively narrow (Fig. 23A).

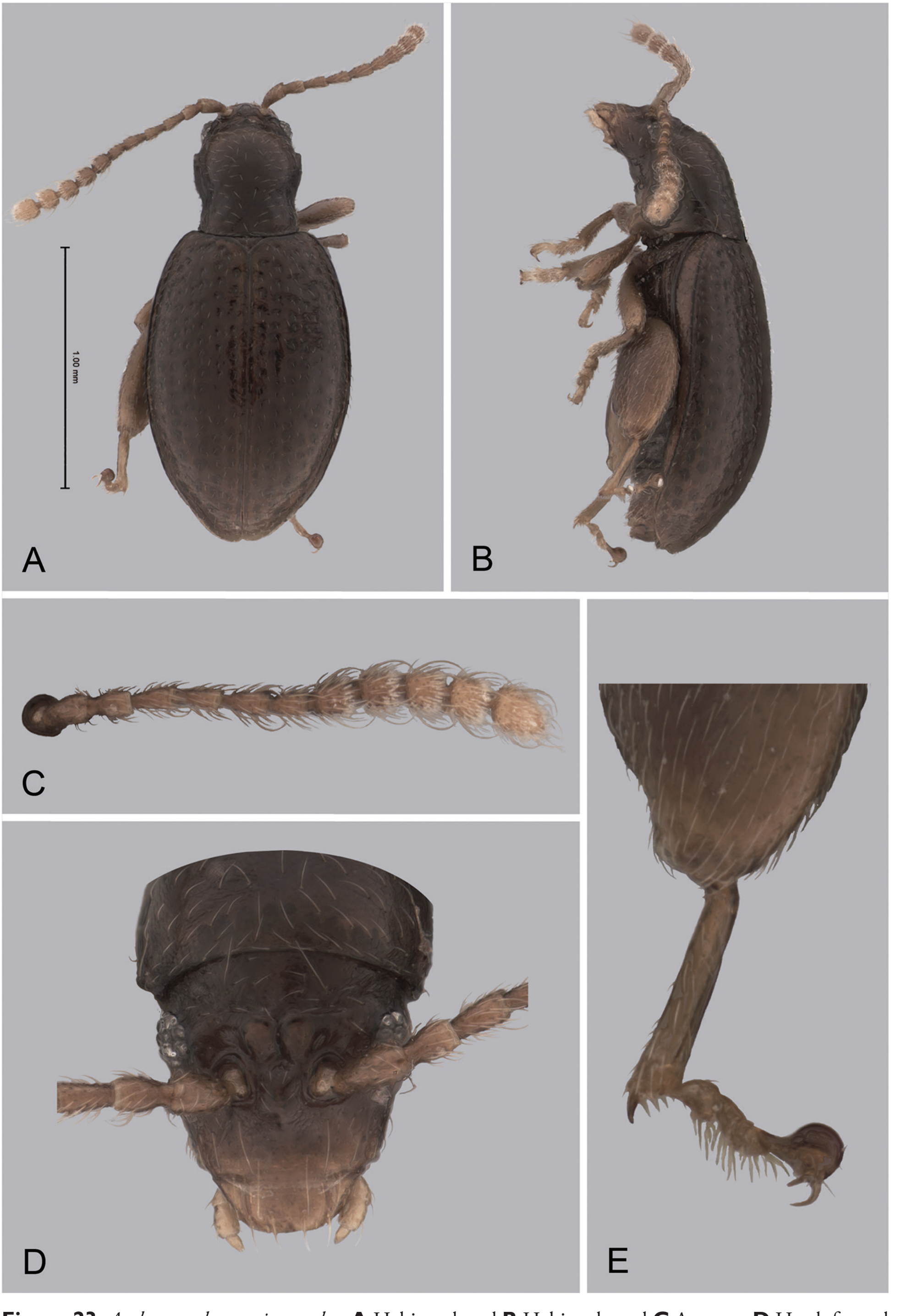

Figure 23. *Andersonoplatus microoculus*. **A** Habitus dorsal **B** Habitus lateral **C** Antenna **D** Head, frontal view **E** Hind leg.

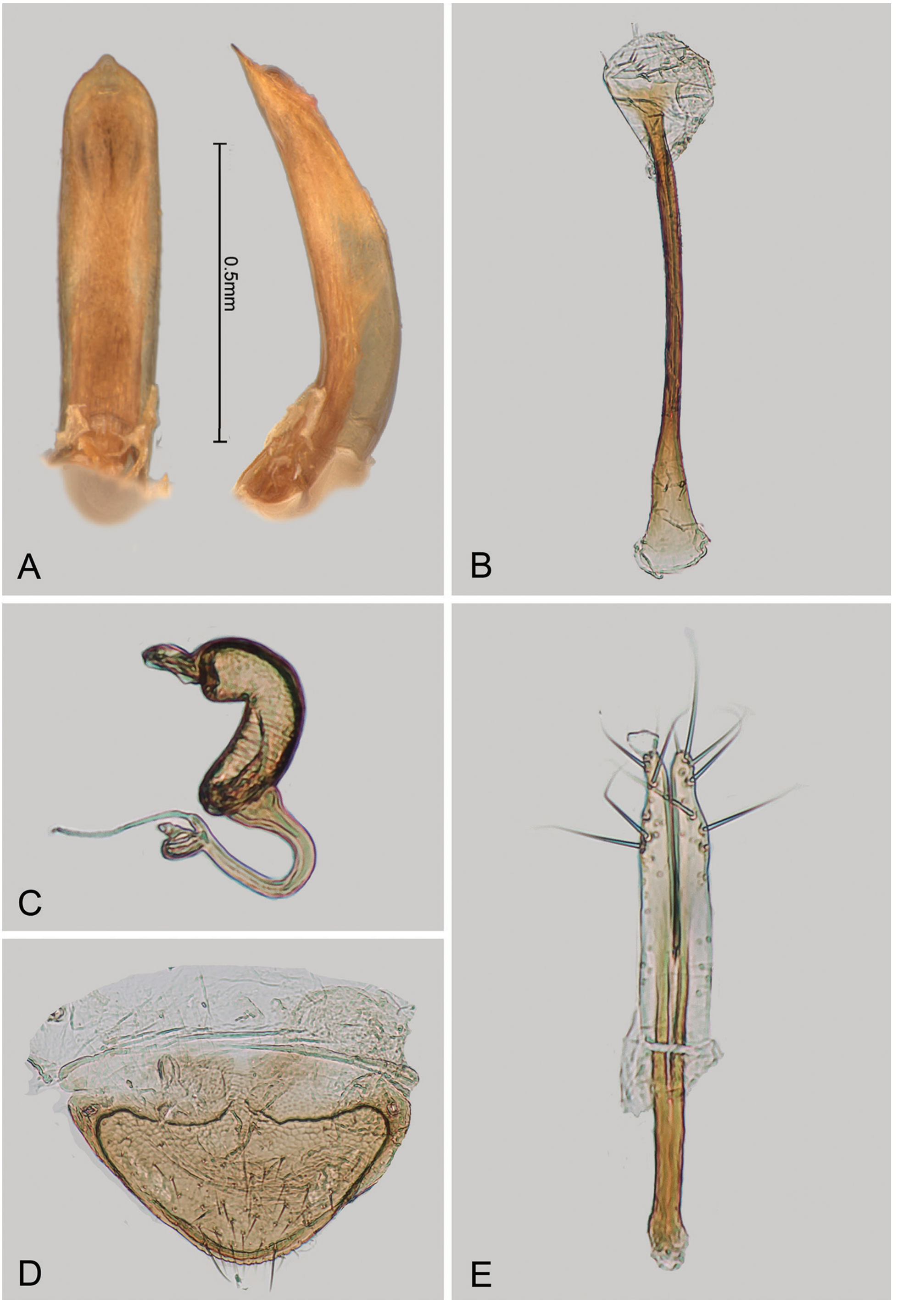

Figure 24. *Andersonoplatus microoculus*. **A** Median lobe of aedeagus, ventral and lateral views **B** Tignum **C** Spermatheca **D** Last abdominal tergite of female **E** Vaginal palpi.

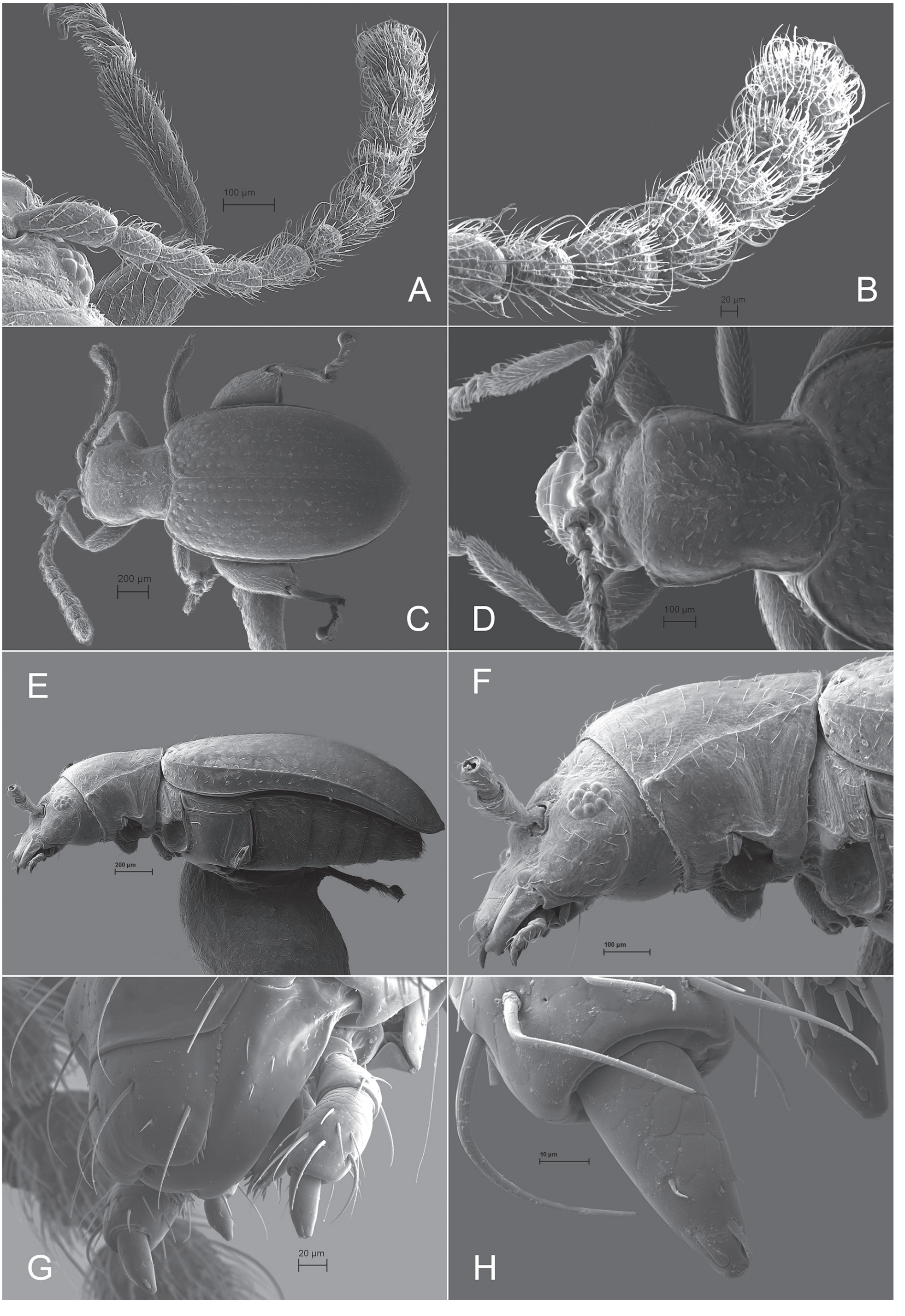

Figure 25. *Andersonoplatus microoculus*. **A** Antenna **B** Seven apical antennomeres **C** Habitus dorsal **D** Pronotum in dorsal view **E** Habitus lateral **F** Head and pronotum in lateral view **G** Mouth parts in lateral view **H** Last maxillary palpomere.

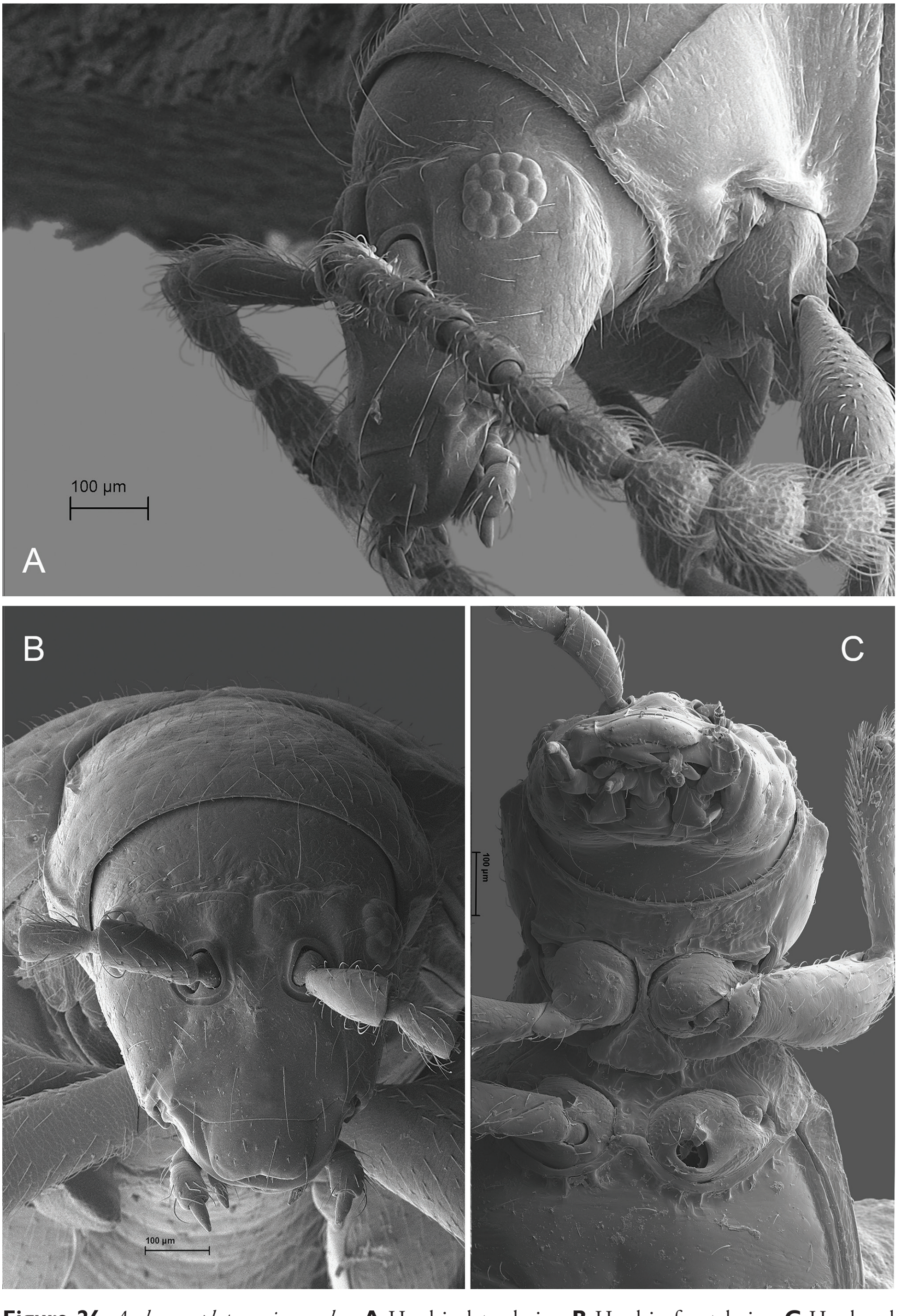

Figure 26. *Andersonoplatus microoculus*. **A** Head in lateral view **B** Head in frontal view **C** Head and pronotum in ventral view.

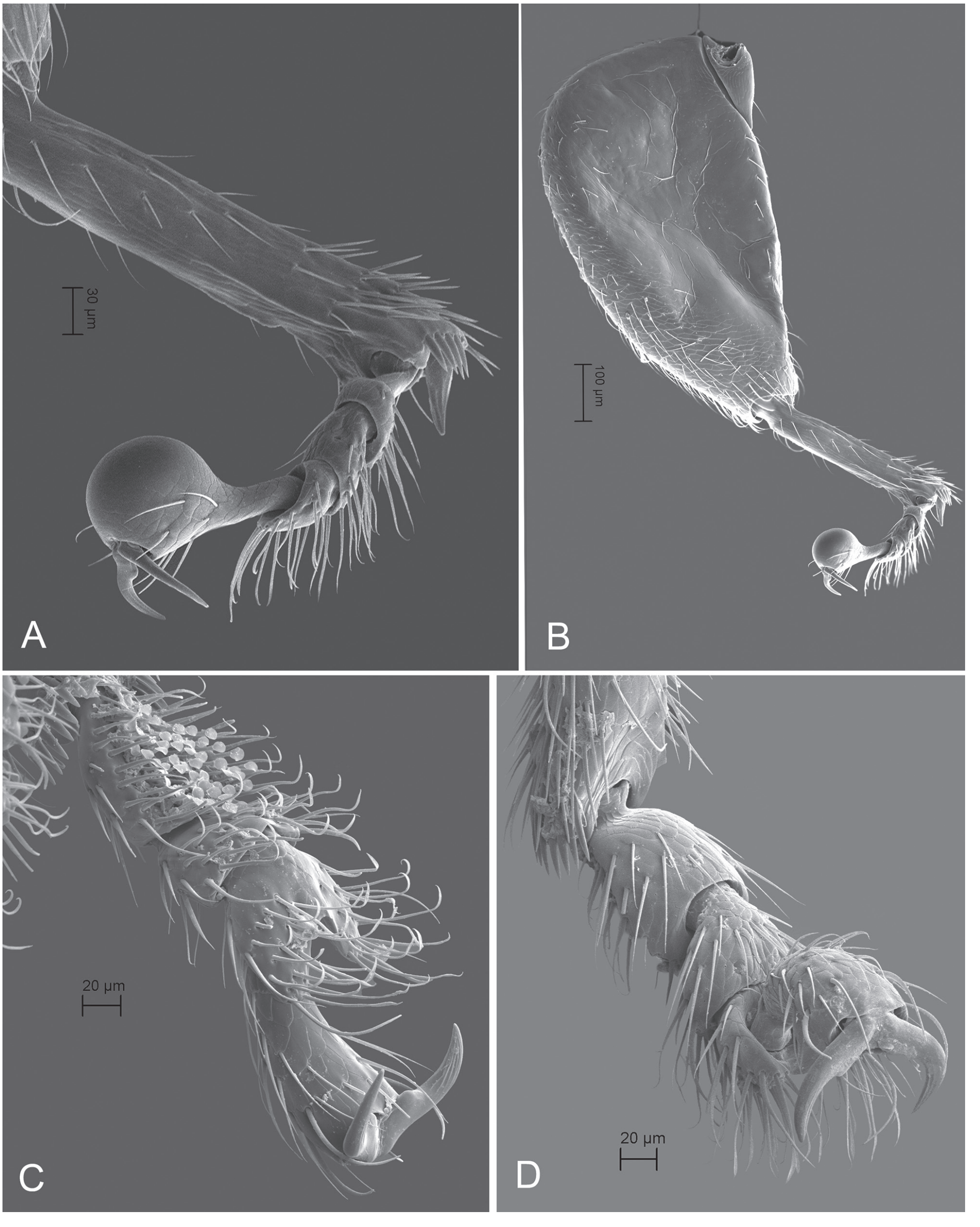

Figure 27. *Andersonoplatus microoculus*. **A** Hind tibia and tarsus in dorsal view **B** Hind leg in dorsal view **C** Protarsomeres in ventral view **D** Protarsomeres in dorsal view.

Andersonoplatus peck **sp. n.**
http://zoobank.org/B35E4FF6-541D-4124-8EFD-F533B99B32D1
Figs 28, 29

Description. Body length 1.62–1.78 mm, width 0.81–0.91 mm, shiny, pilose, with semi-erect hairs, flat in lateral view. Color light brown.

Head (Fig. 28D): slightly convex in lateral view, shiny, generally reticulated, pilose. Frons and vertex at same level in lateral view. Supraorbital pore indistinguishable. Antennal callus delimited from vertex by deep and curved sulcus; not raised; surface uneven, with more than two punctures, some of them bearing setae. Orbital sulcus shallow. Supraorbital absent. Suprafrontal sulcus shallow. Frontolateral sulcus absent. Frontogenal suture well developed. Orbit narrow, nearly two times narrower than transverse diameter of antennal socket. Interantennal space slightly narrower than transverse diameter of eye and as wide as transverse diameter of antennal socket. Frontal ridge wider between antennal sockets abruptly narrowing ventrally. Anterofrontal ridge long, relatively tall, oblique. Eyes very small. Antenna with antennomeres III-XI shorter than second; last five antennomeres wider than preceding ones, moniliform (Fig. 28C).

Thorax: pronotum (Fig. 35A, B) longer than wide, narrower than elytra, notched at middle. Anterior margin wider than posterior, posterior margin slightly convex, lateral margin sinuated. Surface reticulated, pilose with disordered hair. Post basal impression deep, with deep rounded impressions laterally, along notch. Pronotal disc slightly raised. Scutellum rounded, much shorter than wide. Prosternal surface reticulated. Prosternal intercoxal narrow. Posterior end twice as wide as middle. Elytra fused. Elytral surface shiny, pilose, with, semi-erect, disordered hairs, punctate (Fig. 35A). Punctures forming seven striae. Interspaces slightly convex. Second stria reaching elytral base, third stria missing few punctures before elytral base. Epipleura nearly horizontal. Metafemur very enlarged, 2.01 times longer than metatibia. Metatibia almost straight in lateral view, slightly curved in dorsal view. Claws simple and long (Fig. 28E).

Male genitalia (Fig. 29A): ventral side with shallow longitudinal impression running deeper basally; apical denticle well developed, long, apex straight except very tip that faces ventrally.

Female genitalia (Fig. 29B–G): tignum long, narrow, slightly bent, with central canal; anterior sclerotization narrow, posterior sclerotization well delineated, narrower than anterior (Fig. 29B). Vaginal palpi elongate, basally strongly sclerotized, each with approximately eight setae at apex (Fig. 29C). Palpi pointed at apex, enlarged at last third but thinned at apex, situated close together and merged anteriorly for more than half of their length. Posterior sclerotization of vaginal palpi with straight sides. Spermatheca curved, with receptacle and pump not differentiated from each other, receptacle longer than pump. Apex of pump with relatively thick spoon-like projection. Spermathecal duct short, widest at base, without coils, making narrow loop (Fig. 29E).

Type material. Holotype, ♂. VENEZUELA: Merida/ ULA. Biol.Res. LaCarbonerra/ 20km SE Azulita, 28.VI.1989/ 2300m, S.&J. Peck/ Podocarp./ for. litter. 89-240 (MIZA). **Paratype** (1♀ USNM). Same label as holotype.

Etymology. We dedicate this species to Jarmila and Stuart Peck who collected the type series. The specific epithet is a noun in apposition.

Differential diagnosis. *Andersonoplatus peck* is similar to *A. baru* and can be differentiated from it based on the following characters: body 1.62–1.78 mm in length, light brown, vertex sparsely covered with setae; posterior sclerotization of vaginal palpi with straight sides; posterior sclerotization of tignum narrower than anterior. In *A. baru* body is 3.39–3.40 mm, uniformly yellow, vertex densely covered with setae; posterior

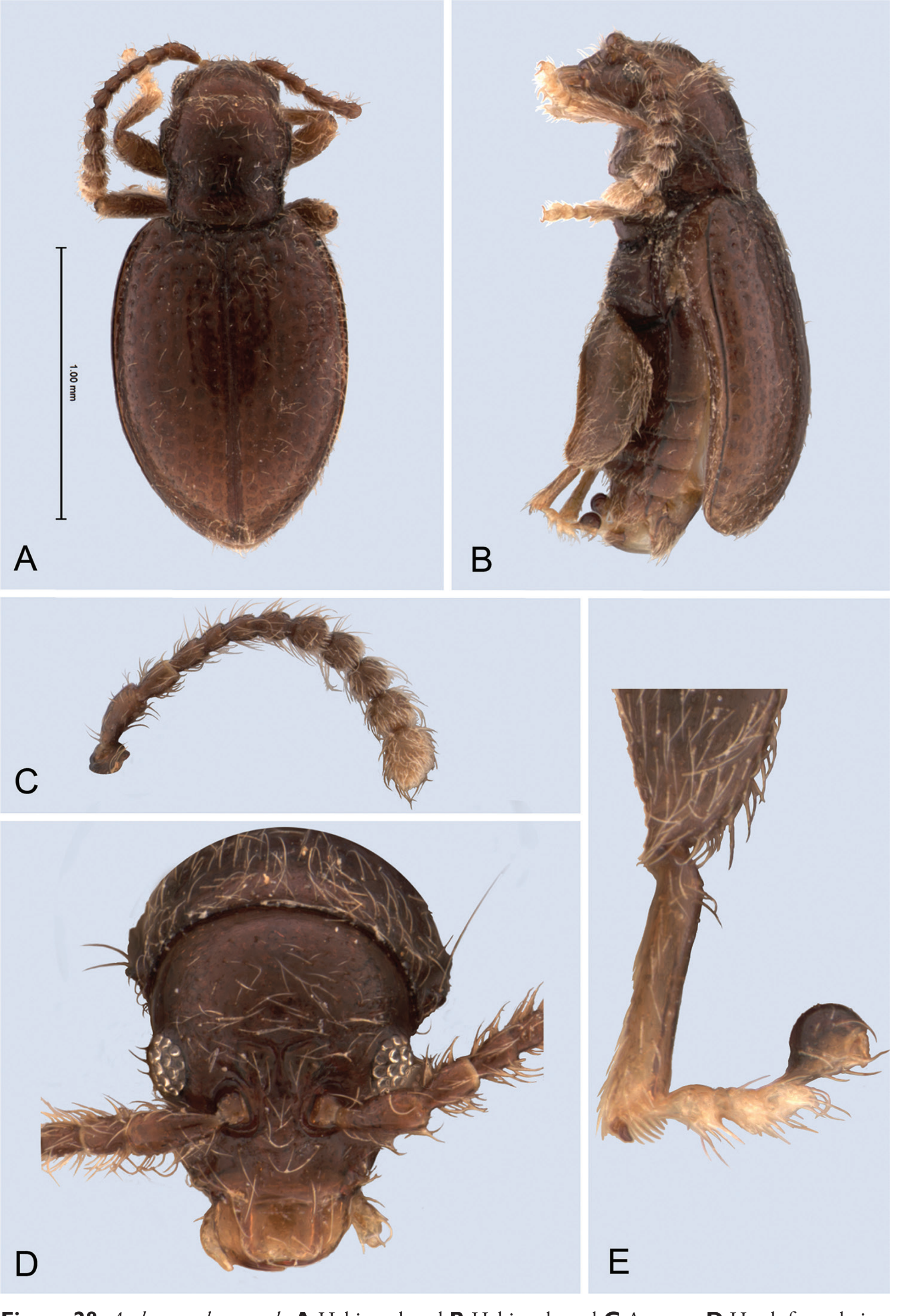

Figure 28. *Andersonoplatus peck*. **A** Habitus dorsal **B** Habitus lateral **C** Antenna **D** Head, frontal view **E** Hind leg.

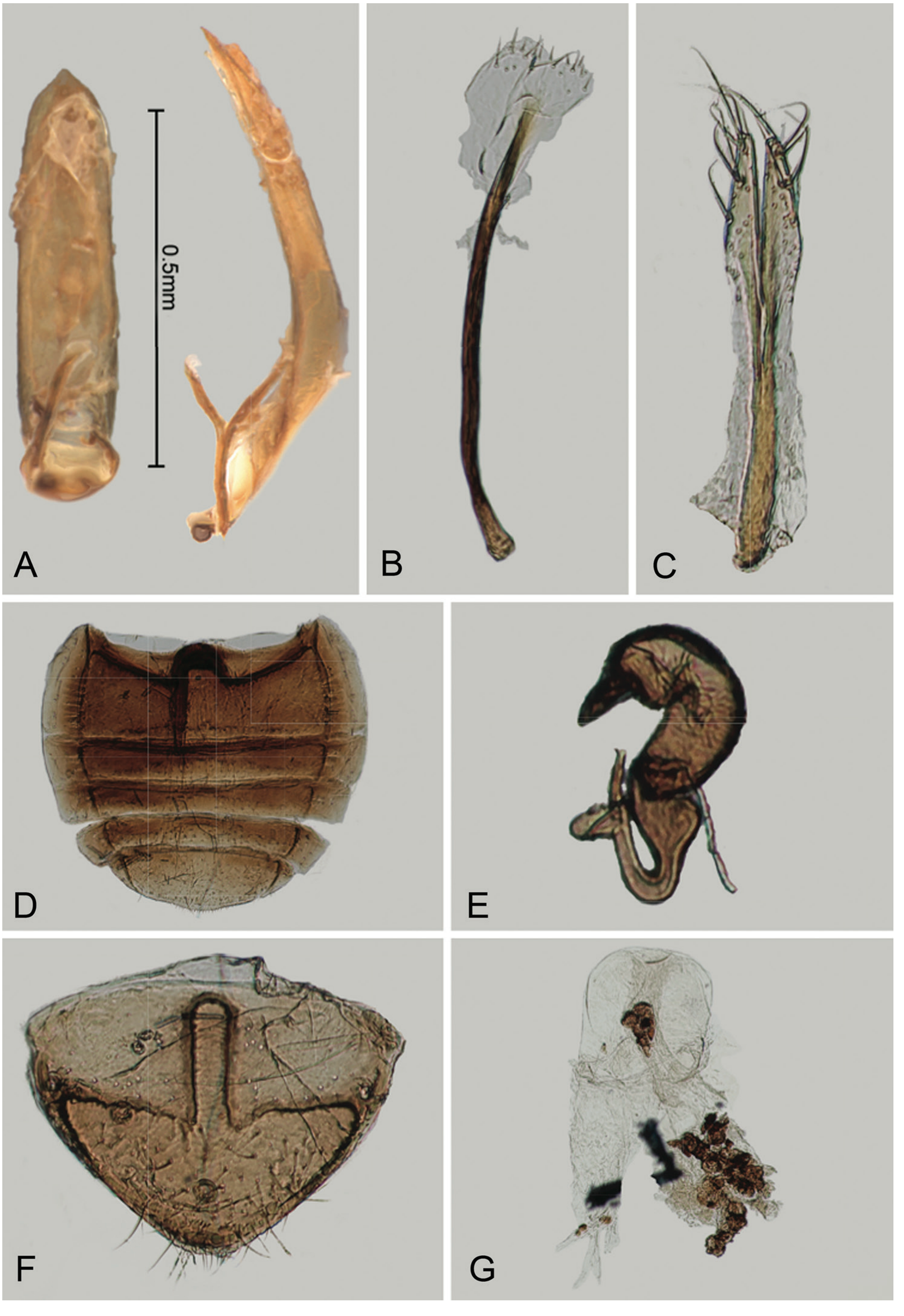

Figure 29. *Andersonoplatus peck*. **A** Median lobe of aedeagus, ventral and lateral views **B** Tignum **C** Vaginal palpi **D** Female abdomen, ventral view **E** Spermatheca **F** Last abdominal tergite of female **G** Gut.

sclerotization of vaginal palpi with curved sides; posterior sclerotization of tignum wider than anterior.

Andersonoplatus rosalesi sp. n.

http://zoobank.org/231080EF-53DD-487D-9C3B-0D7F4C4C4A62

Figs 30, 31

Description. Body length 2.05–2.16 mm, width 1.08–1.18 mm, shiny, pilose, with semi-erect hairs, moderately convex in lateral view. Color castaneous.

Head (Fig. 30D): slightly convex in lateral view, shiny, generally reticulated, with sparse pilosity. Frons and vertex forming nearly a 135° angle in lateral view. Antennal callus delimited from vertex by deep and slightly curved upward supracalinal sulcus. Antennal callus slightly raised, surface even, with no or two punctures, if bearing setae, they are short. Orbital sulcus shallow. Supraorbital sulcus absent. Suprafrontal and frontolateral sulci shallow. Frontogenal suture deep. Orbit narrow, as wide as transverse diameter of antennal socket. Interantennal space narrower than transverse diameter of eye and as wide as transverse diameter of antennal socket. Frontal ridge short and narrow. Antennae filiform; antennomeres III-XI similar in length, the last five antennomeres slightly wider than preceding ones.

Thorax: pronotum (Fig. 30A, B) slightly trapezoidal, almost quadrate, narrower than elytra. Anterior margin wider than posterior, posterior margin slightly concave, lateral margin almost straight. Anterior angles pointed outwards. Surface reticulated, punctuated, pilose, densely covered with well-defined punctures, diameter of which larger than distance between punctures. Pronotal disc weakly raised. Scutellum rounded, shorter than wide. Prosternal intercoxal process narrow. Posterior end nearly twice as wide as middle. Elytra not fused. Elytral surface shiny, with white, semi-erect hairs, deeply punctate (Fig. 30A, B). Punctures forming nine striae, the ninth stria is overlapping marginal one. Interspaces very convex. Second and third striae reaching elytral base. Third and fourth striae merge at apical 2/3rd. Epipleura slightly convex, pilose, nearly vertical, slightly narrowed at elytral apex. Metafemur greatly enlarged, 1.10 times longer than metatibia. Claws appendiculate and long.

Male genitalia (Fig. 31A): ventral side flat apically, with longitudinal impression basally; apical denticle poorly developed, apex bent ventrally.

Female genitalia (Fig. 31B–E): tignum long, narrow, slightly bent, with central canal; anterior sclerotization widening gradually with slightly curved sides and convex apex, posterior sclerotization poorly delineated, wide, wider than anterior (Fig. 31E). Vaginal palpi elongate, basally strongly sclerotized, each with approximately eight setae at apex (Fig. 31B). Palpi pointed at apex, enlarged at last third but thinned at apex, situated close together and merged anteriorly for more than half of their length. Spermatheca curved, with receptacle and pump not differentiated from each other, receptacle longer than pump. Apex of pump with spoon-like projection. Spermathecal duct short, widest at base, without coils, making long and narrow loop (Fig. 31D).

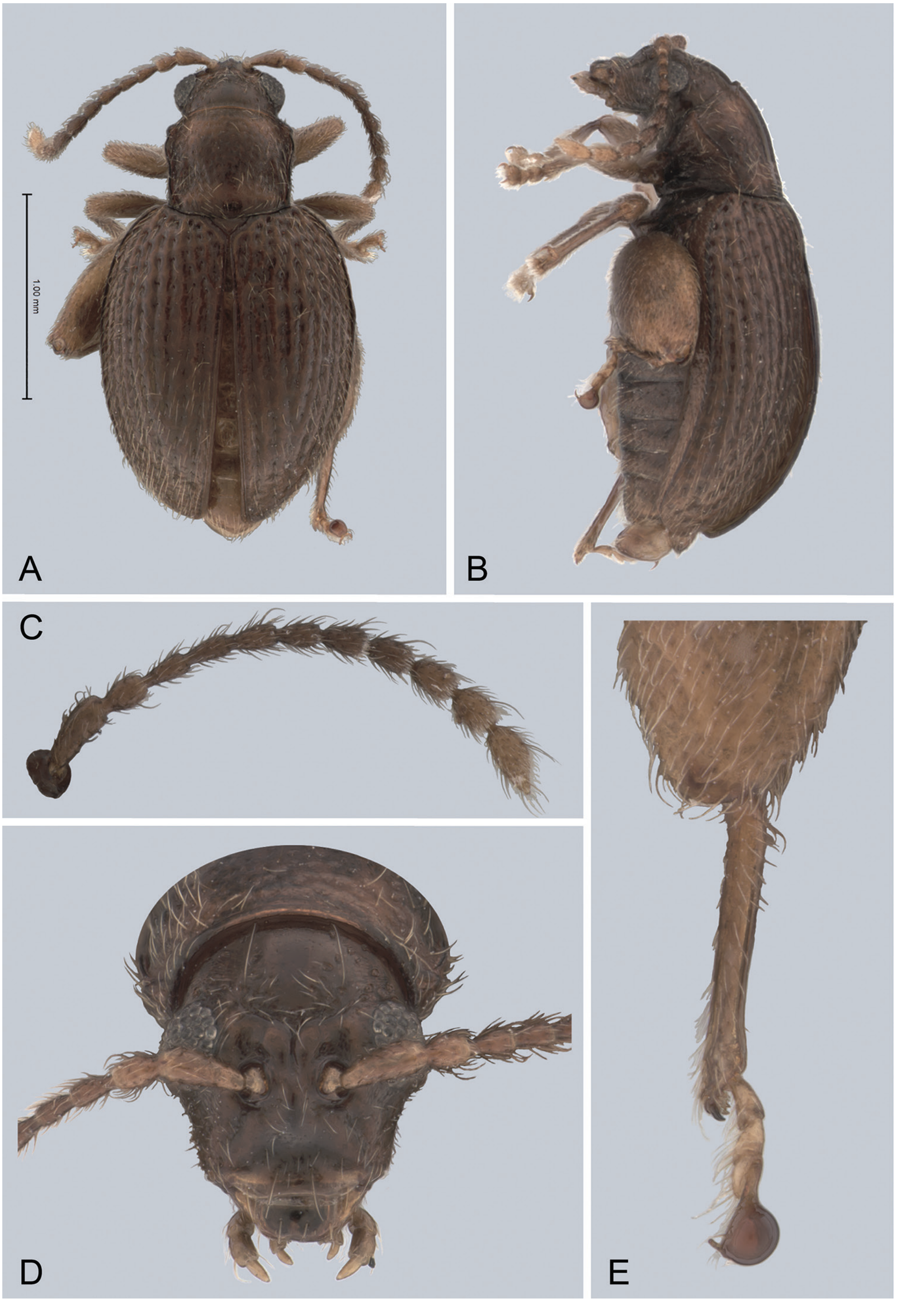

Figure 30. *Andersonoplatus rosalesi*. **A** Habitus dorsal **B** Habitus lateral **C** Antenna **D** Head, frontal view **E** Hind leg.

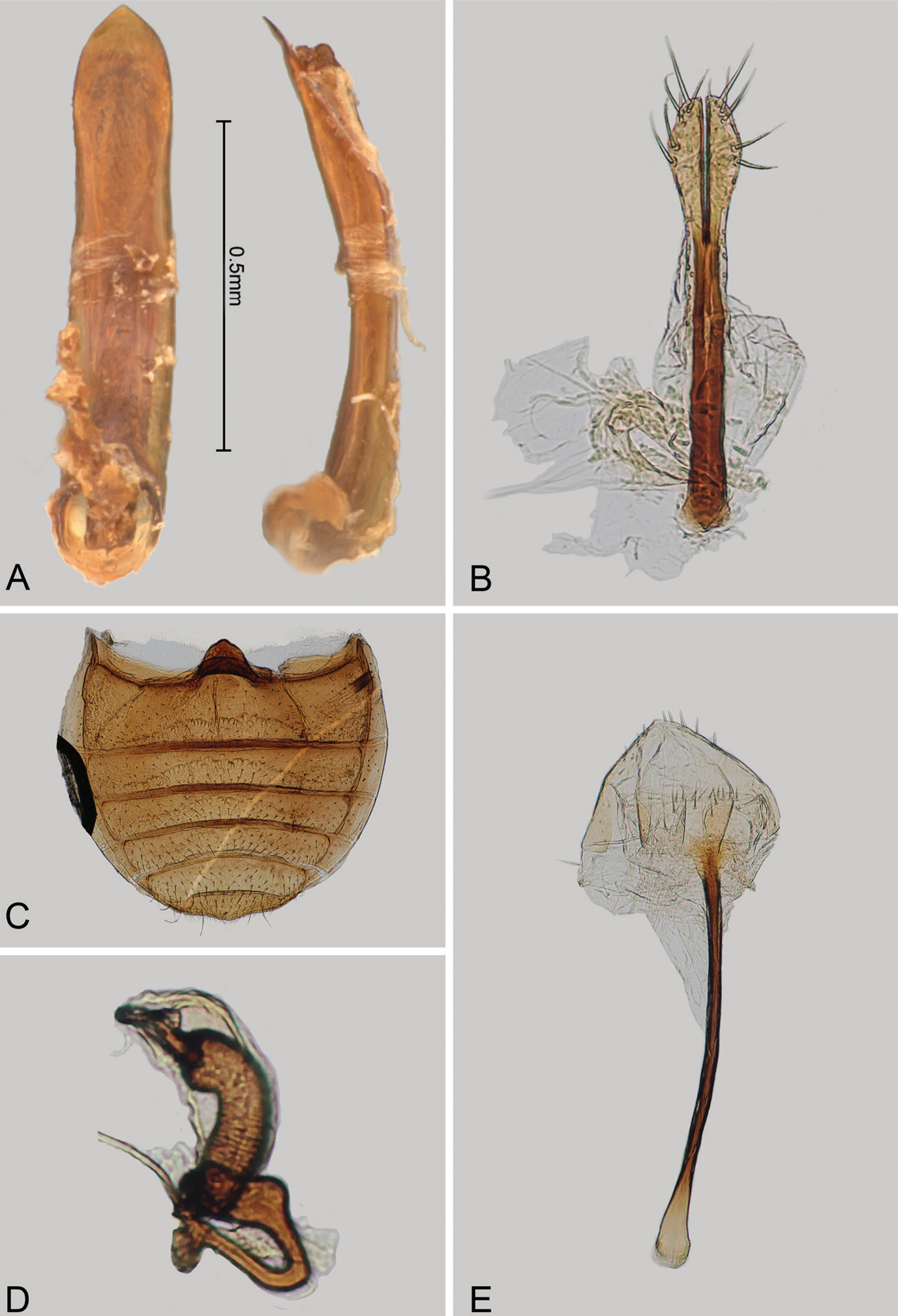

Figure 31. *Andersonoplatus rosalesi*. **A** Median lobe of aedeagus, ventral and lateral views **B** Vaginal palpi **C** Female abdomen, ventral view **D** Spermatheca **E** Tignum.

Type material. Holotype, ♂. VENEZUELA: Merida/ 34km N.W. Merida, Finca/ 'Fundo La Trinidad', 2350m/ 08°37'00"N, 71°20'12"W/ 22.V.1998-027C, R.Anderson/ montane forest litter (MIZA). **Paratypes** (5♂ USNM, CMNC, 1♀ USNM). Same labels as holotype.

Etymology. We name this species after Carlos Rosales of Museo del Instituto de Zoologia, UCV, Maracay, Venezuela, a fellow coleopterist who contributed greatly to our knowledge of beetles of Venezuela.

Differential diagnosis. *Andersonoplatus rosalesi* is similar to *A. andersoni*, *A. flavus* and *A. sanare* and can be separated from them based on the following characters: pronotal surface densely covered with well-defined punctures, diameter of which larger than distance between punctures (Fig. 30A) and second elytral stria reaching base of elytron (Fig. 30A).

Andersonoplatus sanare sp. n.

http://zoobank.org/6D9402CE-5913-4160-B0CF-70F94EBEF0AC
Figs 32, 33

Description. Body length 2.43–3.24 mm, width 1.24–1.59 mm, shiny, pilose, with semi-erect hairs, moderately convex in lateral view. Color light brown to dark brown.

Head (Fig. 32D): slightly convex in lateral view, generally reticulated, with sparse pilosity, gena slightly punctured. Frons and vertex forming nearly a 135° angle in lateral view. Antennal callus delineate from vertex by deep and curved supracalinal sulcus. Antennal callus slightly elevated above vertex, surface even, with no or two punctures, if bearing setae, they are short. Orbital sulcus deep. Supraorbital sulcus shallow. Supraorbital and supracallinal sulci not connected. Suprafrontal sulcus shallow. Frontolateral sulcus shallow. Frontogenal suture deep. Orbit wider than transverse diameter of antennal socket. Interantennal space narrower than transverse diameter of eye and as wide as transverse diameter of antennal socket. Frontal ridge short and narrow. Antenna filiform; last five antennomeres slightly wider than preceding ones; second antennomere shorter (Fig. 32C).

Thorax: pronotum (Fig. 32A) much narrower than elytra. Anterior margin wider than posterior, posterior margin nearly straight, lateral margin slightly sinuated. Surface reticulated, slightly punctated, pilose, sparsely covered with variously defined punctures, diameter of which smaller than distance between punctures. Post basal impression absent in females. Pronotal disc weakly raised. Scutellum triangular, shorter than wide. Prosternal surface reticulated. Prosternal intercoxal process thin. Posterior end twice as wide as middle. Procoxae very close to each other. Elytra fused. Elytral surface shiny, with white, semi-erect hairs, punctate (Fig. 32A, B). Punctures forming nine striae, ninth stria almost merge with marginal one. Interspaces convex. Marginal line of elytra interrupted at base. Second and third striae not reaching elytral base. Epipleura slightly convex, nearly vertical, slightly narrowed at elytral apex. Metafemur greatly enlarged, 1.66 times longer than metatibia. Claws appendiculate and long (Fig. 32E).

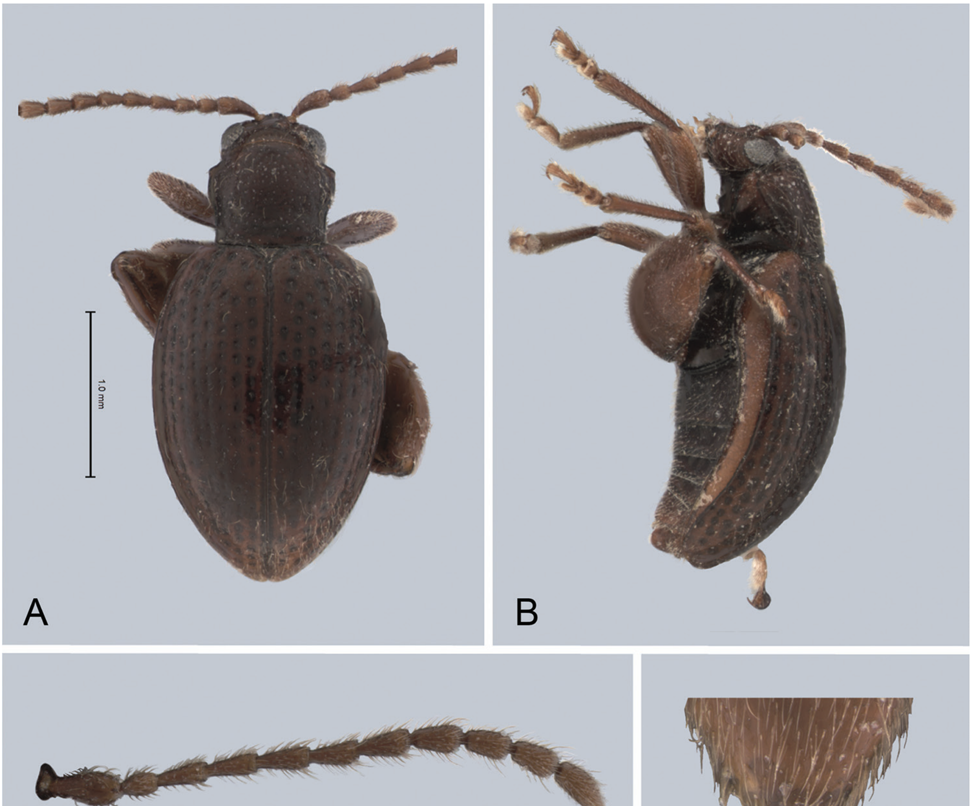

Figure 32. *Andersonoplatus sanare*. **A** Habitus dorsal **B** Habitus lateral **C** Antenna **D** Head, frontal view **E** Hind leg.

Figure 33. *Andersonoplatus sanare*. **A** Median lobe of aedeagus, ventral and lateral views **B** Median lobe of aedeagus, internal structures under compound microscope **C** Vaginal palpi **D** Tignum **E** Spermatheca.

Male genitalia (Fig. 33A, B): ventral side convex and shiny, without longitudinal impression, slightly flattened at apex; apical denticle well developed, long in ventral view, apex slightly bent ventrally.

Female genitalia (Fig. 33C–E): tignum long, narrow, slightly bent, with central canal; anterior sclerotization widening gradually with slightly curved sides and convex apex, posterior sclerotization poorly delineated, narrow, as wide as anterior (Fig. 33D). Vaginal palpi elongate, basally strongly sclerotized, each with approximately eight setae at apex (Fig. 33C). Palpi pointed at apex, enlarged at last third but thinned at apex, situated close together and merged anteriorly for more than half of their length. Spermatheca curved, with receptacle and pump not differentiated from each other. Apex of pump with spoon-like projection. Spermathecal duct short, widest at base, without coils, making small loop (Fig. 33E).

Type material. Holotype, ♂. VENEZUELA: Lara/ P.N.Yacambu, 6.4km/ S.E. Sanare, 1850m/ 09°41'51"N, 69°38'57"W/ 17.V.1998-014C/ R.Anderson, cloud for. Litter (MIZA). **Paratypes** (9♂ 12♀ USNM). (5♂4♀ USNM) Same label as holotype except: (1♂1♀ CMNC) "014A"; (2♂6♀ USNM) "014E"; (1♂1♀ CMNC) "10.4km", "1800m", "013B".

Etymology. The specific epithet is a noun in apposition based on the type locality.

Differential diagnosis. *Andersonoplatus sanare* is similar to *A. andersoni* but can be differentiated from it based on the following characters: ventral side of median lobe without longitudinal impression (Fig. 33A); spermathecal duct making relatively short loop (Fig. 33E).

Andersonoplatus saviniae sp. n.

http://zoobank.org/C96450F3-D40D-4B4D-933F-831E522AB458

Figs 34, 35

Description. Body length 2.54–3.02 mm, width 1.18–1.40 mm, shiny, pilose, with semi-erect hairs, flat in lateral view. Color light brown with elytra darker (almost always in males or with band in middle in females).

Head (Fig. 34D): slightly flat in lateral view, shiny, generally reticulated, with sparse pilosity. Vertex covered with large, poorly defined punctures. Frons and vertex almost at same level in lateral view. Antennal callus delimited from vertex by shallow and slightly inclined supracallinal sulcus; slightly raised above vertex; surface uneven, with more than two punctures, some of them bearing setae. Orbital and supraorbital sulci shallow, represented by punctures. Suprafrontal and frontolateral sulcus shallow. Frontogenal suture shallow. Orbit narrow, punctured, narrower than transverse diameter of antennal socket. Interantennal space narrower than transverse diameter of eye and transverse diameter of antennal socket separately. Frontal ridge short and narrow. Anterofrontal ridge short, relatively tall, oblique. Antenna filiform; the last five antennomeres slightly wider and shorter than preceding ones; second antennomere shortest; sixth antennomere as long as seventh (Fig. 34C).

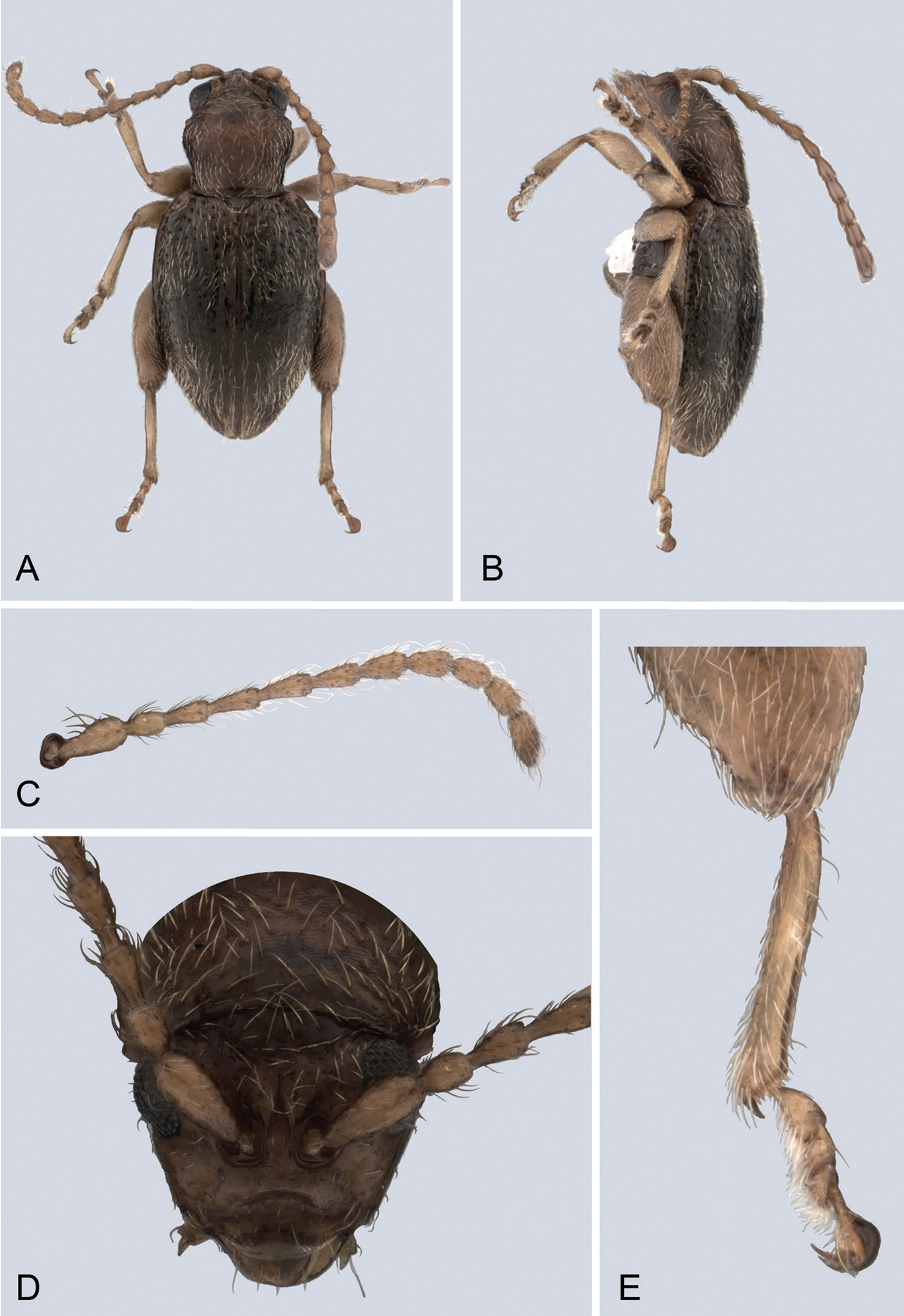

Figure 34. *Andersonoplatus saviniae*. **A** Habitus dorsal **B** Habitus lateral **C** Antenna **D** Head, frontal view **E** Hind leg.

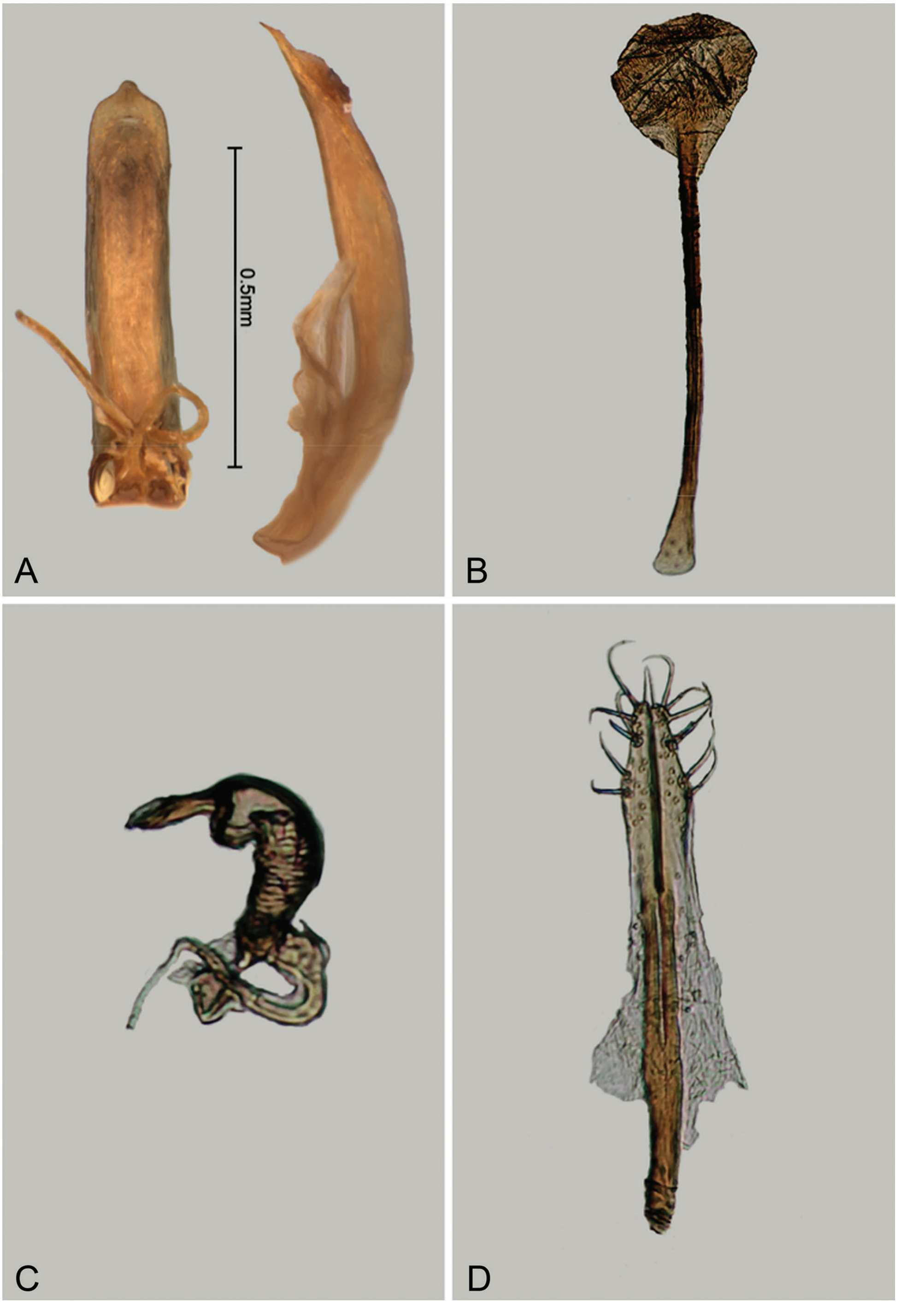

Figure 35. *Andersonoplatus saviniae*. **A** Median lobe of aedeagus, ventral and lateral views **B** Tignum **C** Spermatheca **D** Vaginal palpi.

Thorax: pronotum (Fig. 34A, B) narrower than elytra. Anterior margin wider than posterior, posterior margin slightly convex, lateral margin slightly sinuated. Anterior and posterior angles pointed outwards. Surface reticulated, punctured, pilose. Pronotal disc not raised. Scutellum triangular, wider than long. Prosternal surface reticulated. Prosternal intercoxal process thin. Posterior end twice as wide as middle. Procoxae very close to each other. Elytra weakly fused. Elytral surface shiny, pilose, with white, semi-erect hairs, punctate (Fig. 34A, B). Punctures forming nine striae, ninth stria almost merge with marginal one. Interspaces slightly convex. Distinct impression running on base of fifth and sixth striae. Second and third striae reaching elytral base. Epipleura nearly vertical. Metafemur greatly enlarged, 1.33 times longer than metatibia. Metatibia almost straight in lateral view, slightly curved in dorsal view. Claws simple and long (Fig. 34E).

Male genitalia (Fig. 35A): ventral side flat with shallow longitudinal impression interrupted in middle; apex bent ventrally, in lateral view nearly straight, apical denticle (in ventral view) shorter and less differentiated.

Female genitalia (Fig. 35B–D): tignum long, narrow, slightly bent, with central canal; anterior sclerotization widening gradually with slightly curved sides and convex apex, posterior sclerotization poorly delineated, wide, wider than anterior (Fig. 35B). Vaginal palpi elongate, basally strongly sclerotized, each with approximately eight setae at apex (Fig. 35D). Palpi pointed at apex, enlarged at last third but thinned at apex, situated close together and merged anteriorly for more than half of their length. Spermatheca curved, with receptacle and pump not differentiated from each other, receptacle longer than pump. Apex of pump with spoon-like projection. Spermathecal duct short, widest at base, without coils, making loop (Fig. 35C).

Type material. Holotype, ♂. VENEZUELA: Trujillo/ camino viejo a Trujillo, Paramo/ La Cristalina, km 9.7, 2400m/09°21'21"N, 70°17'51"W/ 20.V.1998-022A/ R.Anderson, elfin for. Litter (MIZA). **Paratypes** (3♂ 3♀ USNM). Same label as holotype except: (1♂1♀ CMNC) “022E”; (2♂ USNM) “022F”; (2♀ USNM) “022J”.

Etymology. We name this species after Vilma Savini of Museo del Instituto de Zoologia, UCV, Maracay, Venezuela, a fellow coleopterist who contributed greatly to our knowledge of beetles of Venezuela.

Differential diagnosis. *Andersonoplatus saviniae* is similar to *A. lagunanegra* and can be differentiated from it based on the following characters: sixth antennomere as long as seventh (Fig. 34C); aedeagus in lateral view nearly straight, apical denticle (in ventral view) shorter and less differentiated (Fig. 35A).

Key to *Andersonoplatus* species

1	Surface of antennal calli uneven, with more than two punctures, some of them bearing long setae	**2**
–	Surface of antennal calli even, with no or two punctures, if bearing setae, they are short	**8**

2 Elytral striae well recognized, often placed in grooves making interspaces convex **3**
– Elytral striae poorly recognized, punctures not in grooves making, interspaces flat **7**
3 Supracallinal sulcus sharply delimited **4**
– Supracallinal sulcus poorly delimited **5**
4 Body 1.62–1.78 mm in length, light brown, vertex sparsely covered with setae. Posterior sclerotization of vaginal palpi with straight sides. Posterior sclerotization of tignum narrower than anterior .... ***Andersonoplatus peck***
– Body 3.39–3.40 mm, uniformly yellowish, vertex densely covered with setae. Posterior sclerotization of vaginal palpi with curved sides. Posterior sclerotization of tignum wider than anterior .... ***Andersonoplatus baru***
5 Vertex with coarse transverse wrinkles most evident near orbital sulci (Fig. 19D). Anterolateral callosity of pronotum long curved denticle-like (Fig. 19A). Body dark in color (Fig. 19A) .... ***Andersonoplatus merga***
– Vertex without coarse transverse wrinkles near orbital sulci (Fig. 17B). Anterolateral callosity of pronotum short, not denticle-like (Fig. 17A). Body lighter in color (Fig. 17A) **6**
6 Vaginal palpi separated on one third of their length (Fig. 18C). Posterior sclerotization of vaginal palpi concave on side (Fig. 18C). Anterior end of tignum narrow (Fig. 18B) .... ***Andersonoplatus macubaji***
– Vaginal palpi separated on more than one third of their length (Fig. 22B). Posterior sclerotization of vaginal palpi slightly curved on side (Fig. 22B). Anterior end of tignum relatively wide (Fig. 22A) .... ***Andersonoplatus merida***
7 Sixth antennomere much smaller than seventh (Fig. 15C). Aedeagus in lateral view strongly curved, apical denticle (in ventral view) longer and better pronounced (Fig. 16A) .... ***Andersonoplatus lagunanegra***
– Sixth antennomere as long as seventh (Fig. 34C). Aedeagus in lateral view nearly straight, apical denticle (in ventral view) shorter and less differentiated (Fig. 35A) .... ***Andersonoplatus saviniae***
8 Elytral interspaces flat **9**
– Elytral interspaces convex **11**
9 Eyes small, with nearly 12 large ommatidia (Fig. 23B, D). Pronotum comparatively narrow (Fig. 23A). Apical denticle of male genitalia well developed, narrow (Fig. 24A) .... ***Andersonoplatus microoculus***
– Eyes large, with more than 20, small ommatidia (Figs 7D, 12 D). Pronotum comparatively wide (Figs 7A, 12A). Apical denticle of male genitalia absent, poorly developed (Fig. 8A), or very wide (Fig. 13F) **10**
10 Supracallinal sulci well developed, deep (Fig. 7D). Apex of median lobe of aedeagus bent ventrally in lateral view (Fig. 8A) .... ***Andersonoplatus castaneus***
– Supracallinal sulci poorly developed, barely perceptible (Fig. 12D). Apex of median lobe of aedeagus straight in lateral view (Fig. 13F) .... ***Andersonoplatus jolyi***

11 Pronotal surface shiny, lacking punctures (Fig. 14A, B, E). Ventral side of median lobe of aedeagus flat with low longitudinal ridge apically (Fig. 14D)... ***Andersonoplatus laculata***

– Pronotal surface dull, covered with punctures (e.g., Fig. 2A). Ventral side of median lobe of aedeagus variously shaped but always without longitudinal ridge (e.g., Fig. 1F) **12**

12 Pronotal surface uneven, covered with relatively large but poorly defined punctures (Fig. 5A). Median lobe of aedeagus ventrally with two ridges and deep groove between them (Fig. 6D) .... ***Andersonoplatus bechyneorum***

Pronotal surface even, covered with moderately sized well defined punctures (e.g., Fig. 30A). Median lobe of aedeagus ventrally without ridges and deep grove between them (e.g., Fig. 1F) **13**

13 Pronotal surface densely covered with well-defined punctures, diameter of which larger than distance between punctures (Fig. 30A). Second elytral stria reaching base of elytron (Fig. 30A)........................ ***Andersonoplatus rosalesi***

– Pronotal surface sparsely covered with variously defined punctures, diameter of which smaller than distance between punctures (e.g., Fig. 32A). Second elytral stria not reaching base of elytron (e.g., Fig. 32A)............................ **14**

14 Body yellow (Fig. 10A, B)...................................... ***Andersonoplatus flavus***

– Body brown (Figs 1A, B, 32A, B) 15

15 Ventral side of median lobe with shallow longitudinal impression, bottom of which covered with transverse wrinkles (Fig. 2F). Spermathecal duct making relatively long loop (Fig. 2E)............................ ***Andersonoplatus andersoni***

– Ventral side of median lobe without longitudinal impression (Fig. 33A). Spermathecal duct making relatively short loop (Fig. 33E) ... ***Andersonoplatus sanare***

Acknowledgements

We are immensely grateful to R. Anderson (Canadian Museum of Nature, Ottawa, Canada), and J. and S. Peck (Ottawa, Canada) for their spectacular flea beetle collecting efforts over the years. The Smithsonian Institution Fellowship Office granted a short-term fellowship to the first author in March of 2011. We thank Meghan Neace for an illustration of *A. castaneus*. Mention of trade names or commercial products in this publication is solely for the purpose of providing specific information and does not imply recommendation or endorsement by the USDA; USDA is an equal opportunity provider and employer.

References

Anderson RS (2010) A taxonomic monograph of the Middle American leaf-litter inhabiting weevil genus *Theognete* Champion (Coleoptera: Curculionidae; Molytinae; Lymantini). Zootaxa 2458: 1–127.

Chapuis F (1875) Histoire naturelle des insectes. Genera des Coléoptères. Vol. 11. Famille des Phytophages. Paris, 420 pp.

Clark H (1860) Catalogue of Halticinae in the collection of the British Museum. Physapodes and Aedipodes. Part I. London, 301 pp. [10 figs]

Konstantinov AS (1998) Revision of the palearctic species of *Aphthona* Chevrolat and cladistic classification of the Aphthonini (Coleoptera: Chrysomelidae: Alticinae). Memoirs on Entomology, International. Associated Publishers, Florida, 429 pp.

Linzmeier AM, Konstantinov AS (2009) A new genus of flea beetles (Coleoptera: Chrysomelidae) from the south of Brazil. Proceedings of the Entomological Society of Washington 111(3): 656–665. ttps://doi.org/10.4289/0013-8797-111.3.656

Linzmeier AM, Konstantinov AS (2012) A new genus of leaf litter inhabiting Neotropical Monoplatina (Coleoptera: Chrysomelidae; Galerucinae: Alticini). Zootaxa 3260: 19–32.

ZooKeys 744: 139–147 (2018)
doi: 10.3897/zookeys.744.22347
http://zookeys.pensoft.net

SHORT COMMUNICATION

A peer-reviewed open-access journal
ZooKeys
Launched to accelerate biodiversity research

X-ray microtomography (microCT) of male genitalia of *Nothybus kuznetsovorum* (Nothybidae) and *Cothornobata* sp. (Micropezidae)

Tatiana V. Galinskaya[1,2], Dina Gafurova (Gilyazetdinova)[3], Olga G. Ovtshinnikova[4]

1 *Faculty of Biology, Lomonosov Moscow State University, Moscow, 119234 Russia* **2** *Museum of Entomology, All-Russian Plant Quarantine Center, Pogranichnaya 32, Bykovo, 140150, Russia* **3** *Faculty of Geology, Lomonosov Moscow State University, Moscow, 119234 Russia* **4** *Zoological Institute, Russian Academy of Sciences, St. Petersburg, 199034 Russia*

Corresponding author: *Tatiana V. Galinskaya* (nuha1313@gmail.com)

Academic editor: *M. Hauser* | Received 17 November 2017 | Accepted 27 February 2018 | Published 20 March 2018

http://zoobank.org/751CAAB3-6BC5-46AD-9631-94E44109D7DA

Citation: Galinskaya TV, Gafurova (Gilyazetdinova) D, Ovtshinnikova OG (2018) X-ray microtomography (microCT) of male genitalia of *Nothybus kuznetsovorum* (Nothybidae) and *Cothornobata* sp. (Micropezidae). ZooKeys 744: 139–147. https://doi.org/10.3897/zookeys.744.22347

Abstract
The results of manual dissection of the musculature of the male genitalia in *Nothybus kuznetsovorum* are fully confirmed by the modern methods of Micro-CT. A comparative analysis of *Neria commutata* and *Cothornobata* sp. shows that an increase in the flexion in the genitalia of males and the displacement of syntergosternite VII to the ventral side in *Cothornobata* sp. caused the disappearance of the muscles ITM6–7r and ITM7–8r. In addition, this increase in flexion apparently caused the fusion of the M18 muscles into one bundle. The muscle ISM5-6c goes on to moving the second segment of the forcipate appendages of sternite V.

Keywords
Cothornobata, Morphology, musculature, *Neria commutata*, *Nothybus kuznetsovorum*, sclerites

Introduction

Micropezidae is an average-sized family of acalyptrate flies (Diptera). It comprises approximately 700 described species in 50 genera (Marshall 2010, 2012; Ferro and

Carvalho 2014). The family is globally distributed, with the greatest species richness found in tropical regions (Steyskal 1968). The body of adult flies is 3.5 to 20.0 mm long (Steyskal 1987).

The family Nothybidae includes only one genus, *Nothybus* Rondani, 1875, distributed in the Oriental Region. These acalyptrate flies are 5.5 to 15.0 mm body long (Lonsdale and Marshall 2016).

Study of the musculature is helpful not only for specifying the functions of genital sclerites, but also for revealing the homology of some poorly traced structures (Ovtshinnikova 1989, 1994, Ovtshinnikova and Yeates 1998; Galinskaya and Ovtshinnikova 2015).

Previously specimens of *Nothybus kuznetsovorum* Galinskaya et Shatalkin, 2015 (Nothybidae) and *Neria commutata* (Czerny, 1930) (Micropezidae) were investigated by manual dissection using light microscopy (Galinskaya et al. 2016, Ovtshinnikova and Galinskaya 2017). In these studies, some muscles were thin and indistinct.

Among the Diptera the X-ray micro-computed tomography (Micro-CT) was used for revealing the morphology of the feeding apparatus of *Philoliche rostrata* and *Ph. gulosa* (Tabanidae) (Karolyi et al. 2014); for the characterization of the morphology of the venom system of *Eutolmus rufibarbis* (Asilidae) (Drukewitz et al. 2018); for revealing the morphology of the proboscis, the food canal and suction pump muscles of *Prosoeca* sp. (Nemestrinidae) (Karolyi et al. 2013); for analysis of the *Drosophila* larvae central nervous system (Drosophilidae) (Mizutani et al. 2007); for revealing the morphology of the late pupa of *Calliphora vicinia* (Calliphoridae) (Metscher 2009); for performing qualitative and quantitative analyses of the morphological changes taking place during the intra-puparial period of *Calliphora vicina* and *Lucilia sericata* (Calliphoridae) (Richards et al. 2012; Hall et al. 2017; Martín-Vega et al. 2016; Martín-Vega et al. 2017a, b); and for the visualization of the three-dimensional movements of flight muscles and thoracic sclerites of *Calliphora vicina* (Calliphoridae) (Walker et al. 2014).

In this study X-ray micro-computed tomography (micro-CT) was utilizzed for revealing genital sclerites and muscles of *Nothybus kuznetsovorum* (Nothybidae), comparing it with results of manual dissection (Galinskaya et al. 2016). The sclerites and muscles of *Cothornobata* sp. (Micropezidae) are also revealed. Males of Micropezidae are characterized by specialized forceps-like processes of variable size, shape, and ornamentation arising from sternite V and by sternite VI sometimes with specialized processes (these processes are secondarily reduced in some spp). The examined species is characterized by elongated forcipate appendages of sternite V, and the musculature of these appendages was investigated.

Materials and methods

One specimen of *Nothybus kuznetsovorum* and one specimen of *Cothornobata* sp. were collected in Northern Vietnam, PhuTho Province, Thanh Son District, Xuan Son National Park; 21°8.333'N; 104°56.25'W; h = 300–900 m, 23 October 2014 by T.V. Galinskaya. The specimens were fixed in 70% ethanol. They were prepared for X-ray micro-computed tomography (micro-CT) analysis by contrasting with iodine as outlined in Gignac and Kley (2014) and by critical point drying. Specimens were glued with the thorax pointing downwards on the tip of a small pin of 1 mm diameter, with the tip of the male abdomen as close to the rotation axis as possible. Micro-CT scans were produced under phase contrast (40 KV, 8 W), using a 4× detector (10 s; 4.15 µm pixel size) and 10× detector (30 s; 1.89 µm pixel size).

The male genital muscles were classified into several groups (muscles of the epandrial complex, muscles of the hypandrial complex, tergosternal muscles, and pregenital muscles) and described according to the system of Ovtshinnikova and Galinskaya (Ovtshinnikova 1989, 2000; Ovtshinnikova and Galinskaya 2017). Male genital sclerites were described according to the Sinclair (2000).

Results

Nothybus kuznetsovorum Galinskaya & Shatalkin, 2015

Figure 1

All sclerites and muscles and their places of attachments revealed using manual dissection and decribed by us previously (Galinskaya et al. 2016) have been confirmed by micro-CT. The only questionable muscle after manual dissection was M7 (Galinskaya et al. 2016). Here the presence and attachment sites of attachment of M7 are confirmed (Figure 1B).

Cothornobata sp.

Figures 2–4

Sclerites. Sternite IV elongate. Sternite V modified into elongated forcipate appendages. Sternite VI elongate. Tergite IV, V, VI not modificated. Ejaculatory apodeme placed at the level of sternites V and VI. Sternite and tergite VII fused into syntergosternite positioned on left side of body. Syntergosternite VIII spherical. Epandrium large, bearing bifurcate surstyli and small cerci.

Muscles. The muscles are grouped by the site of insertion of their proximal parts. Thin paired muscles ISM4–5 attached to basal area of sternite V (Figure 3B). Tergosternal muscle TSM4 poorly developed (Figure 4A).

Muscles of segments V and VI. Two pairs of muscles ISM5–6 lying between sternites V and VI: proximal retractors of sternite VI ISM5–6a broadly fan-shaped, extending from basal area of sternite V to lateral surface of sternite VI (Figures 3C, 4C); median flexors of forcipate appendages ISM5–6c broadly fan-shaped, extending from lateral outgrowths of sternite V to central part of sternite VI (Figures 3B, 4B, G). Contraction of muscles ISM5–6 powers the forcipate appendages of sternite V that participate in the fixation of the female's abdomen during copulation. Tergosternal muscles TSM5 and TSM6 in segments V–VI poorly developed (Figure 4A).

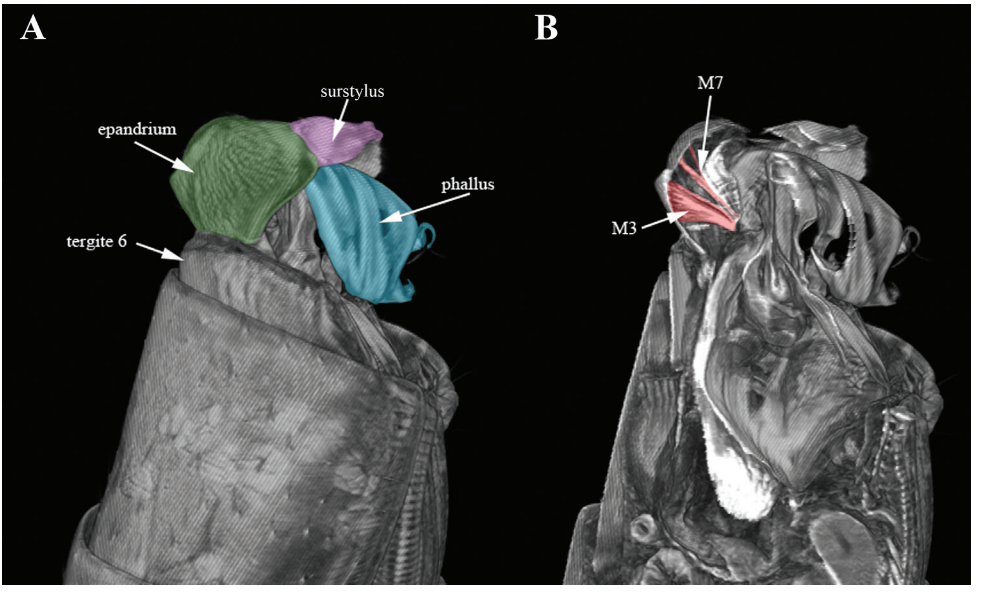

Figure 1. Micro-CT surface rendering (**A**) and volume rendering of virtual sections to median, digitally stained (**B**) of *Nothybus kuznetsovorum* (Nothybidae), lateral view. Cerci shown in yellow, epandrium in dark green, phallus in light blue, surstylus in pink, syntergosternite VIII in violet, syntergosternite VII in light green, sternite VI in orange and sternite V in dark blue.

Muscles associated with segment VII are asymmetrical. Left intersegmental tergal muscle ITM6–7l wide, extending from distal area of tergite VI to left lateral margin of syntergosternite VII (Figure 4G). No muscles TSM6–7 present in sternal area between segments VI and VII. Left muscle ISM7–8l wide, extending from basal margin of syntergosternite VII to syntergosternite VIII (Figure 4G). Tergosternal muscles of segment VII absent, probably due to fusions or reductions.

Pregenital muscles. Muscle of hypandrium M18 connects syntergosternite VIII to hypandrium (Figure 4G). Retractors of epandrium M19 extending from syntergosternite VIII to middle of proximal margin of epandrium (Figure 4C, F).

Tergosternal muscles of segment VIII absent, probably due to fusions or reductions.

Long and powerful symmetrical tergosternal abductors M5 extending from latero-basal margin of epandrium to latero-distal margin of hypandrium.

Muscles of epandrial complex symmetrical. Wide and thin paired cercal muscles M7 extend from distal outgrowths of subepandrial sclerite to cerci (Figure 2B). Paired muscles of subepandrial sclerite M3 well developed, comprise two pairs of muscles: muscles M3b extending from latero-distal lobes of subepandrial sclerite to latero-distal part of epandrium (Figure 2D, 4B, E); muscles M3d extending from median bridge of subepandrial sclerite to distal part of epandrium (Figure 2B, C). Short and narrow adductors of surstylus M4 connecting laterodistal parts of epandrium to basal part of surstylus (Figure 2C, 4B).

Muscles of hypandrial complex symmetrical. Short and powerful paired phallic retractors M1 connecting distal part of phallapodeme to distal inner part of hypandrium

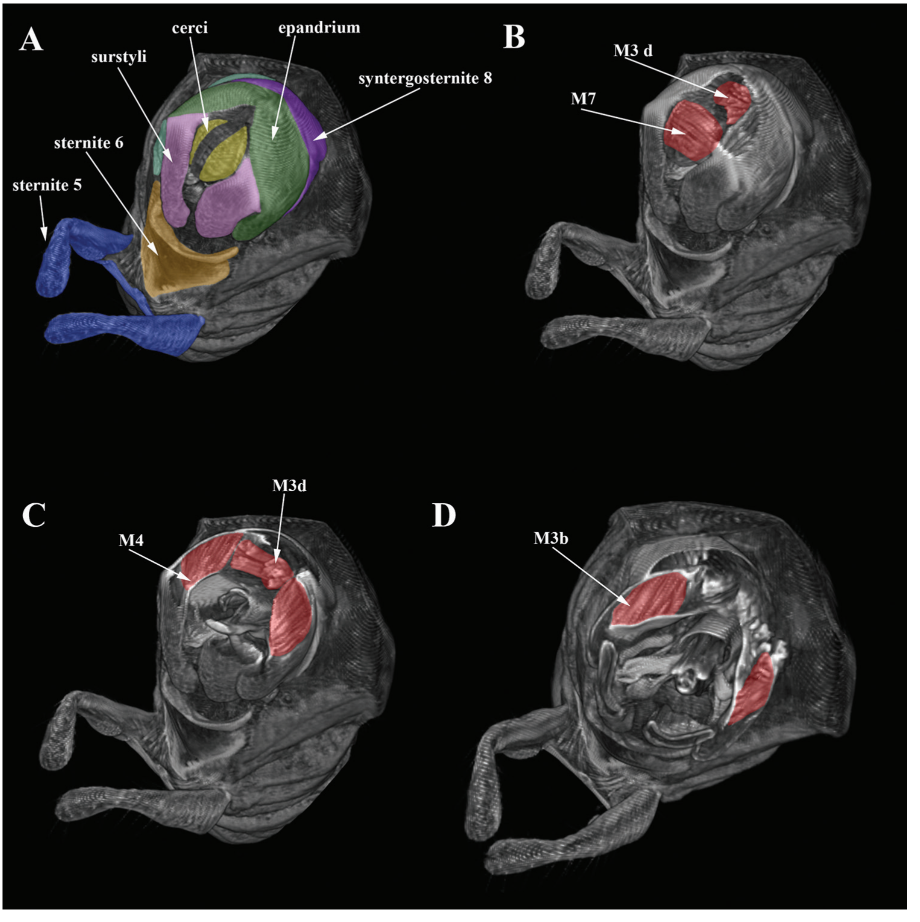

Figure 2. Micro-CT surface rendering (**A**) and volume rendering of virtual sections posteriorly, digitally stained (**B–D**) of *Cothornobata* sp. (Micropezidae), posterior view.

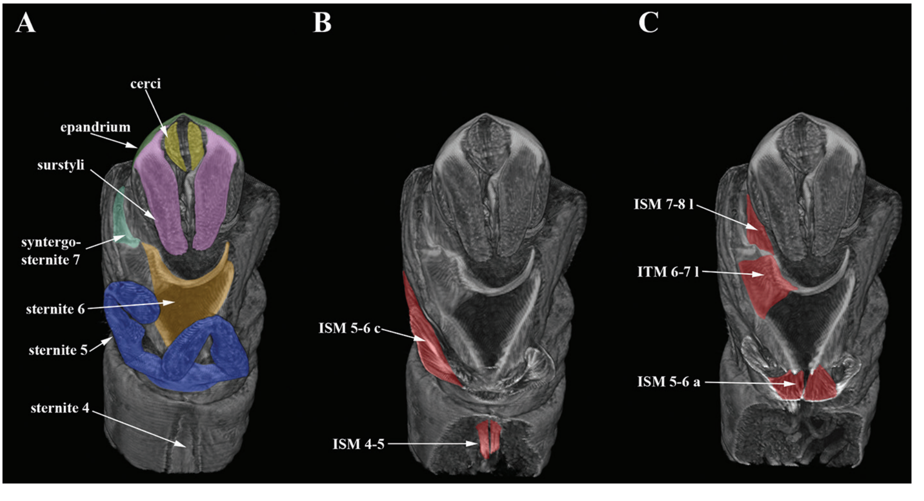

Figure 3. Micro-CT surface rendering (**A**) and volume rendering of virtual sections right to median, digitally stained (**B–C**) of *Cothornobata* sp. (Micropezidae), abdominal view.

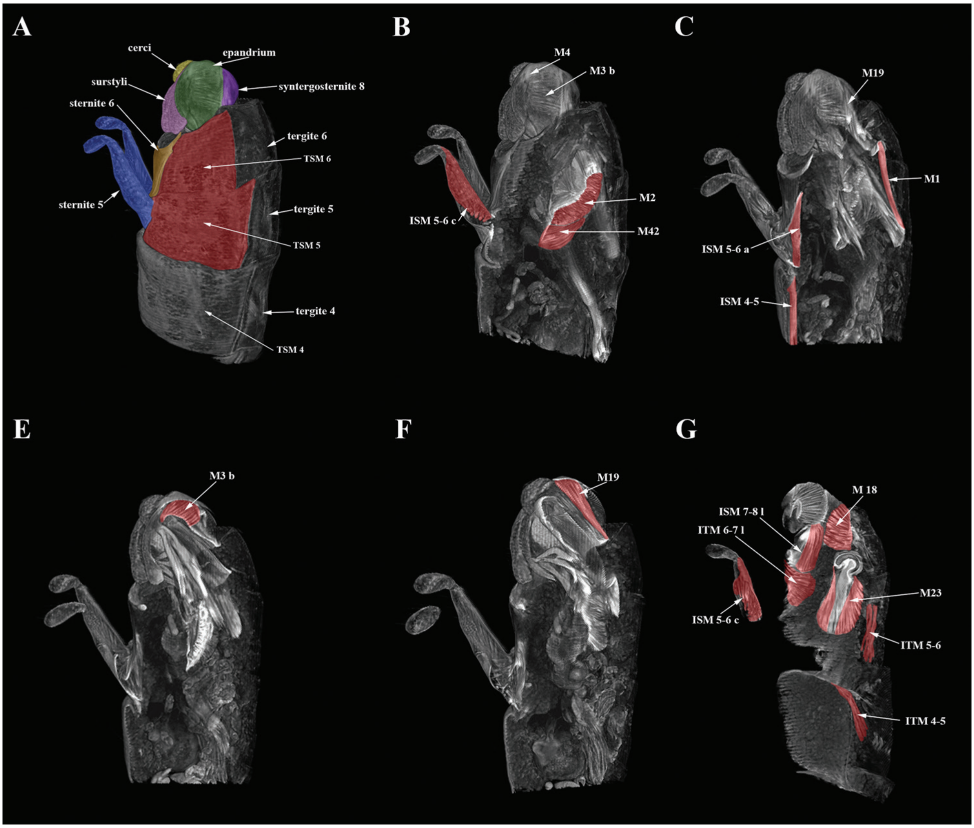

Figure 4. Micro-CT surface rendering (**A**) and volume rendering of virtual sections right to median, digitally stained (**B–G**) of *Cothornobata* sp. (Micropezidae), lateral view.

(Figure 4C). Long and powerful paired phallic protractors M2 connecting distal part of phallapodeme to lateral and median parts of hypandrium (Figure 4B) and lying above M1. Paired retractors of pregonites M42 extending from inner distal part of hypandrium to pregonites (Figure 4B). Compressors of ejaculator M23 well developed (Figure 4G).

Discussion

Since the results of the study of the male genitalia in *Nothybus kuznetsovorum* using micro-CT completely coincide with the results of manual dissection, we conclude that the method of manual anatomy has not lost its significance. However, the micro-CT takes much more time than manual anatomy. The undoubted advantage of micro-CT is its higher accuracy and the fact that only one specimen is needed for the study, while manual anatomy usually needs 4–5 specimens.

We assume that the presence of the elongated appendages of sternite V in the species *Cothornobata* sp. can cause the presence of additional muscles ISM5–6 (due to the complication of sclerites in *Cothornobata* sp. comparing with *Neria commutata*). However, no muscle going from the basal to the distal segments of the appendages of V sternite was discovered. Additionally, we did not find the muscles ISM5–6b and ISM5–6d. *Neria commutata* has the lateral flexors of forcipate appendages ISM5–6d broad and short, extending from inner vanes of sternite V to those of sternite VI and occupying a considerable part of the surfaces of both sclerites; the distal retractors of sternite VI ISM5–6b are narrow, extending from the distal parts of the outgrowths of sternite V to the distal area of sternite VI. Apparently, the muscle ISM5–6c goes on to moving the distal half of the forcipate appendages of sternite V.

In *Cothornobata* sp., unlike *Neria commutata*, no muscles ITM6–7r and ITM7–8r have been detected. *Neria commutata* has the right muscle ITM6–7r narrow, conical, extending from the median part of tergite VI to the membrane in front of syntergosternite VII, and the right muscle ISM7–8r small and short, extending from the membrane at syntergosternite VII to syntergosternite VIII (Ovtshinnikova and Galinskaya 2017). We assume that in *Cothornobata* sp. these muscles are absent due to a stronger flexion of syntergosternite VII to the ventral side. Increased flexion of syntergosternite VII in *Cothornobata* sp. caused the disappearance of muscles ITM6–7r and ITM7–8r. Also, an increase of the flexion apparently caused the fusion of the M18 muscles into one bundle.

Acknowledgments

The authors are grateful to A.I. Shatalkin (Zoological Museum of Lomonosov Moscow State University) and V.A. Krivokhatsky (Zoological Institute of Russian Academy of Sciences) for valuable discussions and advice. The work of T.V. Galinskaya was supported by the Russian Science Foundation (project no. 14-14-00208). The work of O.G. Ovtshinnikova was supported by the Zoological Institute of Russian Academy of Sciences (State Research Program AAAA-A17-117030310205-9) and the Russian Foundation for Basic Research (projects no. 15-04-03457 and 18-04-0035). The work was carried out using a computer X-ray microtomograph Skyscan 1172, purchased from the funds of the Development Program of the Moscow University of Geological Faculty of M.V. Lomonosov Moscow State University.

References

Drukewitz SH, Fuhrmann N, Undheim EAB, Blanke A, Giribaldi J, Mary R, Laconde G, Dutertre S, Reumont BM (2018) A Dipteran's Novel Sucker Punch: Evolution of Arthropod Atypical Venom with a Neurotoxic Component in Robber Flies (Asilidae, Diptera). Toxins 10 (29): 1–23. https://doi.org/10.3390/toxins10010029

Ferro GB, Carvalho CJB (2014) A pictorial key and diagnosis of the Brazilian genera of Micropezidae (Diptera, Nerioidea). Revista Brasileira de Entomologia 58(1): 52–62. https://doi.org/10.1590/S0085-56262014000100009

Galinskaya TV, Ovtshinnikova OG (2015) Musculature of the male genitalia in the tribe Ulidiini (Diptera, Ulidiidae). Entomological Review 95(1): 31–37. https://doi.org/10.1134/S0013873815010042

Galinskaya TV, Shatalkin AI, Ovtshinnikova OG (2016) Skeleton and musculature of the male genitalia in the family Nothybidae (Diptera). Entomological Review 96(9): 1182–1193. https://doi.org/10.1134/S0013873816090037

Gignac PM, Kley NJ (2014) Iodine-enhanced micro-CT imaging: Methodological refinements for the study of the soft-tissue anatomy of post-embryonic vertebrates. Journal of Experimental Zoology Part B 322: 166–176. https://doi.org/10.1002/jez.b.22561

Hall MJR, Simonsen TJ, Martín-Vega D (2017) The 'dance' of life: visualizing metamorphosis during pupation in the blow fly *Calliphora vicina* by X-ray video imaging and micro-computed tomography. Royal Society Open Science 4: 160699. https://doi.org/10.1098/rsos.160699

Karolyi F, Morawetz L, Colville JF, Handschuh S, Metscher BD, Krenn HW (2013) Time management and nectar flow: flower handling and suction feeding in long-proboscid flies (Nemestrinidae: *Prosoeca*). Naturwissenschaften 100: 1083–1093. https://doi.org/10.1007/s00114-013-1114-6

Karolyi F, Colville JF, Handschuh S, Metscher BD, Krenn HW (2014) One proboscis, two tasks: Adaptations to blood-feeding and nectar-extracting in long-proboscid horse flies (Tabanidae, *Philoliche*). Arthropod Structure and Development 43: 403–413. https://doi.org/10.1016/j.asd.2014.07.003

Lonsdale O, Marshall SA (2016) Revision of the family Nothybidae (Diptera: Schizophora). Zootaxa 4098(1): 1–42. https://doi.org/10.11646/zootaxa.4098.1.1

Martín-Vega D, Hall MJR, Simonsen ThJ (2016) Resolving Confusion in the Use of Concepts and Terminology in Intrapuparial Development Studies of Cyclorrhaphous Diptera. Journal of Medical Entomology 53(6): 1249–1251. https://doi.org/10.1093/jme/tjw081

Martín-Vega D, Simonsen ThJ, Wicklein M, Hall MJR (2017a) Age estimation during the blow fly intra-puparial period: a qualitative and quantitative approach using micro-computed tomography. International Journal of Legal Medicine 131(5): 1429–1448. https://doi.org/10.1007/s00414-017-1598-2

Martín-Vega D, Simonsen ThJ, Hall MJR (2017b) Looking into the puparium: Micro-CT visualization of the internal morphological changes during metamorphosis of the blow fly, Calliphora vicina, with the first quantitative analysis of organ development in cyclorrhaphous dipterans. Journal of Morphology 278: 629–651. https://doi.org/10.1002/jmor.20660

Marshall SA (2010) 55. Micropezidae (stilt-legged flies). In: Brown BV, Borkent A, Cumming JM, Wood DM, Woodley NE, Zumbado M (Eds) Manual of Central American Diptera. vol 2. National Research Council Canada, Ottawa, 805–813.

Marshall SA (2012) Flies: the Natural History and Diversity of Diptera. Firefly Books, Ontario, 616 pp.

Metscher BD (2009) MicroCT for comparative morphology: simple staining methods allow high-contrast 3D imaging of diverse non-mineralized animal tissues. BMC Physiology 9: 11. https://doi.org/10.1186/1472-6793-9-11

Mizutani R, Takeuchi A, Hara T, Uesugi K, Suzuki Y (2007) Computed tomography imaging of the neuronal structure of *Drosophila* brain. Journal of Synchrotron Radiation 14: 282–287. https://doi.org/10.1107/S0909049507009004

Ovtshinnikova OG (1989) Muscles of the male genitalia of Brachycera–Orthorrhapha (Diptera). Trudy Zoologicheskogo Instituta Akademii Nauk SSSR 190: 1–166.

Ovtshinnikova OG (1994) On the homology of male genital sclerites of Brachycera Orthorrhapha and Cyclorrhapha (Diptera) based on musculature. Dipterological Research 5(4): 263–269.

Ovtshinnikova OG (2000) Muscles of the Male Genitalia of Hover Flies of the Family Syrphidae (Diptera). Kholodkovsky Memorial Lectures: a Report at the 52nd Annual Meeting, April 1, 1999, St. Petersburg, 70 pp. [In Russian]

Ovtshinnikova OG, Yeates DK (1998) Male genital musculature of Therevidae and Scenopinidae (Diptera: Asiloidea): structure, homology and phylogenetic implications. Australian Journal of Entomology 37(1): 27–33. https://doi.org/10.1111/j.1440-6055.1998.tb01539.x

Ovtshinnikova OG, Galinskaya TV (2017) The male abdominal, genital and pregenital sclerites and musculature in *Neria commutata* (Czerny, 1930) (Diptera, Micropezidae). Entomological Review 97(3): 282–287. https://doi.org/10.1134/S0013873817030022

Richards CS, Simonsen ThJ, Abel RL, Hall MJR, Schwyn DA, Wicklein M (2012) Virtual forensic entomology: Improving estimates of minimum post-mortem interval with 3D micro-computed tomography. Forensic Science International 220: 251–264. https://doi.org/10.1016/j.forsciint.2012.03.012

Sinclair BJ (2000) 1.2. Morphology and terminology of Diptera male terminalia. In: Papp L, Darvas B (Eds) Contributions to a manual of Palaearctic Diptera. vol 1. Science Herald, Budapest, 53–74.

Steyskal GC (1968) Family Micropezidae. In: Vanzolini PE, Papavero N (Eds) A Catalogue of the Diptera of the Americas South of the United States. Departmento de Zoologia, Secretaria da Agricultura, Sau Paulo, 1–33.

Steyskal GC (1987) Micropezidae. In: McAlpine JF (Ed.) Manual of Nearctic Diptera. vol 2. Agriculture Canada, Ottawa, 761–767.

Walker SM, Schwyn DA, Mokso R, Wicklein M, Muller T, Doube M, Stampanoni M, Krapp HG, Taylor GK (2014) In Vivo Time-Resolved Microtomography Reveals the Mechanics of the Blowfly Flight Motor. PLoS Biol 12(3): e1001823. https://doi.org/10.1371/journal.pbio.1001823

ZooKeys 744: 149–149 (2018)
doi: 10.3897/zookeys.744.25059
http://zookeys.pensoft.net

CORRIGENDA

A peer-reviewed open-access journal
ZooKeys
Launched to accelerate biodiversity research

Corrigenda: Davis DR, LaDuc TJ (2018) Amphibians and reptiles of C. E. Miller Ranch and the Sierra Vieja, Chihuahuan Desert, Texas, USA. ZooKeys 735:97–130. https://doi.org/10.3897/zookeys.735.22200

Drew R. Davis[1], Travis J. LaDuc[2]

1 *Department of Biology, University of South Dakota, 414 East Clark Street, Vermillion, South Dakota 57069, USA* **2** *Biodiversity Collections, The University of Texas at Austin, 10100 Burnet Road, PRC 176–R4000, Austin, Texas 78758, USA*

Corresponding author: *Drew R. Davis* (drew.davis@usd.edu)

Academic editor: *A. Herrel* | Received 15 March 2018 | Accepted 15 March 2018 | Published 20 March 2018

http://zoobank.org/C46C9912-3EEC-4893-B2C5-269290811E63

Citation: Davis DR, LaDuc TJ (2018) Corrigenda: Davis DR, LaDuc TJ (2018) Amphibians and reptiles of C. E. Miller Ranch and the Sierra Vieja, Chihuahuan Desert, Texas, USA. ZooKeys 735:97–130. https://doi.org/10.3897/zookeys.735.22200. ZooKeys 744: 149–149. https://doi.org/10.3897/zookeys.744.25059

In our recently published checklist, we mislabeled one of the species of lizards in Figure 6. In error, we listed Figure 6D as a Chihuahuan Spotted Whiptail (*Aspidoscelis exsanguis*) instead of the correct identification as a Little Striped Whiptail (*Aspidoscelis inornata*). Additionally, on 6 February 2018 (ironically, the date this manuscript was published), we received a photographic voucher of an adult Eastern Patch-nosed Snake (*Salvadora grahamiae*) from the Miller family (Jill Miller), taken from the lechuguilla-beargrass association on the top of a mesa in the Sierra Vieja (TNHC 107584). This new voucher reduces the number of species not detected from the historic 1948 survey from three to two.